

# A SIMPLE & ACCESSIBLE FRONT-END SATELLITE RECEIVER FOR COMMUNICATIONS AND E-LEARNING IN EMERGING COUNTRIES

THÈSE N° 3829 (2007)

PRÉSENTÉE LE 29 JUIN 2007

À LA FACULTÉ DES SCIENCES ET TECHNIQUES DE L'INGÉNIEUR  
Laboratoire d'Electromagnétisme et d'Acoustique  
SECTION DE GÉNIE ÉLECTRIQUE ET ÉLECTRONIQUE

ÉCOLE POLYTECHNIQUE FÉDÉRALE DE LAUSANNE

POUR L'OBTENTION DU GRADE DE DOCTEUR ÈS SCIENCES

PAR

Olivier VIDÉMÉ BOSSOU

DEA en génies électrique et des télécommunications, Ecole Nationale Supérieure Polytechnique,  
Université de Yaoundé I, Cameroun  
et de nationalité camerounaise

acceptée sur proposition du jury:

Prof. A. Skrivervik Favre, présidente du jury  
Prof. J. R. Mosig, directeur de thèse  
Prof. A. Azizi, rapporteur  
Dr G. Tejada Guerrero, rapporteur  
Prof. E. Tonye, rapporteur



ÉCOLE POLYTECHNIQUE  
FÉDÉRALE DE LAUSANNE

Lausanne, EPFL

2007



*To Hortense, Firmin, Jordan, Audrey and Irène.*





# Table of Contents

Table of Contents	v
Abstract	ix
Résumé	xiii
Acknowledgements	xvii
Introduction	1
<b>I SYSTEM OF TELECOMMUNICATION</b>	<b>9</b>
<b>1 STATE OF THE ART</b>	<b>11</b>
1.1 Affordable satellite communication systems . . . . .	11
1.1.1 INMARSAT system of telecommunications . . . . .	11
1.1.2 GLOBALSTAR system of telecommunications . . . . .	13
1.1.3 IRIDIUM system of telecommunications . . . . .	16
1.1.4 THURAYA system of telecommunications . . . . .	18
1.1.5 Worldspace system of telecommunications . . . . .	19
1.1.6 Choice of the satellite system of telecommunications . . . . .	21
1.1.7 Block design of the complete receiver . . . . .	23
1.2 State of the art for microstrip antennas . . . . .	26
1.3 State of the art for the LNA . . . . .	30
1.4 Conclusion . . . . .	31
<b>2 WOOD CHARACTERIZATION</b>	<b>33</b>
2.1 Introduction . . . . .	33
2.2 Techniques available to measure the permittivity ( $\epsilon_r$ ) and the permeability ( $\mu_r$ ) . . . . .	34
2.2.1 Microwave cavity . . . . .	34
2.2.2 Microwave ring resonator . . . . .	36
2.2.3 Microwave open resonator . . . . .	37
2.2.4 Microwave waveguide . . . . .	39
2.2.5 Final choice of techniques . . . . .	40
2.3 Theoretical bases for the microwave waveguide technique . . . . .	41
2.3.1 S parameters . . . . .	41

2.3.2	Calculation of the permittivity and of the permeability . . . . .	43
2.3.3	Fundamental relations for anisotropic media . . . . .	47
2.4	Preparation of the wood samples . . . . .	48
2.5	Measurements . . . . .	49
2.5.1	Measurement errors . . . . .	51
2.5.2	Measurement parameters . . . . .	51
2.5.3	Confirmation of the measurements with an open resonator . . . . .	51
2.6	Selection of the species of wood . . . . .	53
2.7	AYOUS WOOD . . . . .	54
2.7.1	Characteristics . . . . .	55
2.7.2	Modelling of Ayous . . . . .	65
2.8	BALSA WOOD . . . . .	67
2.8.1	Characteristics . . . . .	67
2.8.2	Measurement results . . . . .	70
2.8.3	Confirmation of measurements using the Open Resonator . . . . .	76
2.8.4	Modelling of Balsa . . . . .	79
2.9	BUBINGA WOOD . . . . .	80
2.9.1	Characteristics . . . . .	80
2.9.2	Measurement results . . . . .	82
2.9.3	Confirmation of measurements using the Open Resonator . . . . .	85
2.9.4	Modelling of Bubinga . . . . .	87
2.10	DIBETOU WOOD . . . . .	88
2.10.1	Characteristics . . . . .	88
2.10.2	Measurement results . . . . .	90
2.10.3	Confirmation of measurements by using the Open Resonator . . . . .	93
2.10.4	Modelling of Dibetou . . . . .	95
2.11	MBEY WOOD . . . . .	96
2.11.1	Introduction . . . . .	96
2.11.2	Measurement results . . . . .	96
2.11.3	Confirmation of measurements using the Open Resonator . . . . .	99
2.11.4	Modelling of Mbey . . . . .	101
2.12	DIELECTRIC LOSSES VERSUS DENSITY OF THE WOOD . . . . .	102
2.13	CONCLUSION . . . . .	104
<b>3</b>	<b>THE ALUMINIUM-WOOD ANTENNA</b> . . . . .	<b>107</b>
3.1	INTRODUCTION . . . . .	107
3.2	CHOICE OF THE TECHNOLOGY . . . . .	108
3.2.1	Wood - aluminium assembly . . . . .	108
3.2.2	SSFIP antenna type . . . . .	109
3.3	COMPARATIVE STUDY OF ANTENNAS . . . . .	110
3.3.1	Standard SSFIP antenna . . . . .	111
3.3.2	Wood (Balsa) SSFIP antenna . . . . .	112
3.3.3	Balsa antenna . . . . .	114
3.3.4	Ayous antenna . . . . .	114
3.3.5	Ayous - Balsa antenna . . . . .	116
3.3.6	Comparative study . . . . .	118
3.4	LINEARLY POLARIZED ANTENNA . . . . .	120
3.4.1	Balsa antenna . . . . .	120
3.4.2	Ayous-Balsa antenna . . . . .	128
3.4.3	Conclusion . . . . .	131
3.5	CIRCULARLY POLARIZED ANTENNA . . . . .	131
3.6	CONCLUSION . . . . .	136

<b>4</b>	<b>RF FRONT-END</b>	<b>139</b>
4.1	Introduction . . . . .	139
4.2	Simplified strategy for the LNA . . . . .	140
4.2.1	Linear characterization of low noise amplifiers [50]-[51] . . . . .	141
4.2.2	Realization of a low noise amplifier at 1.478 GHz . . . . .	147
4.3	Worldspace satellite receiver system (LNA+Antenna) . . . . .	156
4.4	Conclusion . . . . .	162
<b>II</b>	<b>REMOTE COURSE</b>	<b>163</b>
<b>5</b>	<b>REMOTE COURSE ON ANTENNA TEACHING</b>	<b>165</b>
5.1	Introduction . . . . .	165
5.2	On mathematical developments and programming structures . . . . .	168
5.3	e-Antenna web site . . . . .	168
5.3.1	Functional description of the web site . . . . .	170
5.3.2	Description of the files . . . . .	171
5.3.3	Description of the simulation . . . . .	174
5.4	Some examples of available simulations . . . . .	178
5.4.1	Currents in wire antennas with a TL model . . . . .	181
5.4.2	Method of moments . . . . .	185
5.4.3	Antenna characteristics graphical representation . . . . .	203
5.5	Conclusion . . . . .	206
<b>6</b>	<b>CONCLUSION AND PERSPECTIVES</b>	<b>207</b>
	<b>Bibliography</b>	<b>213</b>
	<b>Curriculum Vitae</b>	<b>219</b>
	<b>Publications</b>	<b>221</b>



# Abstract

For the universities of the emergent countries, and those of Cameroon in particular, the fight to reach a durable development requires to know the needed scientific and technical information for their development, how to get it and to spread it out among partners in the country. Obviously, the complete answer to these preoccupations lies well beyond the framework of this project, but a projection, partial but highly significant, can nevertheless be obtained if one concentrates one's efforts on a specific technological field : in the present study, we shall treat of antennas for telecommunications systems. This subject is highly suitable as example and potential incubator for future achievements.

The ultimate goal is to design and carry out the fabrication of a system of satellite communications adapted to the financial resources and to the development needs of the universities of the South. First of all, we will review the state of the art in satellite communication systems, both for already operating ones and also for new systems, still under development. Then we will determine which system of satellite telecommunications has a receiver and communication fees with affordable costs : our choice will be made on Worldspace satellite system, which was actually designed for developing countries. We will also review the status of planar antenna and low noise amplifier technology, and then explicit the basic challenge involved in our thesis project.

One of the aims of this project is to use local wood as dielectric in SSFIP type antennas. Before using a material as dielectric in an antenna design, it must be characterized. Before carrying the characterization of local wood species, we will begin by reviewing some commonly used dielectric measurement techniques. Then we will carry out a series of measurements to characterize the species of wood growing in the Cameroonian forest. At the

---

end of the series of measurements and according to the dielectric losses observed, we will select the species of wood best suited to make a good substrate for a microstrip antenna.

Next, we will design, manufacture and test low cost antennas. These antennas must satisfy not only technical criteria compatible with those of the telecommunications system chosen but, even most importantly, it must meet socioeconomic criteria : the antennas must be manufactured with low cost and locally available materials, making use of simple technological processes. Once we have found the wood species that exhibits the lowest dielectric losses, we will simulate, and then manufacture the SSFIP type antenna with wood as substrate and aluminium as conducting element. Then we will measure its characteristics and check whether they are compatible with those of a Worldspace receiver.

The signal received from the satellite by the antenna is very weak. It will be important to strengthen the received signal with a low noise amplifier (LNA) before connecting the antenna to the receiver. Thus the antenna and the LNA constitute an active antenna and form what we call here the radiofrequency (RF) front-end. We will design, manufacture and measure the LNA characteristics. A simple manufacturing process must be used to realize these antennas, because later on they must be manufactured locally in Cameroon : this is a determining challenge to ensure the economic independence, which is essential in our thesis project. Afterwards we will join the LNA to the planar antenna and connect the active antenna obtained in this manner to a commercial Worldspace receiver. Finally, we will perform receiving tests of the Worldspace radio station with the system designed.

In parallel, our project includes a second goal, which presents an equivalent significance. We will use existing Matlab codes to develop an online course to teach antenna theory. In addition, at the end of the project and when the Cameroonian local manufacture would have started, we will put all algorithms used for the antenna design on the web site in a multi-media applet, together with a complete documentation of all the manufacturing technologies used. The courses that already exist in Lausanne and Yaounde, relating to the description of other types of antennas will be added, thus leading to a complete teachware that would ensure the durability and the dissemination of the results obtained, and would provide an invaluable tool for teaching and training.

---

**Key words** : Wood characterization, Planar antenna with wood as substrate, Low noise amplifier, Satellite reception system, e-Learning.





# Résumé

Pour les universités des pays émergents, et pour celles du Cameroun en particulier, la lutte pour accéder à un développement durable nécessite la connaissance des sources d'information scientifique nécessaires à leur développement, comment y accéder et ensuite les diffuser parmi les partenaires du pays. La réponse globale à ces préoccupations dépasse bien évidemment le cadre de ce projet, mais une avancée, partielle mais hautement significative, peut néanmoins être obtenue si l'on se concentre sur un domaine technologique spécifique : dans la présente thèse, les antennes pour systèmes de télécommunication. Ce thème est susceptible de servir d'exemple et d'incubateur pour des réalisations futures à long terme.

Le but ultime du projet est de concevoir et de réaliser un système de communication par satellite adapté aux ressources financières et aux besoins de développement des universités du Sud. Dans un premier temps, nous ferons l'état de l'art des systèmes actuelles de télécommunication par satellite qui sont déjà opérationnels ou qui sont en cours de développement. Puis nous déterminerons le système de télécommunication par satellite ayant un coût abordable pour ses équipements de réception : notre choix se portera sur le système de télécommunication par satellite Worldspace, qui a été conçu à l'origine pour les pays émergents. Nous ferons ensuite l'état de l'art des antennes planes et des amplificateurs à faible bruit et nous expliquerons les défis auxquels nous aurons à faire face dans notre projet de thèse.

Un des objectifs de ce projet est d'utiliser le bois que l'on trouve localement au Cameroun comme diélectrique dans une antenne de type SSFIP. L'utilisation de tout matériau

---

comme diélectrique dans la conception d'une antenne plane nécessite au préalable de connaître ses caractéristiques. Avant de commencer la caractérisation proprement dite, nous ferons d'abord l'état de l'art des techniques de mesure couramment utilisées pour la caractérisation des diélectriques. Ensuite nous effectuerons une campagne de mesures pour caractériser des essences de bois disponibles dans la forêt camerounaise. A l'issue de la campagne de mesures, et en fonction des pertes diélectriques observées, nous allons sélectionner les essences les plus susceptibles de jouer le rôle de substrat d'une antenne plane.

Dans un deuxième temps, nous allons concevoir, puis fabriquer et tester des antennes à faibles coûts de revient. Celles-ci doivent satisfaire non seulement des critères techniques compatibles avec ceux du système de télécommunications choisi, mais surtout des critères socioéconomiques : elles doivent pouvoir être fabriquées avec des matériaux de prix abordables, disponibles localement, et en suivant des processus technologiques simples. Lorsque nous aurons choisi l'essence de bois ayant les plus faibles pertes diélectriques, nous allons simuler, puis réaliser une antenne plane de type SSFIP, avec des substrats en bois et des plaques métalliques en aluminium. Nous allons ensuite mesurer ses caractéristiques et contrôler si elles sont compatibles avec celles d'un récepteur Worldspace.

Le signal reçu d'un satellite par une antenne est très faible. Cette situation nécessite une pré-amplification de ce signal à l'aide d'un amplificateur faible bruit (LNA) avant de relier l'antenne au récepteur. L'antenne et le LNA constitueront ainsi une antenne active et formeront ce que nous appellerons ici le "RF front-end". Nous allons associer à l'antenne conçue précédemment cet amplificateur à faible bruit et faire des tests de réception des signaux satellites Worldspace. Cette antenne sera mise au point à l'aide d'un processus de fabrication simple, car la fabrication locale camerounaise de ces antennes présente un défi déterminant pour l'indépendance économique qu'entend promouvoir la conduite de notre projet de thèse. Après nous allons relier l'antenne active ainsi obtenue à un récepteur commercial de Worldspace. Enfin, nous effectuerons des tests de réception des stations radio par satellite de Worldspace avec le système de réception conçu.

En parallèle, notre projet poursuit un second but, d'importance équivalente. Nous ferons usage des codes Matlab existants pour mettre au point un cours en ligne pour

---

enseigner la théorie des antennes. En plus, à la fin du projet et quand la fabrication locale camerounaise aura débuté, nous mettrons tous les algorithmes ayant servi à la conception de ces antennes sous forme de logiciels et d'applets multimédia sur un même site Web, avec une documentation complète des technologies de fabrication. Les cours qui existent déjà à Lausanne et à Yaoundé, relatif à la description d'autres types d'antennes, viendront s'y ajouter, aboutissant ainsi à un didacticiel complet qui assurerait la durabilité et la dissémination des résultats obtenus, et fournirait un outil précieux pour l'enseignement et la formation.

**Mots-clés** : Caractérisation du matériau bois, Antenne plane avec substrat en bois, Amplificateur faible bruit, Système de réception par satellite, e-Learning.



# Acknowledgements

The work presented in this thesis has been carried out with the support and the help of many people.

The first and main acknowledgement goes to Prof. Juan R. Mosig who has given to me the opportunity to perform this work and has made my dream reality. I would like to thank him for his many suggestions and constant support during this research. During my stay in LEMA I have learned a lot especially from a technical viewpoint.

I thank Prof. Tonye Emmanuel for his constant support and for his large contribution to the success of this cooperation project.

I express my gratitude to the members of the jury for accepting to be part of the jury of this thesis and for the useful remarks and interesting discussions held during the exam.

I would also like to thank Jean-François Zürcher for his precious help and collaboration for the development of the wood antennas.

To all the members of the lab : I have enjoyed working with you during my stay in LEMA. Thanks to Anja for taking time to respond to some of my questions. Thanks to Michael for finding time to help me and for valuable comments and suggestions in the revision of the manuscript of my thesis. Thanks to Ivica and Katarina for doing the last revision of my thesis. Thanks to Rainer Koss who learned me Latex, for the experience exchange during the antenna exercises and for the pleasant moments we spent together. Thanks to Sebastien, our system manager, for his contribution in putting online the antenna course. Thanks to Frédéric Bongard for nice moments when we shared the office. Thanks to Ivica, Pedro, Katarina, Juliane, Sergio, Grégoire, Gabriela, Laleh, Roberto, Francesco for technical, social and cultural discussion and pleasant moments we had together. Thanks

---

to acoustics group for their collaboration and the unforgettable moment we spent together. Thanks to Alix and Eulalia for the atmosphere created in the lab.

I would like to thank the printed circuit board and mechanical workshop members for their patience of machining aluminium sheets and wood samples.

I would like to thank Fred and Irene Gardiol for taking me as their child and contributing to make my life more easier in Lausanne. Thanks to Fred Gardiol for valuable comments and suggestions in the revision of the manuscript of my thesis and for taking time to put the manuscript of my thesis into "good English".

I had the pleasure of meeting Penth  r  az Commune resident. They are wonderful people and I am thankful to the way that I was received and that I lived there. My thanks go to Mayor, Roachat and Maccaud families.

My thanks also go to Ma  ro Simon for making at my disposal species of wood and their characteristics. Thanks to Ecam-Placage (Cameroon) for the furniture of Ayous plating especially to Otavio Spotti, Youkessou Roger and Mbia Bene Guy.

I would like to thank the European action COST 284 which supported a collaboration between LEMA and IMST in Germany for measurements on wood antennas. Thanks to Matthias, Patrice and Martin from IMST Germany for their significant contribution to my thesis work.

I thank also JAST (Switzerland) for their contribution in the amplifier design especially Stefano, Ferdinando and Saugy.

I thank "Agence Universitaire de la Francophonie" (AUF) for their grant.

I would also express all my gratitude to EPFL-DDC Cooperation because without their financing this thesis would not be. I want to thank especially Prof. Jean Claude Bolay, Yuri Changkakoti and all the members of the Cooperation unit.

Of course, I am grateful to my parents for their patience and love and to all my family.

I want to thank all those whose name is not mentioned here for all what they have done for the completion of my thesis.

# Introduction

## Context and objectives

This thesis is the result of a collaboration undertaken between the Laboratory of ElectroMagnetism and Acoustics (LEMA) of the Ecole Polytechnique Fédérale de Lausanne (EPFL) in Switzerland and the Electronic and Signal Processing Laboratory (LETS) of the University of Yaounde I in Cameroon. The joint effort was made possible by the financial support provided by EPFL and the Swiss Agency for Development and Cooperation (SDC). The main object of the thesis relates to wireless communication and in particular to satellite telecommunications.

With rich oil resources and favorable agricultural conditions, Cameroon has a wonderful primary commodity economy and potential for growth. Its political stability is a favorable climate for business enterprise. The development of the oil sector led to rapid economic growth between 1970 and 1985. The growth came to an abrupt halt in 1986, precipitated by steep declines in the prices of major exports: petroleum, coffee, and cocoa. Nowadays, the whole country is engaged in a wonderful economic growth rate of 5% per year. Various International Monetary Fund (IMF) and World Bank programs were enacted to support the economic policy of the government. Since 1990, the government has embarked on various IMF and World Bank programs designed to support business investment, increase efficiency in agriculture, improve trade, and recapitalize the nation's banks.

Cameroon's economy is dominated by the tertiary sector, which accounts for 41% to gross domestic product (GDP), followed by the primary sector, 35% and the industrial sector, 24% [1].

Cameroon has a rich and diversified commodity-based economy. Agriculture was the

---

sole engine of growth and foreign-exchange earnings until the late 1970s when oil became the primary engine of growth.

Food and export crops, livestock, fishing and forestry are the mainstay of the economy, accounting for about 29% of GDP, employing some 50% of the active population, and generating more than half of total export earnings. The petroleum and manufacturing sectors represent 20% of GDP. The oil sector accounts for less than 5% of GDP but contributes 35% of government revenue and export receipts. The secondary sector contributes 31% of GDP and employs 15% of the population [2]. The tertiary sector is dominated by commerce, restoration and hotel (47% of tertiary GDP), followed by merchant services other than financial, banking and insurance services. Transports, warehousing and communications are the fourth component of the tertiary sector (14.5%), coming just after merchant services of public administrations (16.5%).

In most developing countries in general and in Cameroon in particular, a growing proportion of workers are devoted to the tertiary sector. In Cameroon communications equipments are all imported. The aim of our project, which is linked with telecommunication systems, is to reduce the importation of these equipments by manufacturing locally antennas using local materials and local labor forces. This will create job and hence reduce the poverty.

Cameroon is also the most important market in the Communauté Economique et Monétaire de l'Afrique Centrale (CEMAC), accounting for nearly half of the GDP.

Nowadays, as all the current projects point out, commercial, institutional and governmental satellites will play an increasing role, by broadcasting information towards regions lacking cable or optical fiber connections. This could be particularly relevant for Africa and for many other rural regions of the world. A receiver for this type of satellite communication typically includes a fairly standard electric part, but also a more specific radiofrequency (RF) front-end (usually consisting of a low noise microwave amplifier and an antenna). This RF front-end provides the "air interface" part of the system, which links directly to electromagnetic (EM) waves and must be tailored to fit the environment reception conditions.



---

The main goal of this thesis has been to investigate the feasibility of an inexpensive RF-system, based essentially on the use of local materials, in order to reduce the technological dependence of emerging countries. Obviously, one cannot avoid the use of some commercial electronic components fabricated elsewhere. However, these are now low-cost items, available everywhere without restrictions. It is rather the design of the receiver system, built up with these basic components, that gives an edge, imposing a high (and frequently unfair) price to all those who lack the technical expertise. A similar situation is encountered at the antenna level. Usually the materials needed for a proper operation of the antenna (low loss dielectrics like Teflon or Kapton, printed copper sheets in thin film technology) are too sophisticated to be manufactured by local workshops in emerging countries. This thesis provides an alternate way, by designing and building antennas based entirely on local materials and unsophisticated technology. In parallel to these efforts, the matter of the information contents has also been addressed. A satellite communication system will essentially broadcast commercial or governmental radio and TV channels. But it can also be used to access Internet and email services, and then to set up small local communication networks for specific communities such as Universities. For instance, teaching material and e-courses can easily be made available from a web-based system at the University of Yaounde. A rich potential does exist for these courses, together with an already proven previous expertise [64].

This project has also provided an opportunity to put together, on an equal basis, the resources available on this matter at LEMA and LETS. The final result is a series of simple teaching supports that can be broadcast without special requirements in terms of bit-rate, bandwidth or data transmission speed. These small pieces of software have been successfully tested at EPFL, mostly within the course "Rayonnement et Antennes" taught to third year Electrical and Electronics (EE) students at the end of Bachelor cycle. They form now a basic staple of this course. These softwares form the main part of an existing antenna course, which can be provided to any student duly registered in a participant university that can receive the satellite broadcasts.

Thus, this thesis is formed by two seemingly dissimilar topics (low cost RF front-end

---

and teaching software) that are here grouped together by the need of addressing the same social target.

### **The specific situation in emergent countries**

For the universities of emergent countries, and those of Cameroon in particular, the fight to achieve a sustainable development requires an answer to the following fundamental questions :

1. Which sources of scientific and technical information should one use in priority ?
2. How can one obtain the relevant scientific information ?
3. Once obtained, how can one diffuse this information among partners within the country ?

Obviously, an exhaustive answer to these questions is well beyond the scope of our thesis project, but nevertheless a projection, partial but highly significant, can at least be obtained while concentrating on a specific technological field : antennas for systems of telecommunications. This subject is well adapted to serve as an example and to provide an incubator to evolve future developments for the long term.

The ultimate goal is to conceive and to carry out the construction of a system of communication via satellite, adapted to the development needs of universities in the South, and thus guaranteeing to answer the third question raised above. In a first stage, we will design, manufacture and test antennas. These antennas must not merely satisfy technical criteria but also, especially, socio-economic criteria : they must be manufactured with indigenous materials, locally available, and following simple technological processes. For example, locally manufacturing Cameroonian antennas sets a determining challenge for economic independence that this project intends to face. Also, the possibility of combining the system with integrated solar cells, which would provide clean autonomous power, would guarantee environmental safeguarding.

As previously mentioned, our project pursues in parallel a second goal of equivalent importance : the development of a web-based antenna course to ensure the durability and

---

the spreading of results obtained. This would provide an invaluable tool for teaching and training.

The steadily increasing number of students, the obsolescence of equipment and the deterioration of the quality of teaching are driving the university authorities of the South to look for sustainable and not too expensive solutions, that would allow them to provide high quality teaching. Two problems arise in African universities in general-and in Cameroonian ones in particular when reaching and/or spreading out information :

- Lightning fast evolution of technologies, which make Internet and wireless communications the principal channels of information flow;
- Recurring costs of subscription fees for the telecommunication operators.

The goals of our thesis project, which aims to mitigate these two problems are :

1. To design low-cost antennas, built with local materials and making use of local manufacturing facilities : this represents a scientific challenge of capital importance. In addition, this approach opens the way to the electromagnetic characterization of various species of wood material available in great quantity in Cameroon, and hopefully to the setting of local industries;
2. To design a web-based antenna course, in order to enhance the relevance and the quality of university teaching;
3. To develop an inter-university system of communication, less expensive than present ones, adapted to the needs for endogenous development for universities in the South, thanks to the realization of receiving satellite micro-stations.

### **Organization of the thesis**

The first chapter of this thesis reviews the state of the art in satellite communication systems, both for already operating ones and also for systems presently under development. The emphasis will be placed here on the cost of the communication equipment because our main objective is to provide Southern countries with an affordable communication tool.

---

Based on these two criteria, one of the telecommunications systems will be selected. This chapter will also review the state of the art of planar antennas and low noise amplifier technology, and then will explicit the basic challenge involved in our thesis project.

The second chapter is devoted to know whether high-tech microwave substrates can be replaced by something as widely available as wood. The quality of wood as a microwave printed antenna substrate will be defined by the complex permittivity and permeability parameters. Before we carry out these measurement, we will begin by reviewing some dielectric measurement techniques commonly used. Among all these measurement techniques we will use at least two available ones in our laboratory. The first one will be considered as reference with the second one used to confirm and to check some critical results. We will measure the characteristics of five species of wood, and will focus especially on the dielectric constant and the losses. After the evaluation of the loss tangent, the woods that can best be used as dielectric substrates will be selected.

In the third chapter we will manufacture a well known type of planar antenna, SSFIP (Strip-Slot-Foam-Inverted-Patch) antenna, and will replace the high-tech microwave substrates by wood substrate and the conducting elements by aluminium. We will progressively go from SSFIP antenna to aluminium-wood antenna using the selected species of wood from the previous chapter and the least expensive way to assemble them. Then, measurements will be carried out for the different manufactured antennas to quantify the quality loss with respect to the reference SSFIP antenna. After this we will select the wood antennas that can be connected to a satellite receiver.

The fourth chapter will review some concepts and calculations relative to low noise amplifiers (LNAs). These amplifiers are essential companions of the antenna in any RF front-end. Then an LNA will be designed, manufactured and its characteristics will be measured to verify the validity of the simulation. Afterwards the LNA will be integrated with the planar antenna, the assembly thus becoming an active antenna, which can be connected to a commercial Worldspace receiver. Finally, receiving tests of the Worldspace radio station will be conducted with the complete system.

The fifth chapter will present a remote course for the teaching of antenna theory, to

---

provide contents and to test the developed transmission system, providing an invaluable tool for teaching and training. Some of the simulations will be illustrated, to allow for a better understanding of the proposed philosophy.

The last chapter will conclude the work done during this thesis project and will highlights some perspectives for future endeavours.



**Part I**

**SYSTEM OF  
TELECOMMUNICATION**





# Chapter 1

## STATE OF THE ART

In this chapter, we will review the state of the art in satellite communication systems, both for already operating ones and also for new systems, still under development. The emphasis will be placed here on the cost of the communication equipment, and also on the communication fees, because our main objective is to provide Southern countries with a low cost communication tool. These two criteria will determine our choice of a system. We will also review the status of planar antenna and low noise amplifier technology, and then explicit the basic challenge involved in our thesis project.

### 1.1 Affordable satellite communication systems

#### 1.1.1 INMARSAT system of telecommunications

Inmarsat [3] (stands for International Maritime Satellite organization) is a commercial system of telecommunications. It comprises 9 active satellites (FIGURE 1.1), with an additional 5 spares, and it provides telephony, data, telex and fax services, carried out with the support of 37 ground stations. It provides an almost global coverage of the terrestrial sphere (FIGURE 1.2).

Inmarsat possesses a large experience in the design and operation of satellite communication networks. It is internationally recognized and keeps introducing new technologies

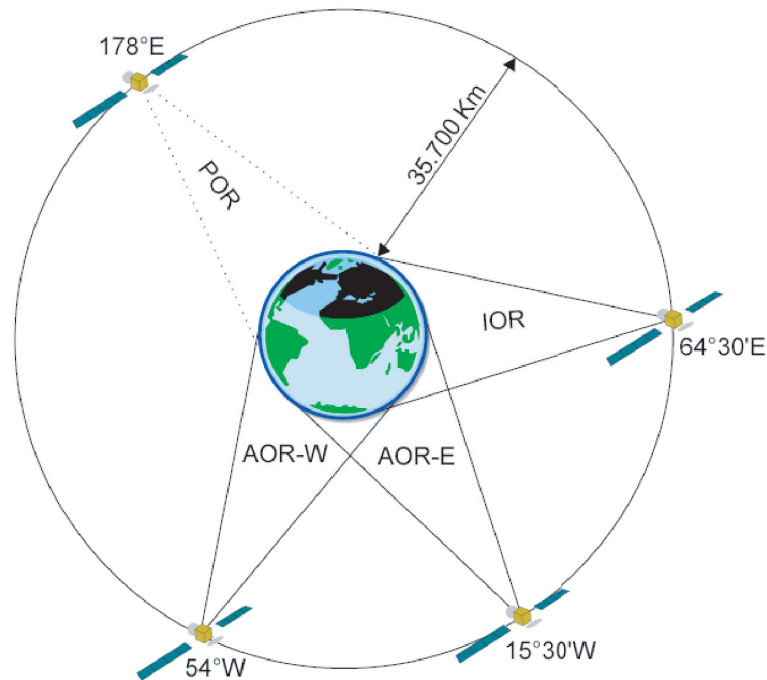


FIGURE 1.1: INMARSAT Satellite Constellation

that upgrade the standard of the industry. It offers a complete portfolio of mobile voice and data services, reaching almost anywhere on the planet, whether on land, on sea or in the air. Its customers include major corporations from the maritime, media, oil and gas, building and aeronautical industries, as well as governments and aid agencies. All these customers have a common need for mobile communications in places where the local network is unreliable or simply does not exist. They rely on Inmarsat to provide mission-critical mobile connectivity and its services are a trusted and integral part of their global operations. Land-based customers already enjoy the benefits of their Broadband Global Area Network service - BGAN - which offers global voice and high-speed data connectivity via terminals of the size of a laptop. It operates in the L band between 1.5 and 1.6 GHz. TABLE 1.1 provides a summary of BGAN receivers [4]. Within sight of the characteristics and prices, our choice would go to the model BGAN-AddValue. But the price of \$ 2,095 remains quite high, as far as the objectives stated at the beginning of our project are concerned.

## 1.1. AFFORDABLE SATELLITE COMMUNICATION SYSTEMS

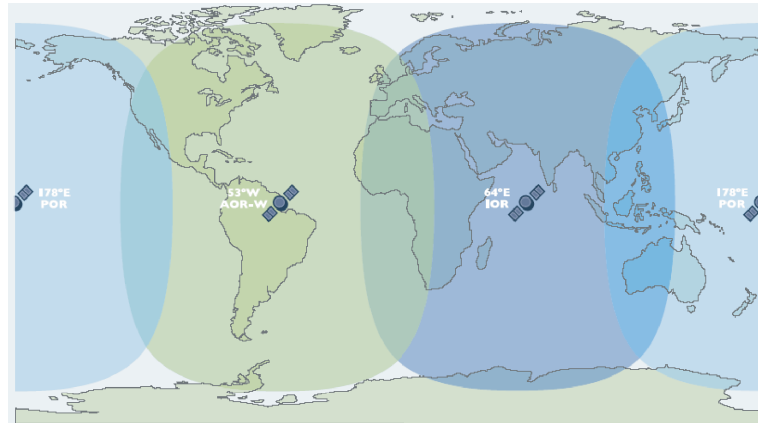


FIGURE 1.2: INMARSAT Cover Zone

### 1.1.2 GLOBALSTAR system of telecommunications

Globalstar [5] provides low cost, dependable high quality satellite voice and data services across North America, and to more than 120 countries worldwide (FIGURE 1.3). When a business is located on a remote worksite, and must operate somewhere beyond the realm of cellular and traditional landline service, Globalstar provides a means to meet the requirements for reliable and low cost communications.

Mobile and fixed units offer voice and data services that meet the needs of business and recreational users. Globalstar data services help deliver information from remote areas, where key business or operational data are collected, saving time and money for countless companies.

Globalstar voice and data customers include businesses that operate in areas where landline service is not available, and where cellular coverage is poor or non-existent. Natural resource companies, long-haul transportation operators, commercial fishermen, government employees, recreational and travel enterprises, geologists, prospectors and public safety organizations all value Globalstar products and services.

Globalstar is a low Earth orbit satellite constellation (FIGURE 1.4) for telephone and low-speed data communications. Globalstar satellites are simple "bent pipe" repeaters without any inter-satellite link. A network of gateway ground stations connects the 48

## CHAPTER 1. STATE OF THE ART

---

TABLE 1.1: BGAN Terminals

	R-BGAN	AddValue	Nera Satcom	Thrane and Thrane	HNS
<b>Terminal's dimension</b>	300 x 240 mm	210 x 140 mm	200 x 140 mm	300 x 200 mm	365 x 275 mm
<b>Weight (kg)</b>	1,8 kg	1,25 kg <	1 kg	1,3 kg	2,5 kg
<b>Sending rate</b>	144 kbit/s	384 kbit/s	384 kbit/s	464 kbit/s	492 kbit/s
<b>Reception rate</b>	144 kbit/s	240 kbit/s	240 kbit/s	448 kbit/s	492 kbit/s
<b>Guaranteed rate</b>	No	32, 64 kbit/s	32, 64 kbit/s	32, 64, 128 kbit/s	32, 64, 128, 256 kbit/s
<b>Connection options</b>	USB, Bluetooth, Ethernet	USB, Bluetooth, (voice/data), RJ11	USB, Bluetooth, (voice/data), RJ45	USB, Bluetooth, (voice/data), RJ11, Ethernet	USB, Bluetooth, WiFi 802.11b hub, RJ45, ISDN 64Kbps
<b>Compatible operating systems</b>	Windows 2000, Windows XP	Windows 2000, Windows XP, Mac OS 10.2, and Linux higher version	Windows 2000, Windows XP, Mac OS 10.2, and Linux higher version	Windows 2000, Windows XP, Mac OS 10.2, and Linux higher version	Windows 2000, Windows XP, Mac OS 10.2, and Linux higher version
<b>Index of protection (dust and moisture)</b>	IP 54	IP 44	IP 44	IP 54	IP 55
<b>Customer applications</b>	Office automation	Voice, Office automation	Voice, Office automation	Voice, Office automation, Heavy file transfer, Acquisition and diffusion of videos, Encrypted traffic	Voice, Office automation, Heavy file transfer, On line videos diffusion, Videoconference, Encrypted traffic
<b>User profile</b>	help solution, Data only, Regional activity	Professional use, help solution use	User in a company, Requirement for professional temporary mobility	User in a company, Workstation, ISDN network connections, Sensible applications	Multi-user environment, Intensive use
<b>Suggested uses</b>	SME, Finance, Supply chain	NGO, Oil industry, Telephony and local Internet	NGO, Oil industry, Mining, Government, BTP	Media, Government	Media, Government, Oil industry, Mining, BTP
<b>Price</b>	\$ 699	\$ 2,095	\$ 2,300	\$ 3,165	\$ 2,950

## 1.1. AFFORDABLE SATELLITE COMMUNICATION SYSTEMS

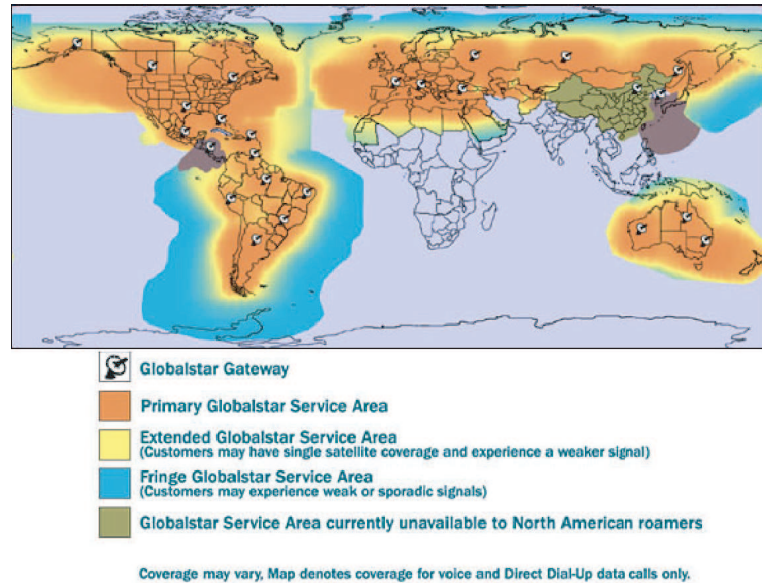


FIGURE 1.3: GLOBALSTAR Cover Zone

satellites to the public switched telephone network; users are assigned phone numbers on the North American Numbering Plan, or on the appropriate phone numbering plan for the country in which the overseas gateway is located. Since satellites are not directly linked to one another, a satellite must always be on the line-of-site of a gateway station to provide service to its customers.

Globalstar utilizes a version of Code Division Multiple Access (CDMA) technology, based upon the IS-95 CDMA standard, to provide high quality, digitally crisp voice, data, and fax services. This standard utilizes digital transmission methods, in which users share time and frequency allocations, and are assigned uniquely defined codes.

In view of all the above considerations, the Globalstar system is very appealing for the kind of project we plan to develop in this thesis. Unfortunately, at the present time, the Globalstar range does not cover Africa. Since our mid-term goal is to demonstrate the feasibility of our approach for Cameroon, we are forced to disregard this option.



FIGURE 1.4: GLOBALSTAR Satellite Constellation

### 1.1.3 IRIDIUM system of telecommunications

The Iridium [6] satellite constellation (FIGURE 1.5) is a system of 66 active communication satellites and spares in orbits around the Earth. The system was originally designed to have 77 active satellites, and as such was named after the element iridium, of atomic number 77. The original name was retained, even though the number of active satellites is smaller than originally planned. Iridium allows for worldwide voice and data communications using handheld devices. The Iridium network is unique in that it covers the whole Earth, including the poles, oceans, and airways, however the use of this service is forbidden in North Korea, Iran, Libya and Sudan, due to American embargoes.

The IRIDIUM system is a satellite-based Personal Communication Services (PCS) or Mobile Satellite Services (MSS) system, which supports global, wireless digital communications. IRIDIUM provides voice, messaging and data services to mobile subscribers using handheld user terminals.

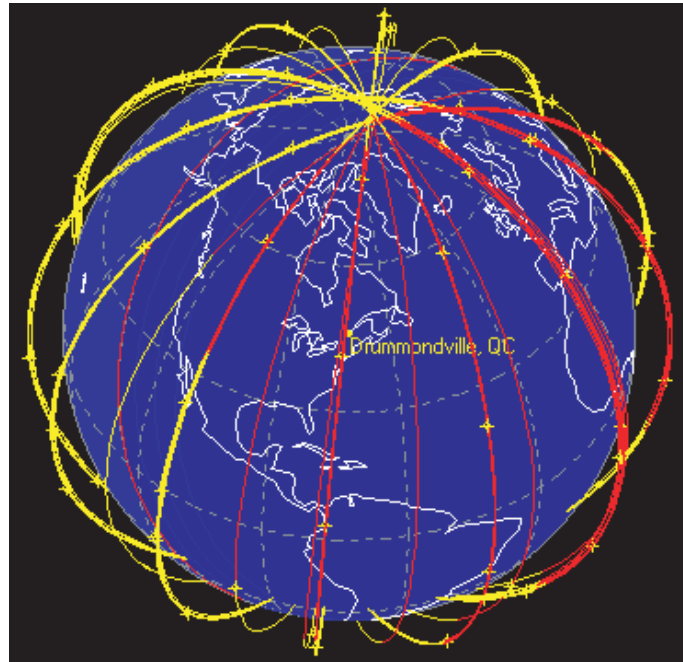


FIGURE 1.5: IRIDIUM Satellite Constellation

Iridium Satellite LLC (Limited Liability Corporation) launched commercial global satellite communications services with enhanced products (TABLE 1.2) and services. Service enhancements include improved voice quality and simplified pricing plans. Soon after launch, Iridium expanded its service portfolio to include also data services. Iridium Satellite LLC is focused on providing affordable, dependable, long-term global communications.

The design of the Iridium network allows for voice and data to be routed virtually anywhere in the world. Voice and data calls are relayed from one satellite to another until they reach the satellite above the Iridium Subscriber Unit (handset) and the signal is relayed back to Earth.

The satellites are on near-polar orbits at an altitude of 780 km. They circle the Earth once every 100 minutes, travelling at a rate of 27,088.5 km per hour. Each satellite is cross-linked to four other satellites; two satellites in the same orbital plane and two in adjacent planes.

TABLE 1.2: MOTOROLA Portable Satellite Phone [7]

Name	Price
9500	\$ 799.99
9505	\$ 1,395



FIGURE 1.6: THURAYA Cover Zone

### 1.1.4 THURAYA system of telecommunications

The Thuraya satellite system [8] is a provider of regional satellite phones. Through partnership with leading national telecom and mobile communications companies, Thuraya provides blanket coverage (Figure 1.6) to more than 110 countries in Europe, North, Central Africa and large parts of Southern Africa, the Middle East, Central and South Asia. The service operates a single active geostationary communications satellite, with one spare for backup, while a third satellite is planned for launch in 2007. The launch of a similar Far East and Australia service is planned for 2007.

The company is based in the United Arab Emirates and provides service through authorized service providers. Its shareholders are a mixture of Middle Eastern and North African Telcos and investment companies.



## 1.1. AFFORDABLE SATELLITE COMMUNICATION SYSTEMS

---

Thuraya provides the following satellite-based services : voice communications with handheld terminals (Hughes and Ascom) and maritime or land-based fixed terminals, short message service, 9.6 kbit/s Data & Fax service, 144 kbit/s high-speed data services, built-in GPS capability, a number of value-added services, such as news, call back, voicemail, WAP, etc.

Thuraya integrates satellite, Global System for Mobile communications (GSM) and Global Positioning System (GPS), all in the same handset. Each handset offers therefore voice, data, fax, messaging and location determination (GPS).

Thuraya's service is valuable to a wide variety of users : from regional roamers to international travellers, from international transportation fleets to national marine operators, from relief and rescue crews to workers in remote industrial sites.

The ThurayaDSL receiver price is \$ 1,525.00. This price remains quite high, as far as the objectives stated at the beginning of our project are concerned.

### 1.1.5 Worldspace system of telecommunications

The Worldspace system of satellites [9] allows to :

- receive radio transmissions in numerical quality within covered zones;
- access a clean channel for data transmission, thanks to the DATACAST service on the zone covered by the Afristar satellite.

WorldSpace is a digital satellite radio network based in Silver Spring in the USA. WorldSpace satellites are "geostationary", orbiting the globe in fixed positions more than 35 000 kilometers above the equator. The satellite network covers (Figure 1.7) most of Asia and Europe, as well as all of Africa. The company is also licensed to serve South America and Central America, but the services for those regions did not start yet. Many channels are free of advertising, and they are known to carry high quality programs.

Currently, two satellites are in use, AfriStar and AsiaStar, which were successfully launched in October 1998 and in March 2000, respectively. AfriStar serves Africa, Europe, and the Middle East, while AsiaStar serves most of South Asia and overlaps in the

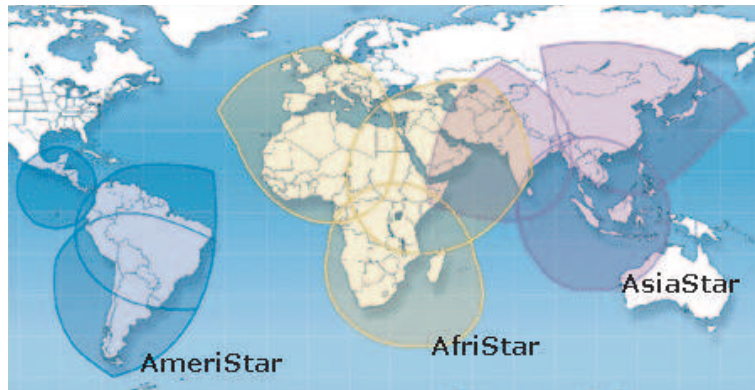


FIGURE 1.7: WORLDSPACE Cover Zone

Middle East. Plans to launch a third satellite, Ameristar, to serve South America were not carried out, because the frequencies used by WorldSpace (L band) are commanded by the United States Air Force. Each satellite provides three transmission beams, which can support 50 channels each, carrying news, music, entertainment, and education, including a computer multimedia service. Using powerful spot beams, the satellites transmit up to three overlapping areas, covering approximately 14 million square kilometers each.

The Worldspace's AfriStar control center is located in Washington, D.C. The WorldSpace Foundation started off with the objective of improving literacy in Africa, and it provided satellite programs to radio stations in small communities of the African continent. The WorldSpace Foundation changed its name to First Voice International. However, the original plan of WorldSpace, to offer low-cost satellite radio services to rural Africa failed, because the receivers were too expensive. As a result, the service provided can only be accessed by expatriates and by the wealthier members of the urban African society. The western beam of the Afristar satellite, ostensibly intended to cover West Africa - but which is also received in most of Western Europe - now carries subscription stations aimed mostly at Europeans.

Despite what has been said Worldspace remains a good candidate for demonstration purpose because simple receivers are available at prices starting at US\$ 100. This also gives us a frame for the "reasonable" prices that should be exhibited by the antenna and RF front-end associated to the full receiver.

## 1.1. AFFORDABLE SATELLITE COMMUNICATION SYSTEMS

---

### 1.1.6 Choice of the satellite system of telecommunications

The satellite systems described here were developed with different goals and objectives. The summary presented in the TABLE 1.3 allows the reader to compare their respective merits and drawbacks, and then to draw his own conclusion.

TABLE 1.3: Summary table

	INMARSAT	GLOBALSTAR	IRIDIUM	THURAYA	WORLDSPACE
<b>Coverage</b>	Global	Spotbeam	Global	Spotbeam	Global
<b>Technology</b>	Digital	Digital	Digital	Digital	Digital
<b>Voice</b>	Yes	Yes	Yes	Yes	No
<b>Fax</b>	Yes	No	No	Yes	No
<b>e-mail</b>	Yes	Yes	Yes	Yes	Yes
<b>Data</b>	Yes	Yes	Yes	Yes	Yes
<b>Telex</b>	Yes	No	No	No	No
<b>Radio</b>	No	No	No	No	Yes
<b>Sim Card</b>	Yes	Yes	Yes	Yes	No
<b>PrePaid Card</b>	Yes	Yes	Yes	Yes	No
<b>Abonnement</b>	No	No	No	No	Yes
<b>Billing</b>	Duration and Volume Based	Duration Based	Duration Based	Duration Based	Volume Based
<b>Receiver Price</b>	\$ 2 095	\$ 1 188.15	\$ 799.99	\$ 1 525	\$ 100

Internet and e-mail services present the greatest interest to us, because they can be used to send and receive data. We notice that all the telecommunication systems listed in the table offer these services. In addition, we must design our antenna and connect it to the least expensive commercial receiver available. A quick look at TABLE 1.3 shows that, when we consider the price only, one receiver stands out all by itself : it is the Worldspace receiver. Its position corresponds to the original vocation of the company, which is to provide direct audio and multi-media broadcasting services by satellite, aimed mainly towards emergent areas in the Middle East, Africa, the Mediterranean basin, Asia, the Caribbean and Latin America, where the choice in the matter of media is often quite limited due to financial

reasons.

The numerical diffusion technology [10] developed for Worldspace is based on the compression technique defined by the international standard ISO MPEG II, layer 3. Satellites operate in the L band (allocated to the service of numerical sound broadcasting by satellite at the World Administrative Radiocommunications Conference in 1992 (CAMR 92)). This technology is different from the Eureka 147 standard developed in Europe.

We plan to test the project in Cameroon, country which is sprinkled over by the western beam of the AfriStar satellite. The characteristics of this satellite, for the reception of which we are going to design our antenna are :

- **Satellite name** : AfriStar;
- **Beam** : West beam;
- **Orbital location** : 21° East;
- **Mode of diffusion** : Numerical;
- **Type of compression** : MPEG 2.5 Layer 3;
- **Polarization** : Circular;
- **Reception band** : L Band;
- **Reception Frequency** : Between 1 452 and 1 492 MHz;
- **West beam frequency [11]** : 1 478 MHz;
- **Sampling Rate (SR)** : 1840 bits/s;
- **Forward Error Correction (FEC)** : 1/2;
- **Type of receiver** : Worldspace;
- **Subscription Global Bouquet only** : 100 € TTC/year;
- **Subscription by receiver** : 20 € HT;

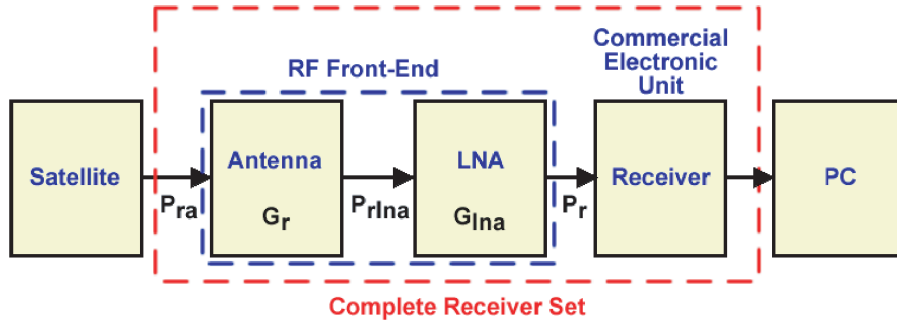


FIGURE 1.8: Worldspace receiving system

- Fees of data transmission per Megabytes (Mo) : 10 € HT;

We notice that, even in terms of subscription and communication fees the Worldspace prices are lower than those of other communication systems. We estimate that these fees could be afforded by the budgets of the Cameroonian universities.

### 1.1.7 Block design of the complete receiver

We will design our communication system for the reception of signals from the Worldspace satellites. Worldspace is a digital broadcaster for audio and multimedia programs, which operates directly from satellites. To decode digital signals from the Worldspace satellite, we need a specifically designed satellite receiver, which functions in conjunction with a suitable antenna. The overall block diagram of the receiver system is shown in FIGURE 1.8. The study that we carried out, while completing our thesis, is mainly focused on the RF front-end of the receiver.

The complete receiver set that transfers the signal received from the satellite to a computer can be considered as the assembly of two parts : a commercial electronic receiver and a RF front-end formed by an antenna and a low noise amplifier (LNA).

After selecting a satellite, we will look at the properties of each block of the reception system. Then we will concentrate on the elements essential to design of our antenna.

Since our interests are mostly e-mails and file transfer, we plan to use the DAMB - A receiver of TONGSHI [12] , which is a low cost receiver designed to transfer directly to a

computer the relevant information broadcasted by the Worldspace site. This means that, to realize an inexpensive reception system, the manufacturing price of our antenna should fall well below US\$ 100.

Here, our work involves the design of the antenna and of the LNA. Cameroon produces and exports wood and aluminium, and therefore we select these indigenous materials to realize our antenna. But before we start to design it, we must find out which species of wood is most likely to play the role of dielectric substrate. In order to choose, we must know the permittivity of the material, and this requires us to carry out a series of measurements on several species of wood that are currently encountered in Cameroon.

By looking at the characteristics of a Worldspace receiver [13] in TABLE 1.4, we see that our antenna can present both a linear or a circular polarization, with at least a gain of 6 dBi. We will first design a linearly polarized antenna which will be used to do all the comparative measurements. Then we will design a circularly polarized antenna in order to confirm that the previous results obtained for linearly polarized antenna are also valid for the antenna with circular polarization. On the other hand, for the LNA we must calculate the necessary gain starting from the Power Flux Density generated by the satellite.

Let us consider the Worldspace geostationary satellite, positioned on a circular orbit at a height  $r = 35\,000$  km above the equator. From that very high position a whole continent is "seen" under a very small angle, and it is therefore necessary to install a very directional antenna on the satellite. The capability of an antenna to concentrate its radiated energy ( $Pt$ ), taking into account a feed loss ( $Lt$ ), in a specified direction can be quantified by the antenna gain ( $Gt$ ). The transmitted power, called Equivalent Isotropic Radiated Power ( $EIRP$ ), is provided by the equation :

$$EIRP = \frac{Pt \times Gt}{Lt} \quad (1.1.1)$$

Let us now consider a sphere of radius  $r$  having its centre at the centre of the radiating antenna. The surface area of this sphere is :

$$A = 4\pi r^2 \quad (1.1.2)$$

The power  $EIRP$  is uniformly distributed across the surface of the sphere, having an

## 1.1. AFFORDABLE SATELLITE COMMUNICATION SYSTEMS

---

TABLE 1.4: Technical Specification for WorldSpace Receiver

<b>Specification</b>	<b>Value</b>
<i>RF frequency range</i>	1452 MHz - 1492 MHz
<i>Active antenna noise temperature T<sub>ant</sub></i>	200 K
<i>Gain(antenna) for Circularly Polarized RF reception</i>	6 dBi
<i>(G/T)(system)</i>	-17 dB/K
<i>Active antenna output level at PFD (Power Flux Density) of -120 dBW/m<sup>2</sup></i>	-88 dBm
<i>Polarization</i>	LHCP (Left Hand Circular Polarization) and RHCP (Right Hand Circular Polarization) or Linear
<i>Minimum Expected WorldSpace Operating signal level for BER (Bit Error Rate) &lt;10<sup>-4</sup></i>	-96 dBm
<i>Minimum Expected WorldSpace RF PFD signal level for BER &lt;10<sup>-4</sup></i>	-120 dBW/m <sup>2</sup>
<i>LNA noise figure</i>	1.8 dB

area  $A$ . We can then define the power flux density, hereafter called  $PFD$ , as the ratio between the power  $EIRP$  crossing the surface of the sphere and its area  $A$  :

$$PFD = \frac{EIRP}{A} \quad (1.1.3)$$

According to the International System measurements the power density is measured in  $W/m^2$ .

The power received by an antenna, whose equivalent area is  $Aeqr$ , located at a distance  $r$  from a transmitting antenna of gain  $Gr$  that is fed by a power  $EIRP$  is :

$$Pra = Aeqr \times PFD \quad (1.1.4)$$

The equivalent area  $Aeqr$  of a receiving antenna of gain  $Gr$  is :

$$Aeqr = \frac{\lambda^2}{4\pi} Gr \quad (1.1.5)$$

Since  $Pr$  and  $Gr$  are given, we can calculate the gain of the Low Noise Amplifier :

$$Glna = \frac{Pr}{Gr \times Pra} \quad (1.1.6)$$

After calculation we obtain :

$$Glna = 14.84 \text{ dB} \quad (1.1.7)$$

Summarizing, these are the parameters that must be satisfied by our design :

1. The antenna must have a gain of 6 dBi;
2. The Low Noise Amplifier must have a gain of 14.84 dB and a noise figure of 1.8 dB.

## 1.2 State of the art for microstrip antennas

Among all the antennas used for satellite communication, which cover the required frequency bands and provide the desired radiation pattern, a printed antenna with a single



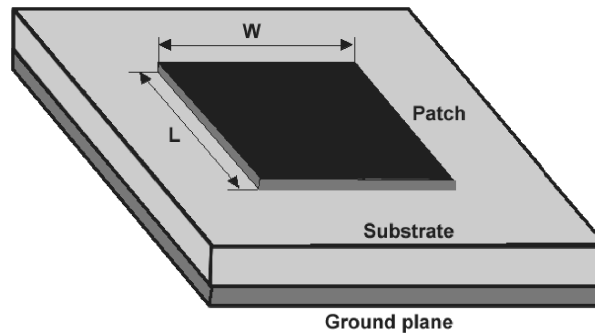


FIGURE 1.9: Microstrip patch antenna

patch appears to be the one that can be realized most easily. Since the 1970s, the international antenna community devoted very large efforts to study of microstrip and printed antennas [15] - [16], both theoretically and experimentally. These antennas offer significant advantages : low profile, compatibility with integrated circuit technology and conformability to shaped or curved surfaces. The driving force for extended studies has been the thirst for low-cost, small-weight, low-profile antennas to fulfill the requirements of modern systems. To achieve low costs, however, one must be able to precisely control the manufacturing process and this, in turn usually demands that the innovative structure selected as prototype can be adequately modelled and characterized mathematically. The results of this research contributed greatly to the success of microstrip antennas, not only for military applications but also in commercial areas such as mobile satellite communications, the direct broadcast satellite (DBS) system, the global positioning system (GPS) and remote sensing.

Printed antennas can be built with a low-cost technology and they should thus be potentially well suited for low-cost consumer applications. Until now, however, designs tended to remain rather expensive, mainly due to high material costs : this drawback limits the use of these antennas. In addition, when compared to traditional antenna structures such as reflectors, horns, slots, or wire antennas, the electrical performance of a basic microstrip antenna or array suffers from other drawbacks, such as narrow bandwidth, large losses in the feed network, large cross polarization and a low power handling capability. These facts must be accounted for in any proper design.

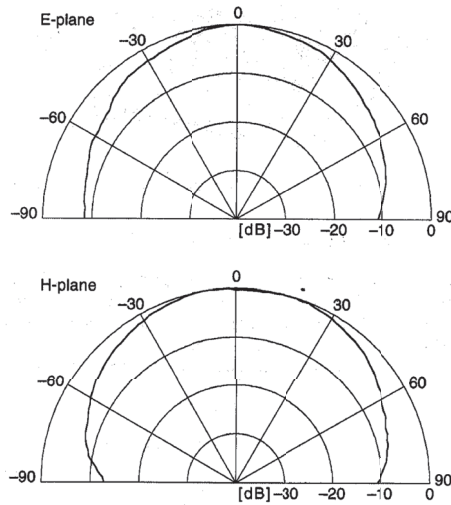


FIGURE 1.10: Measured radiation patterns of a rectangular microstrip patch

A microstrip antenna (FIGURE 1.9) is made of a conducting ground plane, a dielectric substrate and, on top of the substrate, a printed patch, which is the radiating element. The latter can take a variety of shapes : square, rectangle, circle, ring, triangle, ellipse. Excitations for microstrip antennas range from the very simple coaxial probe traversing the ground plane to the strip-slot technique [17]. Since we plan to use aluminium for the radiating patch, we may well have to face the notorious technological problem : connecting aluminium to copper is always difficult and problematic, either by soldering or by welding. Therefore we will use here the SSFIP configuration which is a good compromise between simplicity and performances. With a radiating patch of  $\lambda/2$  size, this kind of microstrip antenna has a gain within the 5-6 dB range, a bandwidth of about 5-10 % and it exhibits a 3 dB beamwidth located somewhere between  $70^\circ$  and  $90^\circ$ . The input impedance can attain the convenient value of  $50 \Omega$  when the position of the feed is properly chosen. Many substrate materials are presently available on the market, providing dielectric constants ranging from 1.17 to about 25, with loss tangents between 0.0001 and 0.004. As an example, the E-plane and H-plane radiation patterns shown in Figure 1.10 were measured for a  $14 \times 9.6$  mm rectangular patch antenna, coaxially excited at 3.6 mm from the center of the patch, on a 0.8 mm thick epoxy substrate (with  $\epsilon_r = 4.3$ ), at its resonant frequency of 4.97 GHz.

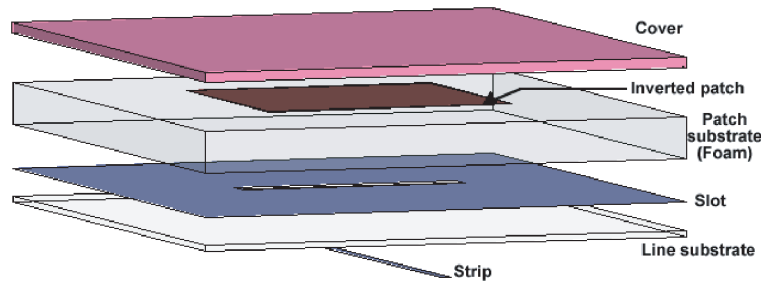


FIGURE 1.11: SSFIP antenna

We plan to use wood and aluminium to manufacture our antenna and determined that the least expensive way to assemble them is by gluing. Since the patch of our antenna will be made out of aluminium, it would be difficult to solder a copper wire feed to an aluminium patch : this can be avoided by feeding the patch through a slot in the ground plane. All these constraints and specifications correspond exactly to the SSFIP antenna geometry. Therefore, we are going to manufacture a SSFIP (FIGURE 1.11) antenna, using wood for the dielectric substrates and aluminium for the patch and the metal connections. Initially we will replace the foam by wood (Balsa). Then we will replace the top layer, which plays the role of protecting cover, by linseed oil. Then we will replace the copper patch by an aluminium patch. Finally we will replace the copper ground plane, in which the slot is cut out, by an aluminium ground plane with a slot having the same size, the dielectric FR4 substrate by wood (Ayouss) and the copper feed line by an aluminium feed line. At the end we will have an antenna only made with wood and aluminium. The system will be assembled by simply gluing the layers with a classical glue of Araldite type.

The SSFIP antenna geometry was found to be particularly tolerant to small changes or errors, both for the geometrical setting as for the material properties. Among its interesting properties, we also notice a frequency band significantly larger than that of other microstrip patch antennas, as well as a slightly larger gain. Our goal will be to build a SSFIP antenna with a maximum of inexpensive materials locally available in Cameroon.

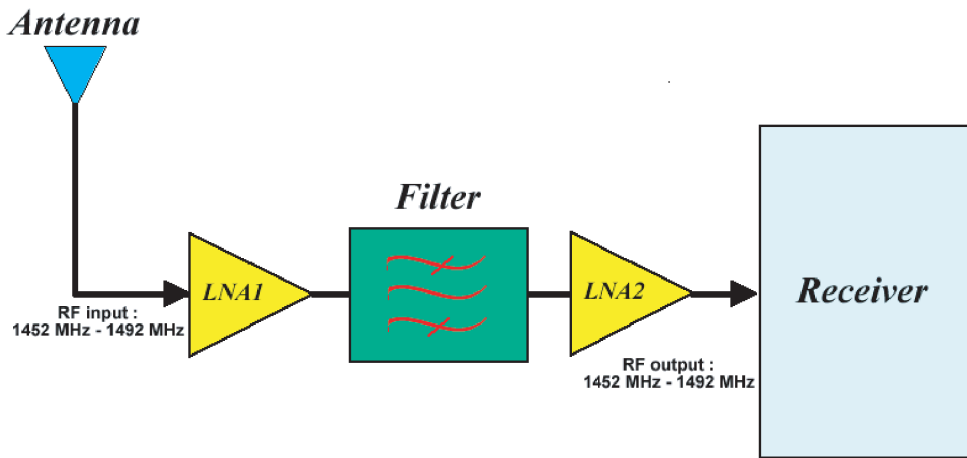


FIGURE 1.12: RF receiver system

### 1.3 State of the art for the LNA

The LNA (Low Noise Amplifier) is a particular kind of microwave amplifier used in communication systems to amplify very weak signals captured by an antenna. Together with the antenna, the LNA is the key piece in the RF front-end of a global receiver defined as the subsystem which processes the signal at the original frequency of the electromagnetic wave (FIGURE 1.12). The LNA is most often located very close to the antenna because this way, the losses in the transmission line feed become less critical. We obtain then an "active antenna" arrangement, which is frequently used in microwave systems like GPS, because long coaxial cable feedlines are very lossy at microwave frequencies.

Placing a LNA next to the antenna reduces the noise of all the subsequent stages by the gain of the LNA, while the noise of the LNA is injected directly into the received signal [51]. Thus, a LNA has to boost the desired signal, while adding as little noise and distortion as possible, to ensure that the signal can be retrieved in the later stages in the system.

Typical receiver front-ends include at least two LNAs separated by a filter (FIGURE 1.12) : the purpose of the first LNA is to strengthen and of the second one is to add power to the signal.

A band-pass filter lets signals with frequencies within a certain range travel across it with little attenuation, but it rejects (or strongly attenuates) signals at frequencies outside of that

range. An ideal filter would have a completely flat passband (e.g. with no gain/attenuation throughout) and would completely cut down signals at all frequencies outside the passband. Additionally, the transition out of the passband should be instantaneous in frequency. In practice however, bandpass filters are never ideal. A real filter does not completely attenuate signals at all frequencies outside the desired frequency range; in particular, over a region just outside the intended passband, signals are attenuated, but not totally rejected. This is known as the filter roll-off, and it is usually expressed in dB of attenuation per octave or decade of frequency.

## 1.4 Conclusion

The objective of this work is to contribute to the development of inexpensive microstations for the reception of satellite signals in emerging countries like Cameroon and its African neighbors. Therefore we have started this chapter with a survey of currently available satellite systems and their associated commercial receivers. The conclusion of this survey have been two-fold. Firstly a satellite system, Worldspace/Afristar emerges as a clear candidate. Secondly an understanding of the receiver organization has led to the decision on which parts should be concerned by this study. On the one hand, it would be naive to seek to replace the basic electronics and integrated chips by a local fabrication. Electronic chips are nowadays easily available standard components where global competition plays actively to keep them at affordable prices. On the other hand, the more specialized parts related to the microwave front-end (antenna and low noise amplifier) are usually more expensive items sold by companies fully using (and sometimes abusing) a monopolistic situation. But precisely with the adequate knowledge and a minimum skill low cost versions of these components can be easily built with local materials and by local workshops. Therefore, we will concentrate in these two components.

After computing the specifications and electric parameters requested for a proper functioning of these components, we have shown through a concise state-of-the-art survey that there is certainly a possibility for designing and fabricating these low cost alternatives for

## CHAPTER 1. STATE OF THE ART

---

both antenna and LNA. Indeed the microwave RF front-end can be reduced to the bare combination of these two items while retaining the essential electrical performances.

All these intuitions will be confirmed in the following chapters of this thesis, where in step by step a fully optional RF front-end will be built based only upon local materials and technologies.

# Chapter 2

## WOOD CHARACTERIZATION

### 2.1 Introduction

As stated in the previous chapter, one of the main goals of this thesis is to find out whether high-tech microwave substrates can be replaced by something as widely available as wood. The suitability of wood as a microwave printed antenna substrate will be determined by the values taken by the complex parameters "permittivity"  $\varepsilon$  and "permeability"  $\mu$  [18]. In particular, the imaginary parts of these complex quantities are related to losses ( $\tan \delta$ ) and must be kept as small as possible to achieve a good design. Following the usual convention [18] we define these quantities with respect to their free space values  $\varepsilon_0$  and  $\mu_0$  and we can then write  $\varepsilon = \varepsilon_0 \varepsilon_r$  and  $\mu = \mu_0 \mu_r$  where  $\varepsilon_r = \varepsilon'_r - j\varepsilon''_r$  and  $\mu_r = \mu'_r - j\mu''_r$ . It is important to note that the choice of sign for time-dependence dictates the sign convention for the imaginary part of permittivity. The signs used here for imaginary parts correspond to those conventionally used in engineering. The dielectric loss tangent is defined as  $\tan \delta = \varepsilon''_r / \varepsilon'_r$  and is the determining factor that will guide us for the choice of the species of wood to use as substrate.

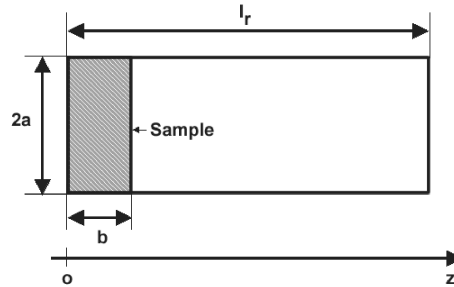


FIGURE 2.1: Dimensions used for  $TE_{01n}$  cavity with dielectric specimen

## 2.2 Techniques available to measure the permittivity ( $\epsilon_r$ ) and the permeability ( $\mu_r$ )

We want to determine the complex values of  $\epsilon_r$  and  $\mu_r$ . Even though we expect wood to be non magnetic and hence to show a relative permeability equal to unity ( $\mu_r' = 1$ ,  $\mu_r'' = 0$ ), we plan to use methods that also provide an estimation of  $\mu_r$ . In this way, we can check the accuracy of the measurements. We also expect "low" values for  $\epsilon_r'$  ( $1 < \epsilon_r' < 3$ ), which will help to increase the bandwidth of printed antennas. Otherwise, when the permittivity becomes too large, spurious surface waves can propagate on the substrate. We would like to obtain a loss tangent ( $\tan \delta$ ) as small as possible. The best technological results are obtained with a dielectric having  $\tan \delta \simeq 10^{-4}$  but a good standard dielectric exhibits  $\tan \delta \simeq 10^{-3}$ . In our case, making use of wood as dielectric, our goal is to obtain at least  $\tan \delta \simeq 10^{-2}$ . Before carrying out actual measurements, however, we will first review the methods commonly used to measure permittivity [19].

### 2.2.1 Microwave cavity

The basic techniques used to measure dielectric samples in microwave cavities are well documented in the literature [20]-[22]. They essentially involve the measurement of the resonant frequency and of the quality factor (Q-factor) of an empty cavity and then, again, the measurement of these parameters with the cavity filled, or partially filled by the dielectric sample under test (FIGURE 2.1). The quality factors are defined as  $Q_U =$  (energy



## 2.2. TECHNIQUES AVAILABLE TO MEASURE THE PERMITTIVITY ( $\epsilon_R$ ) AND THE PERMEABILITY ( $\mu_R$ )

---

stored in cavity) / (energy dissipated in cavity per radian) for an unloaded Q and as  $Q_L =$  (energy stored in cavity) / (energy dissipated in both cavity and external circuit per radian) for a loaded Q. Both rectangular and circular cavities have been used. The  $TE_{01n}$  mode is chosen because it exhibits an interesting property, whereby the attenuation decreases with increasing frequency. Thus very high Q-factors can be achieved at high frequencies : this is an important consideration when measuring low loss dielectrics. A small piece of a bar shaped sample is placed in the position of maximum electric field. The dielectric constant and the loss tangent of the specimen can then be calculated from the changes of resonant frequency and quality factor of the metallic cavity filled at the selected resonant mode. Let the constants  $\beta_1$  refer to the dielectric-filled portion of the cavity extending from  $z = 0$  to  $z = b$ , and  $\beta_0$  refer to air-filled portion of the cavity extending from  $z = b$  to  $z = l_r$ . First we must calculate the value of the constant k, which appears in the expression of the relative permittivity  $\epsilon'_r$ . The solution is given by a Bessel function of the first kind of order one. The condition requires that :

$$J_1(ka) = 0 \tag{2.2.1}$$

where  $2a$  is the height of the cavity. The first root of  $J_1(ka) = 0$  which defines the  $TE_{01n}$  mode is :

$$ka = 3.832 \tag{2.2.2}$$

From the equation (2.2.2) we can easily calculate the value of k. After measuring the resonant frequency and the quality factor of an empty cavity ( $Q_0$ ) and the cavity partially filled by the dielectric ( $Q_d$ ) we can calculate  $\beta_1$  using the equation :

$$\frac{\tan \beta_1 b}{\beta_1} = -\frac{\tan \beta_0 (l_r - b)}{\beta_0} \tag{2.2.3}$$

where :

$$\beta_0 = \omega^2 \mu_0 \epsilon_0 - k^2 \tag{2.2.4}$$

$\omega =$  the angular frequency

Using the equations (2.2.4) and the following :

$$\beta_1 = \omega^2 \mu'_r \mu_0 \varepsilon'_r \varepsilon_0 - k^2 \quad (2.2.5)$$

and knowing that for most dielectric materials  $\mu'_r = 1$ , the relative permittivity  $\varepsilon'_r$  of the specimen is given by :

$$\varepsilon'_r = \frac{\beta_1^2 + k^2}{\beta_0^2 + k^2} \quad (2.2.6)$$

Knowing the relative permittivity and the Q-factors the loss tangent is given by :

$$\tan \delta = \frac{p(2b - s) + (1/\varepsilon'_r)[2(l_r - b) - q]}{p(2b - s)} \left( \frac{1}{Q_d} - \frac{1}{Q_0} \right) \quad (2.2.7)$$

where :

$$p = \frac{\sin^2 \beta_0 (l_r - b)}{\sin^2 \beta_1 b}$$

$$q = \frac{\sin 2\beta_0 (l_r - b)}{\beta_0}$$

$$s = \frac{\sin 2\beta_1 b}{\beta_1}$$

where  $Q_0$  and  $Q_d$  are the values of the quality factor of the air and dielectric filled cavities respectively.

The microwave cavity method has been proved to be the most successful and accurate technique to measure the complex permittivity of low-loss materials. But the accuracy depends critically on the fit of the sample within the cavity.

### 2.2.2 Microwave ring resonator

Microwave microstrip ring resonators (MMRRs) (FIGURE 2.2) have been widely reported as moisture sensors for paper, soil [23], and biomaterial like grains and leaves. MMRRs can also be used to detect the rancidity of oils. MMRRs present many advantages over other kinds of resonators, for instance, there is no end effect as in the case of a straight-line resonator. Since it is a transmission system, the power transmitted at resonance is maximum

## 2.2. TECHNIQUES AVAILABLE TO MEASURE THE PERMITTIVITY ( $\epsilon_R$ ) AND THE PERMEABILITY ( $\mu_R$ )

---

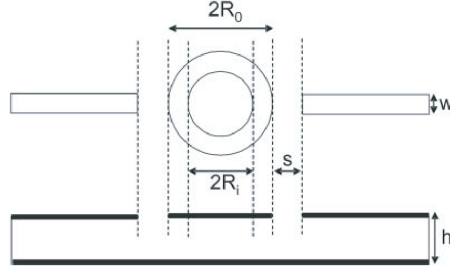


FIGURE 2.2: Ring resonator

(contrary to the rejection filter) and samples can be loaded and unloaded much more easily than in cavity resonators - because the ring uses an open structure. The presence of an abrupt air-dielectric interface in MMRRs excites fringing field components in the air above the structure. The longitudinal components of both electric and magnetic fields correspond to the quasi-TEM mode of the microstrip line. If the material under study is overlaid on top of the MMRR [24], it modifies the effective dielectric constant of the system and, hence, its resonance frequency. The shifts in the effective dielectric constant and in the resonance frequency are linked to the change in the fringing field, and hence depend on the dielectric constant and thickness of the overlay and on the type of overlay. The determination of the dielectric constant of overlaid materials using the MMRRs requires complicated mathematical calculations. The frequency-dependent effective dielectric constant of the system with overlay is calculated using the following expression [24] :

$$\epsilon_{eff,over}(f) = \epsilon_{eff,r} \frac{f_r^2}{f_0^2} \quad (2.2.8)$$

where  $\epsilon_{eff,r}$  and  $f_r$  are the respective effective dielectric constant of the system and the resonant frequency without overlay and  $\epsilon_{eff,over}(f)$  and  $f_0$  are the corresponding quantities with overlay.

### 2.2.3 Microwave open resonator

Various theories and formulations were developed during the past decade to achieve beam conformation inside a Fabry-Perot open cavity. Scalar theory was previously used to develop the Gaussian beam theory for an open resonator. For permittivity measurements,

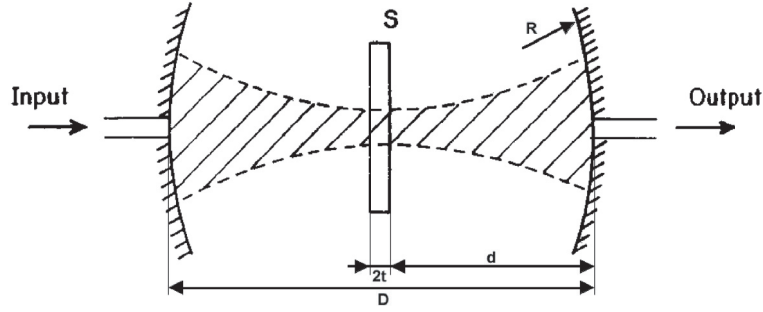


FIGURE 2.3: Fabry-Perot open resonator

the more recently developed vector theory provides a much higher accuracy [19], [25]-[26].

A suitable open-resonator configuration for dielectric measurements is shown in FIGURE 2.3. The spherical mirror resonator has been thoroughly studied and is convenient for flat sheet specimens. Knowing the values of  $D$ ,  $t$  and  $R$  we can measure the resonant frequency  $f_0$  and the quality factor of the open resonator without the dielectric ( $Q_0$ ) and the resonant frequency  $f_L$  and the quality factor of the open resonator with the dielectric in place ( $Q_L$ ). For symmetrical modes, having an antinode of the electric field on the central plane, we can calculate the refractive index  $n$  of the dielectric material with respect to the air by using the equation for resonance :

$$n \tan(nkt - \phi_t) = \cot(kd - \phi_d) \quad (2.2.9)$$

where :

$$\phi_t = \arctan\left(\frac{2t}{nk\omega_0^2}\right) \quad (2.2.10)$$

$$\phi_d = \arctan\left[\frac{2}{k\omega_0^2}\left(d + \frac{t}{n^2}\right)\right] - \arctan\left(\frac{2t}{n^2k\omega_0^2}\right). \quad (2.2.11)$$

$$k = \frac{2\pi}{\lambda} \quad (2.2.12)$$

and

$$\omega_0 = 2\pi f_L \quad (2.2.13)$$

## 2.2. TECHNIQUES AVAILABLE TO MEASURE THE PERMITTIVITY ( $\epsilon_R$ ) AND THE PERMEABILITY ( $\mu_R$ )

---

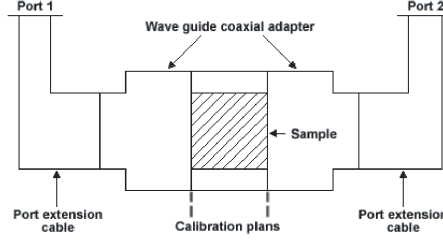


FIGURE 2.4: Microwave waveguide set

Knowing the refractive index of the dielectric material we can easily calculate the relative permittivity  $\epsilon_r$  using the equation :

$$n = \sqrt{\epsilon_r'} \quad (2.2.14)$$

The determination of the loss tangent from the measured Q-factor follows the lines familiar in closed resonator methods. The theory is now quite accurate, and the overall accuracy is at present entirely limited by the accuracy with which the Q-factors can be measured. The relevant formula is :

$$\tan \delta = \frac{1}{Q_\epsilon} \frac{\Delta t + d}{\Delta t + (1/2k) \sin[2(kd - \phi_d)]} \quad (2.2.15)$$

where

$$\Delta = \frac{n^2}{n^2 \sin^2(nkt - \phi_t) + \cos^2(nkt - \phi_t)} \quad (2.2.16)$$

and

$$\frac{1}{Q_\epsilon} = \frac{1}{Q_L} - \frac{1}{Q_0}. \quad (2.2.17)$$

Here  $Q_L$  is the loaded Q-factor when the dielectric is present, and  $Q_0$  is the unloaded Q-factor.

### 2.2.4 Microwave waveguide

The complex permittivity of a number of dielectric materials has also frequently been measured with the waveguide technique [27]-[28]. This technique which is mostly used

## CHAPTER 2. WOOD CHARACTERIZATION

---

for quite lossy materials is based on the measurement of the reflection and transmission coefficients, from which the dielectric or magnetic properties of materials can be extracted. The waveguide method is widely used to measure the permittivity and the permeability of material over a wide range of frequencies, even though this method is less accurate than the cavity technique. It requires a small sample size (for example 22.86 mm x 10.16 mm x 6.95 mm) at microwave frequencies, and the preparation of these samples may be difficult. The sample must be prepared with a regular geometry, with accurately known dimensions. Furthermore, the small sample must be introduced into a waveguide that plays the role of sample holder. The sample sizes allow to cut out a sample in any given direction in the wood. Since we want to measure the anisotropy of the species of wood under test, having samples in all three major directions in the wood will suit our application.

### 2.2.5 Final choice of techniques

Two methods that can be used to measure wood permittivity are available in the laboratory: the waveguide and the open resonator techniques. But these two methods use samples of quite different sizes. The open resonator requires samples of 144 mm x 144 mm, and this wouldn't allow us to machine samples along any direction with the wood that we find in the local Cameroonian market. On the other hand, the waveguide method needs samples of small dimensions, which can be cut along any direction in the commercial Cameroonian wood. Since we are trying to measure the wood anisotropy we need to have wood samples cut along the three axes of coordinates. For this reason, we will consider as reference values the ones obtained with the waveguide measurements, and we will use open resonator measurements to confirm the values measured in the waveguide method. The waveguide method requires to review some microwave circuits theory, which will be done in the next section.

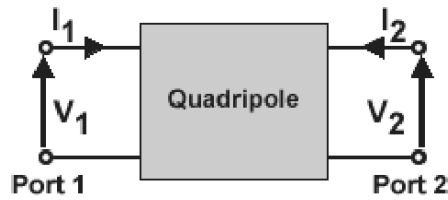


FIGURE 2.5: Quadripole's diagram

## 2.3 Theoretical bases for the microwave waveguide technique

We survey now the basic microwave concepts needed to establish the equations to be used in the microwave waveguide technique. For a rigorous theoretical framework, the reader can consult any standard microwave textbook [29].

### 2.3.1 S parameters

Let us consider the quadripole of FIGURE 2.5. A usual method to determine its functionality and transfer properties is to know its voltage-current transformation matrix (**impedance matrix**) or its current-voltage matrix (**admittance matrix**) summarized by the following equations :

$$\begin{pmatrix} V_1 \\ V_2 \end{pmatrix} = \begin{pmatrix} Z_{11} & Z_{12} \\ Z_{21} & Z_{22} \end{pmatrix} \begin{pmatrix} I_1 \\ I_2 \end{pmatrix} \quad (2.3.1)$$

or

$$\begin{pmatrix} I_1 \\ I_2 \end{pmatrix} = \begin{pmatrix} Y_{11} & Y_{12} \\ Y_{21} & Y_{22} \end{pmatrix} \begin{pmatrix} V_1 \\ V_2 \end{pmatrix} \quad (2.3.2)$$

The knowledge of one of these two matrices defines completely the linear quadripole. To determine the  $Z_{ij}$  and the  $Y_{ij}$  parameters, we must respectively impose conditions of current and of voltage cancellation, i.e. realize either open circuits or short circuits. However above 100 MHz the *open circuit* or the *short-circuit* conditions are difficult, or even sometimes impossible to realize, due to the presence of parasitic capacitances and

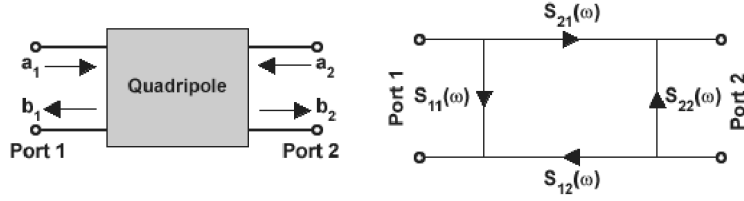


FIGURE 2.6: S Parameters

inductances. Moreover, connecting a short-circuit or an open circuit to a quadripole may create resonances and, in the case of active quadripoles, it may provoke oscillations : at high frequencies, the matrices  $[Z]$  and  $[Y]$  are therefore inadequate. For this reason another kind of matrix has been defined : the scattering matrix  $[S]$ , which is an incident-reflected wave transformation matrix :

$$\begin{pmatrix} b_1 \\ b_2 \end{pmatrix} = \begin{pmatrix} S_{11} & S_{12} \\ S_{21} & S_{22} \end{pmatrix} \begin{pmatrix} a_1 \\ a_2 \end{pmatrix} \quad (2.3.3)$$

where  $a_1$  and  $a_2$  are incident waves and  $b_1$  and  $b_2$  are reflected waves on Ports 1 and 2. These incident and reflected waves are related to voltages and currents by the following equations :

$$a_1 = \frac{V_1 + I_1 Z_c}{2\sqrt{Z_c}} \quad (2.3.4)$$

$$a_2 = \frac{V_2 + I_2 Z_c}{2\sqrt{Z_c}} \quad (2.3.5)$$

$$b_1 = \frac{V_1 - I_1 Z_c}{2\sqrt{Z_c}} \quad (2.3.6)$$

$$b_2 = \frac{V_2 - I_2 Z_c}{2\sqrt{Z_c}} \quad (2.3.7)$$

This representation leads to the new description of the quadripole in FIGURE 2.6.

Consequently if :

- $a_2 = 0$ , this means that the Port 2 (output) of the quadripole is terminated into a matched load, and then we have :

$$S_{11} = \frac{b_1}{a_1} = \text{Input reflection coefficient.}$$



## 2.3. THEORETICAL BASES FOR THE MICROWAVE WAVEGUIDE TECHNIQUE

---

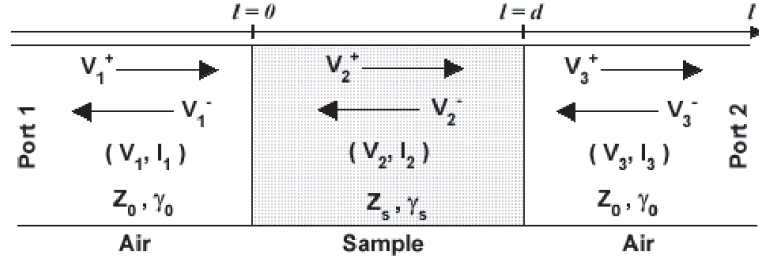


FIGURE 2.7: Waveguide with the device under test diagram

$$S_{21} = \frac{b_2}{a_1} = \text{Input to output transmission coefficient.}$$

- $a_1 = 0$ , this means that the Port 1 (input) of the quadripole is terminated into a matched load, and then we have :

$$S_{22} = \frac{b_2}{a_2} = \text{Output reflection coefficient.}$$

$$S_{12} = \frac{b_1}{a_2} = \text{Output to input transmission coefficient.}$$

### 2.3.2 Calculation of the permittivity and of the permeability

The equations which follow are established by considering the diagram of FIGURE 2.7. The output of the quadripole is terminated into a perfectly matched load : in this case  $a_2 = 0$ . Now we can apply standard transmission line theory [29] to the waveguide sections of FIGURE 2.7.

According to what precedes, we obtain the following equations :

1.  $l \leq 0$

$$V_1 = V_1^+ e^{-j\gamma_0 l} + V_1^- e^{j\gamma_0 l} \quad (2.3.8)$$

$$I_1 = \frac{1}{Z_0} (V_1^+ e^{-j\gamma_0 l} - V_1^- e^{j\gamma_0 l}) \quad (2.3.9)$$

2.  $0 \leq l \leq d$

$$V_2 = V_2^+ e^{-j\gamma_s l} + V_2^- e^{j\gamma_s l} \quad (2.3.10)$$

## CHAPTER 2. WOOD CHARACTERIZATION

---

$$I_2 = \frac{1}{Z_s} (V_2^+ e^{-j\gamma_s l} - V_2^- e^{j\gamma_s l}) \quad (2.3.11)$$

3.  $l \geq d$

$$V_3 = V_3^+ e^{-j\gamma_0(l-d)} \quad (2.3.12)$$

$$I_1 = \frac{1}{Z_0} (V_3^+ e^{-j\gamma_0(l-d)}) \quad (2.3.13)$$

The boundary conditions related to the configuration of FIGURE 2.7 are :

1.  $l = 0$

$$V_1 = V_2 \quad (2.3.14)$$

$$I_1 = I_2 \quad (2.3.15)$$

2.  $l = d$

$$V_2 = V_3 \quad (2.3.16)$$

$$I_2 = I_3 \quad (2.3.17)$$

Writing the equations (2.3.8) - (2.3.13) at the two interfaces between the three media we obtain :

1.  $l = 0$

$$V_1 = V_1^+ + V_1^- \quad (2.3.18)$$

$$I_1 = \frac{1}{Z_0} (V_1^+ - V_1^-) \quad (2.3.19)$$

$$V_2 = V_2^+ + V_2^- \quad (2.3.20)$$

$$I_2 = \frac{1}{Z_s} (V_2^+ - V_2^-) \quad (2.3.21)$$

## 2.3. THEORETICAL BASES FOR THE MICROWAVE WAVEGUIDE TECHNIQUE

---

2.  $l = d$

$$V_2 = V_2^+ e^{-j\gamma_s d} + V_2^- e^{j\gamma_s d} \quad (2.3.22)$$

$$I_2 = \frac{1}{Z_s} (V_2^+ e^{-j\gamma_s d} - V_2^- e^{j\gamma_s d}) \quad (2.3.23)$$

$$V_3 = V_3^+ \quad (2.3.24)$$

$$I_1 = \frac{V_3^+}{Z_0} \quad (2.3.25)$$

However, taking into account the boundary conditions, we have :

$$V_2^+ + V_2^- = V_1^+ + V_1^- \quad (2.3.26)$$

$$V_2^+ - V_2^- = \frac{Z_s}{Z_0} (V_1^+ - V_1^-) \quad (2.3.27)$$

$$V_3^+ = V_2^+ e^{-j\gamma_s d} + V_2^- e^{j\gamma_s d} \quad (2.3.28)$$

$$\frac{Z_s}{Z_0} V_3^+ = V_2^+ e^{-j\gamma_s d} - V_2^- e^{j\gamma_s d} \quad (2.3.29)$$

By summing and subtracting (2.3.26) and (2.3.27), we obtain :

$$V_2^+ = \frac{V_1^+}{2} \left[ 1 + \frac{V_1^-}{V_1^+} + \frac{Z_s}{Z_0} \left( 1 - \frac{V_1^-}{V_1^+} \right) \right] \quad (2.3.30)$$

$$V_2^- = \frac{V_1^+}{2} \left[ 1 + \frac{V_1^-}{V_1^+} - \frac{Z_s}{Z_0} \left( 1 - \frac{V_1^-}{V_1^+} \right) \right] \quad (2.3.31)$$

By replacing the expressions of  $V_2^+$  and  $V_2^-$  in the equations (2.3.28) and (2.3.29) we get :

$$S_{21}(\omega) = \frac{1}{2} \left[ S_{11}(\omega) \left( T(1-K) + \frac{1}{T}(1+K) \right) + T(1+K) + \frac{1}{T}(1-K) \right] \quad (2.3.32)$$

$$K \cdot S_{21}(\omega) = \frac{1}{2} \left[ S_{11}(\omega) \left( T(1-K) - \frac{1}{T}(1+K) \right) + T(1+K) - \frac{1}{T}(1-K) \right] \quad (2.3.33)$$

with :

$$S_{11}(\omega) = \frac{V_1^-}{V_1^+}$$

$$S_{21}(\omega) = \frac{V_3^+}{V_1^+}$$

## CHAPTER 2. WOOD CHARACTERIZATION

---

$$T = e^{-j\gamma_s d}$$

$$K = \frac{Z_s}{Z_0}$$

From (2.3.32) and (2.3.33) we can determine the expression of  $S_{11}(\omega)$  :

$$S_{11}(\omega) = \frac{(T^2 - 1)(1 - K^2)}{(1 + K)^2 - T^2(1 - K)^2} \quad (2.3.34)$$

Knowing that :

$$\Gamma = \frac{Z_s - Z_0}{Z_s + Z_0} = \frac{K - 1}{K + 1} \quad (2.3.35)$$

we easily deduce the final expression of  $S_{11}(\omega)$  :

$$S_{11}(\omega) = \frac{(1 - T^2)\Gamma}{1 - T^2\Gamma^2} \quad (2.3.36)$$

By replacing  $S_{11}(\omega)$  by its expression (2.3.32) we find :

$$S_{21}(\omega) = \frac{(1 - \Gamma^2)T}{1 - T^2\Gamma^2} \quad (2.3.37)$$

Once the values of  $S_{11}(\omega)$  and  $S_{21}(\omega)$  will have been measured, the expressions (2.3.36) and (2.3.37) allow us to calculate  $\Gamma$  and  $T$  :

$$\Gamma = k \pm \sqrt{k^2 - 1} \quad (2.3.38)$$

$$T = \frac{S_{11}(\omega) + S_{21}(\omega) - \Gamma}{1 - [S_{11}(\omega) + S_{21}(\omega)]\Gamma} \quad (2.3.39)$$

with :

$$k = \frac{S_{11}^2(\omega) - S_{21}^2(\omega) + 1}{2S_{11}(\omega)} \quad (2.3.40)$$

Knowing that :

$$\Gamma = \frac{\sqrt{\frac{\mu_r}{\varepsilon_r}} - 1}{\sqrt{\frac{\mu_r}{\varepsilon_r}} + 1} \quad (2.3.41)$$

$$T = e^{-j\omega\sqrt{\mu\varepsilon}d} = e^{-j\frac{\omega}{c}\sqrt{\mu_r\varepsilon_r}d} \quad (2.3.42)$$

## 2.3. THEORETICAL BASES FOR THE MICROWAVE WAVEGUIDE TECHNIQUE

---

we can easily calculate  $\mu_r$  and  $\varepsilon_r$  :

$$\mu_r = \sqrt{x \cdot y} \quad (2.3.43)$$

$$\varepsilon_r = \sqrt{\frac{y}{x}} \quad (2.3.44)$$

with :

$$x = \frac{\mu_r}{\varepsilon_r} = \left( \frac{1 + \Gamma}{1 - \Gamma} \right)^2 \quad (2.3.45)$$

$$y = \mu_r \varepsilon_r = - \left[ \frac{C}{\omega d} \ln \left( \frac{1}{T} \right) \right]^2 \quad (2.3.46)$$

In short, we measured the values of  $S_{11}$  and  $S_{21}$ . From these two measured values we calculated  $\Gamma$  and  $T$ . Knowing the values of  $C$ ,  $\omega$ ,  $d$  and the expressions of  $\Gamma$  and  $T$  we calculated  $x$  and  $y$ . These two values allowed us to calculate the values of  $\varepsilon_r$  and  $\mu_r$ .

### 2.3.3 Fundamental relations for anisotropic media

Since wood is an anisotropic medium, according to standard EM theory, the permittivity must become a 3x3 (tensor or dyadic) matrix :

$$\bar{\varepsilon} = \begin{bmatrix} \bar{\varepsilon}_{xx} & \bar{\varepsilon}_{xy} & \bar{\varepsilon}_{xz} \\ \bar{\varepsilon}_{yx} & \bar{\varepsilon}_{yy} & \bar{\varepsilon}_{yz} \\ \bar{\varepsilon}_{zx} & \bar{\varepsilon}_{zy} & \bar{\varepsilon}_{zz} \end{bmatrix} \quad (2.3.47)$$

For real anisotropic dielectrics, it can be shown that the matrix  $\bar{\varepsilon}$  is symmetric [30], so that  $\bar{\varepsilon}_{ij} = \bar{\varepsilon}_{ji}$ . A particularly interesting transformation of the coordinate system is then possible, because every symmetrical tensor of rank two can be transformed, by rotation of the coordinate system to a diagonal form. Thus for a particular set (O,x,y,z) of coordinates in a given medium the matrix  $\bar{\varepsilon}$  takes the form :

$$\bar{\varepsilon} = \begin{bmatrix} \bar{\varepsilon}_{xx} & 0 & 0 \\ 0 & \bar{\varepsilon}_{yy} & 0 \\ 0 & 0 & \bar{\varepsilon}_{zz} \end{bmatrix} \quad (2.3.48)$$

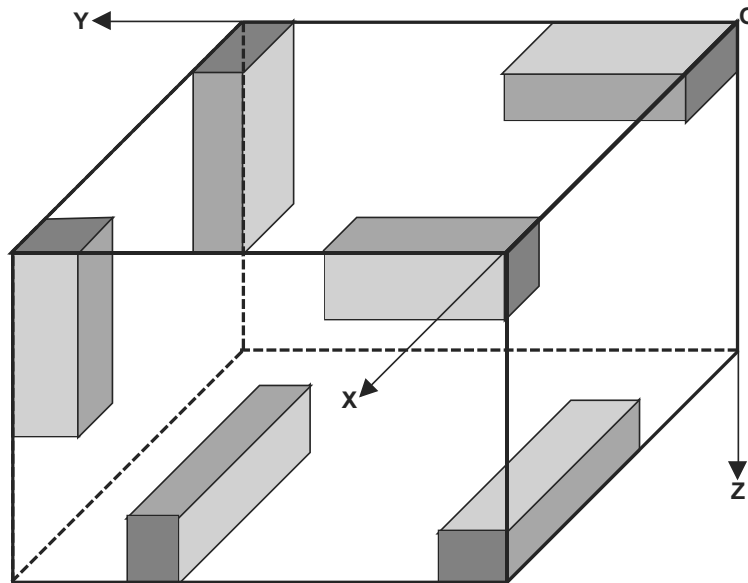


FIGURE 2.8: Directions along which samples are cut

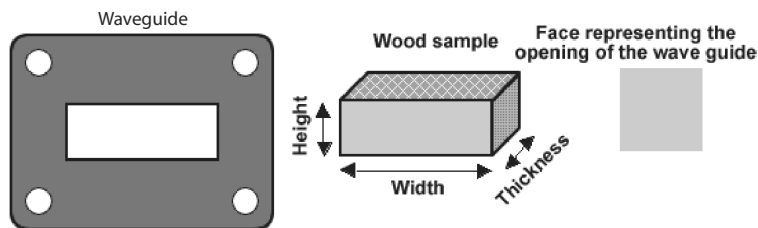


FIGURE 2.9: Sample location in waveguide

The axes of this particular coordinate system  $(O,x,y,z)$  are said to be the *principal axes* of the medium. They correspond to "natural" directions of the medium (for instance to fiber direction in wood). Therefore, our wood samples should be prepared according to these principal axes.

## 2.4 Preparation of the wood samples

The samples were cut in the wood pieces according to the three principal axes (FIGURE 2.8)  $(ox)$ ,  $(oy)$ ,  $(oz)$  and summarized in TABLE 2.1.

The samples were then machined to fit to the dimensions of the X-band waveguide

TABLE 2.1: Directions along which samples are cut

Sample name	Width direction	Height direction	thickness direction
SpeciesLxHyEz	( <i>ox</i> )	( <i>oy</i> )	( <i>oz</i> )
SpeciesLxHzEy	( <i>ox</i> )	( <i>oz</i> )	( <i>oy</i> )
SpeciesLyHzEx	( <i>oy</i> )	( <i>oz</i> )	( <i>ox</i> )
SpeciesLyHxEz	( <i>oy</i> )	( <i>ox</i> )	( <i>oz</i> )
SpeciesLzHxEy	( <i>oz</i> )	( <i>ox</i> )	( <i>oy</i> )
SpeciesLzHyEx	( <i>oz</i> )	( <i>oy</i> )	( <i>ox</i> )

inside which they will be placed (FIGURE 2.9).

*Width of the waveguide* : 22.86 mm

*Height of the waveguide* : 10.16 mm

*Length of the waveguide* : 6.95 mm

## 2.5 Measurements

The network analyzer shown in FIGURE 2.10 allows one to determine the input reflection coefficient and the input to output transmission coefficient by measuring the amplitude and the phase of the incident, reflected and transmitted waves [31]. The measurements of FIGURE 2.11 were made by using a waveguide with the device under test in it.

Measurements were taken in the frequency band from 8.2 GHz to 12.4 GHz. It is one of the lowest range of frequencies for which equipment to measure the permittivity is available in the laboratory. However, the frequency band at which our antenna will function is between 1 GHz and 2 GHz. But since the performances of this type of dielectric tend to degrade with frequency [32], we can consider that measurements between 8.2 GHz and 12.4 GHz provide values in the most unfavorable case.

## CHAPTER 2. WOOD CHARACTERIZATION

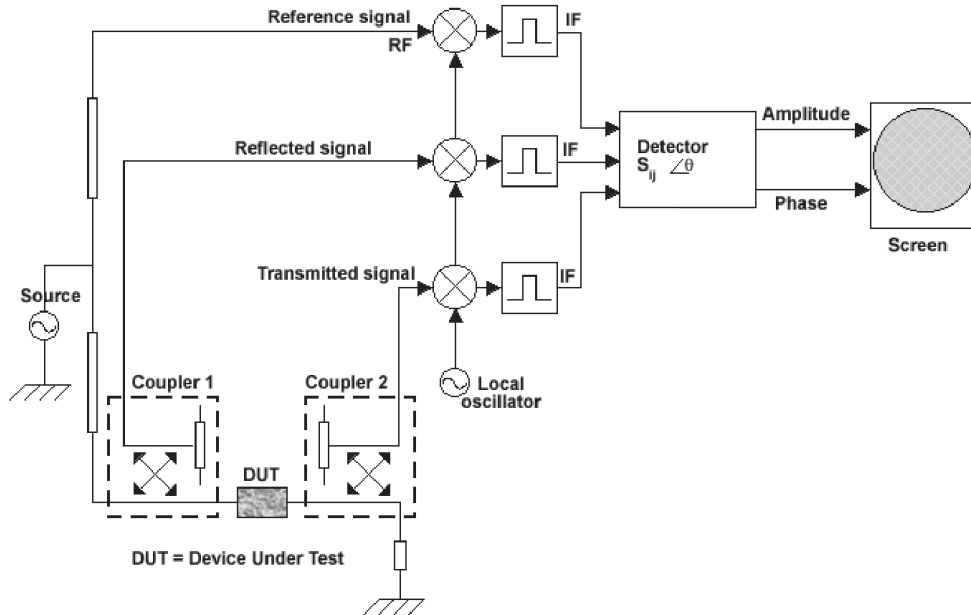


FIGURE 2.10: Simplified block diagram of the network analyzer

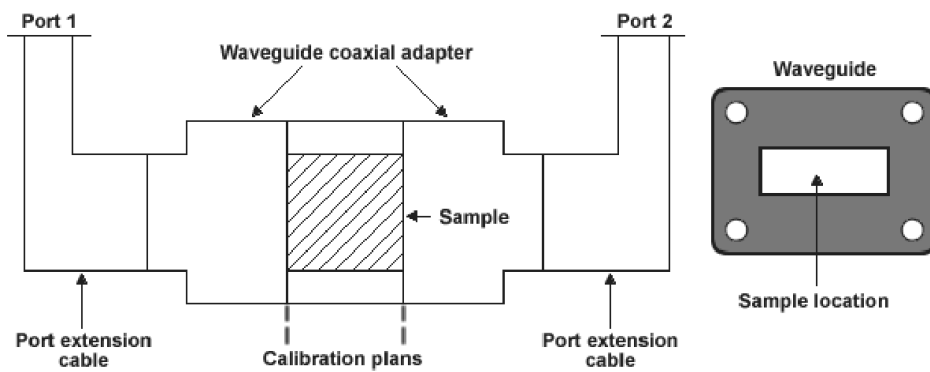


FIGURE 2.11: Assembly diagram



### 2.5.1 Measurement errors

The absolute error (according to the manufacturer) made by measuring using this method is :

$$\Delta\varepsilon'_r = 0.02$$

$$\Delta\varepsilon''_r = 0.02$$

$$\Delta\mu'_r = 0.03$$

$$\Delta\mu''_r = 0.03$$

### 2.5.2 Measurement parameters

*Minimum frequency* : 8.2 GHz

*Maximum frequency* : 12.4 GHz

*Mode* : Waveguide

### 2.5.3 Confirmation of the measurements with an open resonator

The use of an open resonator [33] provides another way to determine the permittivity, which can be used to confirm the values found using the measurements in the waveguide. Measurements can then only be made at the resonant frequencies, which are determined by the system during the calibration. The quality factor is measured at each resonance frequency, and then the system determines the permittivity of the material located in the middle of the Fabry-Perrot resonator.

#### Dimensions of the sample

*Length of sample* : 144 mm

*Width of sample* : 144 mm

*Thickness of sample* : 10 mm

*Length of chamfer* : 20 mm

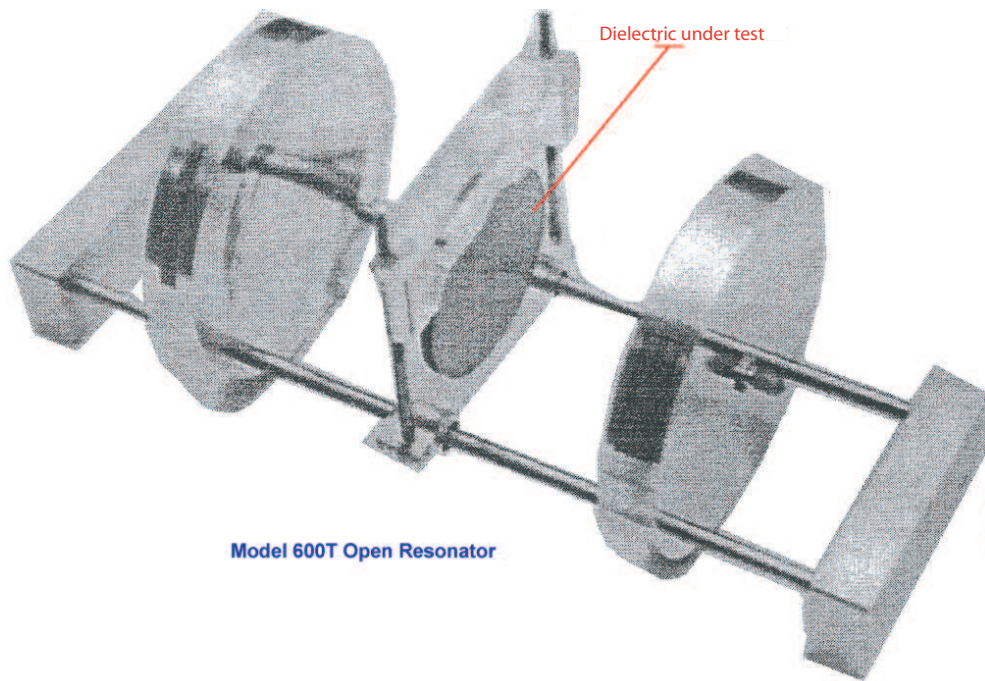


FIGURE 2.12: Open Resonator

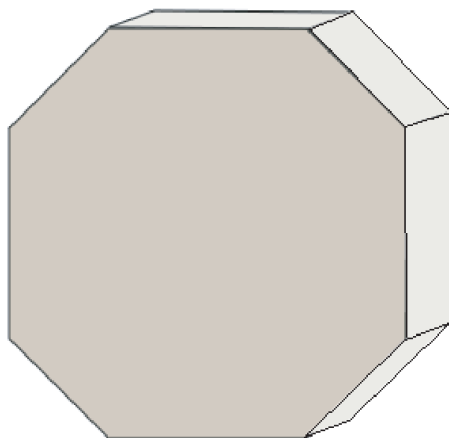


FIGURE 2.13: Wood sample

### 2.6 Selection of the species of wood

As was previously stated, the aim of our project is to manufacture printed antennas using local materials as dielectric substrates. Our thesis work deals with the reception of microwave signals. Since Cameroon produces and exports aluminium and wood, these materials are locally available, so that we will use wood for the dielectric substrates and aluminium for the patches to manufacture our antennas. We would like to use wood from the Central Africa forest as dielectric, but there is apparently no information available on their dielectric characteristics at microwave frequencies. That is why, as pioneers, we must first determine the dielectric characteristics of these wood species at microwaves, which are necessary to design our antenna. We shall carry out a series of measurements on different selected species of wood.

Several researches [34] and measurements were made on wood material [35]. The dielectric properties of wood were measured at microwave frequencies [36] - [38], but for wood species that do not grow in the African forest. For instance, we can find the permittivity of Balsa [39] wood, for a variety that one encounters in Latin America. But we could not find information on the species which one encounters in the African equatorial forest. The characterization of such species is an innovation brought by our thesis work.

The wood samples that we are going to use for these measurements are of dried wood, which one can readily buy in the Cameroonian market place. Since wood is anisotropic, we expect to see that losses increase with the density of the wood. For this reason we will select species of wood, beginning with the wood which has the lowest density among all the wood species indexed in the Cameroon forest.

Our measurements will determine the relative permittivity ( $\epsilon_r$ ) and the relative permeability ( $\mu_r$ ) of wood material. The method of measurement used here allows us to determine the complex permittivity of any dielectric, even when dielectric losses are not negligible ( $\tan(\delta)$ ). The method remains valid when dielectric losses are negligible, but then reliable values are obtained only for  $\epsilon_r'$  while values for  $\epsilon_r''$  are "dubious".

The measurements taken using a Hewlett Packard network analyzer HP8510 and a "PERMES" program developed in LEMA, allow us to simultaneously determine  $\epsilon_r$ ,  $\mu_r$  and

$\tan(\delta)$ .

A special attention must be paid to wood impregnation. Many woods are not suitable for long lasting outdoor operation, and their performances will quickly be downgraded by the attack of moisture and other chemical and biological agents present in tropical areas. Therefore, a surface treatment of the wood, covering or impregnating it with a protective substance (varnish, wax, oil, ...) is of permanent relevance. To be consistent with the overall strategy of this thesis, we have considered linseed oil, which represents a whole class of low-cost protective oils easily available in Cameroon.

The other characteristics of wood quoted in this chapter come from ATIBT [40].

## 2.7 AYOUS WOOD

In this section we will carry out a series of permittivity measurements with the two previously described methods : the waveguide and the Open Resonator measurements. These measurements are required to select the species of wood which will be a good candidate as a dielectric for the antenna we are going to design. The main aim of these measurements is to determine which wood species have a dielectric loss tangent smaller or equal to  $2 \cdot 10^{-2}$  the dielectric loss tangent of FR4 material. Since FR4 is probably the "worst", but still acceptable dielectric used in microwave applications.

We will carry out the same measurements for all the other species of wood in the following sections.



FIGURE 2.14: Ayous wood

### 2.7.1 Characteristics

#### Denomination

<i>Scientific name</i>	: Triplochiton scleroxylon K. Schum
<i>Family</i>	: Sterculiaceae
<i>Origins</i>	: Cameroon, Ivory Coast, Ghana, Equatorial Guinea, Liberia, Nigeria, Republic of Central Africa
<i>Cameroonian local denomination</i>	: Ayous
<i>Other local denominations</i>	: Samba, Obeché, Wawa, Ofa, Aréré

#### Description of sapwood and perfect wood

<i>Description of sapwood</i>	: Not very distinct
<i>Color of perfect wood</i>	: Yellowish white
<i>Line of perfect wood</i>	: Straight
<i>Against-grain of perfect wood</i>	: Slight occasional against-grain
<i>Grain of perfect wood</i>	: Mean to coarse
<i>Duramen characteristic</i>	: Tendency to blueing
<i>Density in a green state</i>	: 570 kg/m <sup>3</sup>

## CHAPTER 2. WOOD CHARACTERIZATION

---

### Physical and mechanical characteristics

<i>Density at 12%</i>	: 330 kg/m <sup>3</sup> ≤ density ≤ 550 kg/m <sup>3</sup>
<i>Total volume withdrawal</i>	: 0.34%
<i>(per moisture percentage in less)</i>	
<i>Total tangential withdrawal</i>	: 5.4%
<i>Total radial withdrawal</i>	: 3.1%
<i>Axial compression at 12%</i>	: 35 MPa
<i>Static inflexion at 12%</i>	: 66 MPa
<i>Elasticity modulus at 12%</i>	: 6,300 MPa
<i>Mushrooms durability</i>	: Non durable
<i>Termites durability</i>	: Sensitive
<i>Vrillette/Lyctus durability</i>	: Sensitive
<i>Impregnability</i>	: Fairly impregnable
<i>Hardness</i>	: Very tender

### Implementation

<i>Sawing</i>	: Easy (use quite sharp tools)
<i>Machining</i>	: Easy (use quite sharp tools)
<i>Nailing</i>	: Easy
<i>Joining</i>	: Good
<i>Completion</i>	: Good (Porage stand-in advised)
<i>Plating</i>	: Unwinding and cutting
<i>Drying</i>	: Easy and fast
<i>Surface treatment</i>	: Is dyed and is varnished well
<i>Uses</i>	: Matches, rods and moulding, plywood, packing-box, skirting, interior wood finishing, movable, lamellate panels, sculpture
<i>Note</i>	: Can cause respiratory disorders

Waveguide measurements

TABLE 2.2: Permittivity values for non-impregnated Ayous (waveguide)

Sample	$\varepsilon_r'$		$\varepsilon_r''$		$\mu_r'$		$\mu_r''$		tan $\delta$	
	$\overline{\varepsilon_r'}$	$\sigma^2$	$\overline{\varepsilon_r''}$	$\sigma^2$	$\overline{\mu_r'}$	$\sigma^2$	$\overline{\mu_r''}$	$\sigma^2$	$\overline{\tan \delta}$	$\sigma^2$
AyousLxHyEz	2.101	9.015 10 <sup>-4</sup>	-0.1903	7.069 10 <sup>-4</sup>	1.059	2.537 10 <sup>-4</sup>	4.715 10 <sup>-3</sup>	7.065 10 <sup>-5</sup>	8.597 10 <sup>-2</sup>	2.853 10 <sup>-5</sup>
AyousLxHzEy	2.080	1.731 10 <sup>-3</sup>	-0.1849	8.078 10 <sup>-4</sup>	1.014	5.555 10 <sup>-5</sup>	-6.577 10 <sup>-3</sup>	5.101 10 <sup>-5</sup>	9.540 10 <sup>-2</sup>	4.361 10 <sup>-5</sup>
AyousLyHxEz	1.743	1.406 10 <sup>-4</sup>	-0.1094	1.270 10 <sup>-6</sup>	1.022	3.022 10 <sup>-6</sup>	7.705 10 <sup>-3</sup>	1.119 10 <sup>-6</sup>	5.523 10 <sup>-2</sup>	2.513 10 <sup>-7</sup>
AyousLyHzEx	1.791	1.330 10 <sup>-4</sup>	-0.0893	3.361 10 <sup>-5</sup>	1.019	5.084 10 <sup>-6</sup>	-5.929 10 <sup>-3</sup>	2.768 10 <sup>-6</sup>	5.567 10 <sup>-2</sup>	3.478 10 <sup>-6</sup>
AyousLzHxEy	1.852	3.794 10 <sup>-4</sup>	-0.1284	1.051 10 <sup>-4</sup>	1.061	2.180 10 <sup>-4</sup>	5.337 10 <sup>-3</sup>	2.212 10 <sup>-5</sup>	6.423 10 <sup>-2</sup>	1.018 10 <sup>-6</sup>
AyousLzHyEx	1.699	3.262 10 <sup>-5</sup>	-0.1298	1.334 10 <sup>-4</sup>	1.056	3.605 10 <sup>-5</sup>	2.181 10 <sup>-2</sup>	3.475 10 <sup>-5</sup>	5.561 10 <sup>-2</sup>	1.245 10 <sup>-6</sup>

With :

- $\overline{\varepsilon_r'}$ ,  $\overline{\varepsilon_r''}$ ,  $\overline{\mu_r'}$ ,  $\overline{\mu_r''}$ ,  $\overline{\tan \delta}$  representing the average values :

$$\overline{X} = \frac{1}{N} \sum_{i=1}^N x_i$$

- $\sigma^2$  representing the variance :

$$\sigma^2 = \frac{1}{N-1} \sum_{i=1}^N (x_i - \overline{X})^2$$

## CHAPTER 2. WOOD CHARACTERIZATION

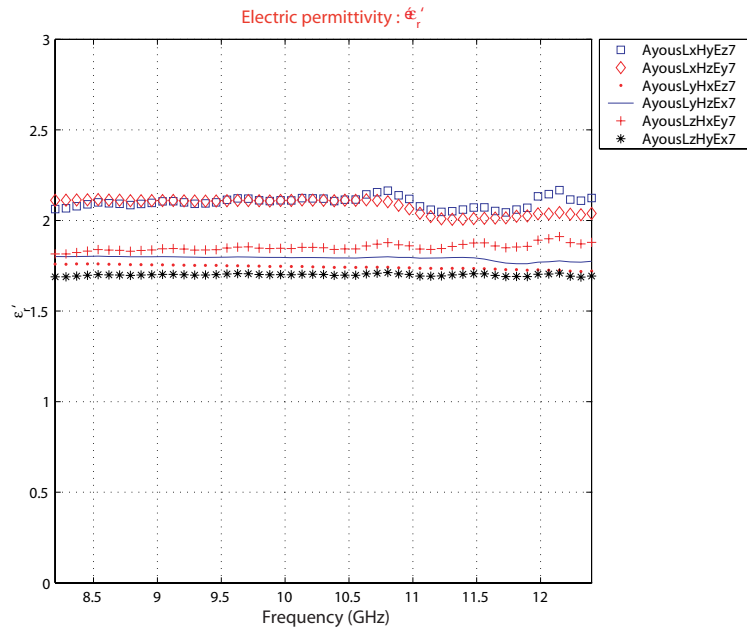


FIGURE 2.15: Relative Permittivity of Ayous wood : real part (waveguide)

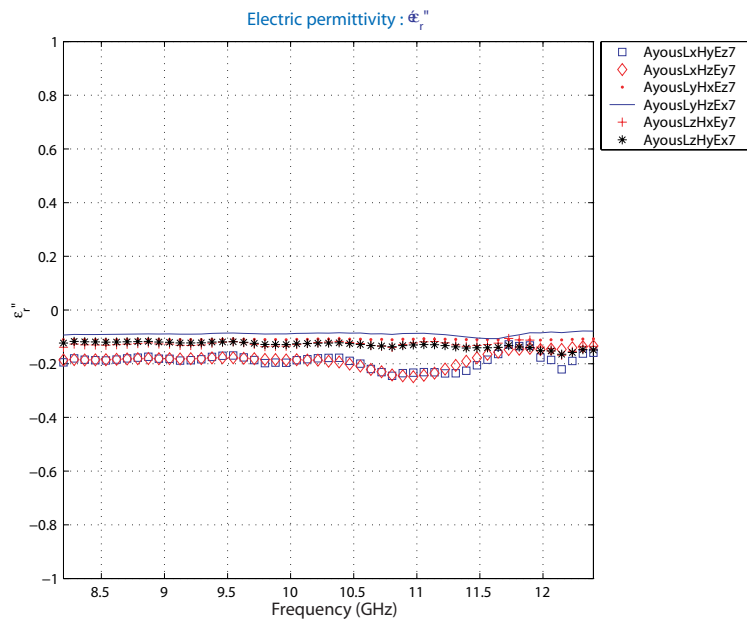


FIGURE 2.16: Relative Permittivity of Ayous wood : imaginary part (waveguide)



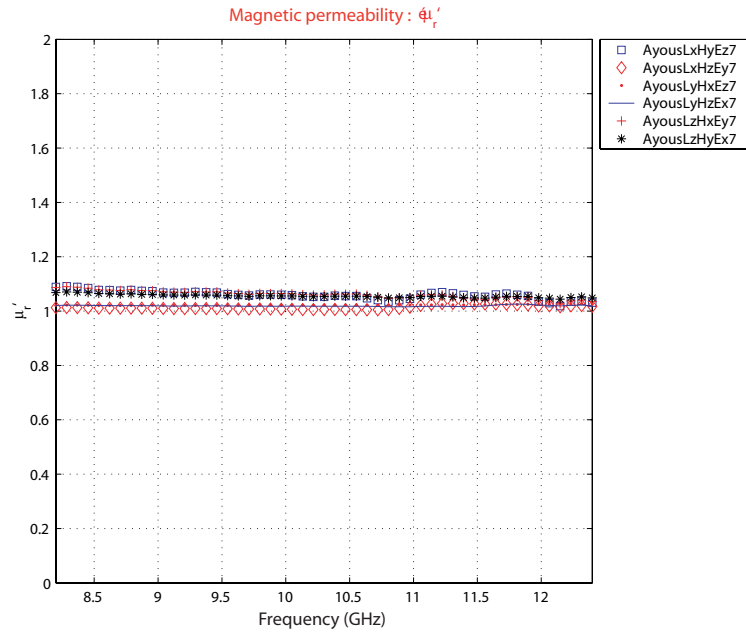


FIGURE 2.17: Relative permeability of Ayous wood : real part (waveguide)

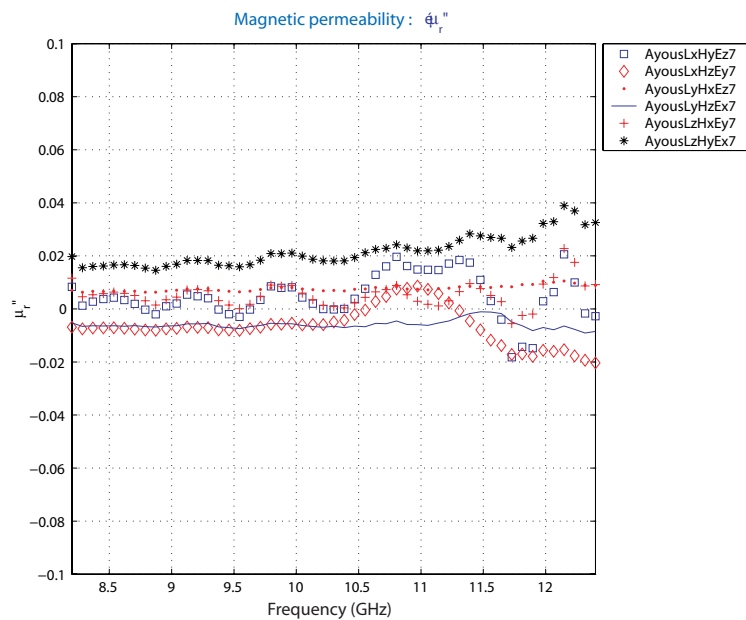


FIGURE 2.18: Relative permeability of Ayous wood : imaginary part (waveguide)

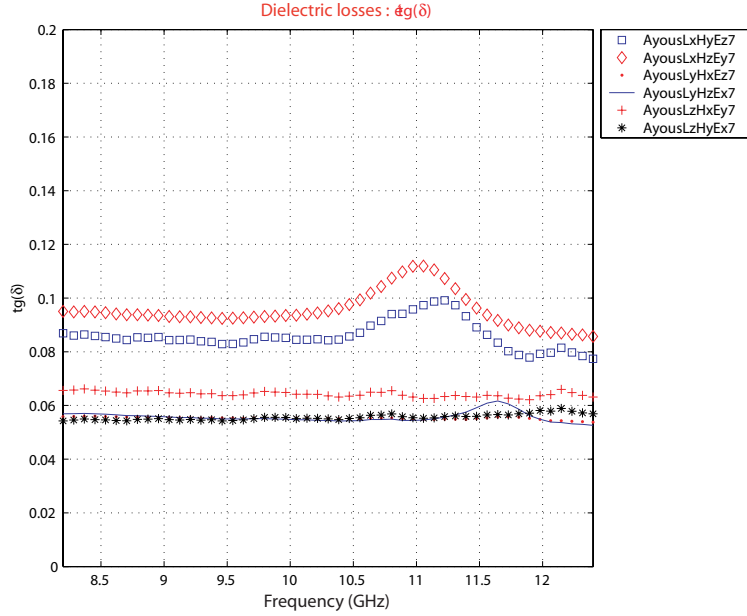


FIGURE 2.19: Dielectric losses of Ayous wood (waveguide)

Open resonator measurements

TABLE 2.3: Permittivity values for non-impregnated Ayous (open resonator)

Sample	$\epsilon'_r$		$\epsilon''_r$		$\tan \delta$	
	$\bar{\epsilon}'_r$	$\sigma^2$	$\bar{\epsilon}''_r$	$\sigma^2$	$\tan \delta$	$\sigma^2$
Ayous1LR	1.5442	$9.2693 \cdot 10^{-4}$	$9.9702 \cdot 10^{-2}$	$3.7117 \cdot 10^{-5}$	$6.4527 \cdot 10^{-2}$	$7.6072 \cdot 10^{-6}$
Ayous1LR90	1.8334	$2.2696 \cdot 10^{-3}$	$2.0767 \cdot 10^{-1}$	$7.5469 \cdot 10^{-4}$	$1.1316 \cdot 10^{-1}$	$1.7623 \cdot 10^{-4}$
Ayous2LR	1.7822	$5.1767 \cdot 10^{-4}$	$1.3991 \cdot 10^{-1}$	$1.0343 \cdot 10^{-4}$	$7.8474 \cdot 10^{-2}$	$2.6473 \cdot 10^{-5}$
Ayous2LR90	2.1038	$5.7721 \cdot 10^{-3}$	$2.1029 \cdot 10^{-1}$	$1.5915 \cdot 10^{-2}$	$1.0024 \cdot 10^{-1}$	$3.5103 \cdot 10^{-3}$

**N.B.** : In the notation “Ayous1LR90” the suffixes “LR” correspond to the “Long” spacing with “Rods” choice during calibration and “90” corresponds to a measurement made with a  $90^\circ$  rotation of the sample.

The results obtained are summarized in TABLE 2.3. By making a rotation of  $90^\circ$  the direction of the fibers is identical to that of the field inside the resonator, that’s why there

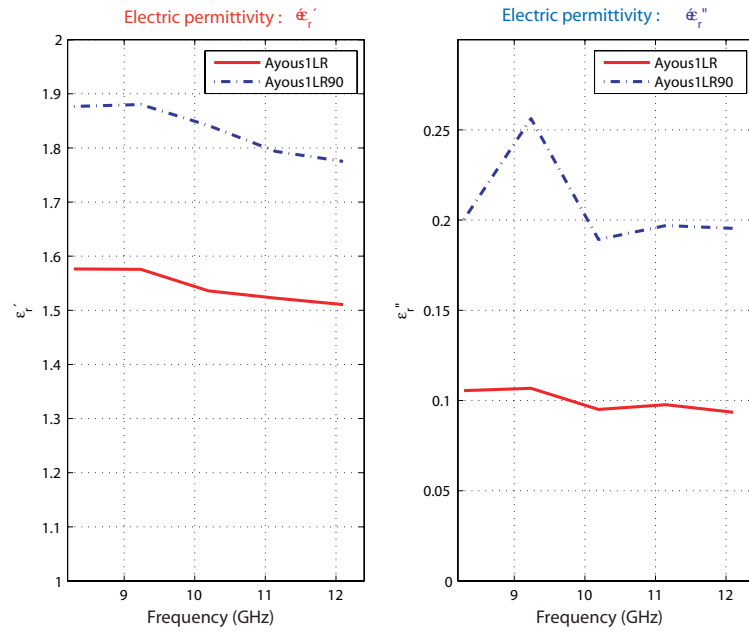


FIGURE 2.20: Relative permittivity of Ayous1LR (open resonator)

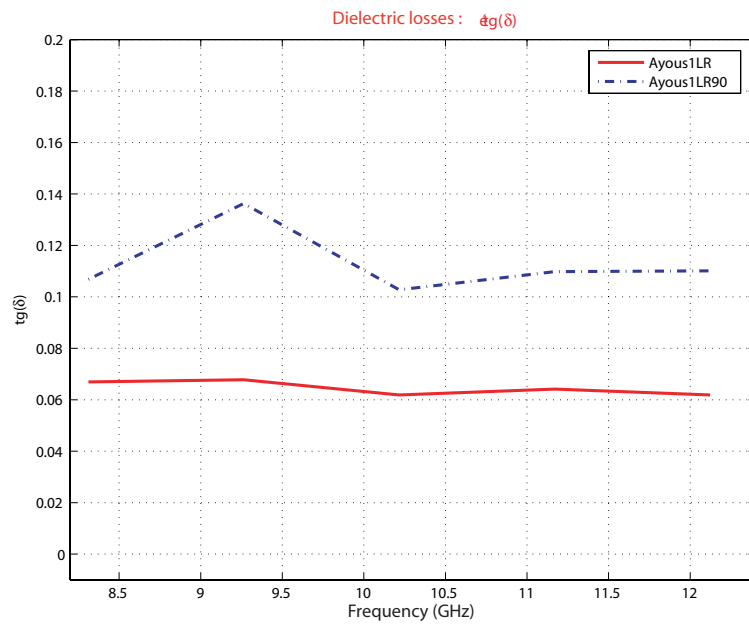


FIGURE 2.21: Dielectric losses of Ayous1LR (open resonator)

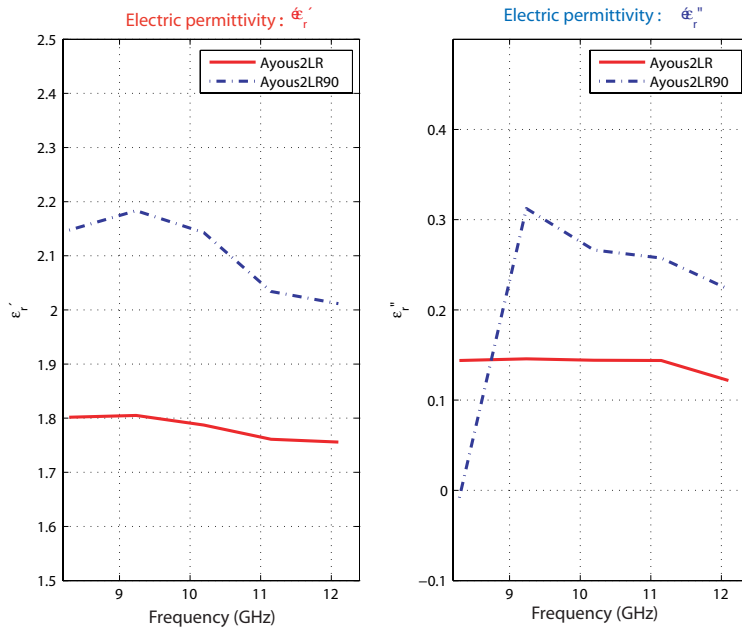


FIGURE 2.22: Relative permittivity of Ayous2LR (open resonator)

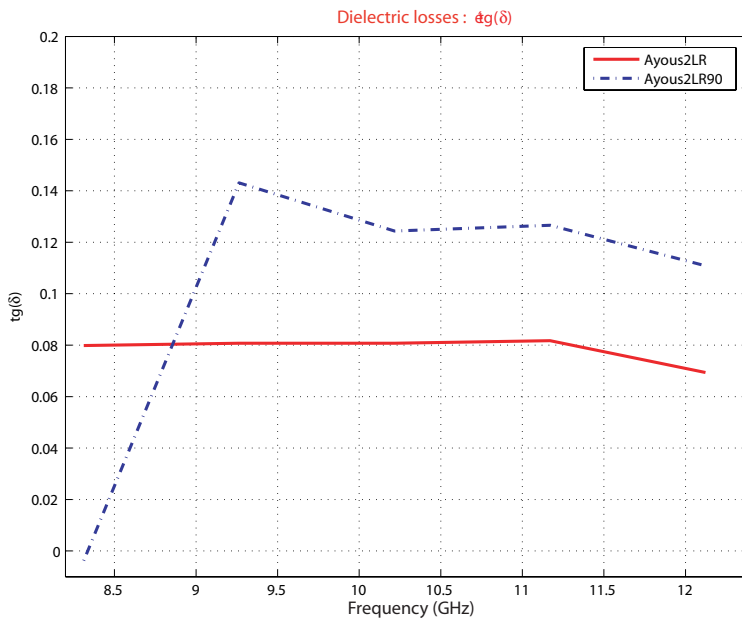


FIGURE 2.23: Dielectric losses of Ayous2LR (open resonator)

is an increase in the values. In addition, for the Ayous2LR90 sample we notice that the first value measured is dubious, explaining why the curve begins below the curve of the Ayous2LR sample. But we remark that the values are similar to those found by the first method of measurement : this enables us to confirm the values of permittivity obtained in the previous measurements.

### Measurement results for Ayous impregnated with linseed oil

The antenna is an element that is placed outdoors. Outside the air is not completely dry, in particular in Africa during the rain season! Since wood is porous and must face the humidity of the air, we need to protect it against moisture. We choose a biological oil in order not to change the dielectric characteristics of the wood and we impregnate it with this oil which will play the protector role.

#### Characteristics of linseed

<i>Botanical Name</i>	: Linum usitatissimum, Lini semen, Olea lini semen
<i>Family</i>	: Linacee
<i>Common name</i>	: Lin, linseed, linseed oil
<i>Used part</i>	: Seeds and oil drawn from the seeds
<i>Origin</i>	: Probably coming from the Mediterranean basin, this : annual plant is today cultivated everywhere : under the moderate and tropical climates
<i>Usage</i>	: Nutrition, Textile industry, Medicinal plant, : Wood's completion and maintains (boiled linseed oil)

We impregnated Ayous in linseed oil in order to be able to measure the permittivity. We noticed that Ayous is not a very porous wood because the linseed oil infiltrated very slightly. By inspecting the TABLE 2.4 we notice that the values did not change significantly with respect to TABLE 2.3.

## CHAPTER 2. WOOD CHARACTERIZATION

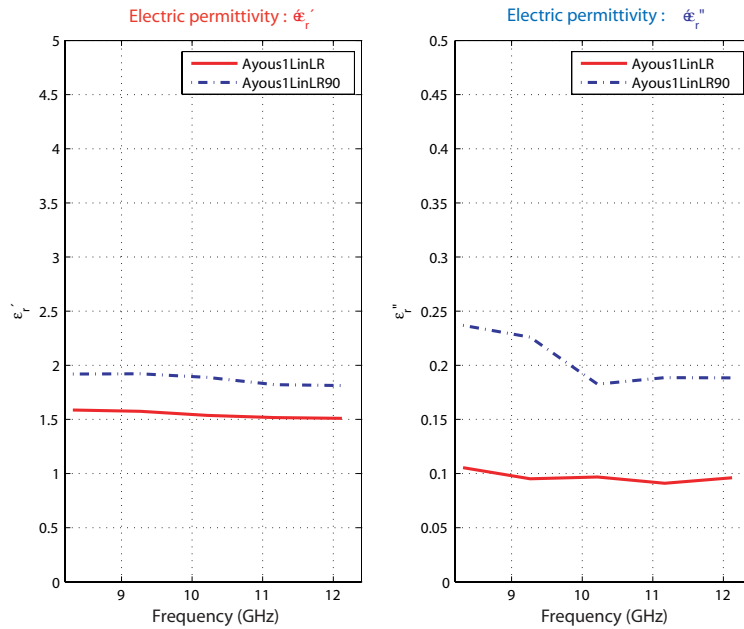


FIGURE 2.24: Relative permittivity of Ayous1LinLR (open resonator)

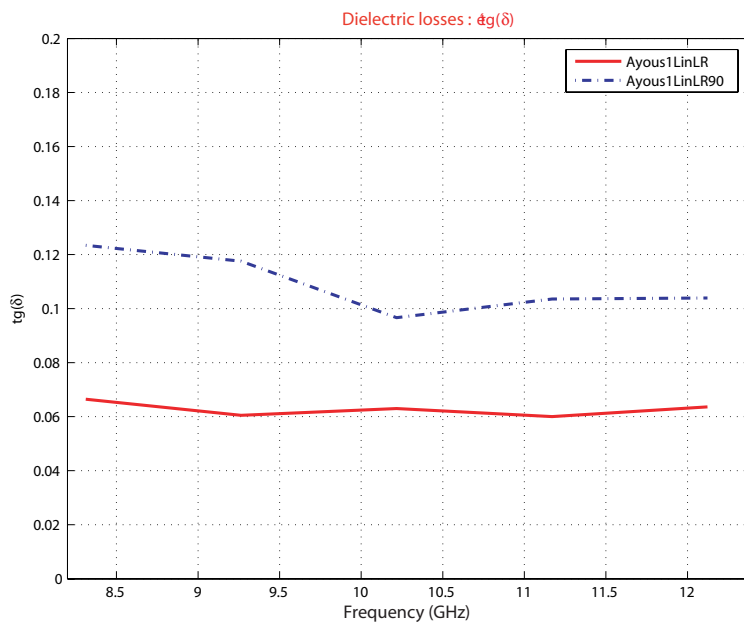


FIGURE 2.25: Dielectric losses of Ayous1LinLR (open resonator)

TABLE 2.4: Permittivity values of impregnated Ayous (open resonator)

Sample	$\varepsilon'_r$		$\varepsilon''_r$		$\tan \delta$	
	$\bar{\varepsilon}'_r$	$\sigma^2$	$\bar{\varepsilon}''_r$	$\sigma^2$	$\tan \delta$	$\sigma^2$
Ayous1LinLR	1.5450	1.1708 10 <sup>-3</sup>	9.6911 10 <sup>-2</sup>	2.7811 10 <sup>-5</sup>	6.2709 10 <sup>-2</sup>	6.8403 10 <sup>-6</sup>
Ayous1LinLR90	1.8729	2.7948 10 <sup>-3</sup>	2.0447 10 <sup>-1</sup>	6.2613 10 <sup>-4</sup>	1.0902 10 <sup>-1</sup>	1.2211 10 <sup>-4</sup>

### 2.7.2 Modelling of Ayous

The samples were machined along three directions :  $(ox)$ ,  $(oy)$  and  $(oz)$ . The width of each sample has one of the three directions. For each direction of the width of the sample (for example  $(ox)$ ), the height is machined according to one of the two other directions ( $(oy)$  or  $(oz)$ ).

In the TABLE 2.2, we notice a very small value of the variance for all the measured values : we can in this fact consider for each characteristic its average value.

#### Relative permeability

According to the results of measurement, the value of the relative magnetic permeability (the imaginary part being negligible) is the same in all the directions and is equal to the unity : the medium is thus non magnetic.

#### Relative permittivity

The relative permittivity values are complex, they differ along the three axes, but remain constant for each direction : we have here a linear anisotropic dielectric medium. The dielectric tensor is :

$$\bar{\varepsilon}_r = \begin{pmatrix} \bar{\varepsilon}_{rx} & 0 & 0 \\ 0 & \bar{\varepsilon}_{ry} & 0 \\ 0 & 0 & \bar{\varepsilon}_{rz} \end{pmatrix} = \begin{pmatrix} 2.091 - j0.1876 & 0 & 0 \\ 0 & 1.767 - j0.0994 & 0 \\ 0 & 0 & 1.776 - j0.1291 \end{pmatrix}$$

According to what precedes, we notice that  $\bar{\varepsilon}_{ry} \approx \bar{\varepsilon}_{rz}$  : this anisotropic linear dielectric medium has a uniaxial character.



FIGURE 2.26: Balsa wood

### Dielectric losses

The tensor of the dielectric losses is :

$$\tan \delta = \begin{pmatrix} \tan \delta_x & 0 & 0 \\ 0 & \tan \delta_y & 0 \\ 0 & 0 & \tan \delta_z \end{pmatrix} = \begin{pmatrix} 9.069 \cdot 10^{-2} & 0 & 0 \\ 0 & 5.545 \cdot 10^{-2} & 0 \\ 0 & 0 & 5.992 \cdot 10^{-2} \end{pmatrix}$$

We notice that the dielectric losses are quite important, because in all directions they remain larger than  $5 \cdot 10^{-2}$ . But if we reduce the thickness and use Ayous as line substrate, we feel that we can still realize an antenna with a gain suitable for the Worldspace receiver characteristics.



## 2.8 BALSAM WOOD

### 2.8.1 Characteristics

#### Denomination

<i>Scientific name</i>	: Ochroma pyramidal, Ochroma lagopus (synonymous)
<i>Family</i>	: Bombacaceae
<i>Origins</i>	: Brazil, Colombia, Ecuador, Guatemala, Honduras, Nicaragua, Peru, El Salvador, Trinidad and Tobago, Venezuela
<i>Main denomination</i>	: Balsa
<i>Other local denominations</i>	: Pau of Balsa, Lanu, Lanilla, Guano, Gatillo, Palo of Balsa, Topa, Algodón, Flood Wood, Balso

#### Description of the bark and wood

##### Description of the bark

<i>Diameter</i>	: From 50 to 80 cm
<i>Thickness of sapwood</i>	: -
<i>Buoyancy</i>	: Floatable
<i>Conservation in forest</i>	: Weak (must be treated)

##### Description of wood

<i>Reference color</i>	: White cream
<i>Sapwood</i>	: Non distinct
<i>Grain</i>	: Coarse
<i>Line</i>	: Straight
<i>Against-grain</i>	: Absent
<i>Note</i>	: White wood cream to rosy white

## CHAPTER 2. WOOD CHARACTERIZATION

---

### Drying

*Speed of drying* : Normal to slow

*Risk of deformation* : High

*Risk of cementing* : Yes

*Risk of cracks* : High

*Risk of collapse* : No

*Note* : Artificial drying is preferable to air drying  
: to reduce the defects. Drying must be carried out  
: slowly and prudently.

### Physical and mechanical characteristics

The properties indicated relate to the "ripe" wood. These properties can vary significantly depending on the source and conditions of the wood growth.

**Physical characteristics**

<i>Density</i> *	: 0.14
<i>Monnin hardness</i> *	: 0.3
<i>Volume withdrawal coefficient</i>	: 0.21%
<i>Total tangential withdrawal</i>	: 5.2%
<i>Total radial withdrawal</i>	: 2.2%
<i>Point of fibres saturation</i>	: 34%
<i>Stability in service</i>	: Fairly stable

**Mechanical characteristics**

<i>Breaking stress in compression</i> *	: 11 MPa
<i>Breaking stress in static inflexion</i> * (4 points inflexion)	: 24 MPa
<i>Longitudinal elasticity modulus</i> * (4 points inflexion)	: 5 140 MPa

\* : with 12% of moisture; 1 MPa = 1 N/mm<sup>2</sup>

**Required treatment for safeguarding**

<i>Against the attacks of seasoned wood insects</i>	: This wood requires a treatment : of adapted safeguarding
<i>In case of temporary humidification</i>	: This wood requires a treatment : of adapted safeguarding
<i>In case of permanent humidification</i>	: The use of this wood is : not advised

### Implementation

#### Sawing and machining

<i>Unsharpen Effect</i>	: Normal
<i>Teeth for sawing</i>	: Ordinary or allied steel
<i>Tools for machining</i>	: Ordinary
<i>Aptitude for unwinding</i>	: Not recommended or without interest
<i>Aptitude for cutting</i>	: Not recommended or without interest

*Note* : Maintain the tools well sharpened to avoid a fluffy  
: surface

#### Assembly

*Nailing-screwing* : Weak behavior

*Joining* : Correct

#### Usage

: Insulation, Floats, Model making

*Note* : A filling-in is necessary to obtain good  
: completion

### 2.8.2 Measurement results

#### Waveguide measurements

TABLE 2.5: Non-impregnated Balsal permittivity values (waveguide)

Sample	$\varepsilon'_r$		$\varepsilon''_r$		$\mu'_r$		$\mu''_r$		tan $\delta$	
	$\overline{\varepsilon}'_r$	$\sigma^2$	$\overline{\varepsilon}''_r$	$\sigma^2$	$\overline{\mu}'_r$	$\sigma^2$	$\overline{\mu}''_r$	$\sigma^2$	tan $\delta$	$\sigma^2$
BalsaLxHyEz	1.096	2.858 10 <sup>-6</sup>	-0.0121	1.084 10 <sup>-6</sup>	1.018	5.589 10 <sup>-6</sup>	-5.159 10 <sup>-3</sup>	4.637 10 <sup>-7</sup>	1.615 10 <sup>-2</sup>	4.326 10 <sup>-7</sup>
BalsaLxHzEy	1.124	1.130 10 <sup>-6</sup>	-0.0211	1.350 10 <sup>-6</sup>	1.009	2.748 10 <sup>-6</sup>	-9.029 10 <sup>-4</sup>	7.935 10 <sup>-7</sup>	1.967 10 <sup>-2</sup>	6.999 10 <sup>-7</sup>
BalsaLyHxEz	1.182	8.205 10 <sup>-6</sup>	-0.0252	4.659 10 <sup>-6</sup>	1.026	1.610 10 <sup>-5</sup>	-6.489 10 <sup>-3</sup>	1.821 10 <sup>-6</sup>	2.763 10 <sup>-2</sup>	1.228 10 <sup>-6</sup>
BalsaLyHzEx	1.242	3.867 10 <sup>-6</sup>	-0.0354	1.084 10 <sup>-5</sup>	1.025	6.656 10 <sup>-6</sup>	-1.056 10 <sup>-2</sup>	2.483 10 <sup>-6</sup>	3.879 10 <sup>-2</sup>	2.146 10 <sup>-6</sup>
BalsaLzHxEy	1.198	5.699 10 <sup>-6</sup>	-0.0325	1.204 10 <sup>-6</sup>	1.025	1.271 10 <sup>-5</sup>	-9.454 10 <sup>-4</sup>	6.173 10 <sup>-7</sup>	2.808 10 <sup>-2</sup>	5.198 10 <sup>-7</sup>
BalsaLzHyEx	1.235	3.993 10 <sup>-6</sup>	-0.0389	2.535 10 <sup>-6</sup>	1.023	5.886 10 <sup>-6</sup>	-4.617 10 <sup>-3</sup>	7.104 10 <sup>-7</sup>	3.601 10 <sup>-2</sup>	1.863 10 <sup>-6</sup>

### Balsal impregnated with linseed oil

Balsal is a very porous wood. We will increase the time of wood immersion in the oil in order to evaluate the effect of the oil on the wood characteristics. Then we immersed the Balsal sample in linseed oil during 6 hours in order to see the influence of this oil on the characteristics of the wood. The drying was made during approximately 30 hours.

TABLE 2.6: Permittivities values of Balsal impregnated with linseed oil (waveguide)

Sample	$\varepsilon'_r$		$\varepsilon''_r$		$\mu'_r$		$\mu''_r$		tan $\delta$	
	$\overline{\varepsilon}'_r$	$\sigma^2$	$\overline{\varepsilon}''_r$	$\sigma^2$	$\overline{\mu}'_r$	$\sigma^2$	$\overline{\mu}''_r$	$\sigma^2$	tan $\delta$	$\sigma^2$
BalsaLxHzEy	1.124	1.130 10 <sup>-6</sup>	-0.0211	1.350 10 <sup>-6</sup>	1.009	2.748 10 <sup>-6</sup>	-9.029 10 <sup>-4</sup>	7.935 10 <sup>-7</sup>	1.967 10 <sup>-2</sup>	6.999 10 <sup>-7</sup>
BalsaLinLxHzEy	1.171	6.320 10 <sup>-4</sup>	-0.0223	5.434 10 <sup>-4</sup>	1.053	5.652 10 <sup>-4</sup>	-7.179 10 <sup>-3</sup>	4.125 10 <sup>-4</sup>	2.589 10 <sup>-2</sup>	2.297 10 <sup>-6</sup>

We notice that when we consider the average values, we obtain almost the same values for the permittivity and for the permeability in the impregnated and in the non-impregnated samples but on the other hand we remark that the dielectric losses increase.

## CHAPTER 2. WOOD CHARACTERIZATION

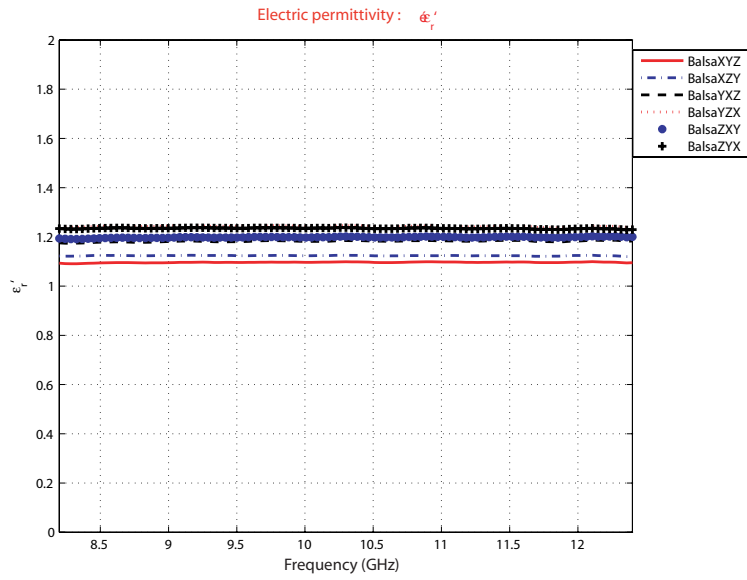


FIGURE 2.27: Relative permittivity of balsa wood : real part (waveguide)

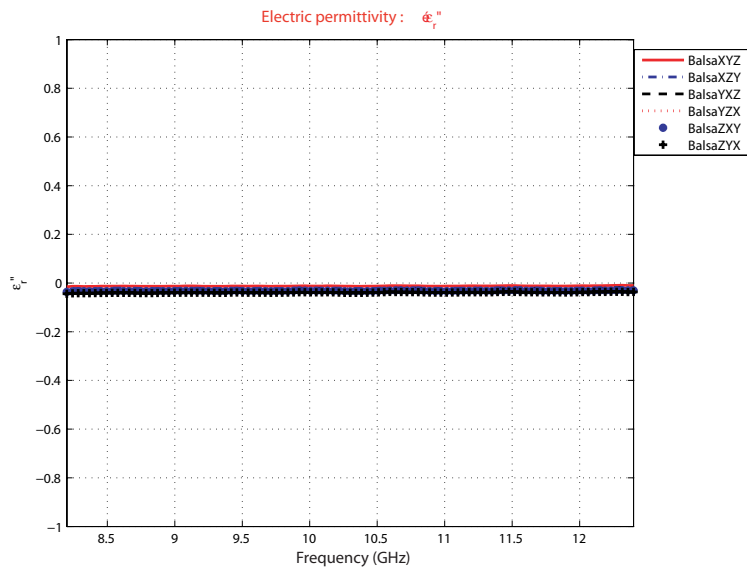


FIGURE 2.28: Relative permittivity of balsa wood : imaginary part (waveguide)

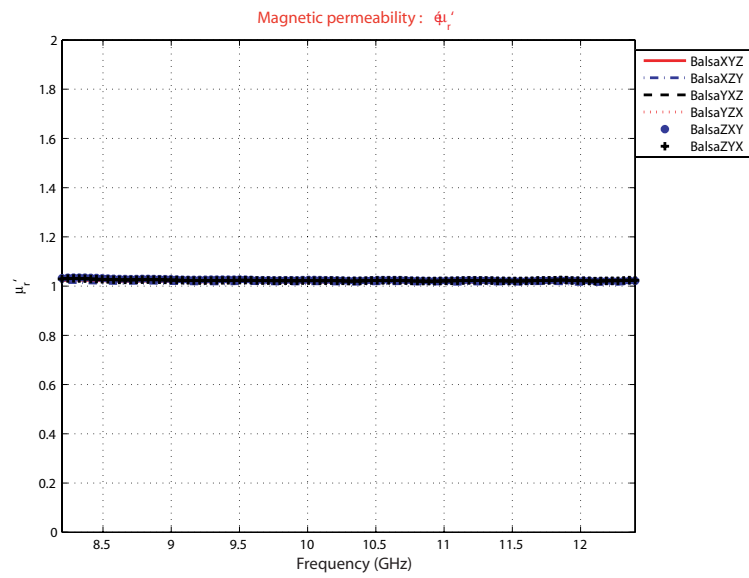


FIGURE 2.29: Relative permeability of balsawood : real part (waveguide)

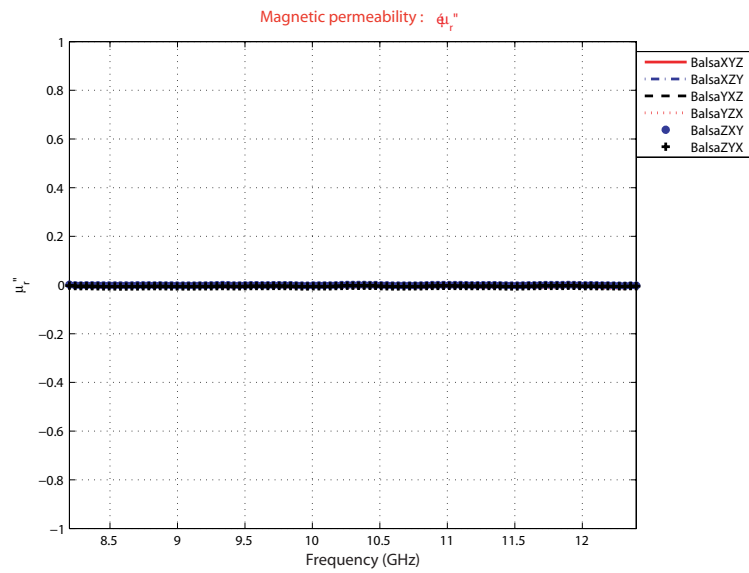


FIGURE 2.30: Relative permeability of balsawood : imaginary part (waveguide)

## CHAPTER 2. WOOD CHARACTERIZATION

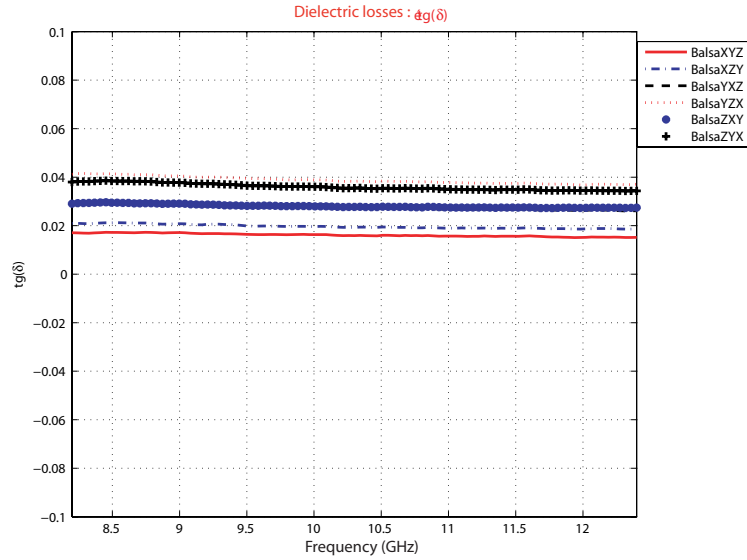


FIGURE 2.31: Dielectric losses of balsa wood (waveguide)

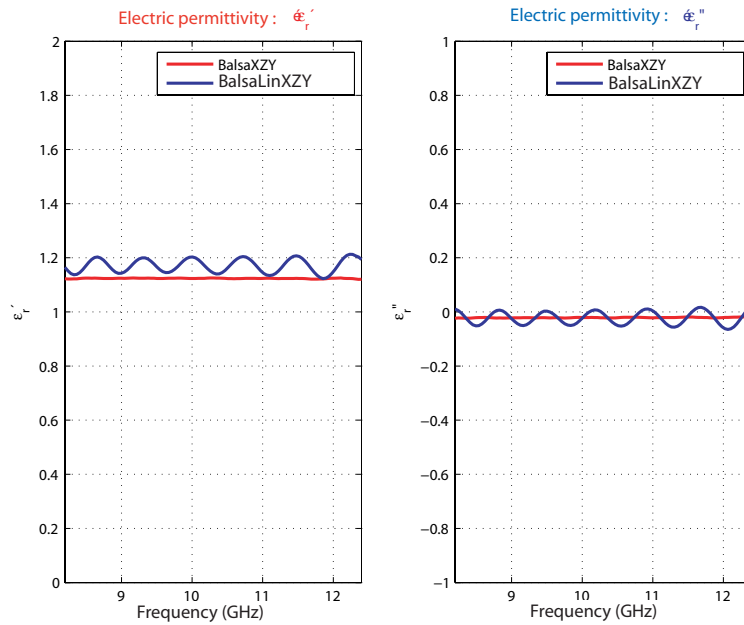


FIGURE 2.32: Comparison of the permittivity between natural Balsa and Balsa impregnated with linseed oil (waveguide)



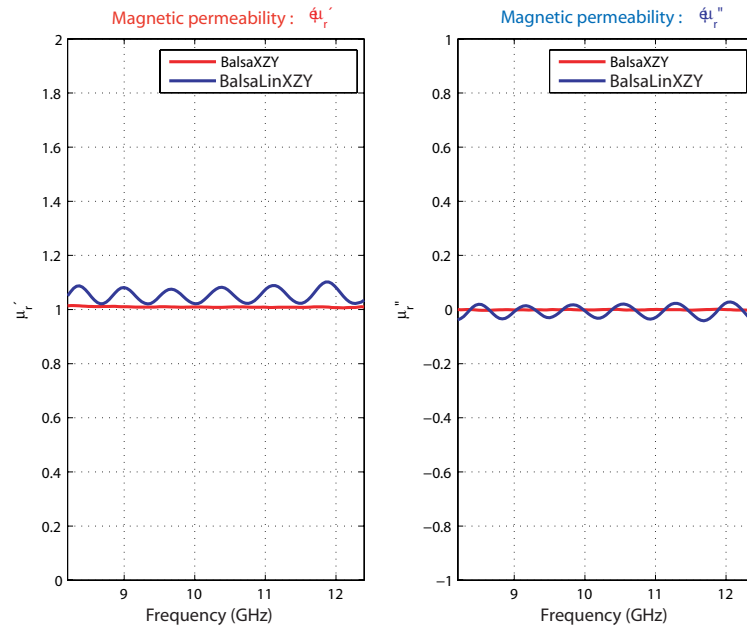


FIGURE 2.33: Comparison of the permeability between natural Balsa and Balsa impregnated with linseed oil (waveguide)

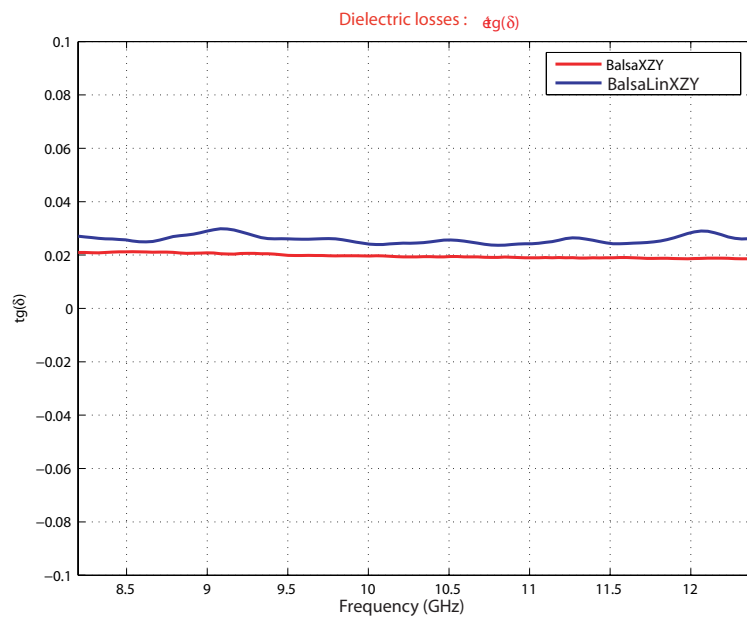


FIGURE 2.34: Comparison of the dielectric losses between natural Balsa and Balsa impregnated with linseed oil (waveguide)

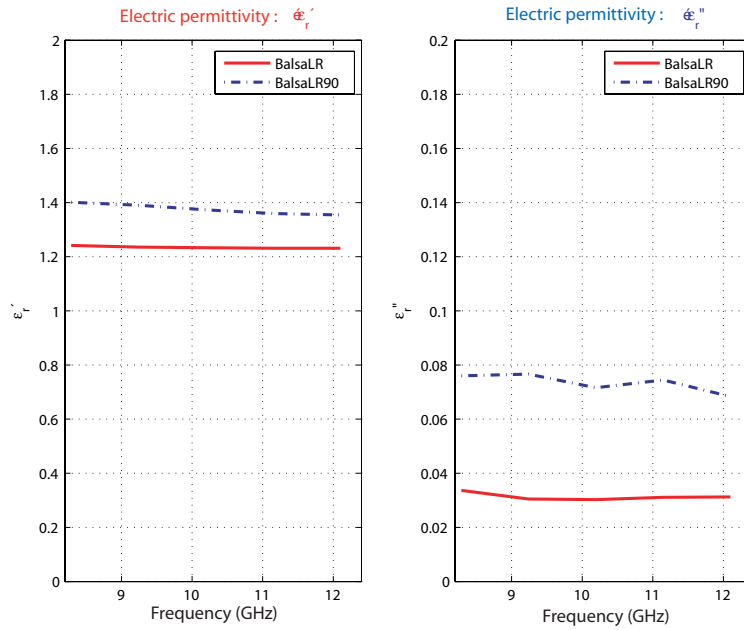


FIGURE 2.35: Relative permittivity of BalsalR (open resonator)

### 2.8.3 Confirmation of measurements using the Open Resonator

#### Measurement results for non-impregnated balsa

In the TABLE 2.7 we notice that the values are similar to the previously made measurements : this allows us to confirm the results obtained by waveguide measurements.

TABLE 2.7: Values of permittivity for balsa wood (open resonator)

Sample	$\epsilon_r'$		$\epsilon_r''$		$\tan \delta$	
	$\bar{\epsilon}_r'$	$\sigma^2$	$\bar{\epsilon}_r''$	$\sigma^2$	$\tan \delta$	$\sigma^2$
BalsalR	1.2348	$1.8893 \cdot 10^{-5}$	$3.1347 \cdot 10^{-2}$	$1.8159 \cdot 10^{-6}$	$2.5384 \cdot 10^{-2}$	$1.0382 \cdot 10^{-6}$
BalsalR90	1.3758	$3.8961 \cdot 10^{-4}$	$7.3406 \cdot 10^{-2}$	$1.1771 \cdot 10^{-5}$	$5.3344 \cdot 10^{-2}$	$3.9337 \cdot 10^{-6}$

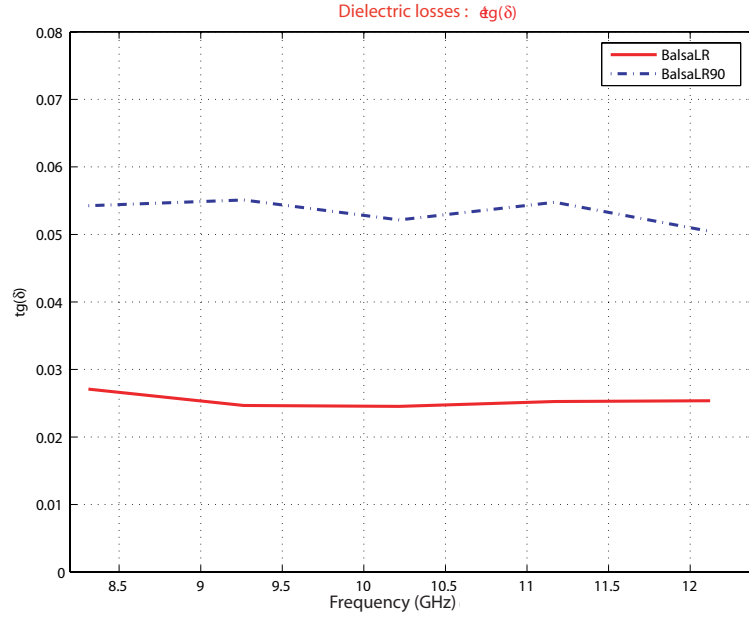


FIGURE 2.36: Dielectric losses of BalsalR (open resonator)

**Measurement results for Balsal wood impregnated with linseed oil**

We impregnated the Balsal in linseed oil in order to be able to measure the permittivities. We noticed that the Balsal is a porous wood. But by observing the TABLE 2.8 we notice that the values did not change significantly : the linseed oil is a valid candidate for wood protection against moisture.

TABLE 2.8: Values of permittivity for balsal wood impregnated with linseed oil (open resonator)

Sample	$\epsilon'_r$		$\epsilon''_r$		$\tan \delta$	
	$\bar{\epsilon}'_r$	$\sigma^2$	$\bar{\epsilon}''_r$	$\sigma^2$	$\overline{\tan \delta}$	$\sigma^2$
BalsalLinLR	1.2604	$5.4864 \cdot 10^{-5}$	$3.1454 \cdot 10^{-2}$	$1.0193 \cdot 10^{-6}$	$2.4953 \cdot 10^{-2}$	$4.8634 \cdot 10^{-7}$
BalsalLinLR90	1.4086	$2.2761 \cdot 10^{-5}$	$7.3016 \cdot 10^{-2}$	$1.9446 \cdot 10^{-5}$	$5.1839 \cdot 10^{-2}$	$9.9323 \cdot 10^{-6}$

## CHAPTER 2. WOOD CHARACTERIZATION

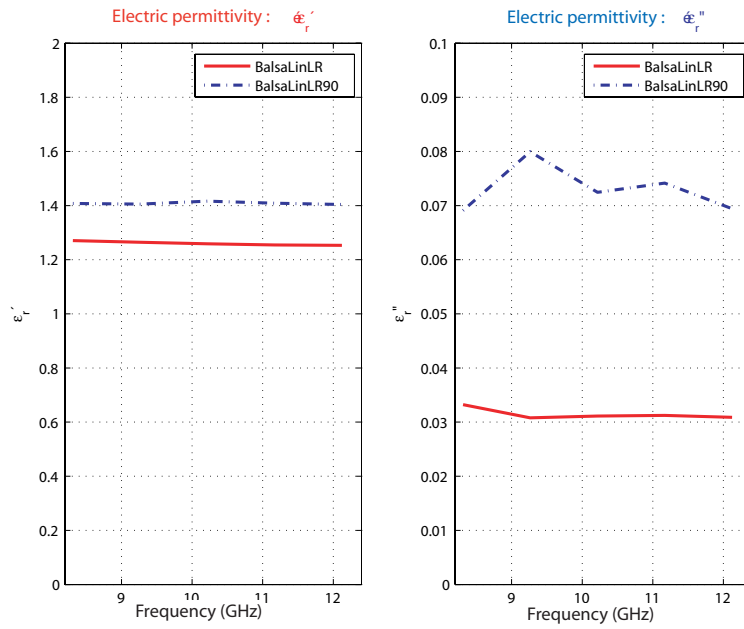


FIGURE 2.37: Relative permittivity of BalsaLinLR (open resonator)

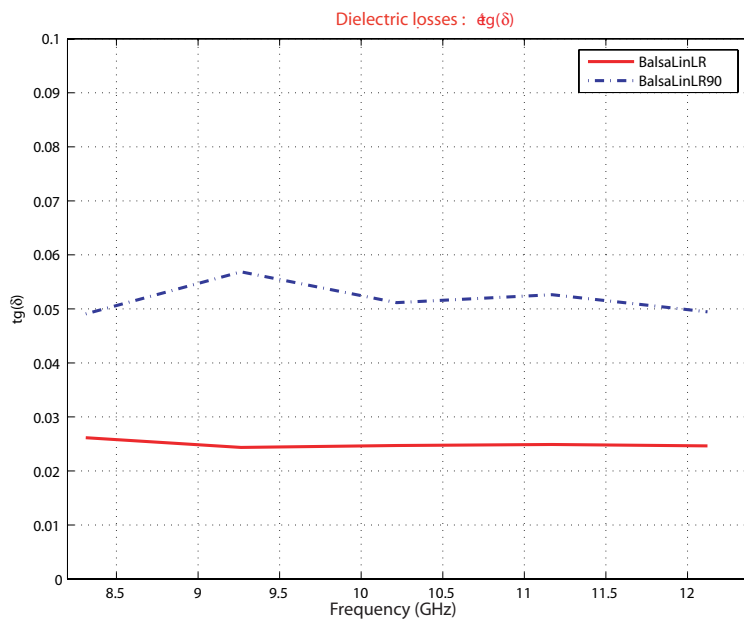


FIGURE 2.38: Dielectric losses of BalsaLinLR (open resonator)

### 2.8.4 Modelling of Balsal

In the TABLE 2.5, we notice very small values for the variance, for all the measured values : we can consider for each quantity its average value.

The results of TABLE 2.5 were confirmed by using another method of measurement : the open resonator. The agreement between the two methods is 1% accuracy. In addition, for the sample impregnated with linseed oil, the values obtained remain almost constant.

#### Relative permeability

According to the results of measurement, the value of the relative magnetic permeability (the imaginary part being negligible) is the same in all the directions and is equal to unity : the medium is thus non magnetic.

#### Relative permittivity

The values of the relative permittivity are complex, they differ along the three axes, but remain constant for each direction : we are in the presence of an anisotropic linear dielectric medium. The dielectric tensor is :

$$\bar{\epsilon}_r = \begin{pmatrix} \bar{\epsilon}_{rx} & 0 & 0 \\ 0 & \bar{\epsilon}_{ry} & 0 \\ 0 & 0 & \bar{\epsilon}_{rz} \end{pmatrix} = \begin{pmatrix} 1.110 - j0.0166 & 0 & 0 \\ 0 & 1.212 - j0.0303 & 0 \\ 0 & 0 & 1.217 - j0.0357 \end{pmatrix}$$

According to what precedes, we notice that  $\bar{\epsilon}_{ry} \approx \bar{\epsilon}_{rz}$  : this anisotropic linear dielectric medium has a uniaxial character.

#### Dielectric losses

The tensor of the dielectric losses is :

$$\tan \delta = \begin{pmatrix} \tan \delta_x & 0 & 0 \\ 0 & \tan \delta_y & 0 \\ 0 & 0 & \tan \delta_z \end{pmatrix} = \begin{pmatrix} 1.791 \cdot 10^{-2} & 0 & 0 \\ 0 & 3.321 \cdot 10^{-2} & 0 \\ 0 & 0 & 3.205 \cdot 10^{-2} \end{pmatrix}$$



FIGURE 2.39: Bubinga wood

We notice that the dielectric losses are greater than  $3 \cdot 10^{-2}$  in two directions ((o,y) and (o,z)). But we notice that in the (o,x) direction the losses are lower than  $2 \cdot 10^{-2}$  (the value for the FR4 dielectric tangent losses). Such losses are acceptable for our application and the use of this species of wood as a substrate looks very encouraging.

## 2.9 BUBINGA WOOD

### 2.9.1 Characteristics

#### Denomination

<i>scientific Name</i>	: Guibourtia demeusei, Guibourtia pellegriniana, Guibourtia tessmannii
<i>Family</i>	: Leguminosae Caesalpinae
<i>Origins</i>	: Cameroon, Congo, Guinea Equatorial, Democratic Republic of Congo.
<i>Cameroonian local denomination</i>	: Bubinga, Essingang
<i>Other local denominations</i>	: Kevazingo, Nomélé, Ebana, Waka, Oveng

**Description of sapwood and perfect wood**

<i>Description of sapwood</i>	: Distinct, Pallid
<i>Color of perfect wood</i>	: Reddish, Purplish Veins
<i>Line of perfect wood</i>	: -
<i>Against-grain of perfect wood</i>	: Frequent, light
<i>Grain of perfect wood</i>	: Fine to semi-fine
<i>Meshing of perfect wood</i>	: Fine
<i>Density in a green state</i>	: 1000 Kg/m <sup>3</sup>

**Physical and mechanical characteristics**

<i>Density at 12%</i>	: 800 Kg/m <sup>3</sup> ≤ density ≤ 950 Kg/m <sup>3</sup>
<i>Total volume withdrawal</i>	: 0.57%
<i>(per percentage of moisture in less)</i>	
<i>Total tangential withdrawal</i>	: 8.3%
<i>Total radial withdrawal</i>	: 5.7%
<i>Axial compression at 12%</i>	: 72 MPa
<i>Static inflexion at 12%</i>	: 146 MPa
<i>Elasticity modulus at 12%</i>	: 14,500 MPa
<i>Mushrooms durability</i>	: Very durable
<i>Termites durability</i>	: Durable
<i>Vrillette/Lyctus durability</i>	: Durable
<i>Impregnability</i>	: Non impregnable
<i>Hardness</i>	: Hard to very hard

## CHAPTER 2. WOOD CHARACTERIZATION

---

### Implementation

<i>Sawing</i>	: Rather difficult (request the power)
<i>Machining</i>	: Difficult (against-grain)
<i>Nailing</i>	: Easy (drilling of before-holes)
<i>Joining</i>	: Difficult
<i>Completion</i>	: Good
<i>Plating</i>	: Cutting (dappled aspect)
<i>Drying</i>	: Rather difficult, slow
<i>Surface treatment</i>	: Very good, sometimes with varnish deteriorations
<i>Usage</i>	: Fitting, Frame, Construction, Cabinet work, Staircases, Musical instruments, Skirting, Interior wood finishing and external, Pieces of furniture, Tools, Parquet floors, Plating, Sculpture, Turning, Cross-pieces

### 2.9.2 Measurement results

#### Waveguide measurements

TABLE 2.9: Non-impregnated Bubinga permittivity values (waveguide)

Sample	$\varepsilon_r'$		$\varepsilon_r''$		$\mu_r'$		$\mu_r''$		tan $\delta$	
	$\bar{\varepsilon}_r'$	$\sigma^2$	$\bar{\varepsilon}_r''$	$\sigma^2$	$\bar{\mu}_r'$	$\sigma^2$	$\bar{\mu}_r''$	$\sigma^2$	tan $\delta$	$\sigma^2$
BubingaLxHyEz	2.667	4.607 10 <sup>-2</sup>	-0.2669	4.793 10 <sup>-2</sup>	0.979	4.146 10 <sup>-3</sup>	2.792 10 <sup>-2</sup>	3.526 10 <sup>-3</sup>	7.239 10 <sup>-2</sup>	7.780 10 <sup>-4</sup>
BubingaLxHzEy	2.715	6.307 10 <sup>-2</sup>	-0.3246	6.916 10 <sup>-2</sup>	0.989	5.019 10 <sup>-3</sup>	3.191 10 <sup>-2</sup>	5.811 10 <sup>-3</sup>	8.637 10 <sup>-2</sup>	8.304 10 <sup>-4</sup>
BubingaLyHxEz	2.753	5.393 10 <sup>-2</sup>	-0.2227	4.841 10 <sup>-2</sup>	0.988	4.647 10 <sup>-3</sup>	8.303 10 <sup>-3</sup>	3.995 10 <sup>-3</sup>	7.362 10 <sup>-2</sup>	7.409 10 <sup>-4</sup>
BubingaLyHzEx	2.780	5.257 10 <sup>-2</sup>	-0.2118	5.572 10 <sup>-2</sup>	0.971	4.140 10 <sup>-3</sup>	8.830 10 <sup>-3</sup>	4.230 10 <sup>-3</sup>	6.807 10 <sup>-2</sup>	8.000 10 <sup>-4</sup>
BubingaLzHxEy	3.318	1.441 10 <sup>-1</sup>	-0.2822	1.367 10 <sup>-1</sup>	0.942	7.543 10 <sup>-3</sup>	-1.194 10 <sup>-2</sup>	7.057 10 <sup>-3</sup>	9.962 10 <sup>-2</sup>	8.568 10 <sup>-4</sup>
BubingaLzHyEx	3.221	1.794 10 <sup>-1</sup>	-0.7059	1.741 10 <sup>-1</sup>	0.968	8.873 10 <sup>-3</sup>	8.583 10 <sup>-2</sup>	1.408 10 <sup>-2</sup>	1.306 10 <sup>-1</sup>	6.744 10 <sup>-4</sup>

Since this wood has important losses, it is not necessary to do measurement with impregnated sample.



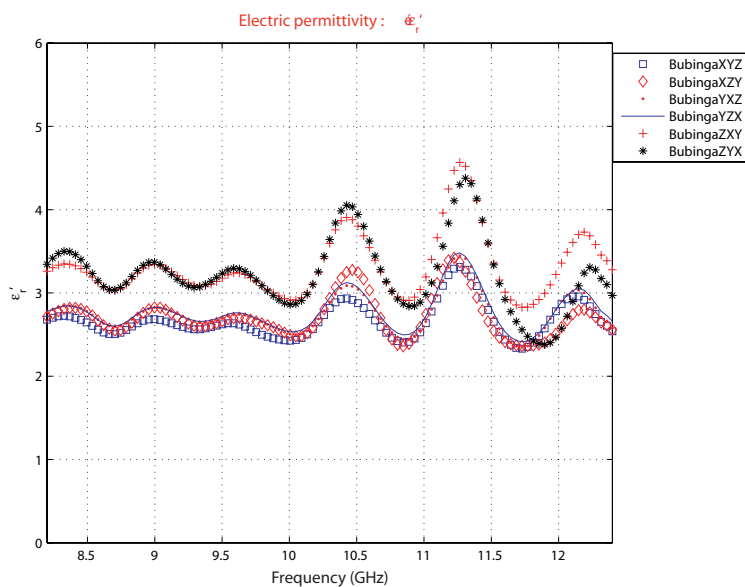


FIGURE 2.40: Relative permittivity of bubinga wood : real part (waveguide)

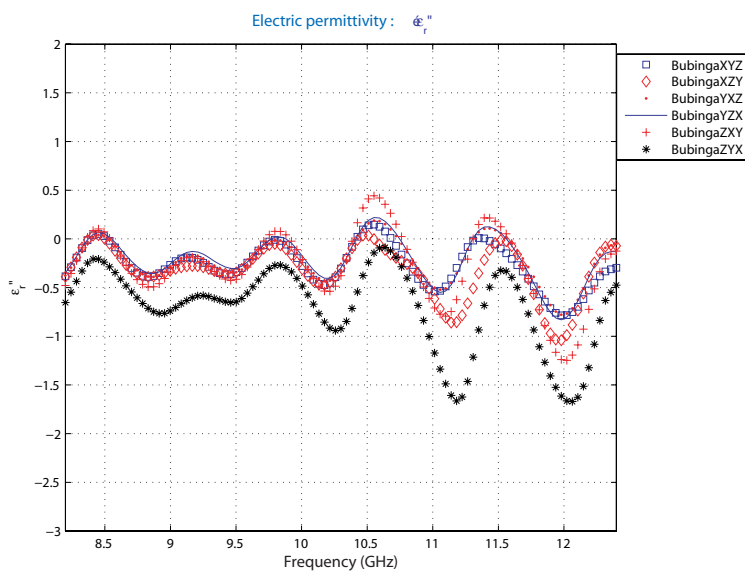


FIGURE 2.41: Relative permittivity of bubinga wood : imaginary part (waveguide)

## CHAPTER 2. WOOD CHARACTERIZATION

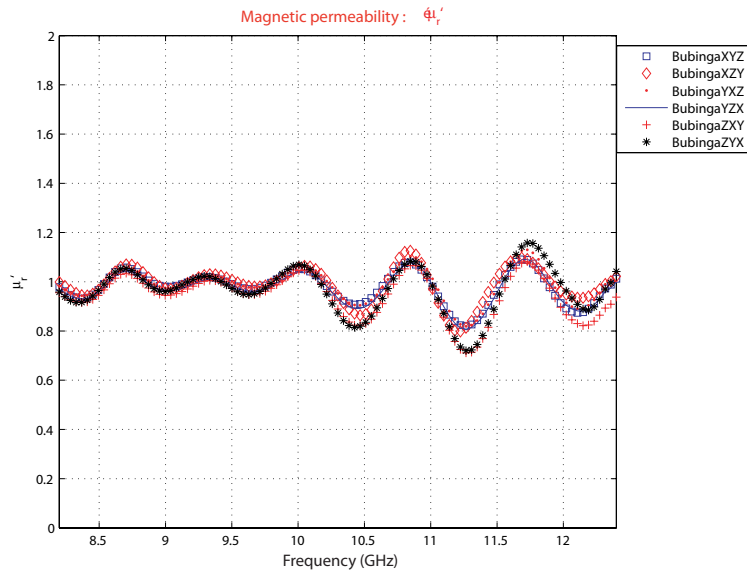


FIGURE 2.42: Relative permeability of bubinga wood : real part (waveguide)

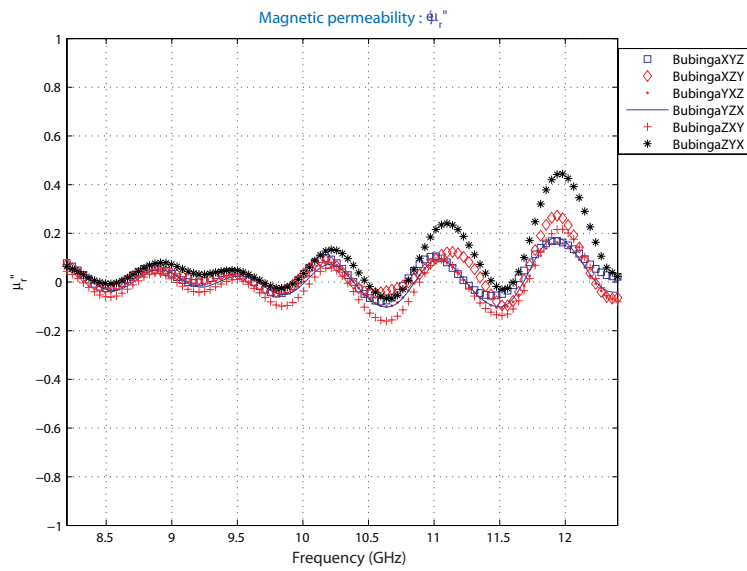


FIGURE 2.43: Relative permeability of bubinga wood : imaginary part (waveguide)

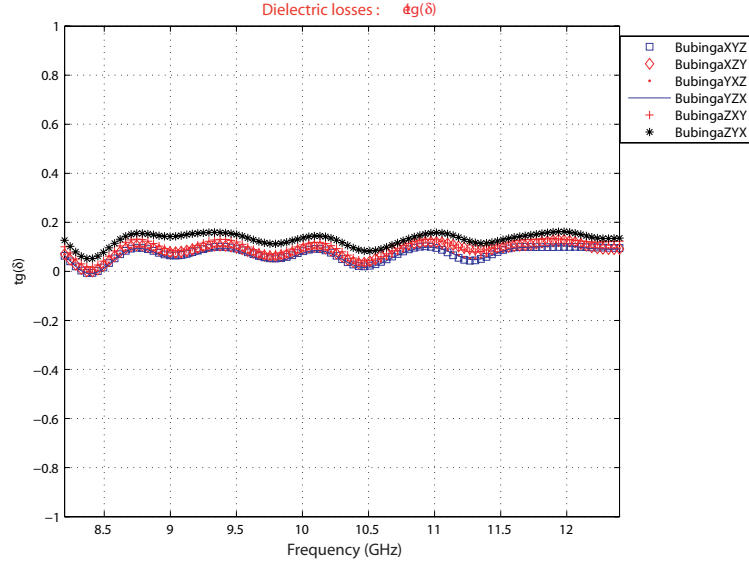


FIGURE 2.44: Dielectric losses of bubinga wood (waveguide)

### 2.9.3 Confirmation of measurements using the Open Resonator

#### Measurement results of non-impregnated Bubinga

Observing the TABLE 2.10, we notice similarities on the average values with previously made measurements, but we also note rather notorious differences on the variances observed in the two methods of measurement. These increased values of variances is due to the variation of the permittivity. To explain this variation, Aron [41] suggested that it arises as a result of coupling between the  $TE_{01n}$  mode and the degenerated  $TM_{11n}$  mode. In spite of the variations compared to the average value we will be able to confirm these results obtained if we stick to the average value.

TABLE 2.10: Permittivity values for non-impregnated Bubinga wood (open resonator)

Sample	$\varepsilon_r'$		$\varepsilon_r''$		$\tan \delta$	
	$\overline{\varepsilon_r'}$	$\sigma^2$	$\overline{\varepsilon_r''}$	$\sigma^2$	$\overline{\tan \delta}$	$\sigma^2$
BubingaLR	2.6316	$3.2479 \cdot 10^{-3}$	$2.7573 \cdot 10^{-1}$	$1.5598 \cdot 10^{-3}$	$1.0457 \cdot 10^{-1}$	$1.6589 \cdot 10^{-4}$
BubingaLR90	3.1067	$2.1980 \cdot 10^{-2}$	$4.4553 \cdot 10^{-1}$	$5.6624 \cdot 10^{-3}$	$1.4298 \cdot 10^{-1}$	$3.7726 \cdot 10^{-4}$

## CHAPTER 2. WOOD CHARACTERIZATION

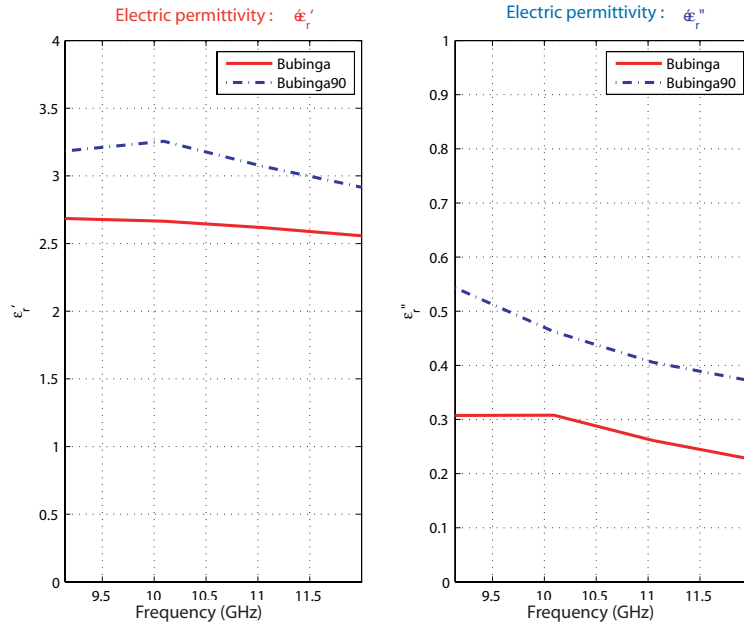


FIGURE 2.45: Relative permittivity of Bubinga wood (open resonator)

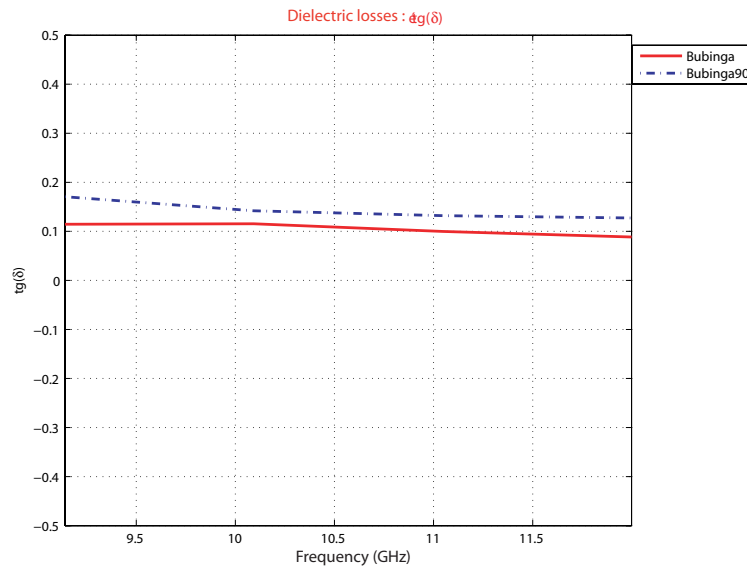


FIGURE 2.46: Dielectric losses of Bubinga wood (open resonator)

### 2.9.4 Modelling of Bubinga

In TABLE 2.9, we notice that variance values go up to about  $10^{-2}$ . These values are too important to let us consider only the average value. But if we compare these measurements with those obtained with the open resonator, where the variance values are small, we notice that the average values are the same. These two measurements let us conclude that we have an oscillation around the average value, which should be the value corresponding to the characteristic properties of this specie of wood.

#### Relative permeability

According to the measurement results, the value of the relative magnetic permeability (the imaginary part being negligible) is the same one in all directions and is equal to the unity : the medium is thus non magnetic.

#### Relative permittivity

If we consider the average value, we can say that the values of the relative permittivity are complex, different along the three axes but remain constant in each direction : this wood is an anisotropic linear dielectric medium. The dielectric tensor is :

$$\bar{\epsilon}_r = \begin{pmatrix} \bar{\epsilon}_{rx} & 0 & 0 \\ 0 & \bar{\epsilon}_{ry} & 0 \\ 0 & 0 & \bar{\epsilon}_{rz} \end{pmatrix} = \begin{pmatrix} 2.691 - j0.2958 & 0 & 0 \\ 0 & 2.767 - j0.2173 & 0 \\ 0 & 0 & 3.270 - j0.4941 \end{pmatrix}$$

According to what precedes, we notice that  $\bar{\epsilon}_{rx} \approx \bar{\epsilon}_{ry}$  : this anisotropic linear dielectric medium has an uniaxial character.

#### Dielectric losses

The tensor of the dielectric losses is :

$$\tan \delta = \begin{pmatrix} \tan \delta_x & 0 & 0 \\ 0 & \tan \delta_y & 0 \\ 0 & 0 & \tan \delta_z \end{pmatrix} = \begin{pmatrix} 7.938 \cdot 10^{-2} & 0 & 0 \\ 0 & 7.085 \cdot 10^{-2} & 0 \\ 0 & 0 & 11.511 \cdot 10^{-2} \end{pmatrix}$$



FIGURE 2.47: Dibetou wood

We notice that the dielectric losses are important in all directions and are higher than  $7 \cdot 10^{-2}$ . These very important losses do not make of Bubinga a good candidate as a dielectric substrate.

## 2.10 DIBETOU WOOD

### 2.10.1 Characteristics

#### Denomination

<i>Scientific name</i>	: <i>Lovoa Trichilloides</i> Harms
<i>Family</i>	: Meliaceae
<i>Origins</i>	: Cameroon, Congo, Ivory Coast, Gabon, Ghana, Equatorial Guinea, Liberia, Nigeria, Sierra Leone, Democratic Republic of Congo.
<i>Cameroonian local denomination</i>	: Bibolo

### Description of sapwood and perfect wood

<i>Description of sapwood</i>	: Distinct, Yellow grayed
<i>Color of perfect wood</i>	: Brown gilded, grayed, very dark veins
<i>Line of perfect wood</i>	: -
<i>Against-grain of perfect wood</i>	: Frequent, light
<i>Grain of perfect wood</i>	: Fine to semi-fine
<i>Mesh of perfect wood</i>	: Fine
<i>Density in a green state</i>	: 800 Kg/m <sup>3</sup>

### Physical and mechanical characteristics

<i>Density at 12%</i>	: 430 Kg/m <sup>3</sup> ≤ density ≤ 650 Kg/m <sup>3</sup>
<i>Total volume withdrawal</i>	: 0.42%
<i>(per percentage of moisture in less)</i>	
<i>Total tangential withdrawal</i>	: 5.8%
<i>Total radial withdrawal</i>	: 3.7%
<i>Axial compression at 12%</i>	: 44 MPa
<i>Static inflexion at 12%</i>	: 85 MPa
<i>Elasticity modulus at 12%</i>	: 10,500 MPa
<i>Mushrooms durability</i>	: Fairly durable
<i>Termites durability</i>	: Fairly durable
<i>Vrillette/Lyctus durability</i>	: Durable
<i>Impregnability</i>	: Not very impregnable
<i>Hardness</i>	: Tender to half-hard

## CHAPTER 2. WOOD CHARACTERIZATION

---

### Implementation

<i>Sawing</i>	: Easy
<i>Machining</i>	: Rather difficult (against-grain)
<i>Nailing</i>	: Easy
<i>Joining</i>	: Good
<i>Completion</i>	: Good
<i>Plating</i>	: Cutting and unwinding after drying
<i>Drying</i>	: Rather easy
<i>Treatment surface</i>	: Is impregnated and varnished very well
<i>Usage</i>	: Fitting, Plywood, Cabinet work, Skirting, Interior wood finishing, Pieces of furniture Plating, Turning

### 2.10.2 Measurement results

#### Waveguide measurements

TABLE 2.11: Permittivity values for non-impregnated Dibetou wood (waveguide)

Sample	$\varepsilon'_r$		$\varepsilon''_r$		$\mu'_r$		$\mu''_r$		tan $\delta$	
	$\bar{\varepsilon}'_r$	$\sigma^2$	$\bar{\varepsilon}''_r$	$\sigma^2$	$\bar{\mu}'_r$	$\sigma^2$	$\bar{\mu}''_r$	$\sigma^2$	$\overline{\tan \delta}$	$\sigma^2$
DibetouLxHyEz	1.845	$9.223 \cdot 10^{-3}$	-0.1251	$9.357 \cdot 10^{-3}$	1.000	$2.451 \cdot 10^{-3}$	$8.239 \cdot 10^{-3}$	$2.174 \cdot 10^{-3}$	$5.960 \cdot 10^{-2}$	$4.353 \cdot 10^{-4}$
DibetouLxHzEy	1.905	$9.742 \cdot 10^{-3}$	-0.1341	$1.034 \cdot 10^{-2}$	0.996	$2.467 \cdot 10^{-3}$	$7.608 \cdot 10^{-3}$	$2.110 \cdot 10^{-3}$	$6.290 \cdot 10^{-2}$	$4.541 \cdot 10^{-4}$
DibetouLyHxEz	1.928	$1.003 \cdot 10^{-2}$	-0.0936	$1.110 \cdot 10^{-2}$	0.989	$2.157 \cdot 10^{-3}$	$-7.868 \cdot 10^{-3}$	$2.366 \cdot 10^{-3}$	$5.683 \cdot 10^{-2}$	$4.804 \cdot 10^{-4}$
DibetouLyHzEx	1.966	$1.098 \cdot 10^{-2}$	-0.1482	$1.236 \cdot 10^{-2}$	0.992	$2.492 \cdot 10^{-3}$	$8.574 \cdot 10^{-3}$	$2.285 \cdot 10^{-3}$	$6.699 \cdot 10^{-2}$	$4.093 \cdot 10^{-4}$
DibetouLzHxEy	2.406	$2.636 \cdot 10^{-2}$	-0.2820	$2.632 \cdot 10^{-2}$	0.979	$2.993 \cdot 10^{-3}$	$2.484 \cdot 10^{-3}$	$3.009 \cdot 10^{-3}$	$1.155 \cdot 10^{-1}$	$6.695 \cdot 10^{-4}$
DibetouLzHyEx	2.465	$2.901 \cdot 10^{-2}$	-0.2745	$2.894 \cdot 10^{-2}$	0.968	$3.035 \cdot 10^{-3}$	$1.092 \cdot 10^{-3}$	$2.983 \cdot 10^{-3}$	$1.111 \cdot 10^{-1}$	$6.986 \cdot 10^{-4}$

Since this wood has important losses, it is not necessary to do measurement with impregnated sample.



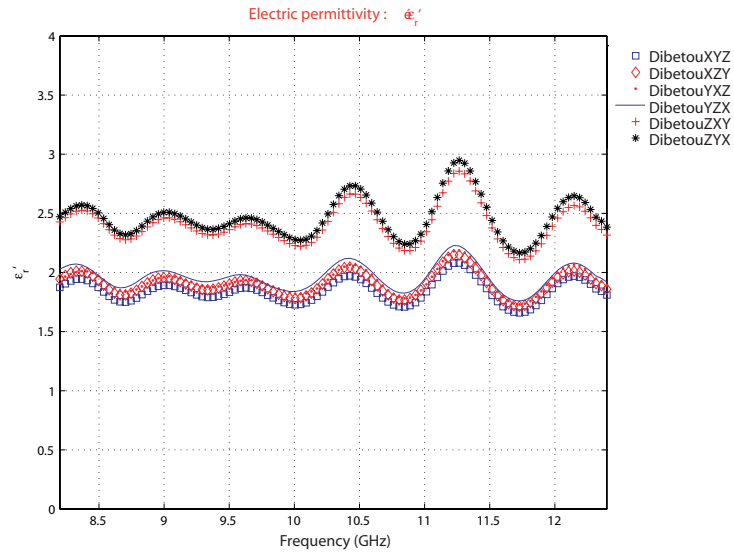


FIGURE 2.48: Relative permittivity of Dibetou wood : real part (waveguide)

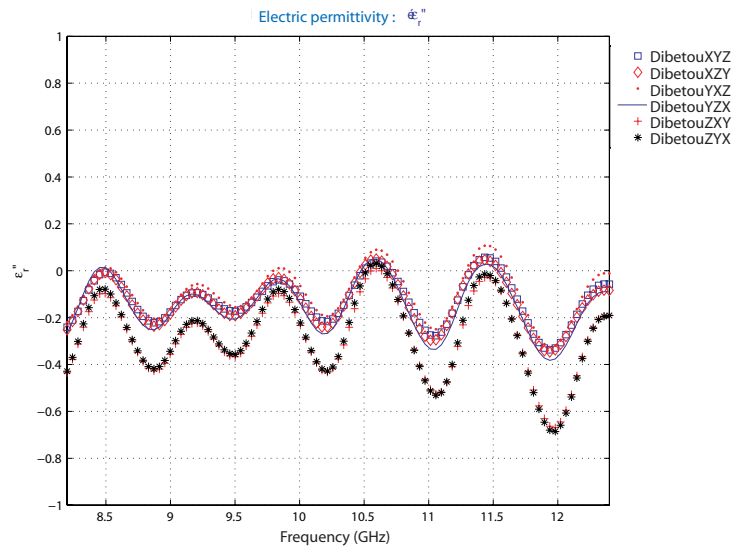


FIGURE 2.49: Relative permittivity of Dibetou wood : imaginary part (waveguide)

## CHAPTER 2. WOOD CHARACTERIZATION

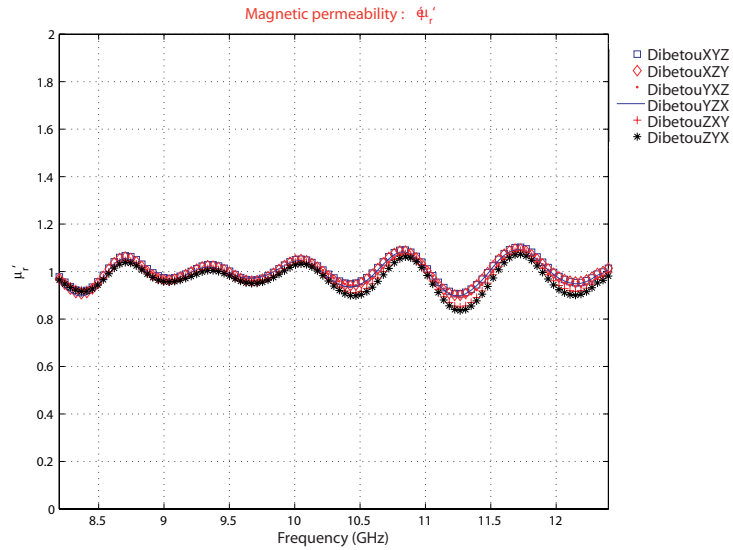


FIGURE 2.50: Relative permeability of Dibetou wood : real part (waveguide)

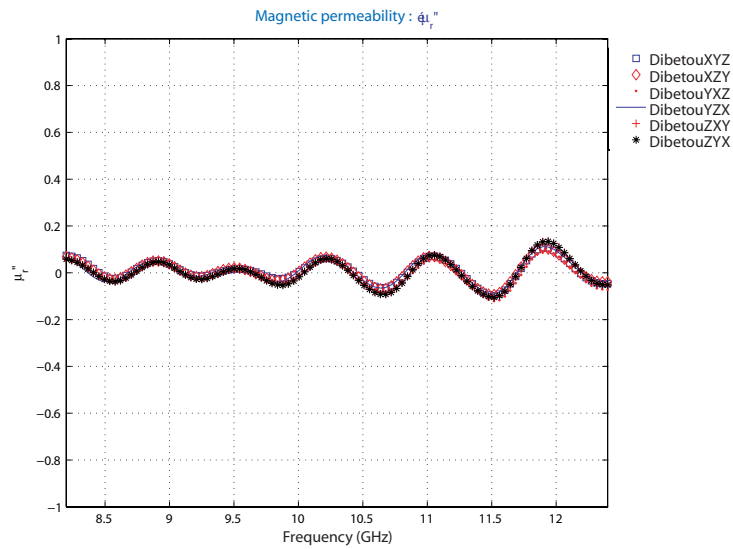


FIGURE 2.51: Relative permeability of Dibetou wood : imaginary part (waveguide)

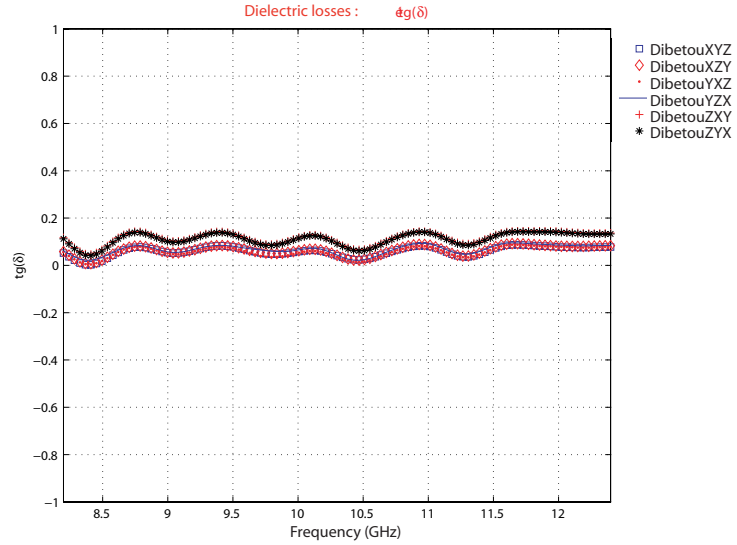


FIGURE 2.52: Dielectric losses of Dibetou wood (waveguide)

### 2.10.3 Confirmation of measurements by using the Open Resonator

#### Non-impregnated Dibetou measurement results

By observing the TABLE 2.12 we notice that the differences are smaller or equal to 10% on the average values for both methods of measurement. Such small differences allow us to say that the two measurements are very close and confirm the obtained results.

TABLE 2.12: Permittivity values of Non-impregnated Dibetou wood (open resonator)

Sample	$\varepsilon_r'$		$\varepsilon_r''$		$\tan \delta$	
	$\bar{\varepsilon}_r'$	$\sigma^2$	$\bar{\varepsilon}_r''$	$\sigma^2$	$\tan \delta$	$\sigma^2$
DibetouLR	1.743	$3.680 \cdot 10^{-4}$	$1.473 \cdot 10^{-1}$	$1.510 \cdot 10^{-4}$	$8.447 \cdot 10^{-2}$	$3.863 \cdot 10^{-5}$
DibetouLR90	2.176	$3.296 \cdot 10^{-3}$	$2.896 \cdot 10^{-1}$	$7.937 \cdot 10^{-4}$	$1.330 \cdot 10^{-1}$	$1.046 \cdot 10^{-4}$

## CHAPTER 2. WOOD CHARACTERIZATION

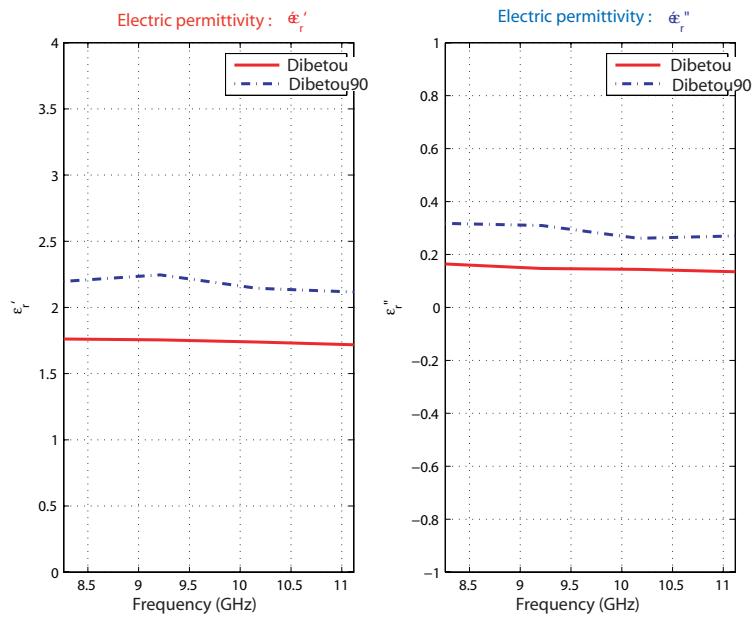


FIGURE 2.53: Relative permittivity of non-impregnated Dibetou (open resonator)

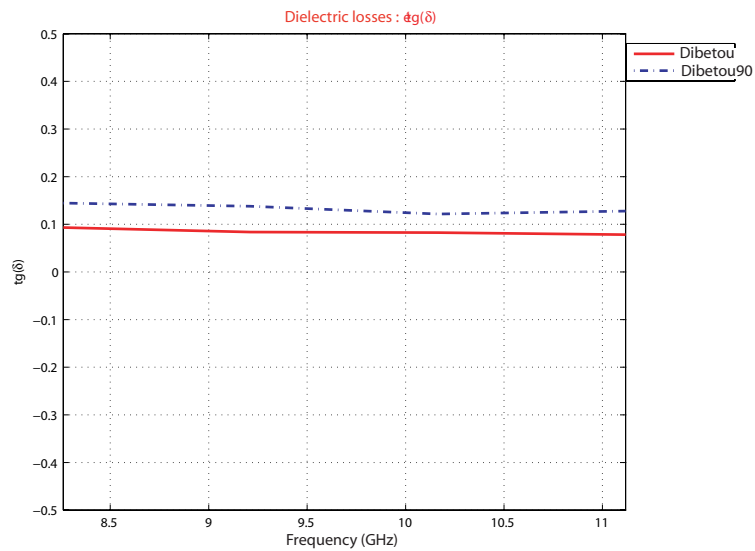


FIGURE 2.54: Relative permittivity of non-impregnated Dibetou (open resonator)

### 2.10.4 Modelling of Dibetou

In the TABLE 2.11, we notice that the values of the variance are about  $10^{-2}$ . These values let us conclude that the results obtained from these two methods of measurement are similar.

#### Relative permeability

According to the results of measurement, the value of the relative magnetic permeability (the imaginary part being negligible) is the same in all the directions and is equal to unity : the medium is thus non magnetic.

#### Relative permittivity

The values of relative permittivity are complex, different along the three axes but remain constant in each direction : we are deal with an anisotropic linear dielectric medium. The dielectric tensor is :

$$\bar{\epsilon}_r = \begin{pmatrix} \bar{\epsilon}_{rx} & 0 & 0 \\ 0 & \bar{\epsilon}_{ry} & 0 \\ 0 & 0 & \bar{\epsilon}_{rz} \end{pmatrix} = \begin{pmatrix} 1.875 - j0.1296 & 0 & 0 \\ 0 & 1.947 - j0.1209 & 0 \\ 0 & 0 & 2.436 - j0.2783 \end{pmatrix}$$

According to what precedes, we notice that  $\bar{\epsilon}_{rx} \approx \bar{\epsilon}_{ry}$  : this anisotropic linear dielectric medium has an uniaxial character.

#### Dielectric losses

The tensor of the dielectric losses is :

$$\tan \delta = \begin{pmatrix} \tan \delta_x & 0 & 0 \\ 0 & \tan \delta_y & 0 \\ 0 & 0 & \tan \delta_z \end{pmatrix} = \begin{pmatrix} 6.125 \cdot 10^{-2} & 0 & 0 \\ 0 & 6.191 \cdot 10^{-2} & 0 \\ 0 & 0 & 11.330 \cdot 10^{-2} \end{pmatrix}$$

We notice that the dielectric losses are important in all the directions and are higher than  $6 \cdot 10^{-2}$ . These very important losses do not make of Dibetou a good candidate for a dielectric substrate.



FIGURE 2.55: Mbey wood

## 2.11 MBEY WOOD

### 2.11.1 Introduction

This species is a wood which is not indexed as a species having commercial value. This name come from Maka of North people who are located in the Department of Lom and Djerem, in Diang division. Sometimes children use it to manufacture bicycle. We try it to see if we will have low losses. Since this wood does not appear in the repertory of tropical wood, we do not have any of its characteristics.

### 2.11.2 Measurement results

#### Waveguide measurements

Since this wood has important losses, it is not necessary to do measurement with impregnated sample.

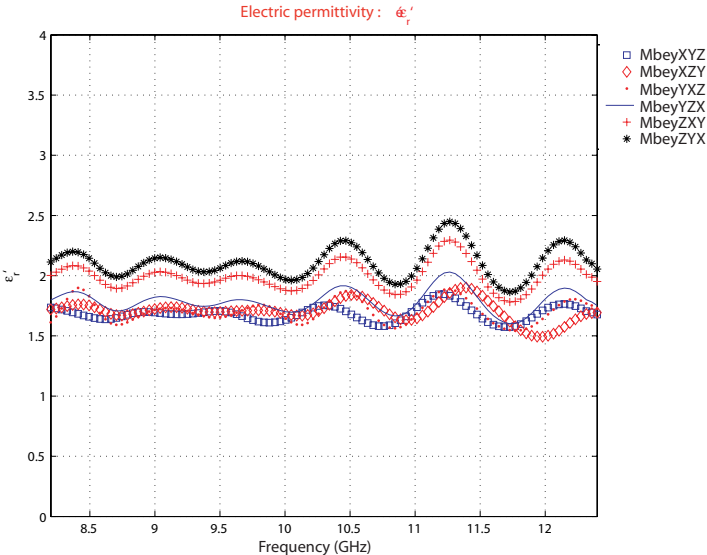


FIGURE 2.56: Relative permittivity of Mbey wood : real part (waveguide)

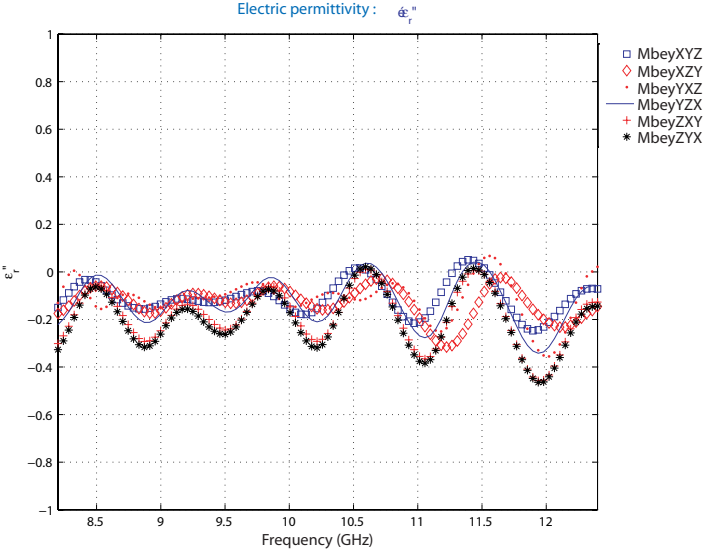


FIGURE 2.57: Relative permittivity of Mbey wood : imaginary part (waveguide)

## CHAPTER 2. WOOD CHARACTERIZATION

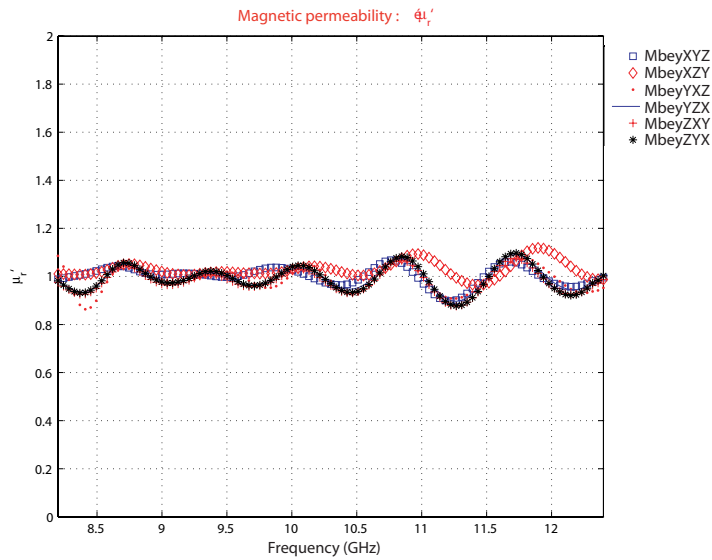


FIGURE 2.58: Relative permeability of Mbey wood : real part (waveguide)

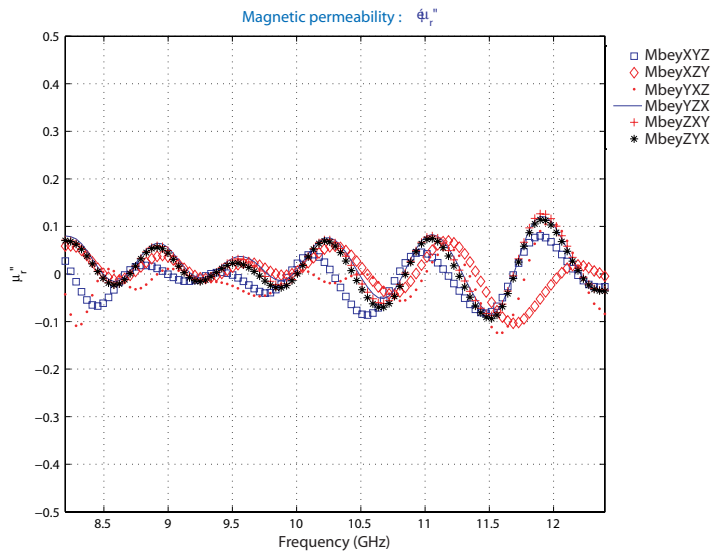


FIGURE 2.59: Relative permeability of Mbey wood : imaginary part (waveguide)



TABLE 2.13: Permittivity values for the non-impregnated Mbey wood (waveguide)

Sample	$\varepsilon'_r$		$\varepsilon''_r$		$\mu'_r$		$\mu''_r$		tan $\delta$	
	$\overline{\varepsilon}'_r$	$\sigma^2$	$\overline{\varepsilon}''_r$	$\sigma^2$	$\overline{\mu}'_r$	$\sigma^2$	$\overline{\mu}''_r$	$\sigma^2$	tan $\delta$	$\sigma^2$
MbeyLxHyEz	1.685	$3.936 \cdot 10^{-3}$	-0.1055	$4.861 \cdot 10^{-3}$	1.002	$1.438 \cdot 10^{-3}$	$-9.554 \cdot 10^{-3}$	$1.630 \cdot 10^{-3}$	$7.229 \cdot 10^{-2}$	$9.452 \cdot 10^{-5}$
MbeyLxHzEy	1.707	$7.493 \cdot 10^{-3}$	-0.1314	$4.665 \cdot 10^{-3}$	1.029	$1.161 \cdot 10^{-3}$	$4.842 \cdot 10^{-3}$	$1.570 \cdot 10^{-3}$	$7.227 \cdot 10^{-2}$	$1.292 \cdot 10^{-3}$
MbeyLyHxEz	1.705	$8.841 \cdot 10^{-3}$	-0.1132	$7.183 \cdot 10^{-3}$	0.988	$2.520 \cdot 10^{-3}$	$-1.542 \cdot 10^{-2}$	$2.236 \cdot 10^{-3}$	$8.169 \cdot 10^{-2}$	$1.443 \cdot 10^{-4}$
MbeyLyHzEx	1.791	$8.360 \cdot 10^{-3}$	-0.1238	$9.010 \cdot 10^{-3}$	0.993	$2.027 \cdot 10^{-3}$	$2.090 \cdot 10^{-2}$	$2.175 \cdot 10^{-3}$	$4.841 \cdot 10^{-2}$	$5.152 \cdot 10^{-4}$
MbeyLzHxEy	1.996	$1.241 \cdot 10^{-2}$	-0.1879	$1.327 \cdot 10^{-2}$	0.981	$2.193 \cdot 10^{-3}$	$1.628 \cdot 10^{-2}$	$2.327 \cdot 10^{-3}$	$7.784 \cdot 10^{-2}$	$5.534 \cdot 10^{-4}$
MbeyLzHyEx	2.109	$1.668 \cdot 10^{-2}$	-0.1998	$1.449 \cdot 10^{-2}$	0.990	$2.6773 \cdot 10^{-3}$	$1.050 \cdot 10^{-2}$	$2.291 \cdot 10^{-3}$	$8.482 \cdot 10^{-2}$	$5.786 \cdot 10^{-4}$

### 2.11.3 Confirmation of measurements using the Open Resonator

#### Non-impregnated Mbey wood measurement results

Observing the TABLE 2.14, we notice differences smaller or equal to 10% on the average values of both methods of measurement. These differences allow us to say that the two measurements are very close and confirm the results obtained.

TABLE 2.14: Permittivity values for the non impregnated Mbey wood (open resonator)

Sample	$\varepsilon'_r$		$\varepsilon''_r$		tan $\delta$	
	$\overline{\varepsilon}'_r$	$\sigma^2$	$\overline{\varepsilon}''_r$	$\sigma^2$	tan $\delta$	$\sigma^2$
MbeyLR	1.677	$2.301 \cdot 10^{-4}$	$1.269 \cdot 10^{-1}$	$8.742 \cdot 10^{-5}$	$7.563 \cdot 10^{-2}$	$2.411 \cdot 10^{-5}$
MbeyLR90	2.014	$1.054 \cdot 10^{-3}$	$2.460 \cdot 10^{-1}$	$6.048 \cdot 10^{-4}$	$1.221 \cdot 10^{-1}$	$1.102 \cdot 10^{-4}$

## CHAPTER 2. WOOD CHARACTERIZATION

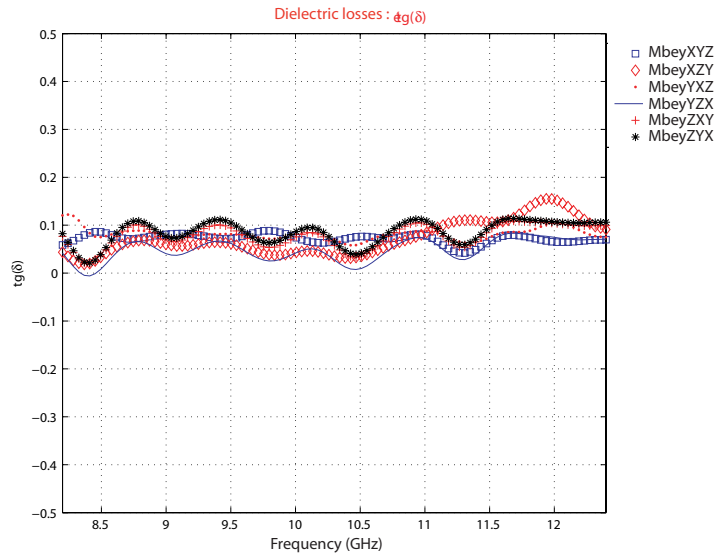


FIGURE 2.60: Dielectric losses of Mbey wood (waveguide)

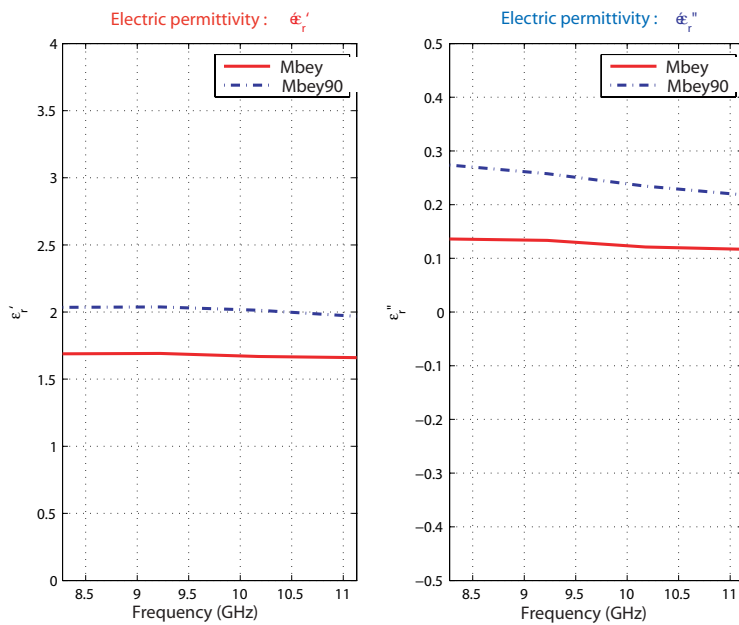


FIGURE 2.61: Relative permittivity of non-impregnated Mbey wood

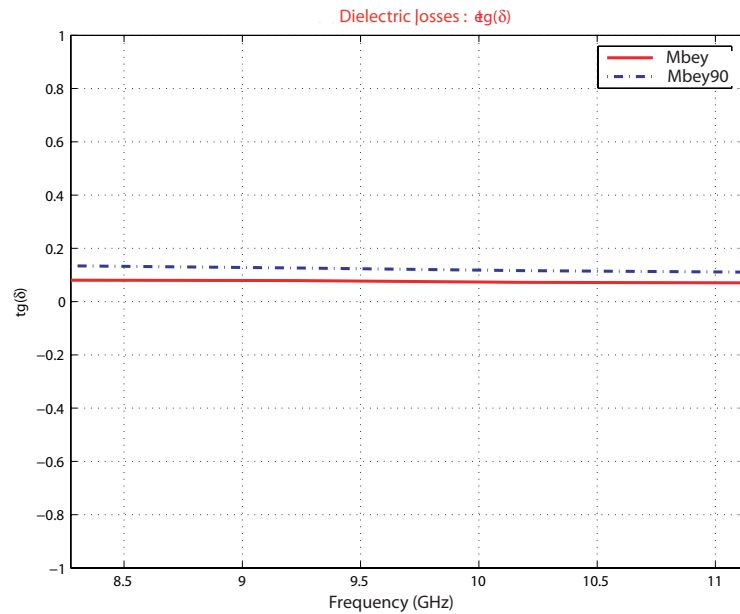


FIGURE 2.62: Dielectric losses of non-impregnated Mbey wood

### 2.11.4 Modelling of Mbey

In tables 2.13 and 2.14, we notice that the values for the two methods of measurement are similar.

#### Relative permeability

According to the results of measurement, the value of the relative magnetic permeability (the imaginary part being negligible) is the same in all the directions and is equal to the unity : the medium is thus non magnetic.

#### Relative permittivity

The values of the relative permittivity are complex, different along the three axes but remain constant in each direction : we have an anisotropic linear dielectric medium. The

dielectric tensor is :

$$\bar{\epsilon}_r = \begin{pmatrix} \bar{\epsilon}_{rx} & 0 & 0 \\ 0 & \bar{\epsilon}_{ry} & 0 \\ 0 & 0 & \bar{\epsilon}_{rz} \end{pmatrix} = \begin{pmatrix} 1.696 - j0.1185 & 0 & 0 \\ 0 & 1.748 - j0.1185 & 0 \\ 0 & 0 & 2.053 - j0.1939 \end{pmatrix}$$

According to what precedes, we notice that  $\bar{\epsilon}_{rx} \approx \bar{\epsilon}_{ry}$  : this anisotropic linear dielectric medium has an uniaxial character.

### Dielectric losses

The tensor of the dielectric losses is :

$$\tan \delta = \begin{pmatrix} \tan \delta_x & 0 & 0 \\ 0 & \tan \delta_y & 0 \\ 0 & 0 & \tan \delta_z \end{pmatrix} = \begin{pmatrix} 7.228 \cdot 10^{-2} & 0 & 0 \\ 0 & 6.505 \cdot 10^{-2} & 0 \\ 0 & 0 & 8.133 \cdot 10^{-2} \end{pmatrix}$$

We notice that the dielectric losses are important in all directions and are higher than  $6 \cdot 10^{-2}$ . These very important losses do not make of Mbey a good candidate for a dielectric substrate.

## 2.12 DIELECTRIC LOSSES VERSUS DENSITY OF THE WOOD

At the beginning of our project we decided to characterize all the species of wood that are available in Cameroon, in order to choose the one that exhibits the lowest losses. We thus became pioneers in the wood characterization in Central Africa. But as we can see, the losses in the wood grow with its density (FIGURE 2.63). We also notice the same phenomena with the variance values (FIGURE 2.64). The variance gives us a degree of confidence in the value of a measurement : if the variance is low, the material can be characterized by the mean value. As we can see in the figure this confidence decreases as the permittivity increases. According to what precedes, since we began the measurements with the less dense among the wood species available in Cameroon, it is not necessary to pursue the characterization of all the woods.

## 2.12. DIELECTRIC LOSSES VERSUS DENSITY OF THE WOOD

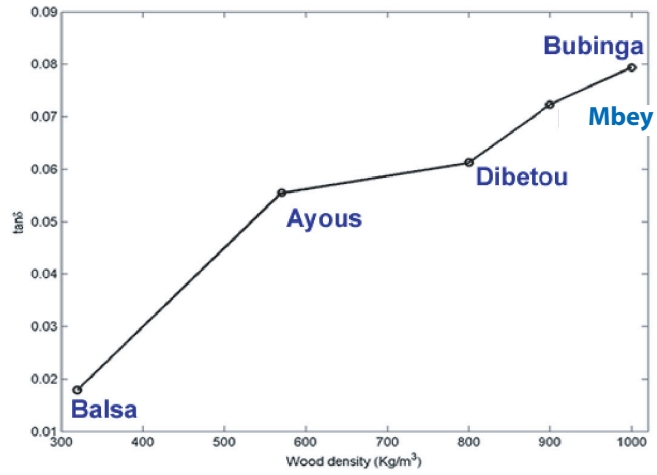


FIGURE 2.63: Dielectric losses versus density

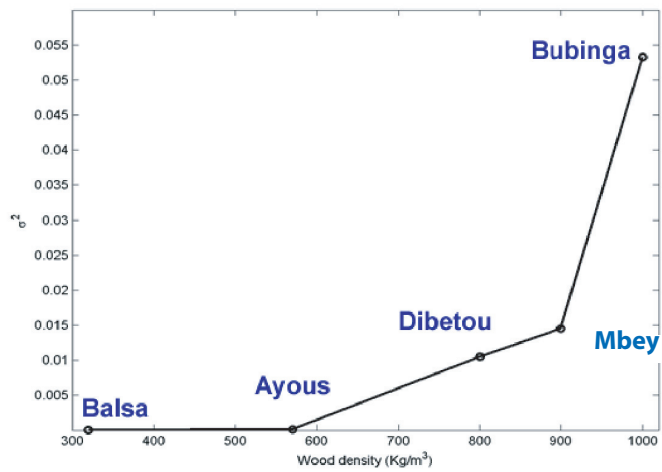


FIGURE 2.64: Variance versus density

### 2.13 CONCLUSION

One of the goals of this project is to use local wood as dielectric in SSFIP type antennas. Before using a material as dielectric in an antenna design, we must know its characteristics. We want to acknowledge the German company IMST which helped us in choosing wood species as substrates, after I had done the first wood characterization. The wood species we used here come mainly from the Central Africa forest. These woods were not yet characterized. This is the first time that the measurement of dielectric constant has been done on Central African wood species. Before we could carry out these measurement, we began by reviewing some commonly used dielectric measurement techniques. Among these measurement techniques, two were available in our laboratory : the waveguide method and the open resonator technique. Since we wanted to measure the anisotropy of wood species, it was necessary to have a sample cut along any of its principal axes. There, only the waveguide method with the small sizes of its samples could allow us to achieve this goal. Therefore, we considered the measurements obtained by this method as reference values. But we still wanted to check whether the measured values were not too far from actual values. This prompted us to conduct a second measurement with open resonator, to determine whether the values from the two methods were close enough. After deriving equations which permitted us to obtain the expressions of dielectric constants, we carried out the two series of measurement on each species wood. First of all, we carried out measurement by using the waveguide method. All the measurement results obtained were summarized in TABLE 2.15. Secondly we carried out measurements using the Open Resonator method. All the measurements obtained by the second method were summarized in TABLE 2.16. Observing the two tables, we can see that the differences between real values and between imaginary values of permittivity  $\epsilon_r$  and loss tangent  $\tan \delta$  provided by the two methods are smaller or equal to 0.1 in absolute value. We can conclude that the values given by the two methods of measurements are sufficiently close, and thus confirm the validity of the measurements. The closeness of the values allows us to say that the values obtained are close to the actual dielectric constants of each species of wood. These measurements reveal that all the species of wood measured possess an anisotropic linear uniaxial dielectric

TABLE 2.15: Waveguide measurement results

Wood specie	$\varepsilon_{rx}$	$\varepsilon_{ry}$	$\varepsilon_{rz}$	$\mu_r$	$\tan \delta_x$	$\tan \delta_y$	$\tan \delta_z$
<i>Ayous</i>	1.767– $j0.0994$	1.776– $j0.1291$	2.091– $j0.1876$	1	5.545 $10^{-2}$	5.992 $10^{-2}$	9.069 $10^{-2}$
<i>Balsa</i>	1.110– $j0.0166$	1.212– $j0.0303$	1.217– $j0.0357$	1	1.791 $10^{-2}$	3.321 $10^{-2}$	3.205 $10^{-2}$
<i>Bubinga</i>	2.691– $j0.2958$	2.767– $j0.2173$	3.270– $j0.4941$	1	7.938 $10^{-2}$	7.085 $10^{-2}$	11.511 $10^{-2}$
<i>Dibetou</i>	1.875– $j0.1296$	1.947– $j0.1209$	2.436– $j0.2783$	1	6.125 $10^{-2}$	6.191 $10^{-2}$	11.330 $10^{-2}$
<i>Mbey</i>	1.696– $j0.1185$	1.748– $j0.1185$	2.053– $j0.1939$	1	7.228 $10^{-2}$	6.505 $10^{-2}$	8.133 $10^{-2}$

character.

Since the antenna will face the humidity of the air, we found biological oil, linseed oil to protect it against the moisture, which does not affect the characteristics of the wood.

Among all the measurements we had made, considering their respective dielectric losses, we could only use two species of wood : we will use Ayous wood as the line substrate, even though it had slightly larger losses, and Balsa wood with its acceptable losses as the patch substrate. We chose Ayous because of its good mechanical characteristics and also because it will be used with a small thickness. Its use, simultaneously with Balsa, will allow us to reach the gain of the Wordspace receiver. The dielectric losses observed with all the other species of wood are much too large, they would not allow us to achieve the characteristics of the Wordspace receiver that we previously mentioned.

These wood characteristics obtained through measurement are not only useful for antenna design. They can also be of interest to industries specializing in microwaves and may find applications in microwave power applications.

Now that the species of wood have been chosen, we can use them to build antennas and find out whether their characteristics will fit the Wordspace receiver requirements.

TABLE 2.16: Open resonator measurement results

Wood specie	$\varepsilon_r$	$\tan \delta$
<i>Ayous</i>	$1.7822 - j0.13991$	$7.8474 \cdot 10^{-2}$
<i>Ayous90</i>	$2.1038 - j0.21029$	$1.0024 \cdot 10^{-1}$
<i>Balsa</i>	$1.2348 - j0.031347$	$2.5384 \cdot 10^{-2}$
<i>Balsa90</i>	$1.3758 - j0.073406$	$5.3344 \cdot 10^{-2}$
<i>Bubinga</i>	$2.6316 - j0.27573$	$1.0457 \cdot 10^{-1}$
<i>Bubinga90</i>	$3.1067 - j0.44553$	$1.4298 \cdot 10^{-1}$
<i>Dibetou</i>	$1.743 - j0.1473$	$8.447 \cdot 10^{-2}$
<i>Dibetou90</i>	$2.176 - j0.2896$	$1.330 \cdot 10^{-1}$
<i>Mbey</i>	$1.677 - j0.1269$	$7.563 \cdot 10^{-2}$
<i>Mbey90</i>	$2.014 - j0.2460$	$1.221 \cdot 10^{-1}$



# Chapter 3

## THE ALUMINIUM-WOOD ANTENNA

### 3.1 INTRODUCTION

In our laboratory, LEMA, several antennas have been designed with conducting materials not made of copper. For instance, our laboratory designed a Beryllium bronze (BzBe) wire antenna for a project to study the terrestrial movements of the European tree frog (*Hyla arborea*) [42]. In another project, called SOLANT, solar cells were used as patch antennas, replacing printed copper sheets [43]-[44]. In the same project, ground planes made of stainless steel were also used in the design of slot antennas [45]. Opening a new and innovative line, in this thesis project we will use aluminium for the radiator, the ground plane and the feed line (it should however be noted that, as far as conductivity is concerned, aluminium is closer to copper than some other metals used elsewhere).

For the antennas that can be usually found in the market, they very seldom make use of wood as an antenna material. For antennas using materials other than the standard high-tech substrates such as FR4, Kapton, Rohacell, the only people who happen to use them are some peculiar individuals like radio amateurs [46]. These particular people sometimes use wood, either as support [47], or to make the mast of their antennas. Cardboard, aluminium foil and materials as curious as potato chips cans [48] are also used to create exciting

antennas very appealing for young people and hence useful for educational purposes. Our work gets inspiration from these attempts and aims to use local materials that can be processed by local people and labor force in order to reduce the price of the antenna. This is another innovation that our work intends to bring.

### 3.2 CHOICE OF THE TECHNOLOGY

The objective of this work is to develop a microstation for the reception of satellite signals, and to make it available to universities in southern countries. Among the antennas operating over the frequency bands used for satellite reception, we selected microstrip antennas, because their size are small and they are easy to manufacture. We plan to use wood and aluminium to manufacture our antenna and we found that the least expensive way to assemble them is by gluing. Since the patch of our antenna will be made out of aluminium, it would be difficult to solder a copper wire feed to an aluminium patch : this can be avoided by feeding the patch through a slot in the ground plane. All these constraints and specifications correspond exactly to the SSFIP antenna [17] geometry. Therefore, we are going to manufacture a SSFIP antenna, using wood for the dielectric substrate and aluminium as patch, ground plane and feed line.

#### 3.2.1 Wood - aluminium assembly

In order to select the best way to assemble our antenna, we carried out four tests by joining Balsa wood with aluminium, using :

- **scotch tape** : it adheres well to wood but can be removed too easily;
- **linseed oil**: wood adheres well to aluminium but it is possible to separate them with a small effort;
- **Araldite glue**: joining is perfect. It requests much effort to separate wood from aluminium;

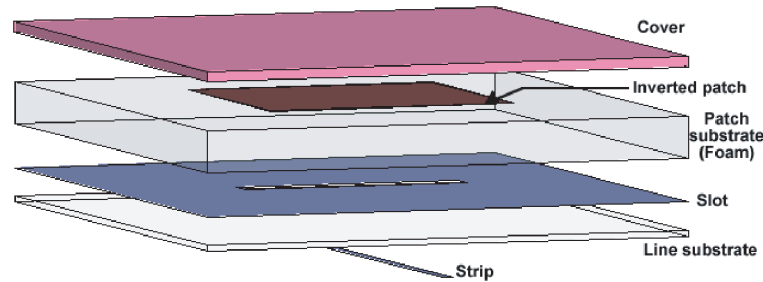


FIGURE 3.1: SSFIP antenna

- **Vlisofix** : it is a joining method which requires heating up to 150 degrees during 30 minutes. Joining is perfect, and it is very difficult to separate wood from aluminium. Unfortunately, this way of assembling reduces the water content and consequently creates constraints in the wood, resulting in some contracting. These constraints and withdrawals create deformations of the wood, which modify the antenna properties. Hence this type of joining is not adapted for our use.

We chose to assemble with Araldite glue, which has a good adherence capacity. This and equivalent local glues are easily available in Cameroon.

### 3.2.2 SSFIP antenna type

The structure of SSFIP antenna is shown in the FIGURE 3.1. Initially we will replace the foam by wood (Balsa). Then we will replace the top layer, which plays the role of protecting cover, by linseed oil. Then we will replace the copper patch by an aluminium patch. Finally we will replace the copper ground plane where the slot is engraved by an aluminium ground plane with the same slot, the FR4 substrate by wood (Ayou) and the copper feed line by an aluminium feed line. At the end we will have an antenna only made of wood and aluminium. The system will be assembled by simply gluing the layers with Araldite.

We will first simulate, and then manufacture antennas with linear polarization and quantify the increase of the losses, which affect particularly the gain of these antennas. Once a linearly polarized antenna has been successfully analyzed and built, the next step

TABLE 3.1: Parameters common to all the antennas

Denomination	Width (mm)	Length (mm)	Thickness (mm)
Strip	-	107.3	-
Line substrate	150	180	-
Ground plane	150	180	-
Patch substrate	150	180	8

will be to move to the realization of a circularly polarized antenna.

### 3.3 COMPARATIVE STUDY OF ANTENNAS

In order to determine whether our project is feasible, we will first find out whether the gain of our antenna built with a wood substrate is large enough for operation with a Worldspace receiver. Then we will measure the gain of all the designed antennas at the same resonant frequency. Since the dimensions of the antenna's patch are related to the resonant frequency and the relative permittivity of the substrate, it will be difficult to have all the antennas with the same size. Equations related to the antenna dimensions are well documented in the literature [15]. For example, the length of microstrip patch antennas is approximately equal to  $\lambda/(2\sqrt{\epsilon_r'})$  where  $\lambda$  is the wavelength of the signal in the air and  $\epsilon_r'$  is the relative permittivity of the substrate. Once the resonance frequency is known, the final dimensions of all the elements of the microstrip antennas were obtained after simulations. All the following antenna's dimensions in this section are related to the wavelength and are optimized through simulations. Since we want to measure the loss of quality, all the antennas must have the same resonant frequency and the same dimensions, especially for substrates because the losses come mainly from substrates. In order to make a valid comparison we will keep constant for each type of antenna the dimensions of elements which have negligible effects on the antennas' resonant frequency or are not dependent on the available dimensions in the market and we will realize linearly polarized antennas. The dimensions which will remain constant are summarized in the TABLE 3.1.

### 3.3. COMPARATIVE STUDY OF ANTENNAS

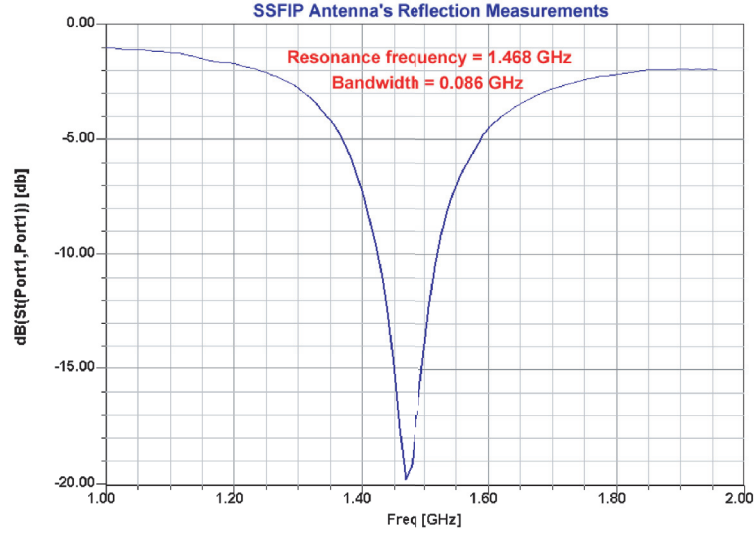


FIGURE 3.2: SSFIP Antenna's reflection measurements

Initially, we will measure the resonant frequencies of each antenna, and then we will take the average of these frequencies to make a comparative measurement of the gain of these antennas. To determine the frequencies of resonance, we will measure the reflection at the antenna input.

#### 3.3.1 Standard SSFIP antenna

In the standard SSFIP antenna we have : a copper patch printed on Kapton which will be used as cover, a Rohacell foam which plays the role of patch substrate, a copper ground plane with the slot and the copper strip which are printed on the FR4 substrate which plays the role of line substrate. All these elements are joined with vlsifix at 150 degrees temperature during 30 minutes. The parameters are summarized in the TABLE 3.2. The reflection measurement (FIGURE 3.2) of this antenna gives us  $f_0 = 1.468$  GHz as resonance frequency and a bandwidth of 5.86%.

TABLE 3.2: SSFIP antenna parameters

Denomination	Width (mm)	Length (mm)	Thickness (mm)	Description
Strip	3	-	0.012	Copper
Line substrate	-	-	1.6	FR4
Ground plane	-	-	0.012	Copper
Slot	42	1.5	0.012	
Patch substrate	-	-	-	Rohacell ( $\epsilon'_r = 1.07$ , $\tan \delta = 0.0008$ )
Patch	80	80	0.017	Copper
Cover	150	180	0.1	Kapton ( $\epsilon'_r = 3.5$ , $\tan \delta = 0.008$ )

### 3.3.2 Wood (Balsa) SSFIP antenna

Here we have all the SSFIP elements but we replace the foam with Balsa wood and all the elements are joined by Araldite glue. The parameters are summarized in the TABLE 3.3. The reflection measurement (FIGURE 3.3) for this antenna gives us  $f_0 = 1.440$  GHz as resonance frequency and a bandwidth of 8%.

### 3.3. COMPARATIVE STUDY OF ANTENNAS

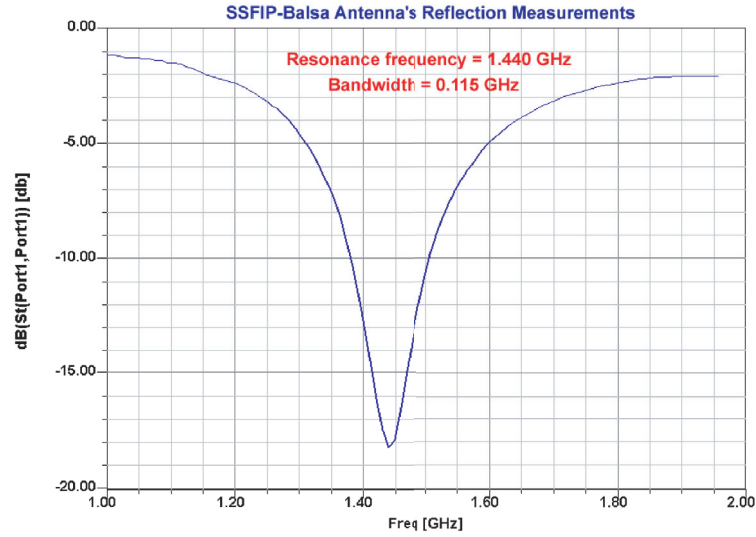


FIGURE 3.3: Wood (Balsa) SSFIP Antenna's reflection measurements

TABLE 3.3: Wood (Balsa) SSFIP antenna parameters

Denomination	Width (mm)	Length (mm)	Thickness (mm)	Description
Strip	3	-	0.012	Copper
Line substrate	-	-	1.6	FR4
Ground plane	-	-	0.012	Copper
Slot	44	1.5	0.012	
Patch substrate	-	-	-	Balsa ( $\epsilon'_r = 1.2$ , $\tan \delta = 0.026$ )
Patch	76	76	0.017	Copper
Cover	150	180	0.1	Kapton ( $\epsilon'_r = 3.5$ , $\tan \delta = 0.008$ )

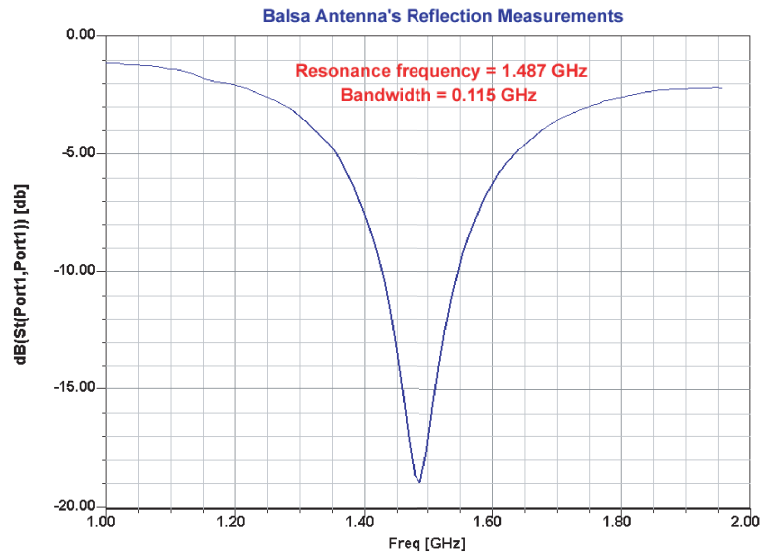


FIGURE 3.4: Balsa Antenna's reflection measurements

### 3.3.3 Balsa antenna

In Balsa antenna we have : an aluminium patch, Balsa wood as patch substrate, a copper ground plane with the slot and the copper strip which are printed on the FR4 substrate which plays the role of line substrate. All these elements are joined with Araldite glue. The parameters are summarized in the TABLE 3.4. The reflection measurement (FIGURE 3.4) for this antenna gives us  $f_0 = 1.487$  GHz as resonance frequency and a bandwidth of 7.73%.

### 3.3.4 Ayous antenna

In Ayous antenna we have : an aluminium patch, Ayous wood as patch substrate, a copper ground plane with the slot and the copper strip which are printed on the FR4 substrate which plays the role of line substrate. All these elements are joined with Araldite glue. The parameters are summarized in the TABLE 3.5. The reflection measurement (FIGURE 3.5) for this antenna gives us  $f_0 = 1.440$  GHz as resonance frequency and a bandwidth of 10.63%.



### 3.3. COMPARATIVE STUDY OF ANTENNAS

TABLE 3.4: Balsa antenna parameters

Denomination	Width (mm)	Length (mm)	Thickness (mm)	Description
Strip	3	-	0.012	Copper
Line substrate	-	-	1.6	FR4
Ground plane	-	-	0.012	Copper
Slot	44	1.5	0.012	
Patch substrate	-	-	-	Balsa ( $\epsilon'_r = 1.2$ , $\tan \delta = 0.026$ )
Patch	76.5	76.5	0.14	Aluminum
Cover				No cover

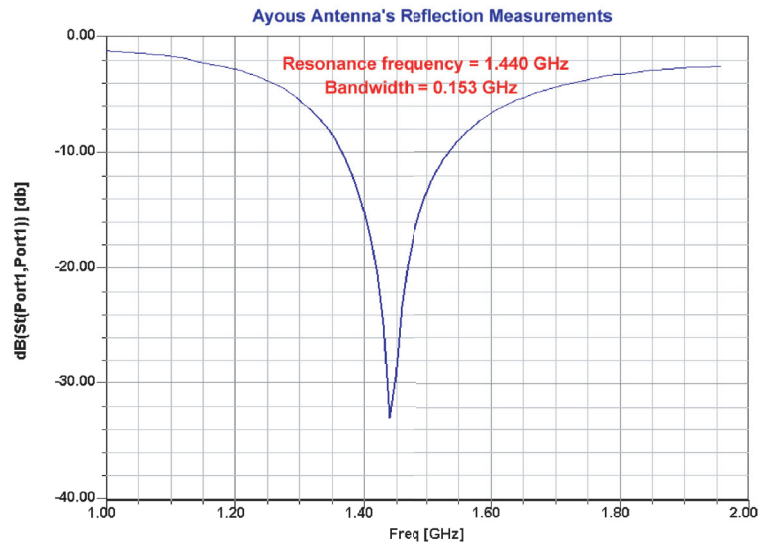


FIGURE 3.5: Ayous Antenna's reflection measurements

TABLE 3.5: Ayous antenna parameters

Denomination	Width (mm)	Length (mm)	Thickness (mm)	Description
Strip	3	-	0.012	Copper
Line substrate	-	-	1.6	FR4
Ground plane	-	-	0.012	Copper
Slot	40	1.5	0.012	
Patch substrate	-	-	-	Ayous ( $\epsilon'_r = 1.77$ , $\tan \delta = 0.0577$ )
Patch	63	63	0.14	Aluminum
Cover				No cover

### 3.3.5 Ayous - Balsa antenna

In Ayous - Balsa antenna we have : an aluminium patch, Balsa wood as patch substrate, an aluminium ground plane with the slot, Ayous wood as line substrate and aluminium strip. All these elements are joined with Araldite glue. The parameters are summarized in the TABLE 3.6. The reflection measurement (FIGURE 3.6) for this antenna gives us  $f_0 = 1.506$  GHz as resonance frequency and a bandwidth of 10.82%.

### 3.3. COMPARATIVE STUDY OF ANTENNAS

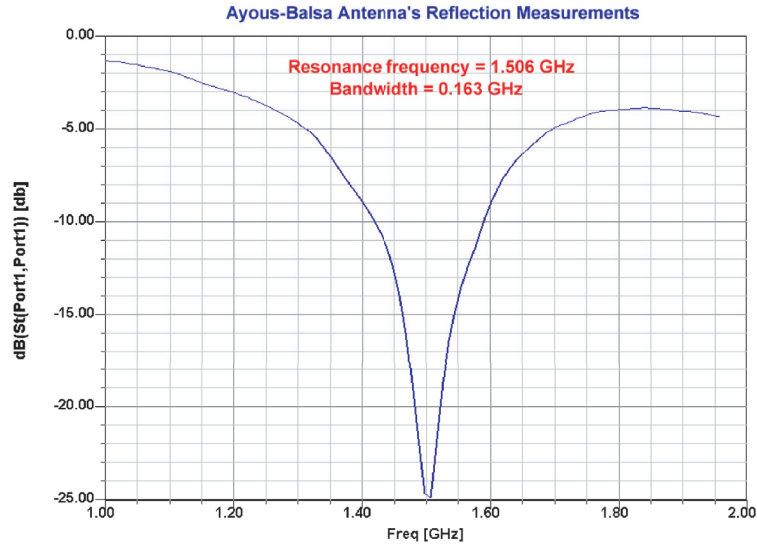


FIGURE 3.6: Ayous-Balsa Antenna's reflection measurements

TABLE 3.6: Ayous-Balsa antenna parameters

Denomination	Width (mm)	Length (mm)	Thickness (mm)	Description
Strip	4	-	0.14	Aluminum
Line substrate	-	-	1.2	Ayous ( $\epsilon'_r = 1.77$ , $\tan \delta = 0.0577$ )
Ground plane	-	-	0.14	Aluminum
Slot	38	4	0.14	
Patch substrate	-	-	-	Balsa ( $\epsilon'_r = 1.2$ , $\tan \delta = 0.026$ )
Patch	75	75	0.14	Aluminum
Cover				No cover

TABLE 3.7: Comparative Gain measurements at 1.468 GHz

Denomination	Gain Loss (dB)	Gain (dB)
SSFIP Antenna	0	10.02
Wood (Balsa) SSFIP antenna	-0.89	9.13
Balsa antenna	-1.05	8.97
Ayous-Balsa antenna	-1.43	8.59
Impregnated Ayous-Balsa antenna	-1.72	8.30
Ayous antenna	-3.64	6.38

### 3.3.6 Comparative study

As we can see, the bandwidths of these antennas fall within the range of those of microstrip antennas. For microstrip antennas the bandwidth decreases when the substrate permittivity increases [49]. In our measurements we note an opposite effect : the measured bandwidths (5.86%–10.82%) grow as the substrate permittivity increases (1.07 ( $\tan \delta = 0.0008$ )–1.77 ( $\tan \delta = 0.0577$ )). This phenomenon observed in measurement values is mainly due to dielectric losses, which play a preponderant role on the increase of the bandwidth. This phenomenon highlights the effect of dielectric losses on the increase in bandwidth of the SSFIP type antenna. In the other hand, using the resonant frequency equation from [15] we verify that the calculated and the measured values of the resonant frequency are very close : this verification confirms the validity of our measurements.

These various measurements show us that it is difficult to simulate, and then to manufacture, at a nonindustrial level, antennas having exactly the same frequencies of resonance. However, the frequency dispersion is not so large, so we will take the average value of all these resonant frequencies and then quantify the gain losses by using the SSFIP antenna as a reference. After calculation we obtain  $f_{0moy} = 1.468$  GHz as average value. Measured reflection coefficients at resonance are always below -15 dB so we can consider that all the antennas are well matched during the gain measurements. At the frequency  $f_{0moy} = 1.468$  GHz we will measure the reduction in gain as compared to that of SSFIP antenna. The results obtained are summarized in TABLE 3.7.

### 3.3. COMPARATIVE STUDY OF ANTENNAS

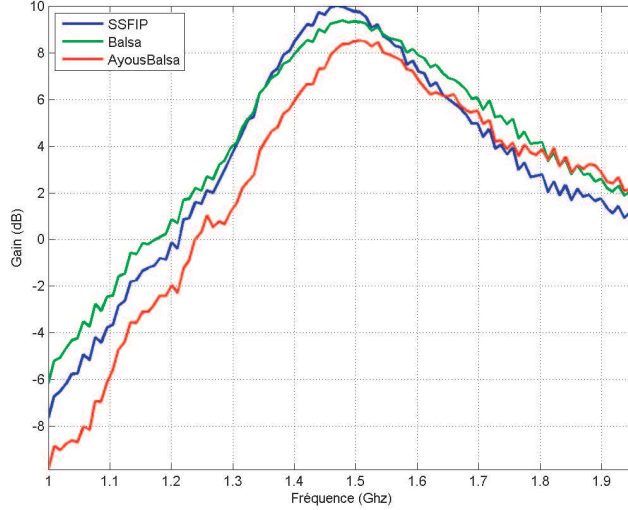


FIGURE 3.7: Three antennas gain measurement method

TABLE 3.7 shows us that all the gain values are greater than the 6 dB gain of the Worldspace receiver antenna. We also notice a large difference, of about 3 dB between the SSFIP antenna and the Ayous antenna. But this difference is reduced by half, down to 1.43 dB between the SSFIP antenna and the Ayous-Balsa antenna : this result confirms the assumption we made earlier, according to which losses in Ayous-Balsa antenna will be definitely lower than those of Ayous antenna. In addition, we notice losses of  $-1.72$  dB when the antenna is impregnated with linseed oil. These losses make a difference of 0.29 dB between the impregnated and the non impregnated Ayous-Balsa antenna. This is not so bad and this result comes to confirm that this oil can be used to protect the wood against moisture. We finally measured the intrinsic gains of the Balsa and Ayous-Balsa antennas by using the method of three antennas [78], taking as third antenna the SSFIP antenna (FIGURE 3.7). We notice that the gains of the three antennas are greater than 7 dB over the DAB frequency band and this is a satisfactory information to use these wood antenna for satellite reception.

Now that our first idea, which is to use wood as substrate has been just confirmed by measurements, we will launch the measurement of the other characteristics of this type of

TABLE 3.8: Linearly polarized Balsa antenna parameters

Denomination	Width (mm)	Length (mm)	Thickness (mm)	Description
Strip	3	107.3	0.017	Copper
Line substrate	150	180	1.6	FR4
Ground plane	150	180	0.017	Copper
Slot	69	1.5	0.017	
Patch substrate	150	180	12.3	Balsa ( $\epsilon'_r = 1.2$ , $\tan \delta = 0.026$ )
Patch	76	76	0.14	Aluminum

antenna.

## 3.4 LINEARLY POLARIZED ANTENNA

We will study in this section the characteristics of antennas that present the larger interest for our project : the Balsa antenna and the Ayou-Balsa antenna.

### 3.4.1 Balsa antenna

The parameters of the Balsa antenna (FIGURE 3.8) are summarized in the TABLE 3.8.

#### Sensitivity to misalignments

Before gluing the patch on the substrate, we made a test of antenna sensitivity. Reflection measurements were made without absorbent. We initially measured the reflection with the patch placed at its initial location. Then we performed measurements with the patch in one of the following positions :

- the patch is moved 5 mm in the (ox) axis only;
- the patch is moved 5 mm in the (oy) axis only;

### 3.4. LINEARLY POLARIZED ANTENNA

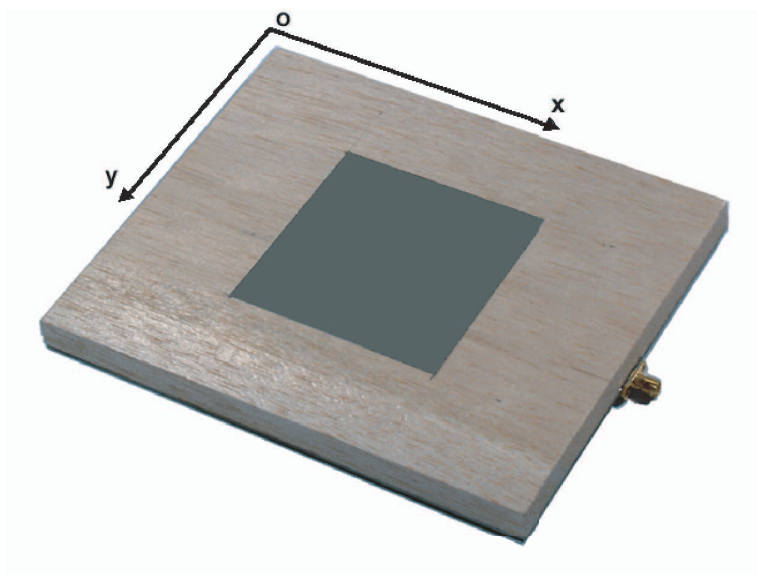


FIGURE 3.8: Balsa antenna

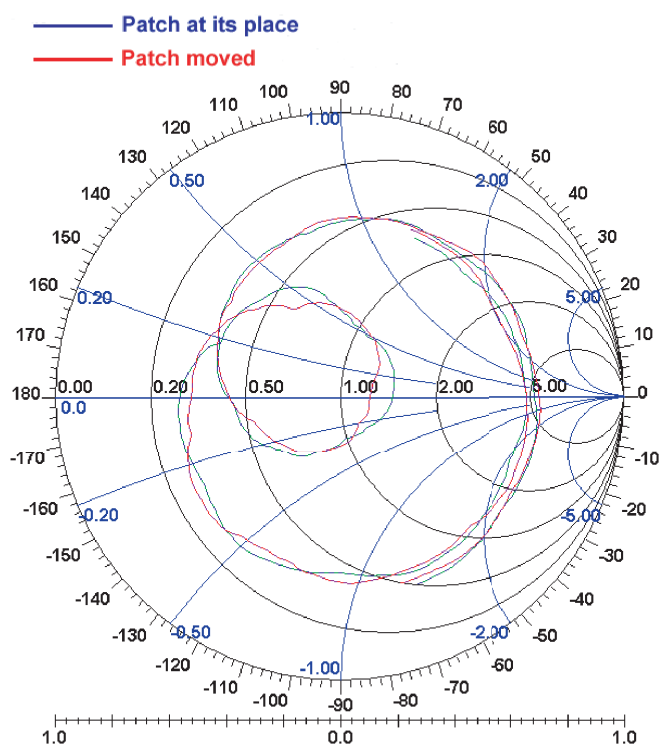


FIGURE 3.9: Antenna with patch on place and moved

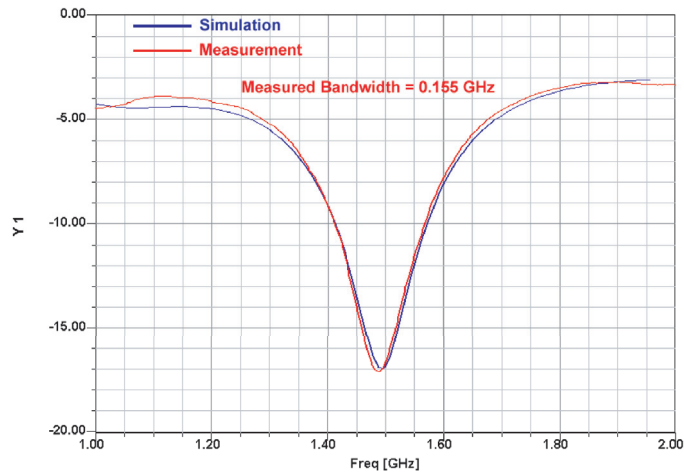


FIGURE 3.10: Antenna reflection : rectangular coordinates diagram

- the patch is moved 5 mm simultaneously in (ox) and (oy) axis;
- the patch has undergone a rotation of  $45^{\circ}$ ;

For each one of these positions of the patch, we have noticed that the adaptation of the antenna did not undergo significant changes (FIGURE 3.9). This enables us to say that the linearly polarized antenna with wood substrate has a very small sensitivity to a displacement lower or equal to 5 mm of the patch.

### Reflection measurement

On the FIGURE 3.10 we have both the simulation and the measurement graphs of the reflection coefficient. From this graph we notice a very small difference between the curve resulting from simulation and that obtained by measurements. We can say that the two results are practically identical. On the Smith chart (FIGURE 3.11) we notice for certain values that the real and imaginary parts differ slightly : we can see a rotation towards the left of the crossing point of the curve. But the adaptation of the antenna with respect to the two methods coincides perfectly.



### 3.4. LINEARLY POLARIZED ANTENNA

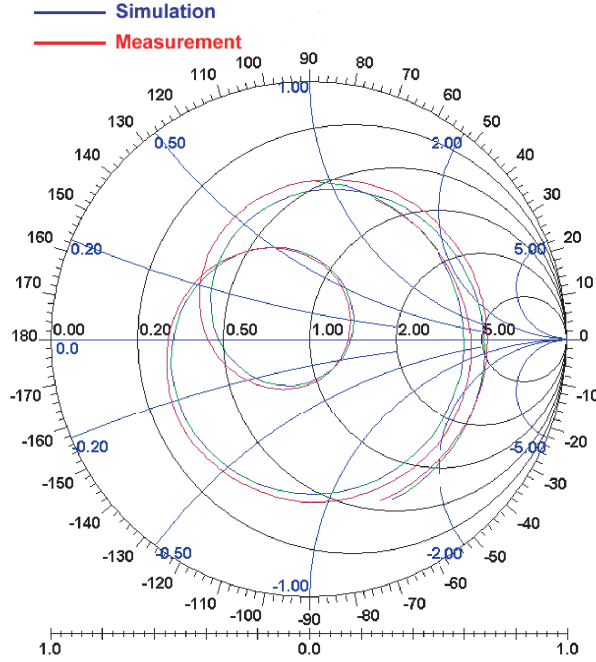


FIGURE 3.11: Antenna reflection : Smith chart

#### Antenna gain

This measurement was made by using a log-periodic antenna as reference antenna (FIGURE 3.12). The error due to measurement by using this antenna is less or equal to  $\pm 0.5$  dB. We observe a difference of  $2.19 \pm 0.5$  dB between simulation and measurements results. In addition the measured gain of 9.856 dB allows us to say that our antenna can be connected to a Worldspace receiver.

#### Radiation pattern

We simulated, and then measured the field in the E plane (FIGURE 3.13, FIGURE 3.14) and in the H plane (FIGURE 3.15, FIGURE 3.16). We note that, according to these figures, all the curves behave in a similar manner.

In the E plane, the measured pattern exhibits a dissymmetry, which must certainly be related to the fact that the antenna presents a manufacture dissymmetry.

In the H plane we have a perfect symmetry.

## CHAPTER 3. THE ALUMINIUM-WOOD ANTENNA

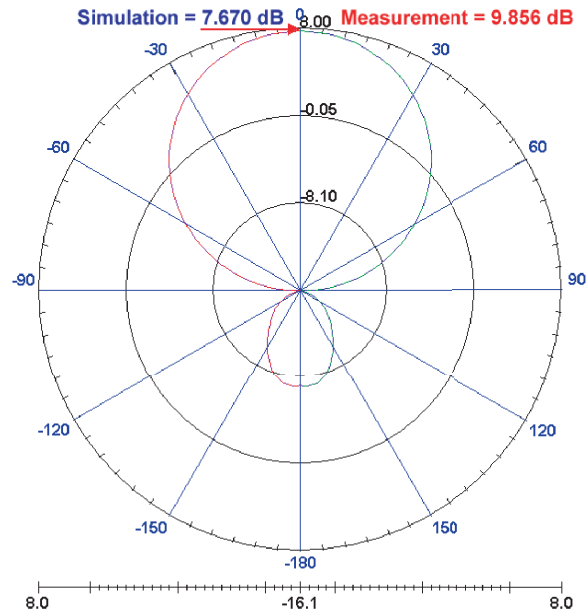


FIGURE 3.12: Radiation pattern

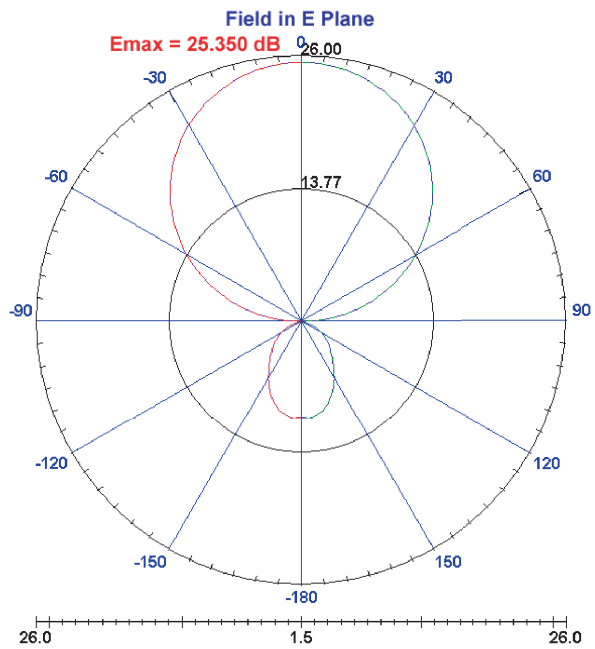


FIGURE 3.13: Simulated Radiation pattern in E plane

### 3.4. LINEARLY POLARIZED ANTENNA

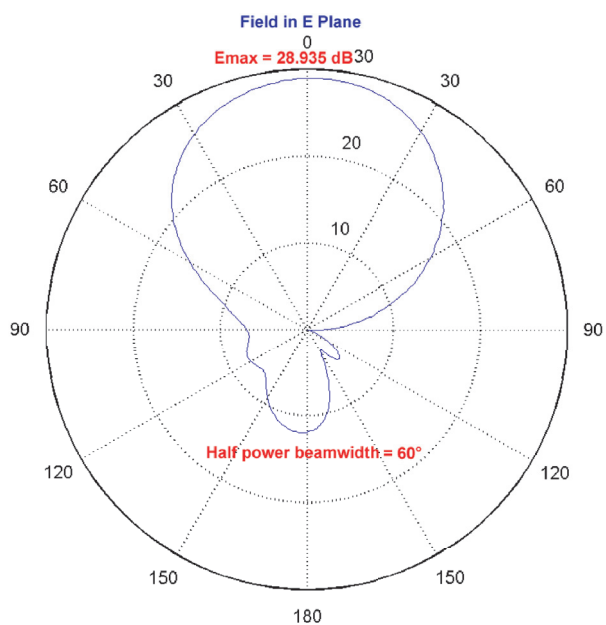


FIGURE 3.14: Measured Radiation pattern in E plane

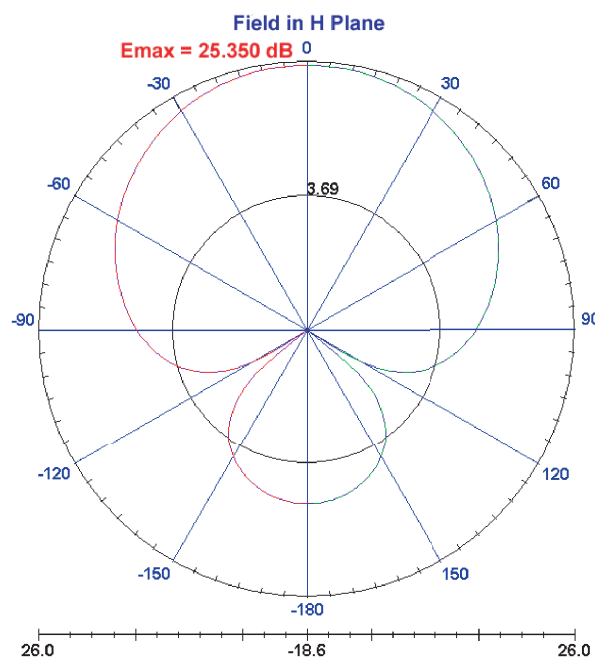


FIGURE 3.15: Simulated Radiation pattern in H plane

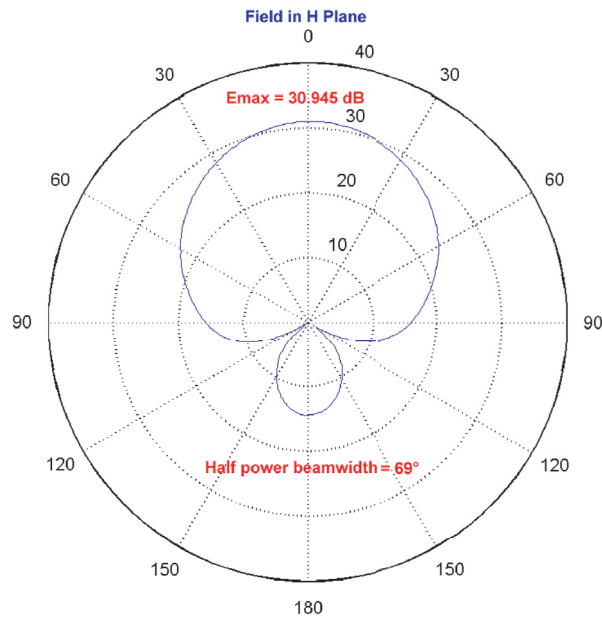


FIGURE 3.16: Measured Radiation pattern in H plane

In term of values we observe a difference (measured E - simulated E) of +3.585 dB in the E plane and of +5.595 dB in the H plane for the maximum values of the field. This is very encouraging for the realization of this antenna.

The measurement of the cross-polar field (FIGURE 3.17) shows that it is very small, and this allows us to verify that our antenna has a linear polarization.

### Influence of protection layer

We whitewashed our antenna with linseed oil. Then we took measurements (FIGURE 3.18) to appreciate the influence of this layer of protection on the antenna properties. We notice that the amplitude did not change but that a small displacement in frequency of  $-0.02$  GHz : this result confirms the fact that we can use linseed oil to protect wood against moisture.

### 3.4. LINEARLY POLARIZED ANTENNA

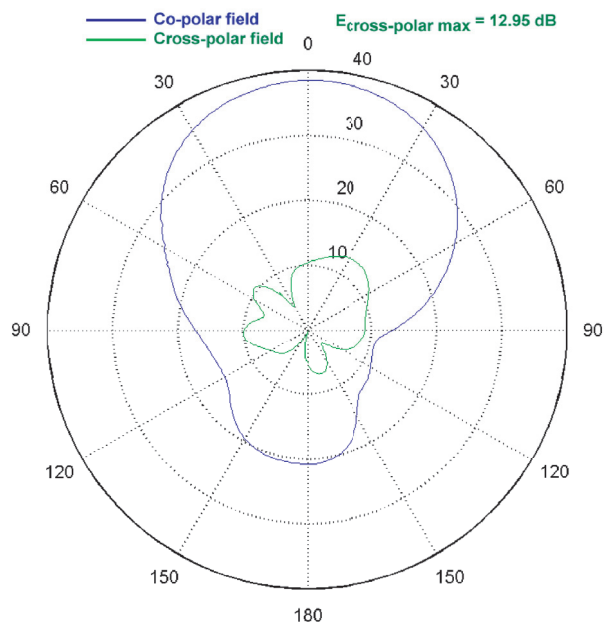


FIGURE 3.17: Measured Co-polar and cross-polar field

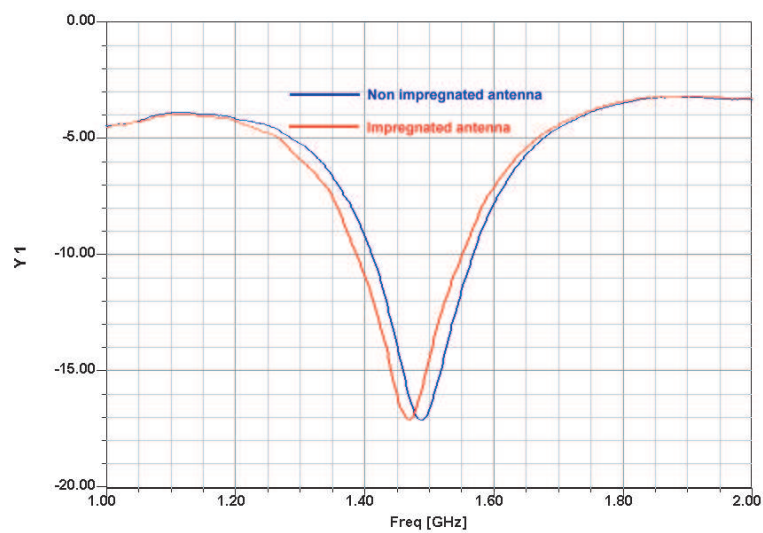


FIGURE 3.18: Comparison between impregnated and non impregnated antennas

TABLE 3.9: Linearly polarized Ayous-Balsa antenna parameters

Denomination	Width (mm)	Length (mm)	Thickness (mm)	Description
Strip	4	107.3	0.14	Aluminum
Line substrate	150	180	1.2	Ayous ( $\epsilon'_r = 1.77$ , $\tan \delta = 0.0577$ )
Ground plane	150	180	0.14	aluminum
Slot	38	4	0.14	
Patch substrate	150	180	8	Balsa ( $\epsilon'_r = 1.2$ , $\tan \delta = 0.026$ )
Patch	75	75	0.14	Aluminum

### 3.4.2 Ayous-Balsa antenna

The Ayous-Balsa antenna's parameters are summarized in TABLE 3.9.

#### Reflection measurement

On the rectangular coordinates graph (FIGURE 3.19) and on the Smith chart (FIGURE 3.20) we have simulated and measured values of reflection coefficient. We notice a frequency shift of 0.04 GHz between measurement and simulation. This frequency shift must certainly come mainly from the assembly and the joining of the various elements. The curves have however the same look.

#### Antenna's gain

We measured the absolute gain (FIGURE 3.7) of this antenna by the method of three antennas. We have for the DAB frequency band a gain above the minimum required value for a Worldspace receiver.

### 3.4. LINEARLY POLARIZED ANTENNA

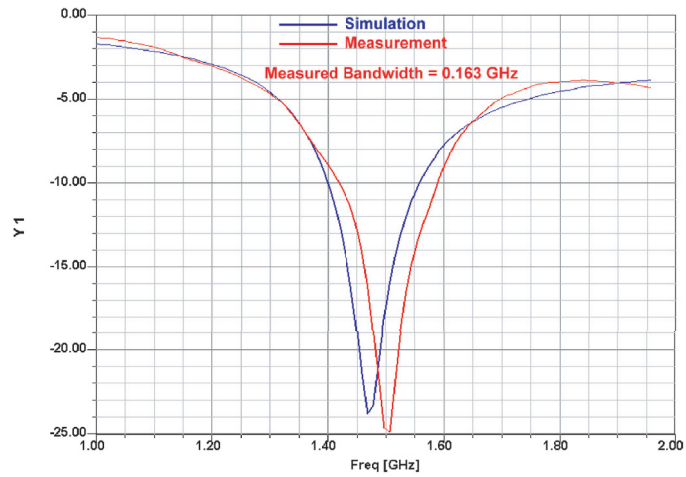


FIGURE 3.19: Antenna reflection : cartesian coordinates diagram

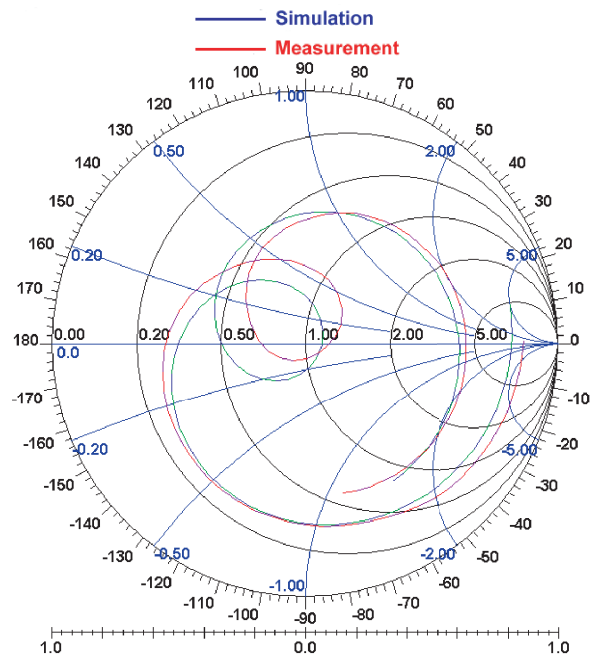


FIGURE 3.20: Antenna reflection : Smith chart

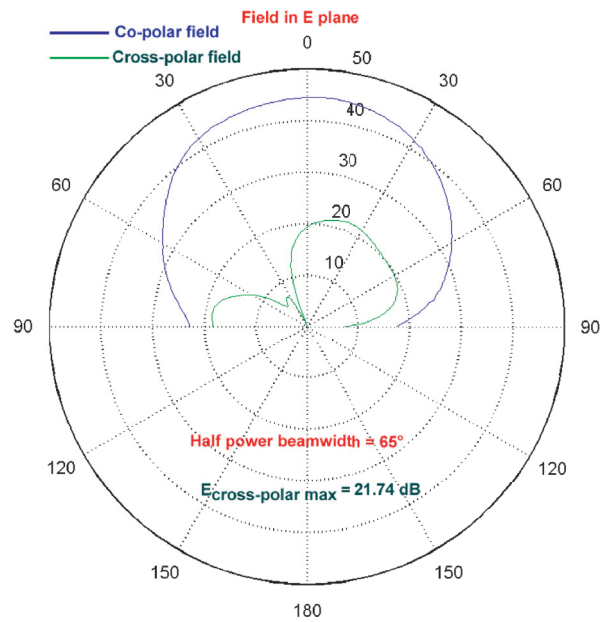


FIGURE 3.21: Measured Co-polar and cross-polar patterns in the E plane

### Radiation pattern

We measured the co-polar and cross-polar field patterns in the E plane (FIGURE 3.21) and in the H plane (FIGURE 3.22). We notice a perfect symmetry of the curves, with the values slightly larger than those for the Balsa antenna.

In addition we notice a good linear polarization.

### Influence of protection layer

We whitewashed our antenna with linseed oil. Then we took measurements (TABLE 3.7) to appreciate the influence of this layer of protection on the antenna properties. We do notice a slight difference of 0.29 dB between the impregnated and the non impregnated antenna. This result confirms once more that we can use linseed oil to protect wood against moisture.



## 3.5. CIRCULARLY POLARIZED ANTENNA

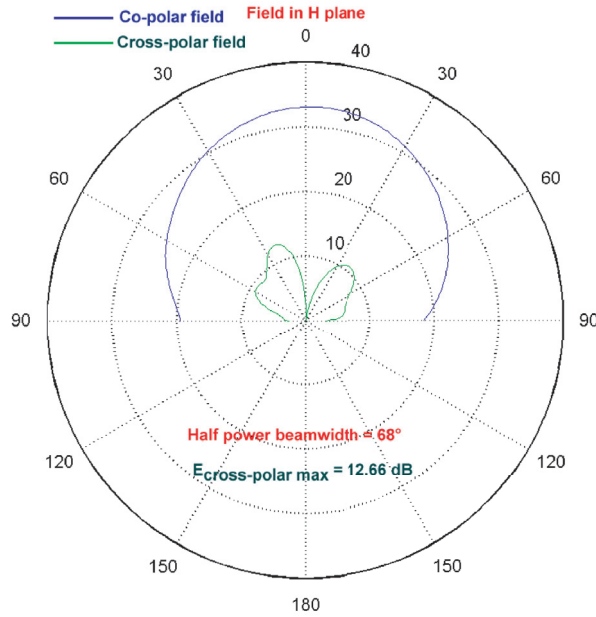


FIGURE 3.22: Measured Co-polar and cross-polar patterns in the H plane

### 3.4.3 Conclusion

In view of its good behaviour and best results obtained, we can confirm that wood and aluminium can be used to manufacture an antenna with the SSFIP geometry, using wood as substrate. In the following section we will show that the results obtained and the conclusion drawn remain valid for a circularly polarized antenna.

## 3.5 CIRCULARLY POLARIZED ANTENNA

Since the results for the analysis of circularly polarized antennas are similarly independent of the antenna type, we will focus on the Ayous-Balsa left circularly polarized antenna. The schematic of the circularly polarized antenna in the plane is represented by the FIGURE 3.23 and its feed line is represented by the FIGURE 3.24.

The parameters of the antenna are summarized in TABLE 3.10.

We notice here a notorious difference between measurements and simulation on the level of the reflection (FIGURE 3.25, FIGURE 3.26). This difference comes mainly from

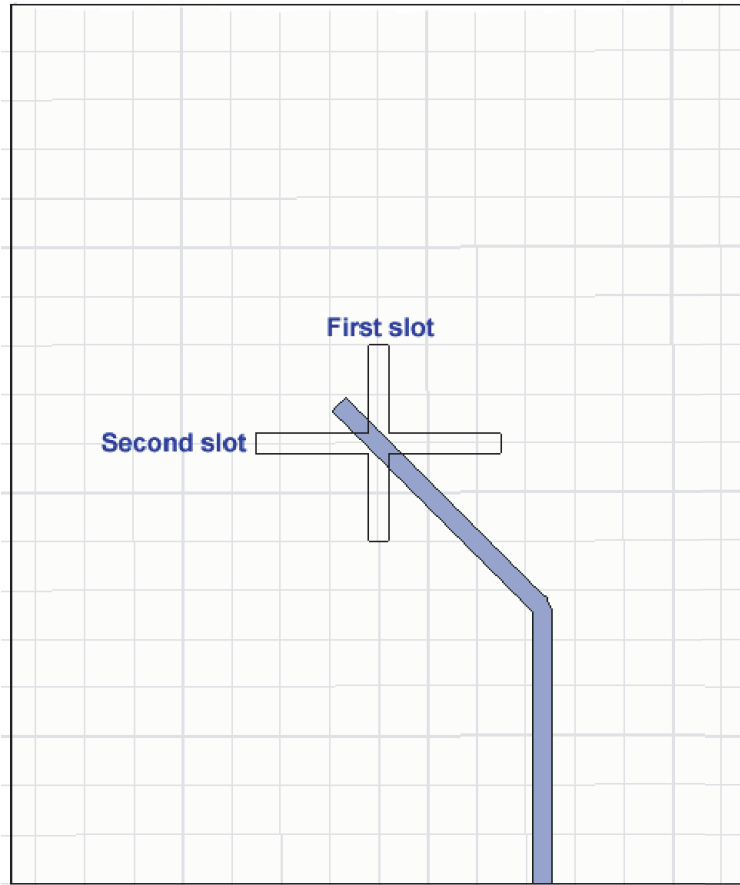


FIGURE 3.23: Left circularly polarized antenna

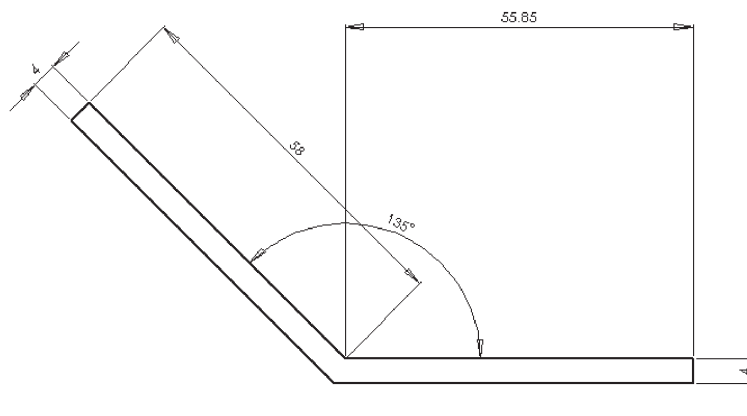


FIGURE 3.24: Strip dimensions of left circularly polarized antenna

### 3.5. CIRCULARLY POLARIZED ANTENNA

---

TABLE 3.10: Left circular polarized Ayous-Balsa antenna parameters

Denomination	Width (mm)	Length (mm)	Thickness (mm)	Description
Strip	-	-	0.14	Aluminum
Line substrate	150	180	1.2	Ayous ( $\epsilon'_r = 1.77$ , $\tan \delta = 0.0577$ )
Ground plane	150	180	0.14	Aluminum
First slot	4	40	0.14	
Second slot	50	4	0.14	
Patch substrate	150	180	8	Balsa ( $\epsilon'_r = 1.2$ , $\tan \delta = 0.026$ )
Patch	70	76	0.14	Aluminum

manufacture errors.

In addition the measurement of the radiation pattern (FIGURE 3.27) with a spinning dipole gives a better ellipticity. Nevertheless this ellipticity can be improved.

Finally, the measured gain is 5.153 dB (FIGURE 3.28). This value is smaller than that of the Worldspace antenna. But we can compensate this drawback by using a low noise amplifier with a gain higher than the one specified in the Worldspace characteristics. This result can also be improved upon by seeking the best parameters in the simulation. We will be able to connect our Ayous-Balsa antenna to the Worldspace receiver by using an amplifier with a gain higher than 14.84 dB.

## CHAPTER 3. THE ALUMINIUM-WOOD ANTENNA

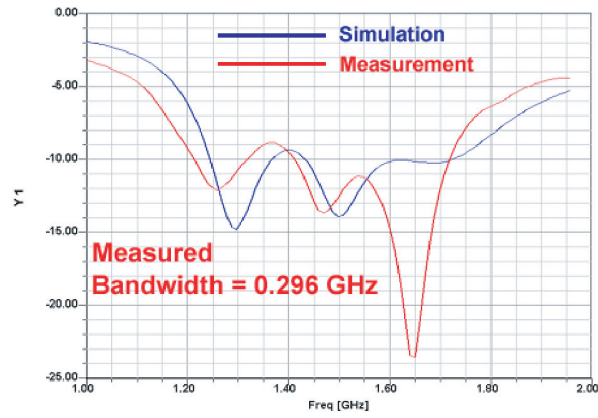


FIGURE 3.25: Antenna reflection : cartesian coordinates plot

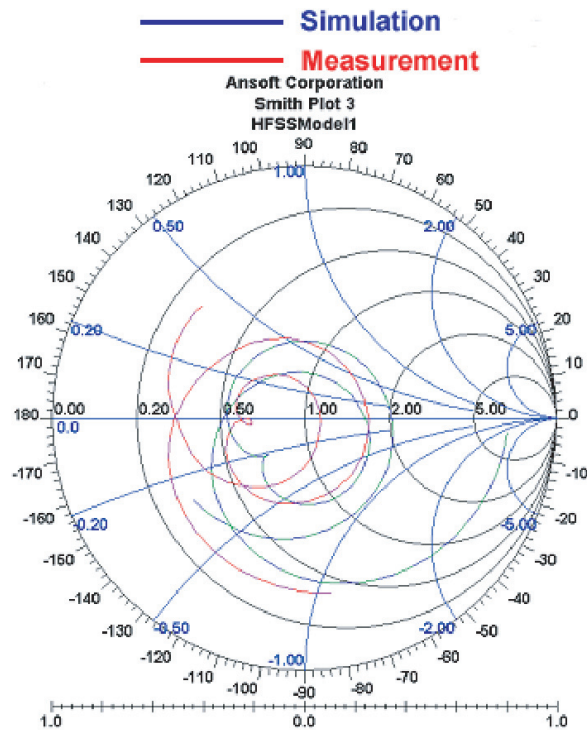


FIGURE 3.26: Antenna reflection : Smith chart

### 3.5. CIRCULARLY POLARIZED ANTENNA

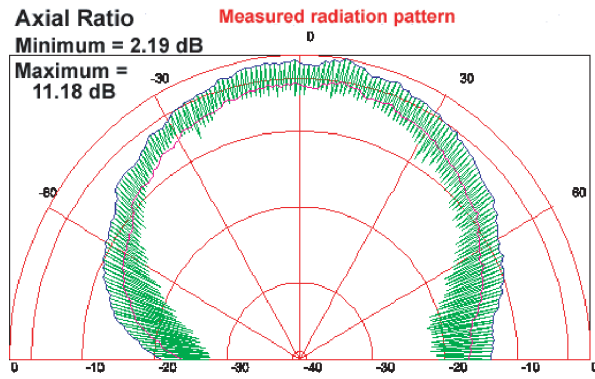


FIGURE 3.27: Measured radiation pattern

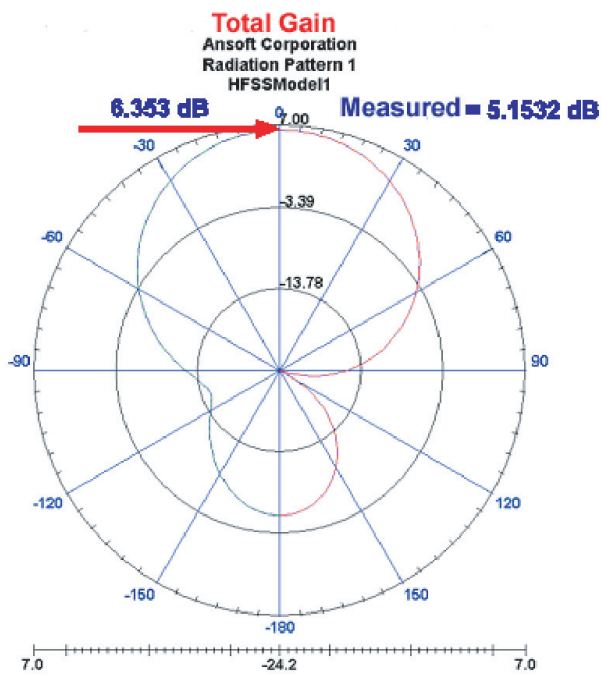


FIGURE 3.28: Measured gain

### 3.6 CONCLUSION

Our first idea was to use local materials to design antennas. Since we planned to use aluminium for the radiating patch, we might well had to face the notorious technological problem : connecting aluminium to copper was always difficult and problematic, either by soldering or by welding. Therefore we used here the SSFIP configuration, which was a good compromise between simplicity and performances. The different blocks of the antenna were assembled by simply gluing the layers with a classical glue of Araldite type, which was locally available in Cameroon. As far as our knowledge goes, this was the first time that antennas were designed and manufactured with wood as line and patch substrates, and aluminium as patch, ground plane and feed line. We manufactured antennas with different technologies and we did compare measurements, essentially to quantify the reduction in gain with respect to the reference SSFIP antenna. All the designed antennas (Balsa, Ayous-Balsa, impregnated Ayous-Balsa and Ayous antennas) exhibited a large enough gain to be connected to a Worldspace receiver. But if we looked carefully at the gain values, we would notice that the gain of the Ayous antenna was just at the borderline for the Worldspace requirement : no manufacturing error would be tolerated! Since we would like to have non professional people manufacture these antennas, we chose the Balsa antenna and the Ayous-Balsa antenna. As we could expect, we observed a reduction in gain of -1.43 dB for a non-impregnated Ayous-Balsa antenna and of -1.72 dB for an impregnated Ayous-Balsa antenna, which were smaller than those of the Ayous antenna. These measurements, which we had just taken, confirmed that antennas can be manufactured at a lower cost, by using only wood and aluminium, with a simple assembling process : gluing. It also confirmed that linseed oil could protect the wood against moisture. The best antenna built upon a wood substrate gave us a highest maximum gain of 8.54 dB, value which was only 1.46 dB below the maximum value of the SSFIP reference antenna. In addition we achieved a better radiation diagram in linear polarization, both in the E and the H plane, and in circular polarization too. We also remarked that the wood antenna tolerates manufacturing errors when the patch was displaced laterally. These results led us to confirm that an antenna with a wood substrate could be used for the reception of the Worldspace satellites signals.

In order to make use of these encouraging results, we will, in the next chapter, design a low noise amplifier, associate it to the antenna and then carry out satellite receiving tests.

## CHAPTER 3. THE ALUMINIUM-WOOD ANTENNA

---



# Chapter 4

## RF FRONT-END

### 4.1 Introduction

In the previous chapter we designed an aluminium-wood antenna. In order to verify if the designed antenna can be used for satellite reception, the next step will be to connect it to a commercial satellite receiver and use the system for reception tests of satellite signals. The signal received from the satellite by this kind of antenna is very weak. If we want to use the antenna for the reception of satellite signals it will be important to strengthen the received signal with a low noise amplifier (LNA) before connecting it to the receiver. Since the received signal's amplitude is too small, the LNA must be placed as close as possible to the antenna. The easiest way of doing it is to integrate directly the LNA with the antenna. Thus the antenna and the LNA constitute an active antenna and form what we call here the radiofrequency (RF) front-end.

Our application targets to provide a global system for the reception of satellite signals. To achieve this goal, we need an active antenna. In this chapter we will review some calculations relative to LNA. Then we will design, manufacture and measure the LNA characteristics. Afterwards we will join the LNA to the planar antenna and connect the active antenna obtained in this manner to a commercial Worldspace receiver. Finally, we will perform receiving tests of the Worldspace radio station with the system designed.

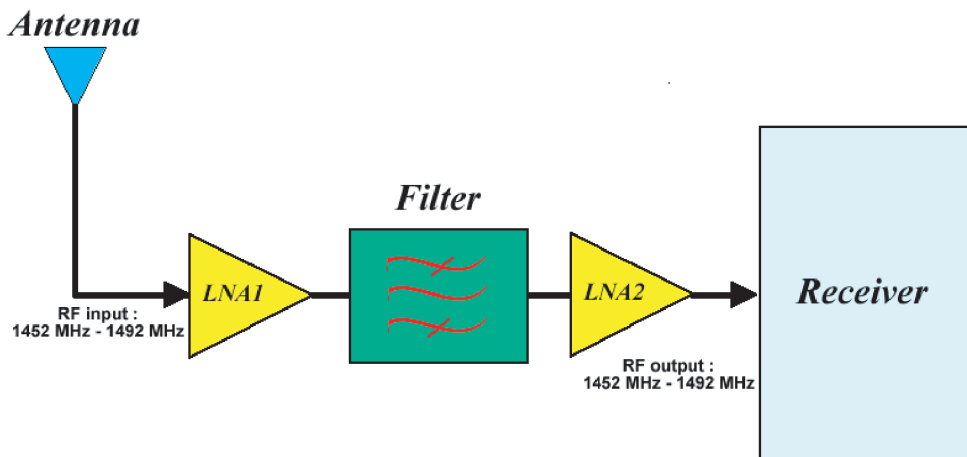


FIGURE 4.1: RF receiver system

## 4.2 Simplified strategy for the LNA

In professional RF receiver and front-end systems the amplification of the signal at the microwave level is often achieved with a chain of two cascade low noise amplifier separated by a filter (FIGURE 4.1). Indeed, it is essential to select a preamplifier (LNA) having a noise figure as low as possible, because this first stage generally determines to a large extent the noise performance of the whole system. The Low Noise Amplifier allows one to combine a low noise figure and a reasonable gain, as well as a good stability over the whole frequency range of operation. This preamplifier is usually located as close as possible to the antenna and is frequently fully integrated with it, giving rise to a true "active antenna". The second amplifier (LNA2) provides the final power boost to the system.

Within the framework of our project, as we try to reduce the manufacturing costs of the system, we will remove the filter and the second amplifier LNA2, which we do not consider essential for our design : the antenna will then be directly connected to the receiver through a single amplifier LNA1.

Moreover, we will propose for the LNA1 a simplified design whose block-scheme is given in FIGURE 4.2. It is hoped that the impedance matching networks around the active chip element can be easily fabricated with a very cheap and elementary printed substrate technology.

## 4.2. SIMPLIFIED STRATEGY FOR THE LNA

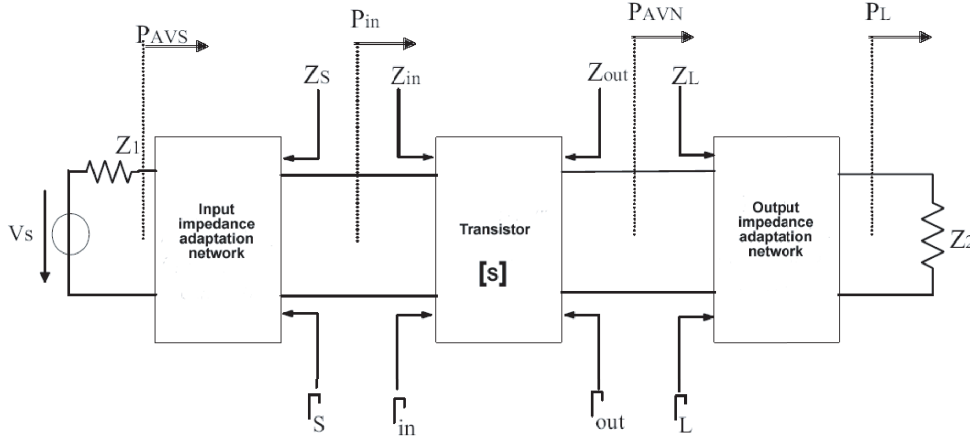


FIGURE 4.2: General configuration selected for our amplifier

The FIGURE 4.2 illustrates the general structure of the resulting design. It includes an active device (in general a transistor), characterized by its S parameters and surrounded on both sides by impedance matching networks. The analysis of this configuration enables us to determine the main parameters characterizing a low noise amplifier : the gain, the noise factor and the stability.

### 4.2.1 Linear characterization of low noise amplifiers [50]-[51]

We will provide the expressions for the main parameters that one must take into account when designing low noise amplifiers.

#### Amplifier gain

**Transfer gain :** The transfer gain or transductive gain is defined as the ratio of the power delivered to the load  $P_L$  by the power available from the source  $P_{AVS}$  :

$$G_T = \frac{1 - |\Gamma_S^2|}{|1 - S_{11}\Gamma_S|^2} |S_{21}|^2 \frac{1 - |\Gamma_L^2|}{|1 - \Gamma_{out}\Gamma_L|^2} = G_1 G_0 G_2 \quad (4.2.1)$$

with :

$$G_0 = |S_{21}|^2$$

$$G_1 = \frac{1 - |\Gamma_S^2|}{|1 - S_{11}\Gamma_S|^2}$$

$$G_2 = \frac{1 - |\Gamma_L^2|}{|1 - \Gamma_{out}\Gamma_L|^2}$$

$\Gamma_{out}$  is the reflection coefficient at the output of the quadripole when it is terminated by an impedance  $Z_S$  corresponding to the reflection coefficient  $\Gamma_S$ . These coefficients are given by :

$$\Gamma_{in} = S_{11} + \frac{S_{12}S_{21}\Gamma_L}{1 - S_{22}\Gamma_L} \quad (4.2.2)$$

$$\Gamma_{out} = S_{22} + \frac{S_{12}S_{21}\Gamma_S}{1 - S_{11}\Gamma_S} \quad (4.2.3)$$

Note :

If  $Z_S = Z_L = R_0$ , then,  $G_T = |S_{21}|^2$ .

**Available gain :** The available gain  $G_A$  or associated gain is equal to the transductive gain when the output of the quadripole is conjugate matched. It is obtained by setting  $\Gamma_L = \Gamma_{out}^*$  in the equation (4.2.1).

$$G_A = \frac{1 - |\Gamma_S^2|}{|1 - S_{11}\Gamma_S|^2} |S_{21}|^2 \frac{1}{1 - \Gamma_{out}^2} \quad (4.2.4)$$

This gain reaches its maximum when the input and the output are simultaneously matched. The maximum available gain ( $MAG$ ) is then defined by setting  $\Gamma_L = \Gamma_{out}^*$  and  $\Gamma_S = \Gamma_{in}^*$  in the equation (4.2.1) :

$$MAG = \frac{(1 - |\Gamma_{in}^2|)|S_{21}|^2}{|1 - S_{11}\Gamma_{in}^*|^2(1 - \Gamma_{out}^2)} = \frac{|S_{21}|^2(1 - |\Gamma_{in}^2|)}{(1 - \Gamma_{in}^2)|1 - S_{22}\Gamma_{out}^*|^2} \quad (4.2.5)$$

Note :

If  $Z_S = R_0$ , then  $\Gamma_{in} = 0$  and the available gain becomes :

$$MAG = \frac{|S_{21}|^2}{|1 - S_{22}\Gamma_{out}^*|^2} \quad (4.2.6)$$

### Stability of an amplifier

The stability considered in this section corresponds to stability defined in terms of the load impedances ( $Z_S$  and  $Z_L \implies \Gamma_S$  and  $\Gamma_L$ ). Actually, when connecting input and output matching networks, one can sometimes create instability, in which case the amplifier can start to oscillate. It is therefore very important to determine whether the system is stable.

**Definition :** An amplifier is called unconditionally stable when, for any source and load impedances, the real parts of the input and output impedances of the amplifier are greater than zero at any given frequency. This requirement yields the following inequality condition for the reflection coefficients :

$$\forall |\Gamma_S| < 1 \text{ and } \forall |\Gamma_L| < 1, \text{ we have } |\Gamma_{in}| < 1 \text{ and } |\Gamma_{out}| < 1$$

On the other hand, an amplifier is conditionally stable if :

$$\forall |\Gamma_S| < 1 \text{ and } \forall |\Gamma_L| < 1, \text{ we have } |\Gamma_{in}| > 1 \text{ and } |\Gamma_{out}| > 1$$

To define stability criteria, we consider the limit of stability defined by  $|\Gamma_{in}| = 1$  and  $|\Gamma_{out}| = 1$ . After analysis :

- The locus of  $|\Gamma_{in}| = 1$  is a circle, of centre  $OC_L$  and of radius  $R_L$  :

$$OC_L = \frac{(S_{22} - \Delta S_{11}^*)^*}{|S_{22}|^2 - |\Delta|^2} \tag{4.2.7}$$

$$RC_L = \frac{|S_{21}||S_{12}|}{||S_{22}|^2 - |\Delta|^2|} \tag{4.2.8}$$

- The locus of  $|\Gamma_{out}| = 1$  is a circle, of centre  $OC_S$  and of radius  $R_S$  :

$$OC_S = \frac{(S_{11} - \Delta S_{22}^*)^*}{|S_{11}|^2 - |\Delta|^2} \tag{4.2.9}$$

$$RC_S = \frac{|S_{21}||S_{12}|}{||S_{11}|^2 - |\Delta|^2|} \tag{4.2.10}$$

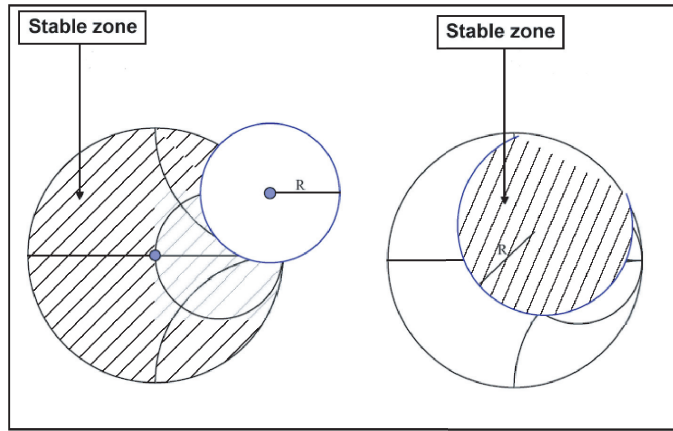


FIGURE 4.3: Stability zones for  $|S_{11}| < 1$

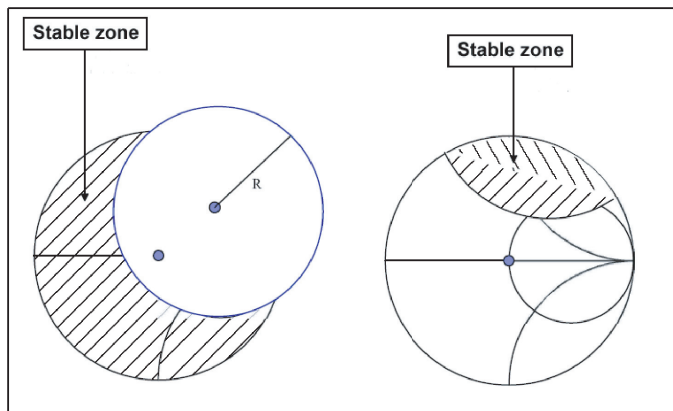


FIGURE 4.4: Stability zones for  $|S_{11}| > 1$

with  $\Delta = S_{11}S_{22} - S_{12}S_{21}$

The stability range is thus defined either inside or outside of these circles, which correspond to the limit of stability.

The analysis of stability is done graphically by determining the stability circles for the amplifier input. We distinguish four cases, corresponding to two inequalities :

- $|S_{11}| < 1$  : the zone containing the centre of the Smith chart is stable (FIGURE 4.3).
- $|S_{11}| > 1$  : the zone containing the centre of the Smith chart is unstable (FIGURE 4.4).

**Analysis of unconditional stability :** In the unconditionally stable operation of an amplifier, we want that all the interior of the Smith chart involve an unstable behaviour of the quadripole (at input and at output).

The inequalities expressed above for unconditional stability can be written in terms of the S parameters of the quadripole, using the Rollet factor K :

$$K = \frac{1 - |S_{11}|^2 - |S_{22}|^2 + |\Delta|^2}{2|S_{12}||S_{21}|} \quad (4.2.11)$$

We can thus show that the necessary conditions to ensure the unconditional stability of an amplifier are :

$$|S_{11}| < 1 \quad |S_{22}| < 1 \quad K > 1$$

If these conditions are not satisfied, the amplifier is conditionally stable and it becomes then necessary to draw the stability circles.

### Simultaneous input-output power matching

Generally, the power at the input of a system is determined by evaluating the effects of the connections. It is thus important to maximize the gain of the amplifying stage, in order to minimize the number of stages of the amplifying chain. To do this, we must provide the complex conjugate impedances  $Z_1 = Z_{in}^*$  and  $Z_2 = Z_{out}^*$  that must be connected at the input and the output of the transistor in order to guarantee the maximum power transfer from the source to the load. The simultaneous input-output matching is only possible if the quadripole is unconditionally stable ( $K > 1$ ). The transductive gain can be expressed as :

$$G_T = \frac{|S_{21}|}{|S_{12}|} (K + \sqrt{K^2 - 1}) \quad (4.2.12)$$

If the quadripole is only conditionally stable, the maximum gain is obtained for values of  $\Gamma_{Smax}$  and  $\Gamma_{Lmax}$  which fall outside of the Smith chart, and thus cannot be realized with passive components. It is then useless to try to obtain the maximum gain by combined complex conjugate matching. Terminations of sources and loads allowing one to satisfy the

conditional stability criterion will only give a gain lower than the maximum absolute gain. We then define the circles with constant gain which allow to determine the places of the points in the planes  $\Gamma_S$  and  $\Gamma_L$  for which the gains  $G_1$  and  $G_2$  are constant, locuses which describe a circle of centre  $O_S$  and of radius  $R_S$  at the input and a circle of centre  $O_L$  and of radius  $R_L$  at output :

$$R_S = \frac{\sqrt{1 - G_1(1 - |S_{11}|^2)}}{1 + G_1|S_{11}|^2} \quad (4.2.13)$$

$$O_S = \frac{G_1}{1 + G_1|S_{11}|^2} S_{11}^* \quad (4.2.14)$$

$$R_L = \frac{\sqrt{1 - G_2(1 - |S_{22}|^2)}}{1 + G_2|S_{22}|^2} \quad (4.2.15)$$

$$O_L = \frac{G_2}{1 + G_2|S_{22}|^2} S_{22}^* \quad (4.2.16)$$

### Noise circles and noise matching

It is possible to minimize the noise contribution of a transistor by presenting at its input a particular source impedance  $\Gamma_S = \Gamma_{opt}$ . This is always possible if the transistor is unconditionally stable ( $K > 1$ ). In this case, the output can be adapted in power by setting  $\Gamma_L = \Gamma_{out}^*$ . In the case of a conditionally stable transistor, it is necessary for  $\Gamma_{opt}$  to be in a stable area of the Smith chart. If this is not the case, it will be necessary to choose a value for  $\Gamma_S$  in the stable area, at the price of an increased noise factor. Then the output is power matched by taking a load impedance located in the stable zone of the stability circle. The place for which the noise factor  $F$  is constant corresponds to a circle of centre  $C_{fb}$  and of radius  $R_{fb}$  :

$$C_{fb} = \frac{\Gamma_{opt}}{1 + N} \quad (4.2.17)$$



$$R_{fb} = \frac{\sqrt{N^2 + N(1 - |\Gamma_{opt}|^2)}}{1 + N} \quad (4.2.18)$$

with :

$$N = \frac{F - F_{min}}{4r_n} |1 + \Gamma_{opt}|^2$$

The layout of these circles makes it possible to quantify the degradation of the noise factor when the reflection coefficient presented at the input moves away from the optimum load impedance. While designing a low noise amplifier, it is sometimes necessary to find a compromise between the maximum gain and the minimum noise factor by locating the intersection between constant noise circles and those with constant gain.

### The importance of these formulas in LNA design

The design of an amplifier at microwave frequencies is perfectly controlled by the theory described in the previous paragraph. This theory gives to the designer a powerful tool to have a control in all the stages of the design process and allows him to design with ease the LNA taking into account all the encountered parameters. Nowadays, after a preliminary design, commercial softwares can easily automatize any iterative optimization process. In our case, instead of starting again all the calculations, our laboratory has a commercial software, Ansoft Designer, which has a tool (Smith Tool) integrating all the above calculations and is used to design input and output impedance adaptation network. The above equations allow us to understand all the steps of the LNA design and can provide a useful starting point. Then, we will use “Smith Tool” of the Ansoft Designer software to design our LNA.

### 4.2.2 Realization of a low noise amplifier at 1.478 GHz

#### Choice of the technology and the transistor

The size, the cost, and the reproducibility are key parameters in the selection of a technology. Here, we will choose a technology using discrete elements, taking into account its

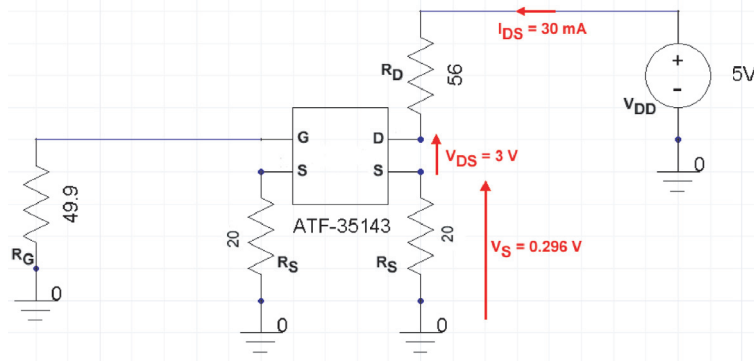


FIGURE 4.5: Transistor polarization circuit

moderate cost, its simplicity and the fact that components can be easily changed. Obviously, integrated circuits would provide further miniaturization and better performances but are out of scope here. The amplifier will be manufactured on FR4 epoxy dielectric, the cheapest dielectric in microwave applications. The FR4 dielectric has high dielectric losses but for our application these losses will not prevent us to achieve the noise figure required by the Worldspace receiver. The FR4 losses will be taken into account while drawing the noise circle and the circle with constant gain on the Smith chart (section 4.2.1)

The transistor selected for the design of the amplifier is an ATF-35143, a PHEMT (Pseudomorphic Hight Electron Mobility Transistor) type marketed by Agilent. This transistor, polarized at  $V_{DS} = 3 V$ ,  $I_{DS} = 30 mA$ ,  $V_G = 0 V$ ,  $V_{GS} = -0.296 V$  is particularly suitable for RF low cost applications [52].

### Transistor polarization

The diagram of the polarization circuit is represented by FIGURE 4.5. The resistor values are calculated by taking into account the desired drain current ( $I_{DS}$ ), the bias voltage ( $V_{DS}$ ) and the source-gate voltage  $V_{GS} (= -V_S)$  in the following way :

$$R_S = \frac{V_S}{I_{DS}} \tag{4.2.19}$$

$$R_D = \frac{V_{DD} - V_{DS} - V_S}{I_{DS}} \tag{4.2.20}$$

## 4.2. SIMPLIFIED STRATEGY FOR THE LNA

---

The  $R_G$  resistor increases the stability of the amplifier at low frequency. The two  $R_S$  resistors are connected in parallel, so that it is appropriate to take  $R_S$  equal to the value obtained in equation (4.2.19) multiplied by two.

### Input-output impedance matching

Impedance matching is a very important step in the design of an amplifier. It actually allows to obtain the maximum power transfer and to improve the signal to noise ratio by increasing the input signal level. This network behaves like an intermediate circuit between two non identical impedances (section 4.2.1). The selection of a matching network with smaller losses is always possible, as long as the impedance of the load is not purely imaginary.

At first, we will determine the transistor characteristics that intervene in the design of the matching circuit at 1.478 GHz frequency. These parameters are summarized in the TABLE 4.1

TABLE 4.1: Transistor ATF-35143 parameters

Frequency	K	Gamma Opt	GA	NF	FMIN
1.478 GHz	0.303	0.652 + j 0.312	18.533 dB	0.691 dB	0.228 dB

The input and output impedance matching networks are made out of inductances and capacitances. The design of the input matching network requires to draw the noise circle and the available gain circle on the Smith chart in such a way as to have a point of tangency between the two circles. The input matching network should provide a path from the point of tangency to the Smith chart origin. This path to the Smith chart center provides us the values of the input matching circuit  $C_{in}$  and  $L_{in}$ . The design of the output matching network requires to use the conjugate point of the tangency point of the noise circle and the available gain circle as starting point. The output matching network should provide a path from the conjugate point of the tangency point to the Smith chart origin. This path to the Smith chart center provides us the values of the output matching circuit  $C_{out}$  and

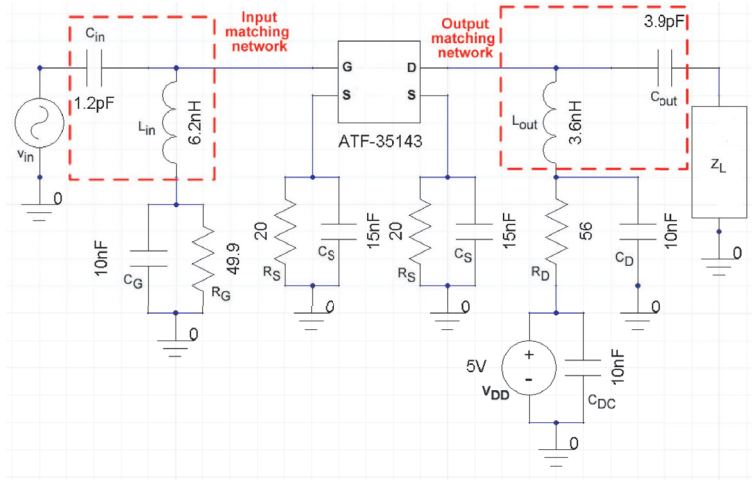


FIGURE 4.6: Low Noise Amplifier Diagram

$L_{out}$ .

Then the use of the “Smith Tool” of the Ansoft Designer software gives us the values of the components of the input matching circuit ( $C_{in}$ ,  $L_{in}$ ) and of the output matching circuit ( $C_{out}$ ,  $L_{out}$ ). The resistances  $R_G$ ,  $R_S$  and  $R_D$  are designed only for polarization purpose. Since in the amplifier circuit there are continuous and variable signals, these resistances bring only their contribution in presence of continuous signals. The capacitors  $C_G$ ,  $C_S$ ,  $C_D$ , and  $C_{DC}$  are decoupling capacitors : they short-circuit the variable signal to the ground. The normalized values of all these components are shown on the amplifier diagram (FIGURE 4.6).

The image of our amplifier is represented by the FIGURE 4.7. We can see, if we compare it with a standard design used in professional applications (FIGURE 4.8), that we keep only the essential block. Despite the big reduction in complexity our amplifier is able to meet the required specifications as shown in the next paragraph.

### Measurement results

After finishing the design and building the amplifier, we measured and compared the measured values with the data obtained from simulations (FIGURE 4.9 - FIGURE 4.11). We notice a difference between the measured and the simulated values. In the measured noise

## 4.2. SIMPLIFIED STRATEGY FOR THE LNA

---

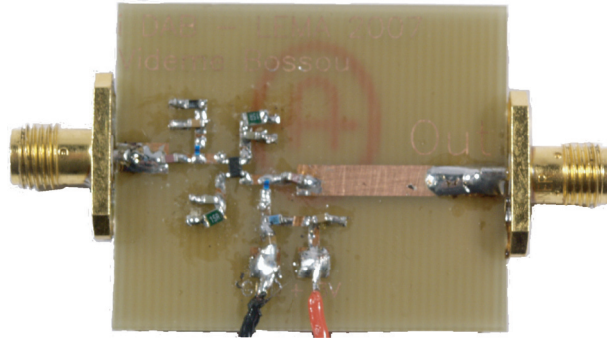


FIGURE 4.7: The Low Noise Amplifier

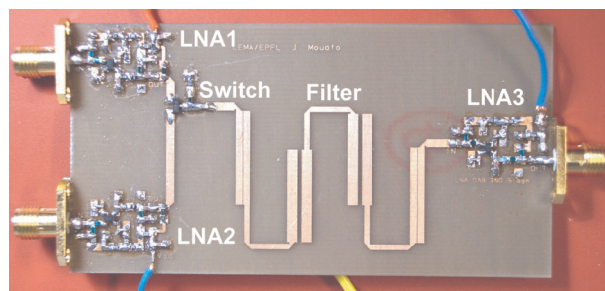


FIGURE 4.8: The standard Low Noise Amplifier

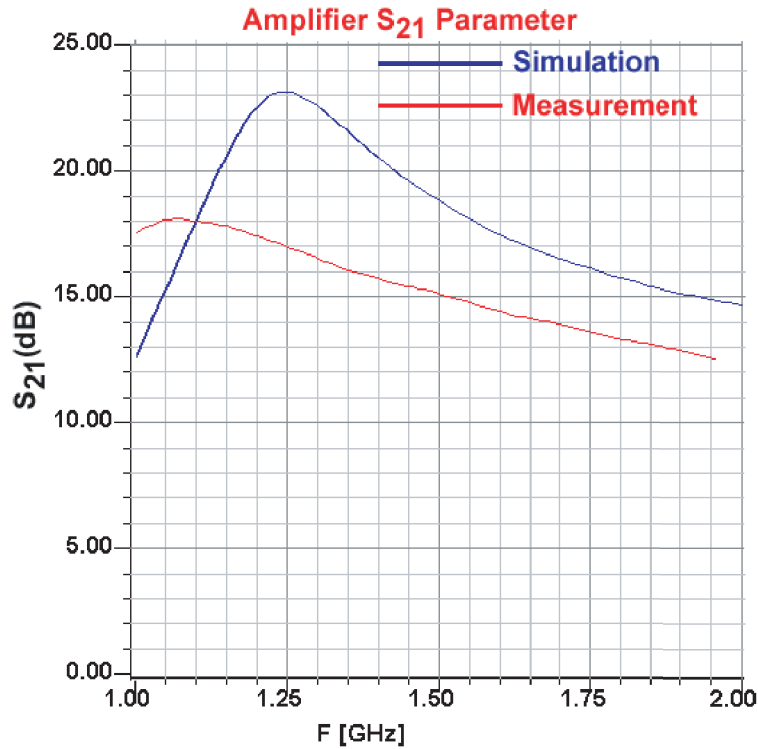


FIGURE 4.9: Measured and simulated  $S_{21}$  parameter of the amplifier

figure curve we have some dubious values. However, we note that the curves resulting from simulation and measurements behave in a similar manner. According to the measurements, we have a noise figure of 0.975 dB, lower than that fixed for the Worldspace receiver and a gain of 15.39 dB larger than the value previously mentioned for the same receiver.

This first design method wasn't considered satisfactory as it leads to a too large difference between predicted and measured values. Therefore, we performed a new iteration, using a second method expected to alleviate the problem. On the first hand we have used more reliable parameters for the transistor description. On the other hand a more rigorous mathematical procedure has been adopted to cope with the weaknesses of the previous model. The new approach aims to determine the tangent point of the circle of constant gain  $G_1$  and the circle of constant noise factor  $F$  which correspond to  $\Gamma_S$ . We used the following data from the data sheet of the transistor at the frequency  $f = 1.478$  GHz :

- $S_{11} = 0.4367 - j * 0.7661$

## 4.2. SIMPLIFIED STRATEGY FOR THE LNA

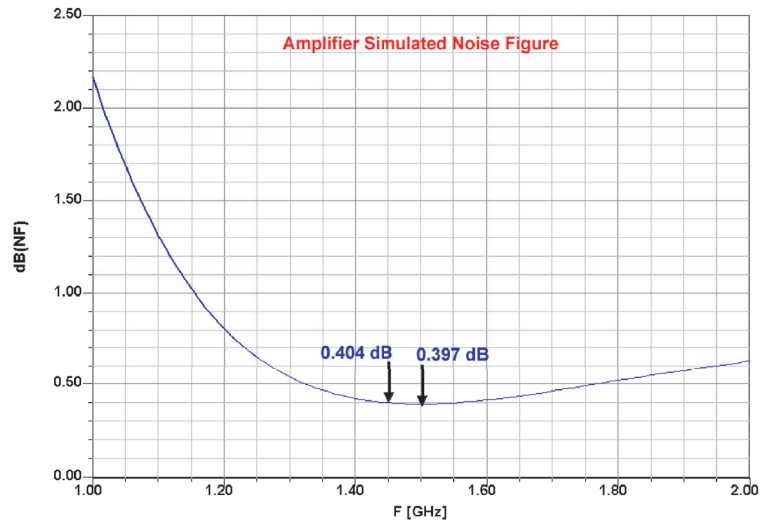


FIGURE 4.10: Simulated Noise Figure parameter of the amplifier

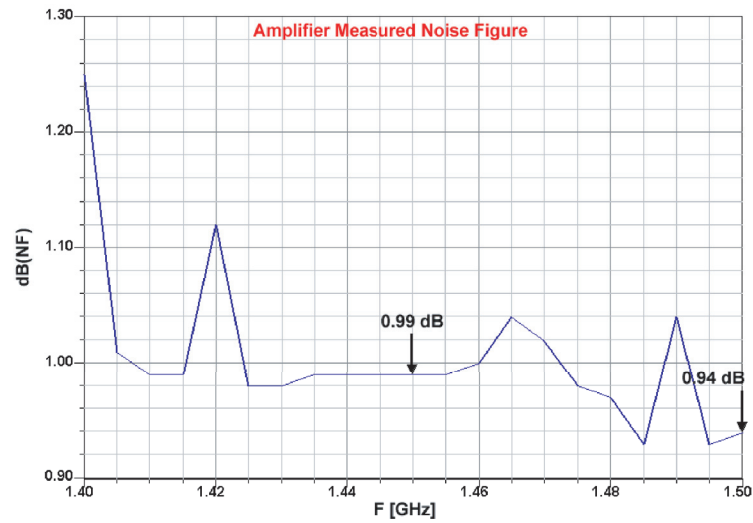


FIGURE 4.11: Measured Noise Figure parameter of the amplifier

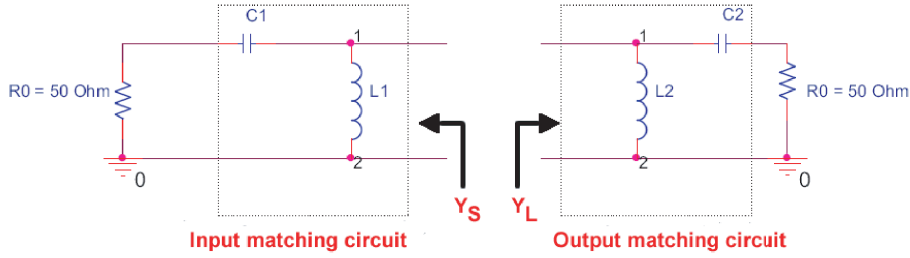


FIGURE 4.12: Input and Output matching circuits

- $S_{12} = 0.0311 + j * 0.0434$
- $S_{21} = -4.8422 + j * 5.6613$
- $S_{22} = 0.3581 - j * 0.3061$
- $F_{min} = 0.2278 \text{ dB}$
- $\Gamma_{opt} = 0.6516 + j * 0.3122$
- $r_n = 0.1602$

Then we used  $G_1 = 1.68 \text{ dB}$ ,  $F = 0.23 \text{ dB}$  and equations (4.2.13), (4.2.14), (4.2.17), (4.2.17) to determine the value of  $\Gamma_S$  :  $\Gamma_S = 0.1980 - j * 0.2643$ . This value of  $\Gamma_S$  corresponds to  $Y_S = 0.0118 + j * 0.0070$ . Afterwards, we used equation (4.2.3) to determine the value of  $\Gamma_L$  :

$$\Gamma_L = \Gamma_{out}^* = S_{22}^* + \frac{S_{12}^* S_{21}^* \Gamma_S^*}{1 - S_{11}^* \Gamma_S^*}$$

This equation gives us the value of  $\Gamma_L$  :  $\Gamma_L = 0.3037 + j * 0.2053$  which corresponds to  $Y_L = 0.0099 - j * 0.0047$ .

According to FIGURE 4.12 we have :

$$Y_S = G_S + jB_S = -jB_1 + \frac{1}{50 - jX_1} = \frac{50}{50^2 + X_1^2} + j \left[ \frac{X_1}{50^2 + X_1^2} - B_1 \right] \quad (4.2.21)$$

and

$$Y_L = G_L + jB_L = -jB_2 + \frac{1}{50 - jX_2} = \frac{50}{50^2 + X_2^2} + j \left[ \frac{X_2}{50^2 + X_2^2} - B_2 \right] \quad (4.2.22)$$



with :

$$X_1 = \frac{1}{C_1\omega}$$

$$X_2 = \frac{1}{C_2\omega}$$

$$B_1 = \frac{1}{L_1\omega}$$

$$B_2 = \frac{1}{L_2\omega}$$

From equations (4.2.21) and (4.2.22) we have the following expressions :

$$X_1 = \sqrt{50 \left( \frac{1}{G_S} - 50 \right)} \quad (4.2.23)$$

$$B_1 = \sqrt{G_S \left( \frac{1}{50} - G_S \right)} - B_S \quad (4.2.24)$$

$$X_2 = \sqrt{50 \left( \frac{1}{G_L} - 50 \right)} \quad (4.2.25)$$

$$B_2 = \sqrt{G_L \left( \frac{1}{50} - G_L \right)} - B_L \quad (4.2.26)$$

Using the frequency  $f = 1.478$  GHz we can calculate the values of  $L_1$ ,  $C_1$ ,  $L_2$  and  $C_2$  :

$$L_1 = 39 \text{ nH}$$

$$C_1 = 2.7 \text{ pF}$$

$$L_2 = 7.5 \text{ nH}$$

$$C_2 = 2.2 \text{ pF}$$

We manufactured a LNA with these values and then compared the simulated and measured values (FIGURE 4.13 - FIGURE 4.15). We realized that the results are better than the previous ones and we notice that these values are very close to each other. We can conclude that to have a good agreement between simulation and measurement, we must use

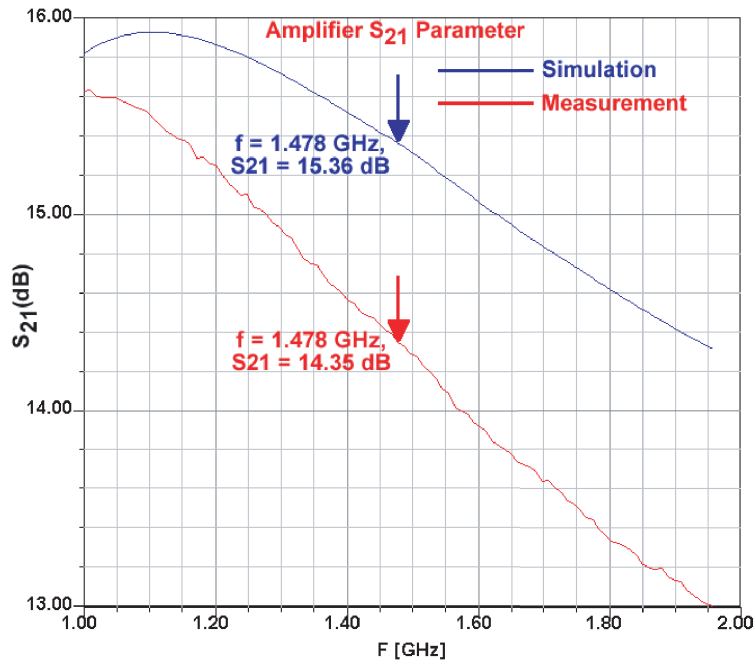


FIGURE 4.13: Measured and simulated  $S_{21}$  parameter of the amplifier (second method)

the parameters given in the data sheet of the transistor and then use rigorous equations to calculate the matching network components values. This put simulated gain values at just 1 dB difference (14.3 dB instead of 15.3 dB) from measured values (FIGURE 4.13). If for some applications still more precision is needed, we must measure the characteristics values given in the data sheet of the transistor, calculate the values of capacitors and inductors and then use their equivalent circuits for simulation.

Definitely, the results obtained for the amplifier are satisfactory for our application. We can now connect the amplifier to the antenna and test the reception of actual Worldspace satellite radio signals.

### 4.3 Worldspace satellite receiver system (LNA+Antenna)

We will now associate the amplifier designed in the previous section with our antenna designed in Chapter 3 : we will call the resulting device the Strip Wood Slot Wood Patch (SWOSWOP) antenna. Our SWOSWOP device should play the role of active antenna

### 4.3. WORLDSPACE SATELLITE RECEIVER SYSTEM (LNA+ANTENNA)

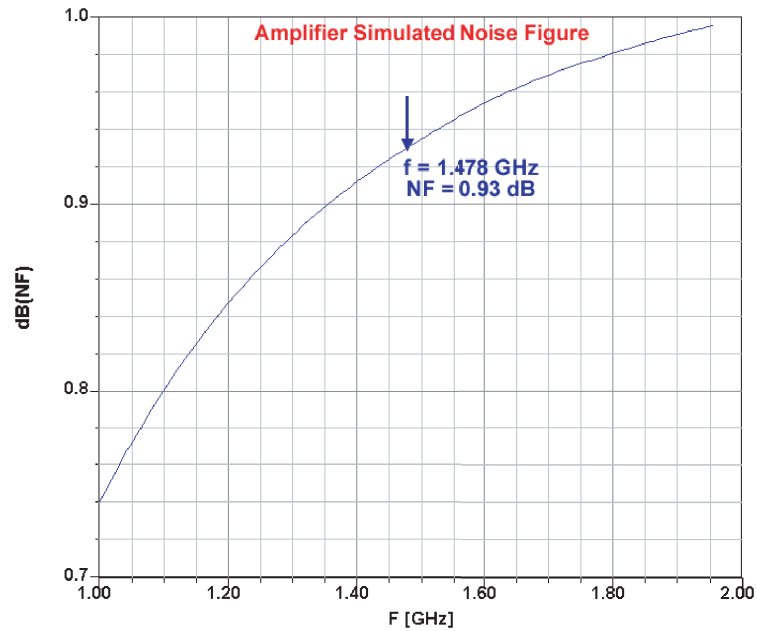


FIGURE 4.14: Simulated Noise Figure parameter of the amplifier (second method)

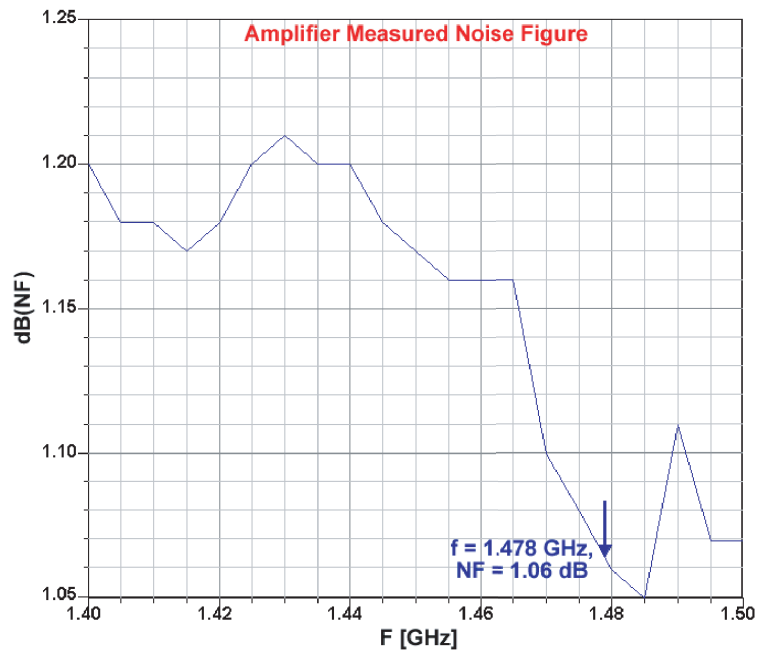


FIGURE 4.15: Measured Noise Figure parameter of the amplifier (second method)

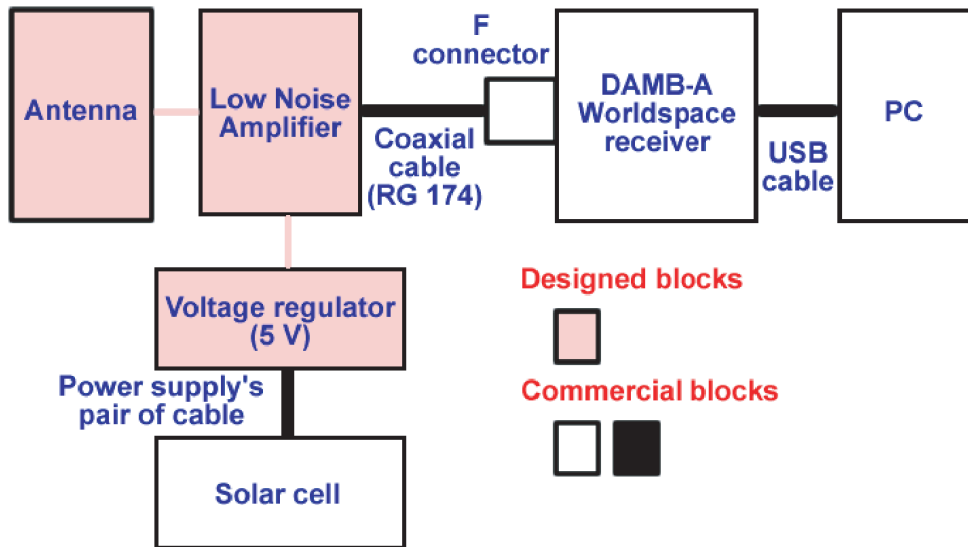


FIGURE 4.16: Worldspace receiver station

in the Worldspace radio station. The block diagram of the system is represented by FIGURE 4.16.

In Chapter 3 we selected two type of antennas : the Balsa antenna and the Ayous-Balsa antenna. The integration of the low noise amplifier which includes the voltage regulator will be different from one antenna to the other :

- in the case of Balsa antenna the LNA will be directly printed with the feed line of the antenna (FIGURE 4.17);
- in the case of Ayous-Balsa antenna the LNA will be printed and then joined with the antenna ground plane by using a conducting glue (FIGURE 4.18).

The power supply of the amplifier needed to activate the voltage regulator and to bias the transistor will be provided by a solar cell, which will be connected to the voltage regulator by a pair of wire. The output of the amplifier will be connected to the DAB receiver by a RG 174 coaxial cable. The connection between the coaxial cable and the receiver will be done with a male F connector.

The cable RG 174 has a characteristic impedance of 50 ohms and an attenuation of 28 dB per 100 m at the frequency of 1.478 GHz. Since we will not need a line longer

### 4.3. WORLDSPACE SATELLITE RECEIVER SYSTEM (LNA+ANTENNA)

---



FIGURE 4.17: The LNA printed with the feed line



FIGURE 4.18: The LNA glue on the ground plane



FIGURE 4.19: Balsa antenna

than 5 m to connect our antenna, the maximum attenuation will be 1.5 dB. However, the calculations of the Worldspace antenna characteristics took into account an attenuation of 5 dB in the feed cable. In addition, we notice that the coaxial wire specifications are compatible with those of Worldspace receiver.

As the problem of compatibility is solved, we carried out receiving tests of Worldspace radios. We successfully received at least all Worldspace radio stations from Afristar satellite with the Balsa antenna (FIGURE 4.19) and with the Ayous-Balsa antenna (FIGURE 4.20).

The image of the complete receiver system is given in the (FIGURE 4.21). In this figure we see the solar cell providing the power supply to the active Ayous-Balsa antenna. This power supply is needed to bias the transistor of the LNA. The active Ayous-Balsa antenna is connected to Tongshi Worldspace receiver which is directly connected to the computer. The receiver system set is in receiving mode. We can see on the computer the list of received radio stations. This receiving test proves once more that our original idea to receive satellite signals using aluminium-wood antenna and a simplified LNA is possible.



### 4.3. WORLDSPACE SATELLITE RECEIVER SYSTEM (LNA+ANTENNA)

---

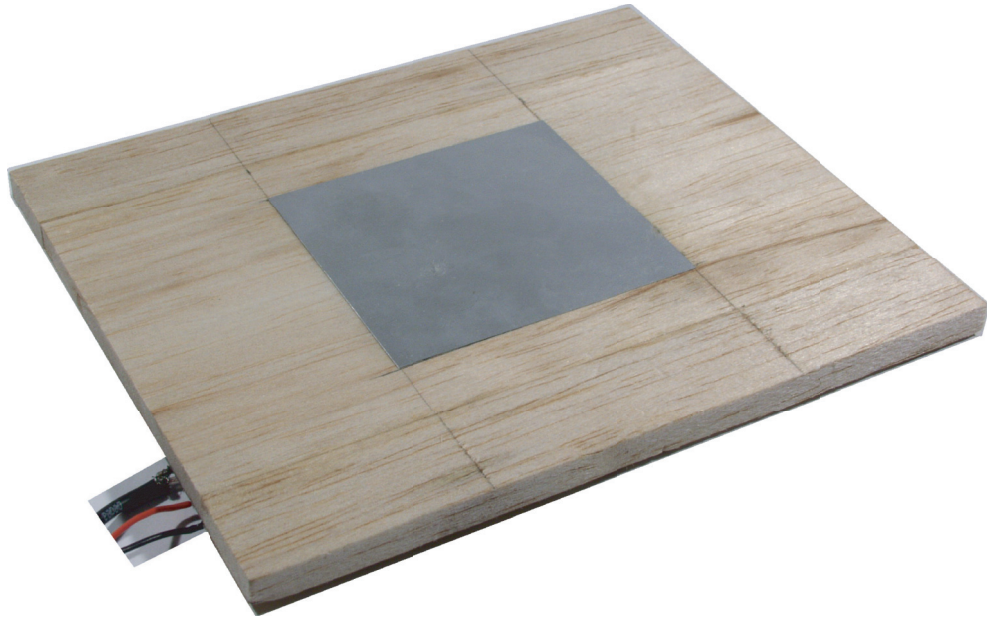


FIGURE 4.20: Ayous-Balsa antenna



FIGURE 4.21: Worldspace signals' receiver system

### 4.4 Conclusion

To build and demonstrate a receiver matching the goals of this thesis, we required a RF front-end with at least the antenna and a Low Noise Amplifier (LNA). For this purpose, we designed an LNA that transformed our antenna into the equivalent of an active antenna. For our application, we didn't need a high quality LNA with stringent requirements, but we needed an amplifier having a gain of 14.84 dB and a noise figure of 1.8 dB. We attempted to design such an amplifier using the relevant theory and the "Smith tool" of the Ansoft Designer software. This tool gave us directly the needed values for the components of the input and output matching circuit. We didn't look deeply into the validity of the simulation but used then as guidelines giving us confidence in the worthiness of building and measuring a given topology of the amplifier. The measured values for the designed LNA were 0.975 dB for the Noise Figure and a gain of 15.39 dB. These values fit the Worldspace specifications and were adequate for our application. In a further step we connected the aluminium-wood antenna to the LNA and launched the reception tests of Worldspace satellite signals. We obtained successful results from these tests, which confirmed that the combination of the simplified LNA and the aluminium-wood antenna functioned perfectly : that was the proof of the feasibility of our original idea - to use local materials and a simple process to manufacture antennas of the microstrip type. This was the first time in antenna design that an antenna was manufactured with wood as substrate and aluminium as conducting element : this antenna would be called Strip Wood Slot Wood Patch antenna (SWOSWOP). The RF front-end designed here was simple and inexpensive. This simplified RF front-end could be manufactured locally and easily, with little specific training.

The next step will be to use this system to transmit scientific information. To achieve this goal, we need to start by producing the information to be transmitted. We have designed the first block of a remote course to teach antenna theory. This task will be described in the next chapter.



## Part II

# REMOTE COURSE



# Chapter 5

## REMOTE COURSE ON ANTENNA TEACHING

### 5.1 Introduction

The second purpose of our project is to develop a remote course for the teaching of antenna theory, which would ensure the durability and the dissemination of the obtained results, and would provide an invaluable tool for teaching and training.

Currently, the literature shows quite a few antenna courses, as it can be easily checked by a fast search in the web. Universities offer online courses which include antennas courses [53] - [58]. As we notice, most universities are located in English speaking area : almost all these courses are in English language. We can also notice that few of them include simulations in their online courses. However, to access these courses one must be student of these universities or must pay for these courses. There are also some books written for teaching enhance purposes based especially on Matlab and including a CD-Rom which contained Matlab tutorials and codes [60]. These books are excellent tools for teaching but for obvious commercial reasons their content is not available on the net and then not accessible to any student.

There are also some professional companies which are specialized in on designing and

selling teaching antenna equipments [61] - [63]. They propose antenna courses which introduce first the basic function and applications of antenna and then build the functioning of special antenna and antenna systems. The antenna training system is a "Blended Learning" system of teaching. Practical exercises using real techniques, are combined with the theoretical studies in one system. The entire range of test instruments required is also part of the system and there is no requirement for any separate individual test instruments. For instance, by selection of the frequencies available in the range of 8 to 10 GHz, several workplaces can be operated close to each other without any danger of interference. These companies propose also course in microwave techniques. The basic idea of the microwave techniques training system is to teach the fundamental principles of high-frequency technology in practical exercises. In the basic package, emphasis is given to wave propagation in waveguide and in free space. Various materials are examined for their properties of propagation and their attenuation. Also, the fundamentals are established for understanding the function of various waveguide components for controlling the flow of energy. The basic system consists of a collection of various waveguide components for use in the X-band, that are fixed together. Measurements in the basic system are made using an oscilloscope or a computer-aided measurement system [61] - [63].

Our aim is to propose a free teaching course accessible by all the students for French speaking areas and to use a convivial graphic user interface to make this course more attractive.

The system designed to receive Worldspace satellite signals will be used to download scientific information from the North universities and to exchange information between local countries. An excellent example of the scientific information that can be transmitted by these systems is the "on-line course" (also known as e-course) that can be partially interactive and partially based on the Internet resources. From the satellite transmission point of view this is also a very convincing test. If properly designed, such a course can be readily included in the available bandwidth of satellite channels and requires a minimum of reactivity and the capacity of working in real-time from the system. Moreover, developing these courses presents a joint interest in the case of the Yaounde and Lausanne

partners, which are both modernizing their teaching approaches. Therefore, this activity was included as a deliverable item in the joint Swiss-Cameroon proposal that has been at the root of this thesis. The development of remote courses began in the partner laboratory from Cameroon since 1993 [64] - [66]. Our work will be thus a complement of what exists already in order to improve the education system in South countries.

Before this thesis, the two partner laboratories at Lausanne and Yaounde had developed teaching tools in a MatLab environment that could only be used in a non-interactive "ex cathedra" way, where the teacher illustrates his course in front of an essentially passive auditorium [67], [68]. To make this process more interactive, and also to access a much wider number of students, we are proposing to use the nowadays well developed web-based tools for e-learning [69], [70]. Also, although in the original version the demonstration tools were available only to students who registered for the course, a more widely available system including a password can be easily implemented. The Matlab package was selected for our codes because of the well known inherent Matlab facilities : conviviality, simplicity, ease of programming, impressive graphical interfaces. But in addition Matlab has now standardized its Matlab Web Server, making it the best choice to make codes widely available and to maintain them easily. Therefore, we chose the simplest configuration with a Web browser running on the client's workstation, while Matlab, the Matlab Web Server (matlabserver), and the Web server daemon (httpd) run on another external machine [72]. This way, the end user only needs the most basic computer facilities, nowadays available almost everywhere in the world. More precisely, we have created the HTML documents to collect the input data from users and to display output with PHP codes [73], [74]. In addition to the Matlab codes, we use a data base server linking to an Access data base, which will be used by the Matlab programs. Keeping an inner consistence with the strategy of the first part of this thesis, the bandwidth required by this strategy is really small and with a basic personal computer (PC) and the simple receiver developed in the first part, the user will not be excessively disturbed. Although not the simplest possible, this strategy reduces to a minimum the hardware and software complexity required from the end user (client) and puts all the computational burden on the remote server. All these programs are run only

inside of the university and are transparent for the end user. As mentioned, outside of the root university a password attributed by the teacher responsible for the course will permit students to access them.

In addition and after a few discussions, French has been used as working language. In general, e-learning tools are less common in French and it is believed that this choice will be helpful for all French speaking countries, starting with the universities that are partners in this project. In the next section we will describe the functioning of the website and we conclude with some specific examples that have been specifically created for this thesis.

### **5.2 On mathematical developments and programming structures**

In several cases, these software tools have called for new and original developments in the area of computational electromagnetism. In these cases, for the sake of completeness and future reference, all the mathematical developments have been included in this thesis. This is important for those who would like to upgrade, evolve and improve upon our codes. However, it must be recalled that all the mathematics is fully transparent to the user, who only sees the input/output graphical interfaces. The same thing can be said about the functional description of the web site including the description of the files and classes being used. Essential for the webmaster and the future developers, these aspects of our work will remain fully hidden from average user.

### **5.3 e-Antenna web site**

In our web site architecture (FIGURE 5.1) we have two components : the web server and the customer. On the customer's web browser, the student can access the teacher's slides used for the course. Before a student accesses this course, he must be registered as an EPFL student. After logging in (name and password) he can view the course, provided in pdf format. On the other hand, no password is required to enter input parameters and

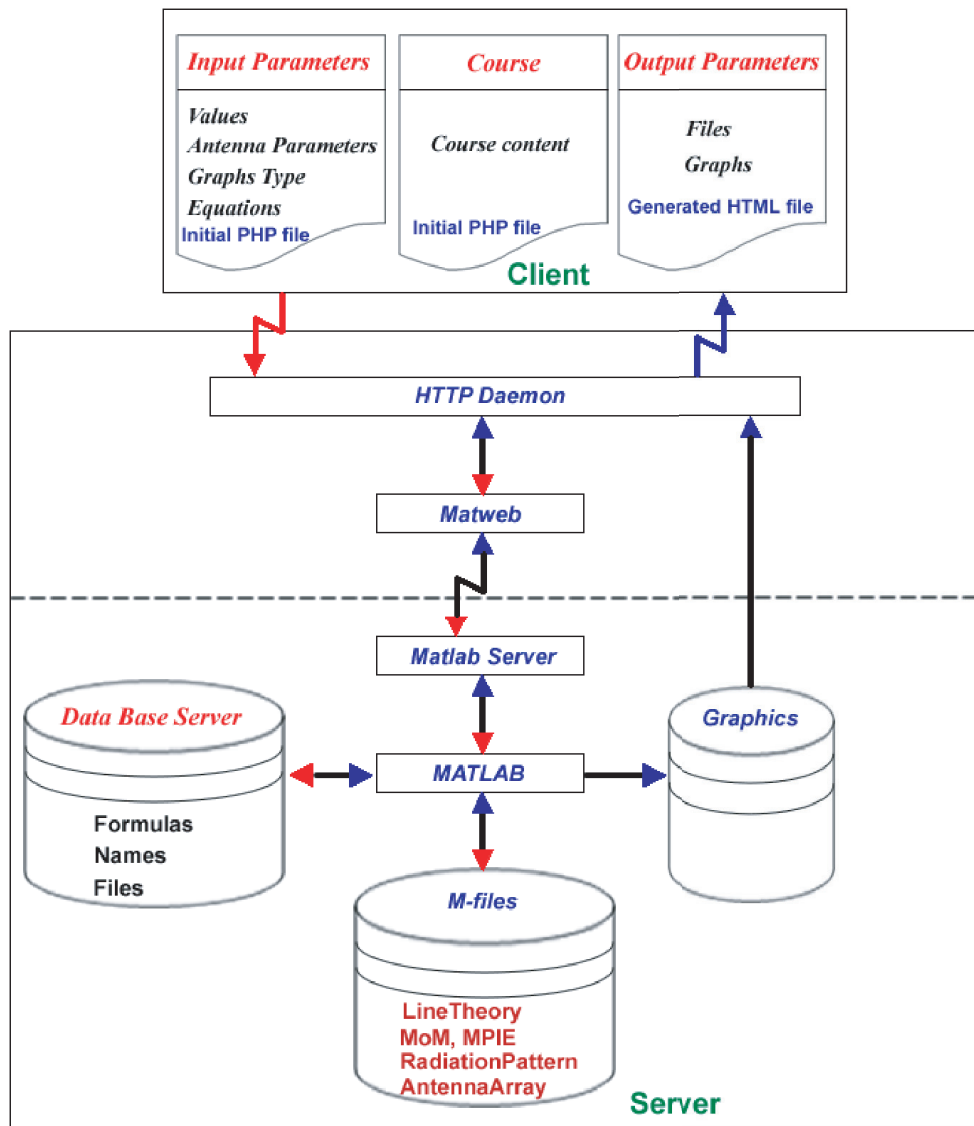


FIGURE 5.1: e-Antenna architecture

then launch the Matlab server. After a while, and depending on which operations are being performed, the server sends to the client's browser the resulting files and graphs, the output parameters of the Matlab execution of the files.

Schematically the web server collects the data from input parameters via the HTTP daemon and calls the `matweb` file. The `matweb` file will then call the `matlabserver` file and transfer the data to the Matlab file, which will be executed, and will save the results as figures and files. The `matlabserver` collects data from an access data base, chooses the appropriate Matlab file to perform the operation, saves the results and puts them in a HTML file. The web server sends the HTML file to the clients browser. The results come in another web page file, different from the first one. In order to put all data in the same file, the user has to click on the button "Show the Graphs" to be able to evaluate the graphs and the results saved in the files.

### 5.3.1 Functional description of the web site

The entire web site is built around one file (`index.php`), which can call many subroutines to execute the tasks. The web site is divided into directories :

- The main directory lists several files and folders. Each folder represents a chapter.
- In each chapter's directory we have a simulation directory, the teacher's course directory and the HTML files and figures related to the chapter.
- In each simulation directory, we have a Matlab directory and the HTML file and figures related to the simulation.
- In the Matlab directory we have the Matlab program and the input and output directories.

In the simulation folder, the PHP program will create a session directory, which contains the sessions' number and the users' directories. The directory of each session's number has a copy of the Matlab directory contents. All the input and output data obtained during simulations are stored in the input and output directories, which are located in the sessions' number directories. Every output parameter of the simulation is saved in a different folder, located in the output directory. The simulation output parameters are all not directly



accessible to users. Later on, if a user needs to access output parameters, he must save the data in his folder after logging in. So, the users' directories only contain historical data. To make all the process work properly, some basic rules must be observed when writing the main.m file and the Matlab main program related to the simulation to be conducted. The main.m file contains the input parameters that will be used for the input parameter menu, and the main matlab file must collect the data from the HTML web page. The flow chart (FIGURE 5.2) shows globally how the web site works when a user is connected. This web site is directly accessible only when inside of the university. Outside of the university, you will need a password, which will be given by the teacher responsible of the course. To access the teacher's slides, you need to be a student registered at the root university.

### 5.3.2 Description of the files

#### **index.php**

This file is the main file around which all the web site is build. It calls the lots of subroutines that are located in other files. At the beginning these files are loaded in order to use their subroutines.

#### **phpantenne.config**

This file is a configuration file. It provides the main program with the name of directories and files, and then permits better navigation through the web site architecture.

#### **php-nav-classes.php**

This file contains two subroutines :

- the first one is the function `read_file_tree($root)`. This function reads the main web site directory, collects the names of all the directories and sub-directories and writes the course menu. The main directory contains directories that provide the name of chapters. Each chapter directory has subdirectories devoted to simulations.

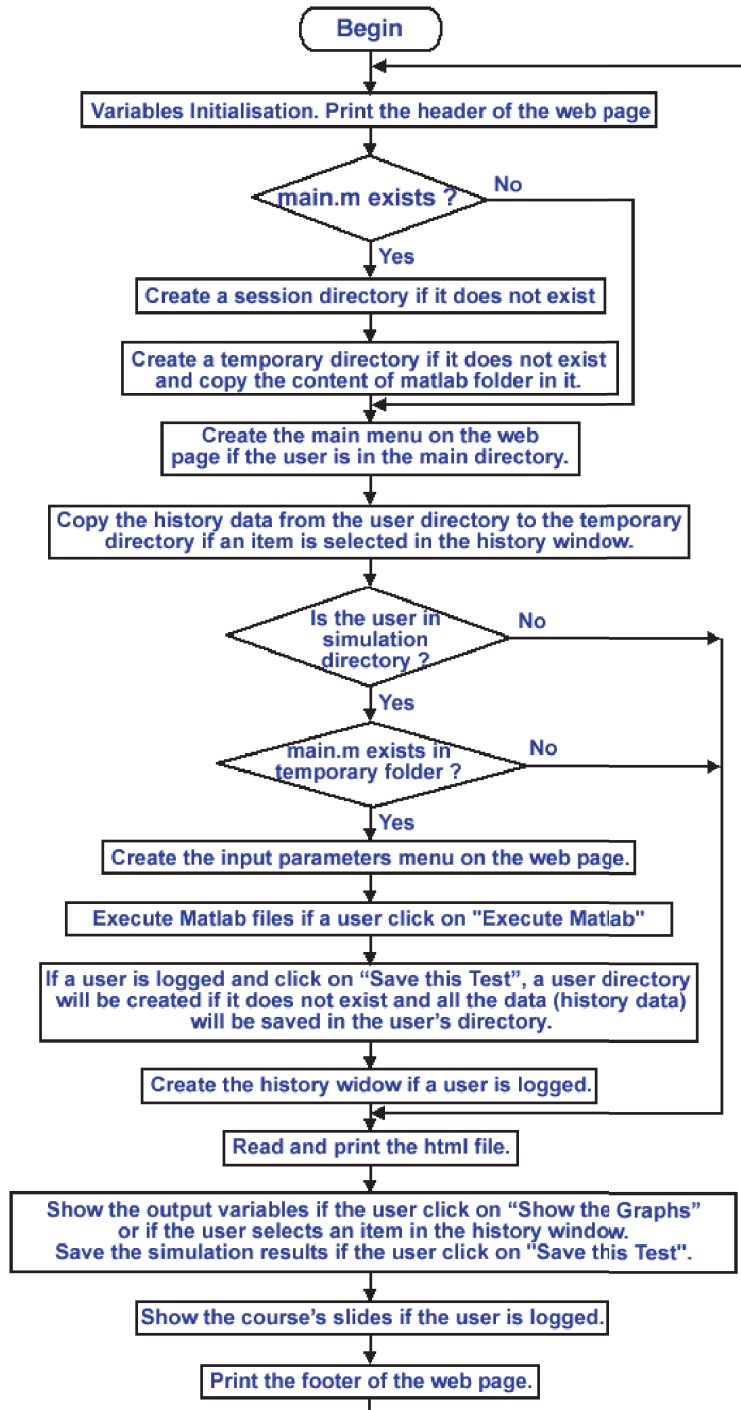


FIGURE 5.2: e-Antenna flow chart

- the second one is the function `draw_secrets()`. This function will check whether the user is logged in. When the user is logged in, then a link to the pdf course will appear on the web page, otherwise there will be no link to the related course.

#### **php-antenne-layout-classes.php**

This file contains different classes :

- the class `header` : this class will draw the header of the web page.
- the class `banner` : this class will draw the EPFL and the laboratory banners.
- the class `footer` : this class will draw the footer of the web page.
- the class `text` : this class will draw all the text which appears on the web page.
- the class `bottom` : this class will draw the date of the last update of the text file.
- the classes `left_menu`, `right_menu`, `main`, `box` are classes for the web page settings.

#### **php-matlab-classes.php**

This file contains different functions :

- the function `handle_session()` : This function will check whether the file `main.m` exists. If this file exists, it will create a session directory if there isn't one as yet. In the session directory, it will create a session number directory and will copy in this directory all the contents of the matlab directory.
- the function `draw_output($object)` : This function will collect the matlab results saved in the image files and the text files and put them on the web site.
- the function `paint_input($objects)` : this function will create the input parameters menu.
- the function `send_input($objects)` : this function will serialize the input parameters. The serialized format is suitable for data exchange.

- the function `translator($file)` : this function will copy all the input parameters values saved in `main.m` file and put them in input parameters.

### **matweb.conf**

This configuration file must be located in the `cgi-bin` directory. In the same directory the file `matweb.exe` must be copied too. In the configuration file we have the name without the matlab extension of all the matlab files that are called by the web page. The structure of this file is as follows :

```
[filename1]
```

```
mlserver = "server name" or "server address"
```

```
mldir = "the directory path where the file filename1.m is located"
```

```
[filename2]
```

```
mlserver = "server name" or "server address"
```

```
mldir = "the directory path where the file filename2.m is located"
```

```
[filenameN]
```

```
mlserver = "server name" or "server address"
```

```
mldir = "the directory path where the file filenameN.m is located"
```

### **5.3.3 Description of the simulation**

We describe here how simulations generally operate on this web site. After the user has launched the antenna remote course, he will see the main page (FIGURE 5.3) appear on his browser. Then he can proceed : the user can be logged in or not. Depending on these two ways, the web site will react differently.

First of all we will consider the situation where the user is not logged in. When clicking on any chapter, he can only see the simulation (FIGURE 5.4). Afterwards, he can click on

### 5.3. E-ANTENNA WEB SITE

FIGURE 5.3: e-Antenna main page

FIGURE 5.4: Chapter's web page when the user is not logged in

the simulation and get the web page of FIGURE 5.5. When clicking on "Execute Matlab" the web server will launch the execution of matlab file. At the end of this operation, the user can click on "Show the graph". Then he will see the result of his simulation. For instance, in FIGURE 5.6 we show the result of using one of the simulations ("Diagramme") which will be fully described in the next section.

Consider now that the user uses his EPFL log name and password. When clicking on the chapter, he can see the simulation and the PDF course (FIGURE 5.7). He can read the course by clicking on it, or he can carry the simulation by clicking on the simulation item.

## CHAPTER 5. REMOTE COURSE ON ANTENNA TEACHING

The screenshot shows the EPFL LEMA website interface. At the top, there is a navigation bar with the EPFL logo and the text "LABORATOIRE D'ELECTROMAGNETISME ET D'ACOUSTIQUE (LEMA)". Below this, there is a breadcrumb trail: "EPFL > LEMA > R&ANT > COURS > Chapitre3 > Diagramme". A "Log in" link is visible in the top right corner.

The main content area is titled "PARAMETRES CARACTERISTIQUES D'UNE ANTENNE". It is divided into two columns. The left column contains a "Paramètres" sidebar with several sections:

- Champ Electrique**: Includes "Données Analytiques" and "Données Numériques" (with a "Browse..." button).
- Type de Représentation**: Radio buttons for "Dimension 2" (selected), "Dimension 3", and "Projection".
- Paramètres de Sortie**: Includes "Résultat Numérique" (with a "W" icon), "Caractéristique à Représenter" (radio buttons for "Puissance", "Champ", "Directivité", and "Polarisation"), and buttons for "Executer Matlab" and "Reset".
- A button at the bottom: "Afficher les graphes".

The right column contains the following text:

Cette simulation permet de faire une représentation graphique en 2D, en 3D et en projection de certains paramètres caractéristiques d'une antenne. Elle utilise soit des données numériques enregistrés dans un fichier, soit des expressions analytiques des deux composantes transverse du champ électrique :  $(E_\theta, E_\phi)$

Les expressions analytiques sont enregistrées dans une base de donnée. Vous pouvez les consulter en [cliquant ici](#).

Pour rentrer les données analytiques il suffira juste de mettre dans les cases ci-contre le numéro d'enregistrement de Etheta et de Ephi dans la base de données.

Pour rentrer les données numériques vous devez envoyer un fichier texte contenant les données numériques des champs Etheta et Ephi. Ce fichier devra avoir soit **361 lignes et 364 colonnes**, soit **361 lignes et 724 colonnes**. Les colonnes correspondent aux valeurs de l'angle theta alors que les lignes correspondent aux valeurs de l'angle phi. La structure du fichier devra être la suivante :

**Valeur réelle(Etheta) Valeur Imaginaire(Etheta) Valeur réelle(Ephi) Valeur imaginaire(Ephi).**

©2006 Olivier Vidémé Bossou [olivier.videmebossou@epfl.ch](mailto:olivier.videmebossou@epfl.ch)  
Mise à jour : January 12 2007 18:22:01.

FIGURE 5.5: Simulation's web page when the user is not logged in

### 5.3. E-ANTENNA WEB SITE

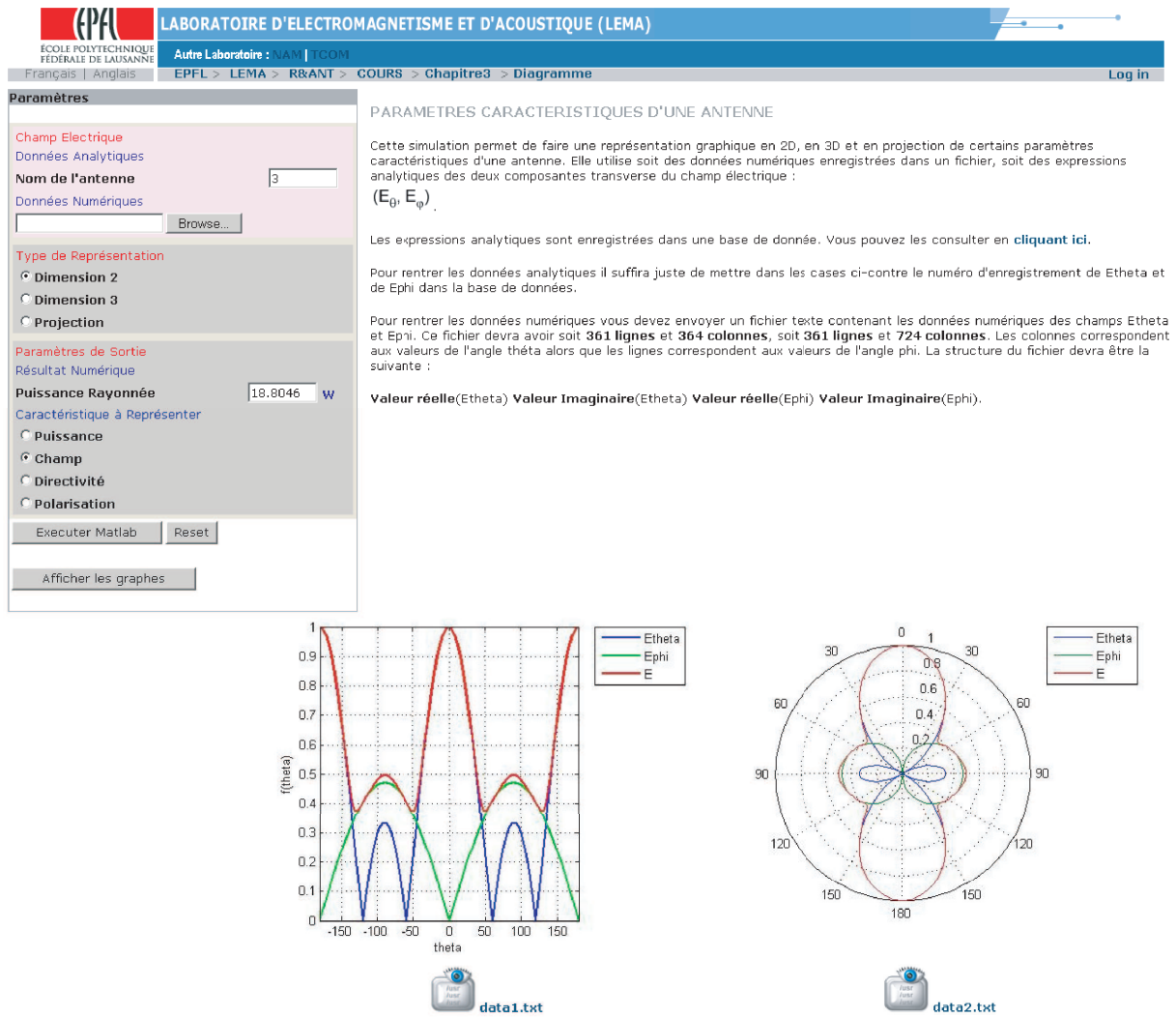


FIGURE 5.6: Simulation results on the web page when the user is not logged in

## CHAPTER 5. REMOTE COURSE ON ANTENNA TEACHING

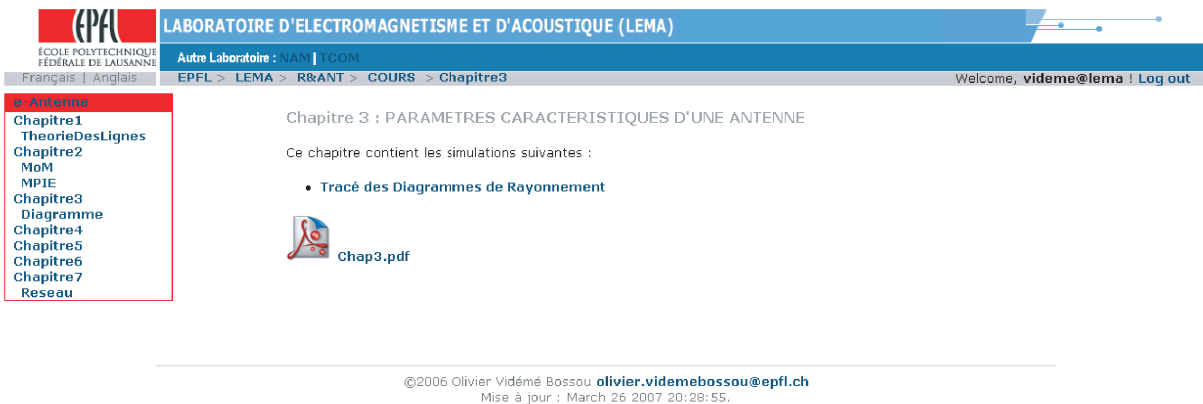


FIGURE 5.7: Chapter's web page when the user is logged in

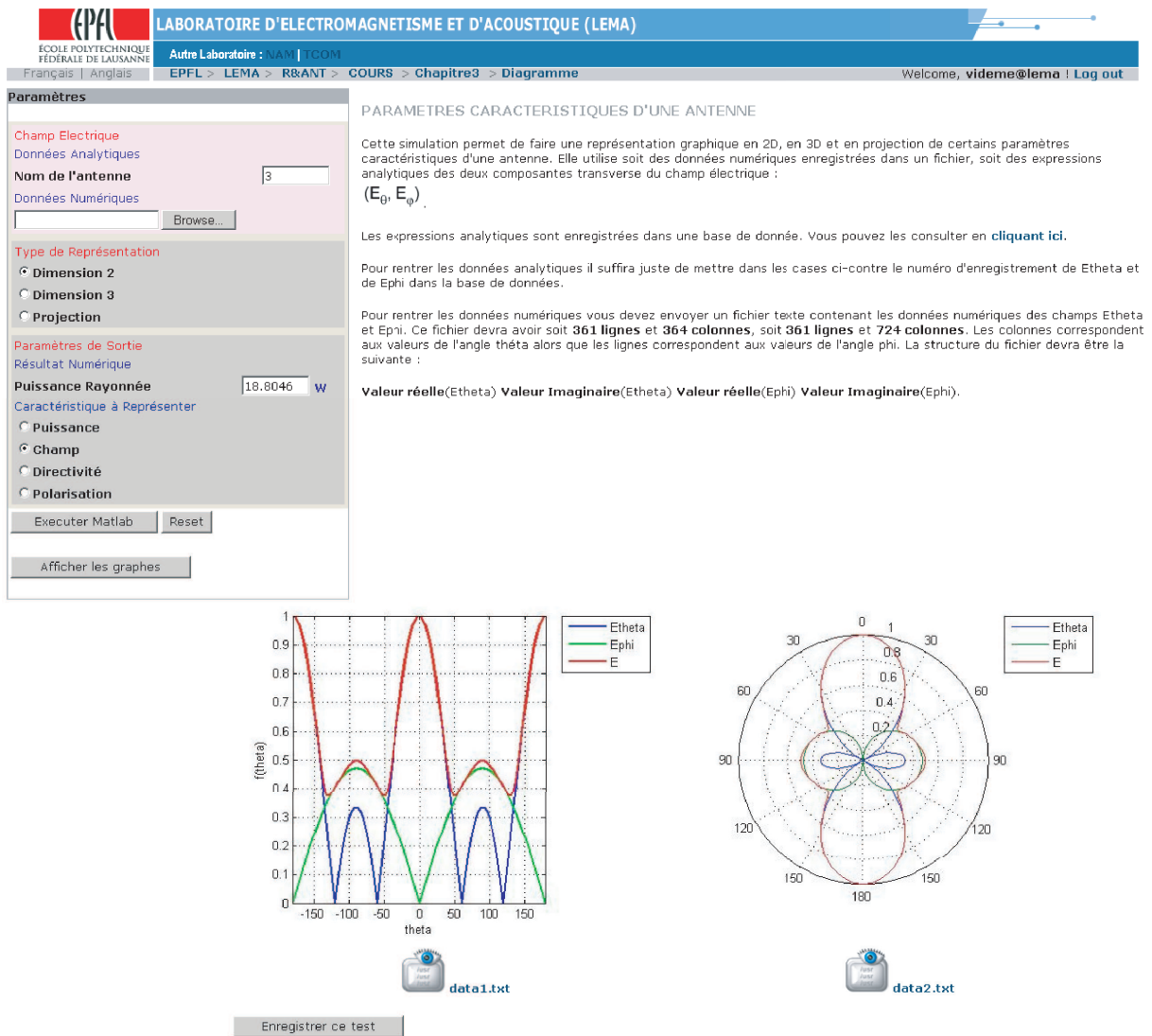
If he clicks on the simulation item, the web page will be the same one as the web page on FIGURE 5.5. Then when clicking on "Execute Matlab" and, after a while, on "Show the graph" he will see his simulation results (FIGURE 5.8). Here he can save his results in his own folder by clicking on "Save this test". After clicking on this button, the history menu will appear on the web site (FIGURE 5.9). The saved simulation can be seen at any time the user wants.

### 5.4 Some examples of available simulations

While the number of possible Matlab programs that can be used in a basic antenna course is particularly boundless, we will just illustrate here a reduced set especially selected because it allows one to better understand our proposed philosophy. However it must be pointed out that the e-antenna website described in section 5.2 is fairly independent on the specific mathematical or numerical problem we are considering. Thus almost every practical problem of antenna theory can be treated within this framework and indeed new softwares are currently and ceaselessly being added. One of the most classical problems in antenna theory is provided by the wire antenna. We design here an "open" strategy courseware (FIGURE 5.10) since the user can introduce numerical values or his own numerical values stored in files as input parameters. By practicing himself the operations at each stage of the simulation process he can verify his understanding of the course. Among all



## 5.4. SOME EXAMPLES OF AVAILABLE SIMULATIONS



©2006 Olivier Vidémé Bossou [olivier.videmebossou@epfl.ch](mailto:olivier.videmebossou@epfl.ch)  
 Mise à jour : January 12 2007 18:22:01.

FIGURE 5.8: Simulation results on the web page when the user is logged in

# CHAPTER 5. REMOTE COURSE ON ANTENNA TEACHING

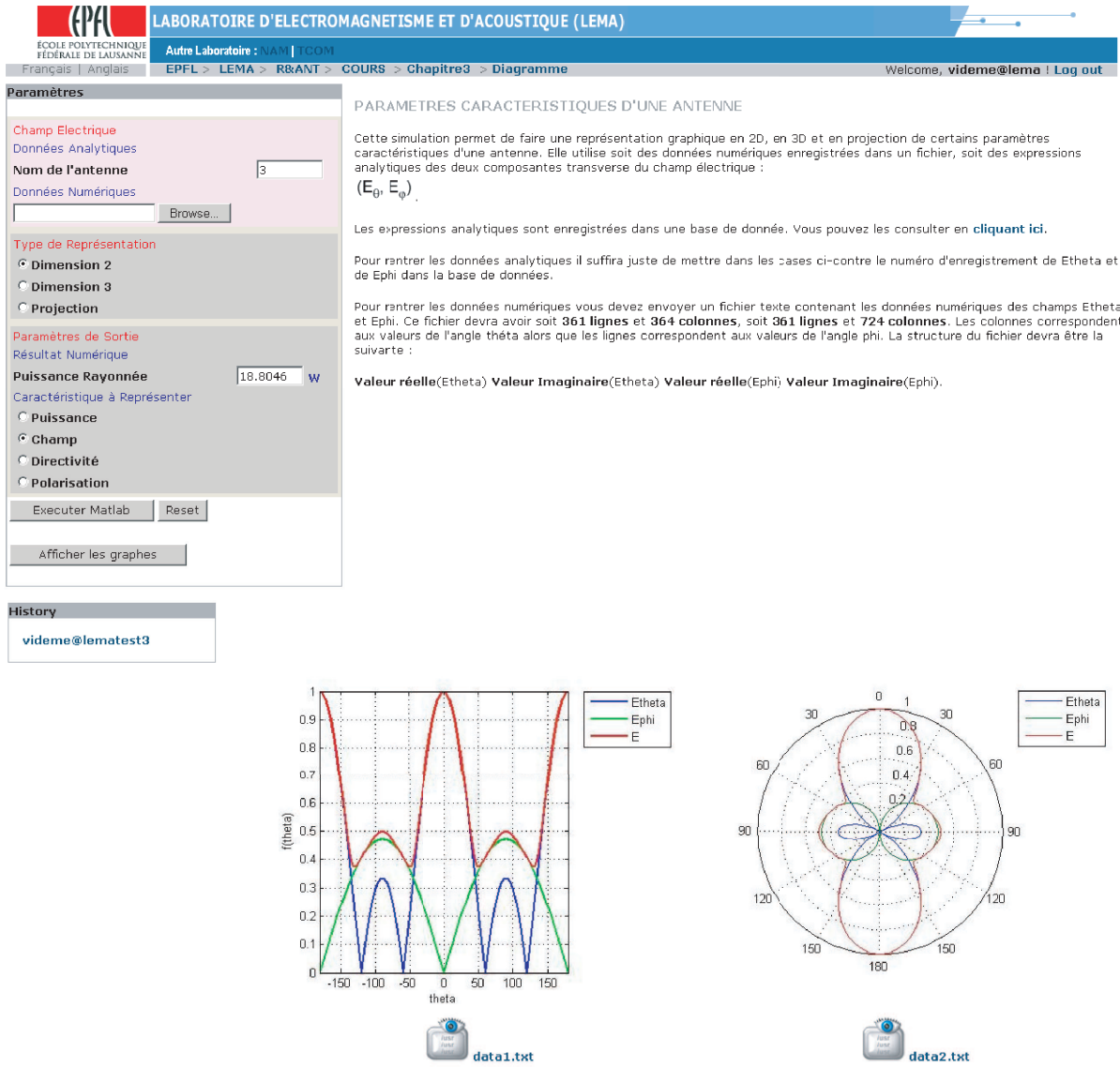


FIGURE 5.9: Simulation results with the history menu on the web page when the user is logged in

## 5.4. SOME EXAMPLES OF AVAILABLE SIMULATIONS

---

the simulations we will describe in this thesis three of them to highlight our philosophy. These simulations are :

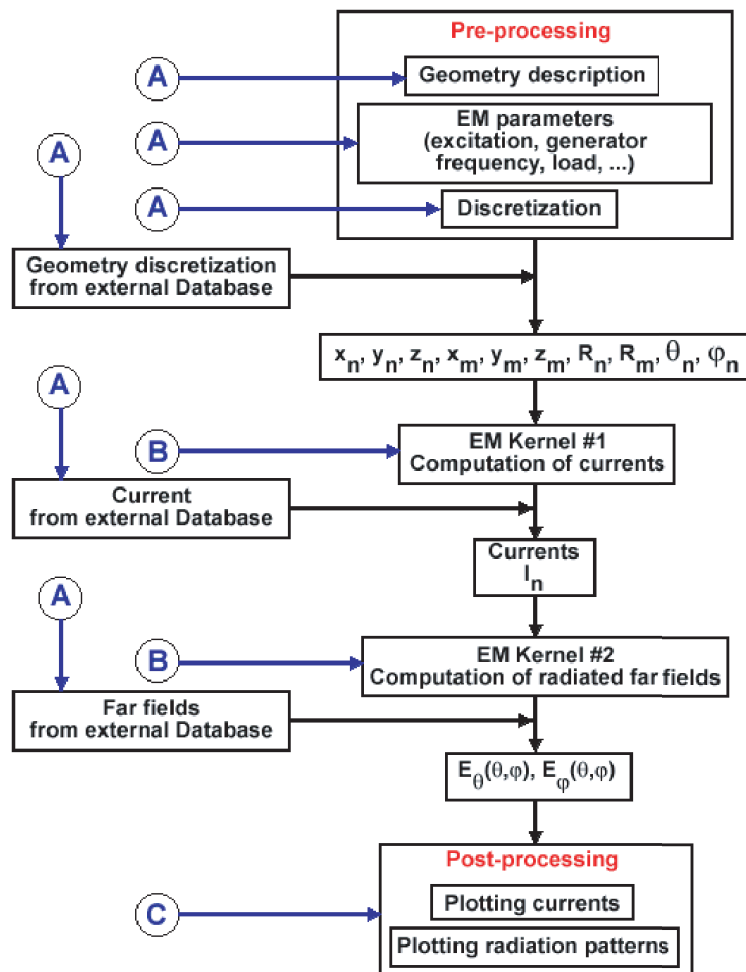
- "TheorieDesLignes" which uses transmission line model to calculate the current distributions on a wire antenna.
- "MoM" which uses method of moment to calculate the current distributions on a wire antenna.
- "Diagramme" which uses the theoretical or numerical expression of the fields to calculate and draw some antenna characteristics.

These simulations are used here only for educational, but not for design purposes. Thus the rigorous mathematical developments and algorithm precisions would be out of scope here. Instead of using rigorous mathematical expressions, we choose a best conviviality and great simplicity usage of the simulations in order to put the user at ease in antenna course learning.

### 5.4.1 Currents in wire antennas with a TL model

The purpose of this simulation is to calculate the distribution of current along a thin wire antenna by using transmission line (TL) theory. In particular the TL model gives accurate results for straight or slightly bent wires solving a bilateral symmetry with a generator in it. A reasonable approximation to find the current in a wire antenna of length  $D = 2d$  excited at its center, is to approach it with a transmission line with a length which is half of that of the antenna ( $d = D/2$ ). The line is excited by a Thevenin voltage generator  $V_g$  with an internal complex impedance  $Z_g$ , and charged with a complex termination  $Z_L$ . On the basis of the expressions of current and voltage in transmission line theory on which we rely, we can calculate the expression of the current, the voltage, the reflection coefficient, the impedance at any point of the transmission line :

$$\rho(z) = \rho_L e^{j2\beta(z-d)} \tag{5.4.1}$$



- A :** Matlab is used as an easy way of processing input data and database, including user-friendly graphical user interfaces.
- B :** Matlab is used as a numerical engine for performing sophisticated numerical algorithms.
- C :** Matlab is used as a flexible graphical tool for plotting numerical results.

FIGURE 5.10: Open strategy courseware

#### 5.4. SOME EXAMPLES OF AVAILABLE SIMULATIONS

---

$$v(z) = 0.5V_g \frac{1 - \rho_g}{1 - \rho_g \rho_L e^{-j2\beta d}} e^{-j\beta z} (1 + \rho(z)) \quad (5.4.2)$$

$$I(z) = 0.5 \frac{V_g}{Z_c} \frac{1 - \rho_g}{1 - \rho_g \rho_L e^{-j2\beta d}} e^{-j\beta z} (1 - \rho(z)) \quad (5.4.3)$$

$$Z(z) = Z_c \frac{1 + \rho(z)}{1 - \rho(z)} \quad (5.4.4)$$

As input parameters we have :

- $N$  : the transmission line is divided into several segments.  $N$  is the total number of segments.
- $Z_c$  : the characteristic impedance of the transmission line.
- $v_{phi}$  : the phase velocity of the signal in the transmission line.
- $d$  : the length of the transmission line.
- $f$  : frequency of the signal.
- $U_g$  : voltage of Thevenin generator.
- $Z_g$  : internal impedance of the Thevenin generator.
- $Z_L$  : load impedance.


For the internal impedance of the Thevenin generator and the load impedance, the information can be entered in two ways :

- the canonic form : in this form we enter the real and imaginary part of the impedance value.
- the exponential form : in this form we enter the amplitude and the phase in degrees of the impedance value.

For instance, if we enter :

- $N = 100$


# CHAPTER 5. REMOTE COURSE ON ANTENNA TEACHING



ÉCOLE POLYTECHNIQUE  
FÉDÉRALE DE LAUSANNE

**LABORATOIRE D'ELECTROMAGNETISME ET D'ACOUSTIQUE (LEMA)**

Autre Laboratoire : NAM | TCOM



Français | Anglais
EPFL > LEMA > R&ANT > COURS > Chapitre1 > TheorieDesLignes
Welcome, [videme@lema](mailto:videme@lema) ! [Log out](#)

**Paramètres**

*Ligne de Transmission*

Nombre de Segments (N)

Impédance Caractéristique (Zc)  ohms

Vitesse de Phase (Vphi)  m/s

Longueur (d)  m

*Variables Complexes*

Forme canonique  Forme exponentielle

*Générateur*

Fréquence (f)  Hz

Tension (Ug)  v

*Impédance interne (Zg)*

Partie réelle/Amplitude  ohms

Partie imaginaire/Phase  ohms/degré

*Charge ZL*

Partie réelle/Amplitude  ohms

Partie imaginaire/Phase  ohms/degré

*Variable de sortie*

Courant

Tension

Coefficient de réflexion

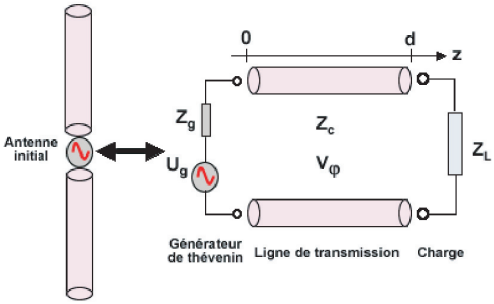
Impédance

LA THEORIE DES LIGNES

Une approximation raisonnable pour trouver le courant dans une antenne filaire de longueur  $D=2d$  excitée dans son centre est de l'approcher par une ligne de transmission dont la longueur est la moitié de celle de l'antenne soit  $d=D/2$ . La ligne est excitée par un générateur de Thévenin de tension  $V_g$  et d'impédance interne complexe  $Z_g$ , et chargée avec une terminaison complexe  $Z_L$ . Une valeur que l'on utilisera le plus souvent pour  $Z_L$  est le circuit ouvert (impédance infinie). La meilleure façon de l'indiquer sous **MatLab** est de lui attribuer la valeur réelle maximale **REALMAX** que peut fournir l'ordinateur. Partant des expressions des courant et tension dont nous disposons, nous pouvons calculer l'expression du courant en tout point de la ligne de transmission soit :

$$Z_c I(z) = 0.5 V_g \frac{1 - \rho_g}{1 - \rho_g \rho_L e^{-j2\beta d}} e^{j\beta z} (1 - \rho_L e^{j2\beta(z-d)})$$

Puis en posant pour l'antenne que  $I(z) = I(-z)$ , cela nous permet de tracer la distribution du courant sur l'antenne.



©2006 Olivier Vidémé Bossou [olivier.videmebossou@epfl.ch](mailto:olivier.videmebossou@epfl.ch)  
 Mise à jour : September 21 2006 16:09:26.

FIGURE 5.11: Transmission line theory on the web page

- $Z_c = 1 \Omega$
- $v_{phi} = 3 \cdot 10^8 \text{ m/s}$
- $d = 0.25 \text{ m}$
- $f = 3 \cdot 10^9 \text{ Hz}$
- $U_g = 1 \text{ V}$
- $Z_g = 1 + j0 \Omega$
- $Z_L = \text{realmax} + j0 \Omega$

as input values, we will obtain the results shown on FIGURE 5.12.

### 5.4.2 Method of moments

The method of moments is a numerical technique used to model antennas, which determines the current distribution on the radiating elements and highlights the influence of the geometry and the geometric disposition of these elements on the characteristics of an antenna. The antennas we are going to study here are wire antennas having any kind of shape, where wires have a negligible radius and width, as compared to the wavelength of the signal.

#### Discretization

Before discretizing our antenna, we must first determine whether there are corners in the geometry of the antenna. If there are corners, each corner must be located at the beginning or at the end of a segment. Once all the corners have been considered, we can discretize our antenna and determine the coordinates of each segment. When all the elements have been discretized, we can have different forms of segments for the same antenna, which are summarized in FIGURE 5.13. The coordinates of each segment will be the following ones :

- the points on the axis of symmetry will have  $x_n$ ,  $y_n$  and  $z_n$  as coordinates.

# CHAPTER 5. REMOTE COURSE ON ANTENNA TEACHING

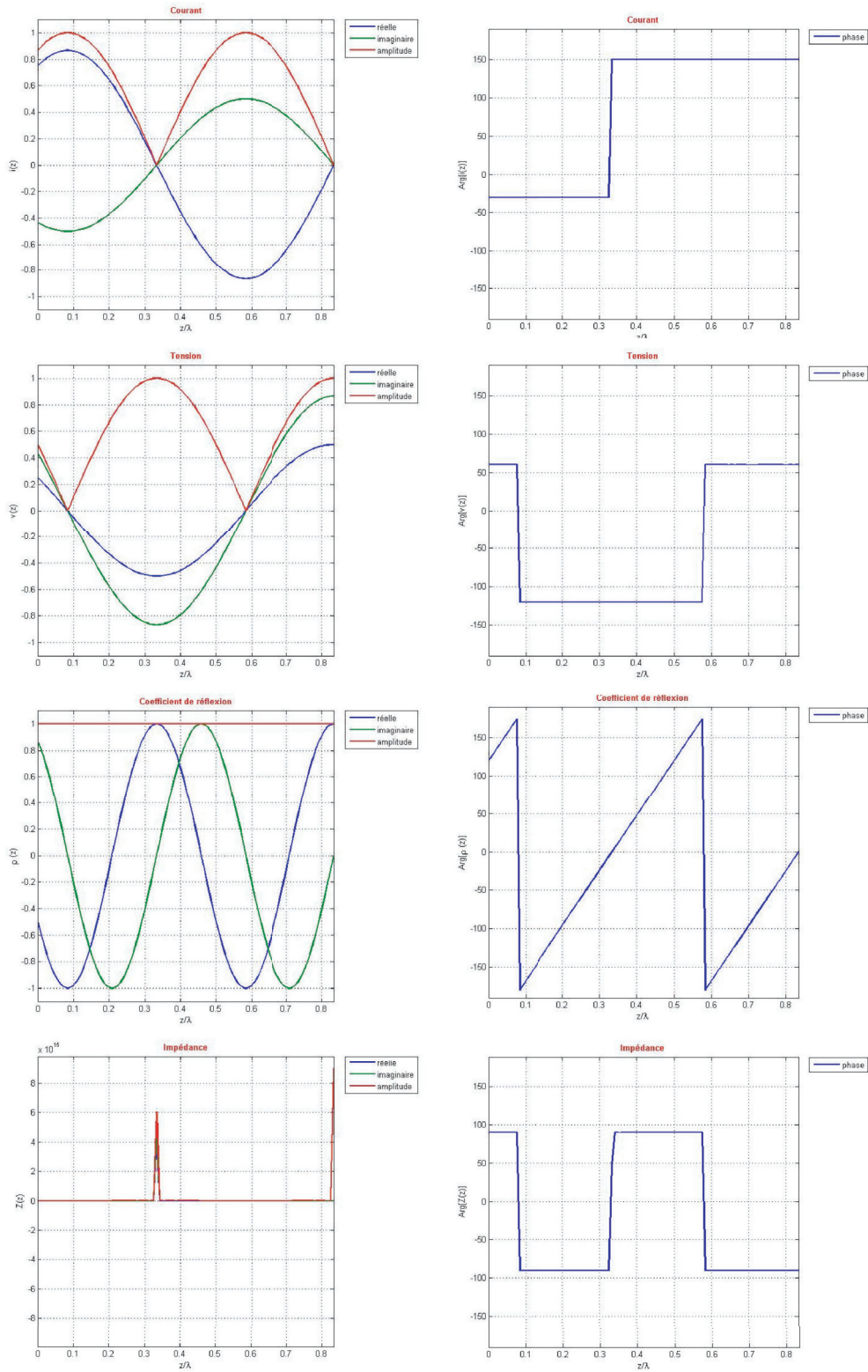


FIGURE 5.12: Example of transmission line theory simulation



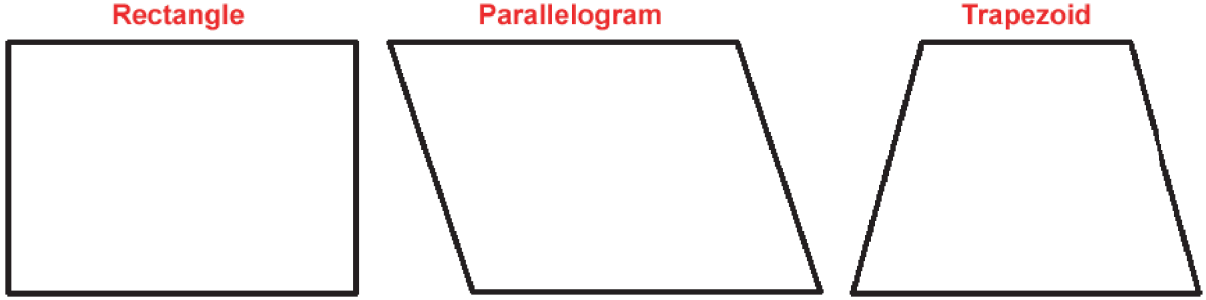


FIGURE 5.13: Segment forms

- the points on the surface of the wire (in the case of a cylindrical wire) or at the edge of the wire (in the case of a rectangular parallelepipedic wire) will have  $x_m$ ,  $y_m$  and  $z_m$  as coordinates.

The beginning and the end of a segment will be distinguished by adding the sign (-) for the beginning of a segment ( $x_{n-}$ ,  $y_{n-}$  and  $z_{n-}$ ) and the sign (+) for the end of a segment ( $x_{n+}$ ,  $y_{n+}$  and  $z_{n+}$ ). An example is shown on FIGURE 5.14.

### Basis functions

As basis functions for the approximation, we will use rooftop functions, as shown in FIGURE 5.15

### Matrix solution

The method of moments was developed by Harrington [75]. From its development, we can calculate the impedance matrix by using the equation :

$$Z_{mn} = j\omega\mu\Delta l_n\Delta l_m\psi(n, m) + \frac{1}{j\omega\varepsilon} [\psi(n^+, m^+) - \psi(n^-, m^+) - \psi(n^+, m^-) + \psi(n^-, m^-)] \quad (5.4.5)$$

with :

$$\psi(n, m) = \frac{1}{\Delta l_n} \int_{\Delta l_n} \frac{e^{-jkR_m}}{4\pi R_m} \quad (5.4.6)$$

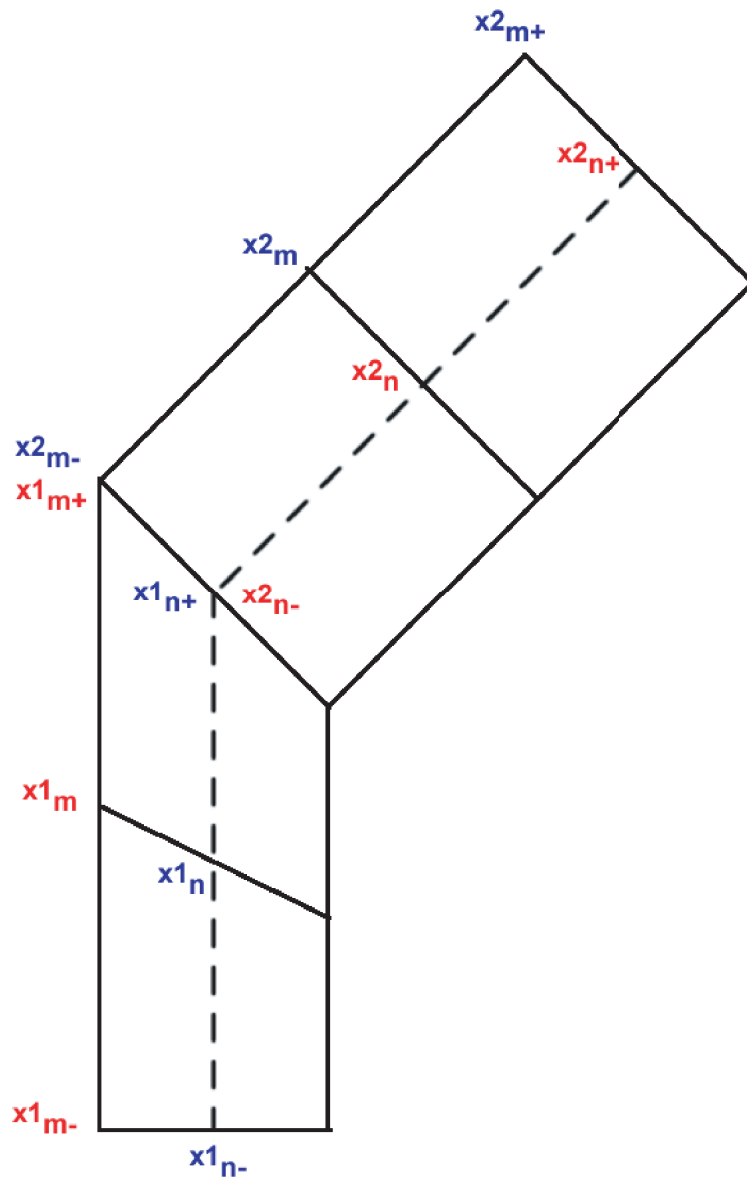


FIGURE 5.14: Segment coordinates

#### 5.4. SOME EXAMPLES OF AVAILABLE SIMULATIONS

---

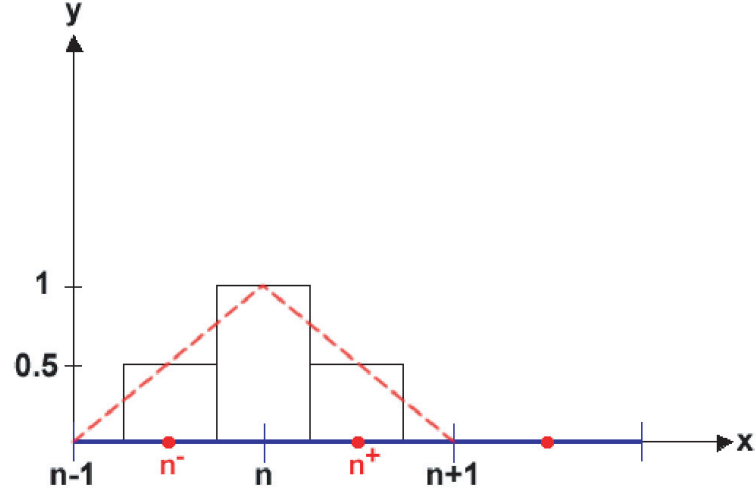


FIGURE 5.15: Basis function

$$R_m = \sqrt{(x_n - x_m)^2 + (y_n - y_m)^2 + (z_n - z_m)^2} \quad (5.4.7)$$

$$\Delta l_n = \sqrt{(x_{n+} - x_{n-})^2 + (y_{n+} - y_{n-})^2 + (z_{n+} - z_{n-})^2} \quad (5.4.8)$$

$$\Delta l_m = \sqrt{(x_{m+} - x_{m-})^2 + (y_{m+} - y_{m-})^2 + (z_{m+} - z_{m-})^2} \quad (5.4.9)$$

To calculate the impedance matrix, we define on each segment a local coordinate system with its origin at the center of the segment and as  $(o, z)$  axis the symmetrical axis of the segment as shown by FIGURE 5.16. The resulting expression for  $\psi(m, n)$  is :

$$\psi(m, n) = \frac{1}{8\pi\alpha} \int_{-\alpha}^{+\alpha} \frac{e^{-jkR_m}}{R_m} dz \quad (5.4.10)$$

with :

$$R_m = \sqrt{x_m^2 + y_m^2 + (z - z_m)^2} \quad (5.4.11)$$

$$2\alpha = \Delta l_n \quad (5.4.12)$$

To approximate the value of  $\psi(m, n)$ , we propose to expand the function to be integrated over a MacLaurin series, including only the terms until order 4. In order to accelerate the convergence of the function to be integrated, we will consider two cases :

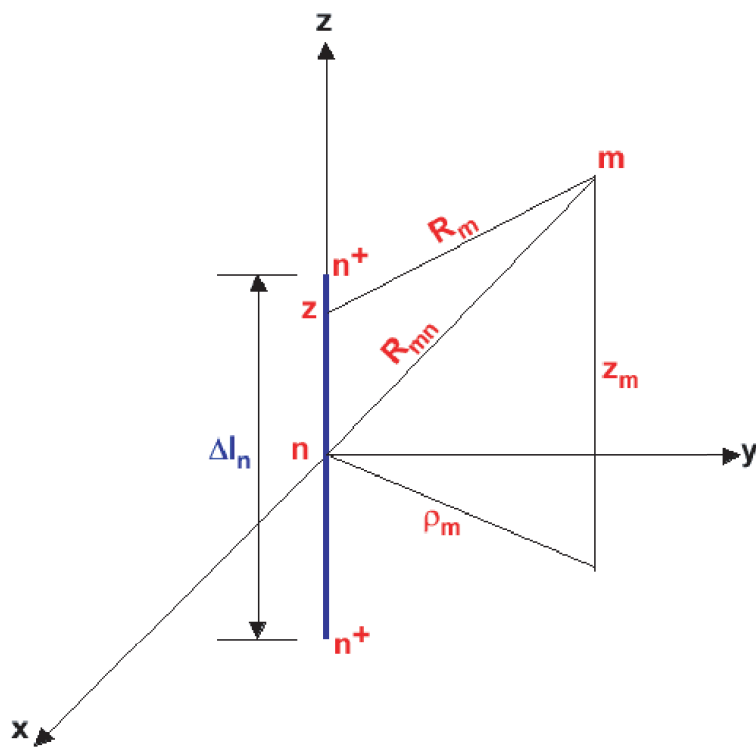


FIGURE 5.16: Geometry for the calculation of  $\psi(m, n)$

#### 5.4. SOME EXAMPLES OF AVAILABLE SIMULATIONS

---

1.  $r < 10\alpha$ ;
2.  $r \geq 10\alpha$ .

with :

$$r = \sqrt{x_m^2 + y_m^2 + z_m^2} \quad (5.4.13)$$

##### FIRST CASE :

In the first case we will only express the exponential as a MacLaurin series until order

4. In recall we know that :

$$e^x = 1 + x + \frac{x^2}{2} + \frac{x^3}{6} + \frac{x^4}{24} + \dots \quad (5.4.14)$$

Knowing that :

$$e^{-jkR_m} = e^{-jkr} e^{-jk(R_m-r)} \quad (5.4.15)$$

and by setting  $x = -jk(R_m - r)$  we have :

$$e^{-jk(R_m-r)} = 1 - jk(R_m - r) - \frac{k^2(R_m - r)^2}{2} + j\frac{k^3(R_m - r)^3}{6} + \frac{k^4(R_m - r)^4}{24} \quad (5.4.16)$$

The equation (5.4.10) becomes :

$$\begin{aligned} \psi(m, n) = \frac{e^{-jkr}}{8\pi\alpha} \int_{-\alpha}^{+\alpha} & \left( \frac{1}{R_m} - \frac{jk(R_m - r)}{R_m} - \frac{k^2(R_m - r)^2}{2R_m} \right. \\ & \left. + j\frac{k^3(R_m - r)^3}{6R_m} + \frac{k^4(R_m - r)^4}{24R_m} \right) dz \end{aligned} \quad (5.4.17)$$

To calculate this integral, we will divide it into several parts :

$$\begin{aligned} I_1 &= \int_{-\alpha}^{+\alpha} \frac{dz}{R_m} = \left[ -\ln(z_m - z + \sqrt{x_m^2 + y_m^2 + (z_m - z)^2}) \right]_{-\alpha}^{+\alpha} \\ &= \ln \left( \frac{z_m + \alpha + \sqrt{x_m^2 + y_m^2 + (z_m + \alpha)^2}}{z_m - \alpha + \sqrt{x_m^2 + y_m^2 + (z_m - \alpha)^2}} \right) \end{aligned} \quad (5.4.18)$$

$$\begin{aligned}
 I_2 &= \int_{-\alpha}^{+\alpha} -\frac{jk(R_m - r)}{R_m} dz = \int_{-\alpha}^{+\alpha} \left( -jk + \frac{jkr}{R_m} \right) dz \\
 &= -jk(2\alpha - rI_1)
 \end{aligned} \tag{5.4.19}$$

$$\begin{aligned}
 I_3 &= \int_{-\alpha}^{+\alpha} R_m dz = \left[ -\frac{(z_m - z)}{2} \sqrt{x_m^2 + y_m^2 + (z_m - z)^2} \right. \\
 &\quad \left. - \frac{x_m^2 + y_m^2}{2} \ln(z_m - z + \sqrt{x_m^2 + y_m^2 + (z_m - z)^2}) \right]_{-\alpha}^{+\alpha} \\
 &= \frac{\alpha + z_m}{2} \sqrt{x_m^2 + y_m^2 + (\alpha + z_m)^2} + \frac{\alpha - z_m}{2} \sqrt{x_m^2 + y_m^2 + (\alpha - z_m)^2} \\
 &\quad + \frac{x_m^2 + y_m^2}{2} I_1
 \end{aligned} \tag{5.4.20}$$

$$\begin{aligned}
 I_4 &= \int_{-\alpha}^{+\alpha} -\frac{k^2(R_m - r)^2}{2R_m} dz = -\frac{k^2}{2} \int_{-\alpha}^{+\alpha} \left( R_m - 2r + \frac{r^2}{R_m} \right) dz \\
 &= -\frac{k^2}{2} (I_3 - 4r\alpha + r^2 I_1)
 \end{aligned} \tag{5.4.21}$$

$$\begin{aligned}
 I_5 &= \int_{-\alpha}^{+\alpha} R_m^2 dz = \int_{-\alpha}^{+\alpha} (x_m^2 + y_m^2 + (z_m - z)^2) dz \\
 &= \left[ (x_m^2 + y_m^2)z - \frac{1}{3}(z_m - z)^3 \right]_{-\alpha}^{+\alpha} \\
 &= 2\alpha(x_m^2 + y_m^2) + \frac{2\alpha^3 + 6\alpha z_m^2}{3}
 \end{aligned} \tag{5.4.22}$$

$$\begin{aligned}
 I_6 &= \int_{-\alpha}^{+\alpha} j \frac{k^3(R_m - r)^3}{6R_m} dz = j \frac{k^3}{6} \int_{-\alpha}^{+\alpha} \left( R_m^2 - 3rR_m + 3r^2 - \frac{r^3}{R_m} \right) dz \\
 &= j \frac{k^3}{6} (I_5 - 3rI_3 + 6\alpha r^2 - r^3 I_1)
 \end{aligned} \tag{5.4.23}$$

#### 5.4. SOME EXAMPLES OF AVAILABLE SIMULATIONS

---

$$\begin{aligned}
 I_7 &= \int_{-\alpha}^{+\alpha} R_m^3 dz \\
 &= \left[ -\frac{1}{8} \sqrt{x_m^2 + y_m^2 + (z_m - z)^2} (5(x_m^2 + y_m^2) + 2(z_m - z)^2) (z_m - z) \right. \\
 &\quad \left. - \frac{3}{8} (x_m^2 + y_m^2)^2 \ln(z_m - z + \sqrt{x_m^2 + y_m^2 + (z_m - z)^2}) \right]_{-\alpha}^{+\alpha} \\
 &= \frac{3}{8} (x_m^2 + y_m^2)^2 I_1 \\
 &\quad + \sqrt{x_m^2 + y_m^2 + (\alpha + z_m)^2} \left( \frac{5}{8} (x_m^2 + y_m^2) (\alpha + z_m) + \frac{1}{4} (\alpha + z_m)^3 \right) \\
 &\quad + \sqrt{x_m^2 + y_m^2 + (\alpha - z_m)^2} \left( \frac{5}{8} (x_m^2 + y_m^2) (\alpha - z_m) + \frac{1}{4} (\alpha - z_m)^3 \right) \quad (5.4.24)
 \end{aligned}$$

$$\begin{aligned}
 I_8 &= \int_{-\alpha}^{+\alpha} \frac{k^4 (R_m - r)^4}{24 R_m} dz \\
 &= \frac{k^4}{24} \int_{-\alpha}^{+\alpha} \left( R_m^3 - 4r R_m^2 + 6r^2 R_m - 4r^3 + \frac{r^4}{R_m} \right) dz \\
 &= \frac{k^4}{24} (I_7 - 4r I_5 + 6r^2 I_3 - 8\alpha r^3 + r^4 I_1) \quad (5.4.25)
 \end{aligned}$$

And finally we have :

$$\psi(m, n) = \frac{e^{-jkr}}{8\pi\alpha} (I_1 + I_2 + I_4 + I_6 + I_8) \quad (5.4.26)$$

#### SECOND CASE :

In this second case, we will develop the complete function over a MacLaurin series :

$$\psi(m, n) = \frac{1}{8\pi\alpha} \int_{-\alpha}^{+\alpha} \left( f(0) + f'(0)z + \frac{1}{2!} f''(0)z^2 + \frac{1}{3!} f^{(3)}(0)z^3 + \frac{1}{4!} f^{(4)}(0)z^4 \right) dz \quad (5.4.27)$$

where :

$$f(z) = \frac{e^{-jk\sqrt{x_m^2 + y_m^2 + (z_m - z)^2}}}{\sqrt{x_m^2 + y_m^2 + (z_m - z)^2}}$$

After calculation we have the following expressions :

$$f(z) = \frac{e^{-jkR_m}}{R_m} \quad (5.4.28)$$

$$f'(z) = \frac{(z_m - z)e^{-jkR_m}}{R_m^2} \left( jk + \frac{1}{R_m} \right) \quad (5.4.29)$$

$$f''(z) = \frac{e^{-jkR_m}}{R_m} \left[ \left( \frac{1}{R_m^2} + j\frac{k}{R_m} \right) \left( -1 + 3 \left[ \frac{z_m - z}{R_m} \right]^2 \right) - k^2 \left( \frac{z_m - z}{R_m} \right)^2 \right] \quad (5.4.30)$$

$$f^{(3)}(z) = \frac{e^{-jkR_m}}{R_m} \left[ \frac{3(z_m - z)}{R_m^3} \left( \frac{1}{R_m} + jk \right) \left( -3 + 5 \left[ \frac{z_m - z}{R_m} \right]^2 \right) + \frac{3k^2(z_m - z)}{R_m^2} \left( 1 - 2 \left[ \frac{z_m - z}{R_m} \right]^2 \right) - jk^3 \left( \frac{z_m - z}{R_m} \right)^3 \right] \quad (5.4.31)$$

$$f^{(4)}(z) = \frac{e^{-jkR_m}}{R_m} \left[ \frac{3}{R_m^3} \left( \frac{1}{R_m} + jk \right) \cdot \left( 3 - 30 \left[ \frac{z_m - z}{R_m} \right]^2 + 35 \left[ \frac{z_m - z}{R_m} \right]^4 \right) + \frac{3k^2}{R_m^2} \left( -1 + 12 \left[ \frac{z_m - z}{R_m} \right]^2 - 15 \left[ \frac{z_m - z}{R_m} \right]^4 \right) + j\frac{2k^3(z_m - z)^2}{R_m^3} \left( 3 - 5 \left[ \frac{z_m - z}{R_m} \right]^2 \right) + k^4 \left( \frac{z_m - z}{R_m} \right)^4 \right] \quad (5.4.32)$$

Equation (5.4.27) becomes :

$$\psi(m, n) = \frac{1}{8\pi\alpha} \left( 2\alpha f(0) + \frac{\alpha^3}{3} f''(0) + \frac{\alpha^5}{60} f^{(4)}(0) \right) \quad (5.4.33)$$



#### 5.4. SOME EXAMPLES OF AVAILABLE SIMULATIONS

---

where :

$$f(0) = \frac{e^{-jkr}}{r} \quad (5.4.34)$$

$$f''(0) = \frac{e^{-jkr}}{r} \left[ \frac{1}{r} \left( \frac{1}{r} + jk \right) \left( -1 + 3 \left[ \frac{z_m}{r} \right]^2 \right) - k^2 \left( \frac{z_m}{r} \right)^2 \right] \quad (5.4.35)$$

$$\begin{aligned} f^{(4)}(0) &= \frac{e^{-jkr}}{r} \left[ \frac{3}{r^3} \left( \frac{1}{r} + jk \right) \left( 3 - 30 \left[ \frac{z_m}{r} \right]^2 + 35 \left[ \frac{z_m}{r} \right]^4 \right) \right. \\ &\quad \left. + \frac{3k^2}{r^2} \left( -1 + 12 \left[ \frac{z_m}{r} \right]^2 - 15 \left[ \frac{z_m}{r} \right]^4 \right) \right. \\ &\quad \left. + j \frac{2k^3 z_m^2}{r^3} \left( 3 - 5 \left[ \frac{z_m}{r} \right]^2 \right) + k^4 \left( \frac{z_m}{r} \right)^4 \right] \end{aligned} \quad (5.4.36)$$

This gives us the following final form :

$$\psi(m, n) = \frac{e^{-jkr}}{4\pi r} \left( g(0) + \frac{\alpha^2}{6} g''(0) + \frac{\alpha^4}{120} g^{(4)}(0) \right) \quad (5.4.37)$$

with :

$$g(0) = 1 \quad (5.4.38)$$

$$g''(0) = \frac{1}{r} \left( \frac{1}{r} + jk \right) \left( -1 + 3 \left[ \frac{z_m}{r} \right]^2 \right) - k^2 \left( \frac{z_m}{r} \right)^2 \quad (5.4.39)$$

$$\begin{aligned} g^{(4)}(0) &= \frac{3}{r^3} \left( \frac{1}{r} + jk \right) \left( 3 - 30 \left[ \frac{z_m}{r} \right]^2 + 35 \left[ \frac{z_m}{r} \right]^4 \right) \\ &\quad + \frac{3k^2}{r^2} \left( -1 + 12 \left[ \frac{z_m}{r} \right]^2 - 15 \left[ \frac{z_m}{r} \right]^4 \right) \\ &\quad + j \frac{2k^3 z_m^2}{r^3} \left( 3 - 5 \left[ \frac{z_m}{r} \right]^2 \right) + k^4 \left( \frac{z_m}{r} \right)^4 \end{aligned} \quad (5.4.40)$$

Knowing  $Z$  we can easily determine the current  $I$  by :

$$[I] = [Z^{-1}][V] \quad (5.4.41)$$

### Field calculation

Once we have obtained the matrix impedance, and knowing the matrix excitation  $[V]$ , we can calculate the distribution of the current on the antenna. This enables us to calculate the vector potential  $\vec{A}$  :

$$\vec{A} = \frac{\mu e^{-jkR}}{4\pi R} \sum_n I(n) \Delta l_n e^{jk(x_n \sin(\theta) \cos(\varphi) + y_n \sin(\theta) \sin(\varphi) + z_n \cos(\theta))} \vec{e}_n \quad (5.4.42)$$

The vector potential  $\vec{A}$  is a sum of vectors. Each element of vector  $\vec{A}$  is aligned along the segment to which it refers. We can then determine its three components in the rectangular system of coordinates :

$$A_x(\theta, \varphi) = \sum_n A_n(\theta) \sin(\theta_n) \cos(\varphi_n) \quad (5.4.43)$$

$$A_y(\theta, \varphi) = \sum_n A_n(\theta) \sin(\theta_n) \sin(\varphi_n) \quad (5.4.44)$$

$$A_z(\theta, \varphi) = \sum_n A_n(\theta) \cos(\theta_n) \quad (5.4.45)$$

with :

$$A_n = \frac{\mu e^{-jkR}}{4\pi R} I(n) \Delta l_n e^{jk(x_n \sin(\theta) \cos(\varphi) + y_n \sin(\theta) \sin(\varphi) + z_n \cos(\theta))} \quad (5.4.46)$$

These three components enable us to calculate the polar components along  $\theta$  and  $\varphi$  :

## 5.4. SOME EXAMPLES OF AVAILABLE SIMULATIONS

---

$$A_{\theta}(\theta, \varphi) = A_x \cos(\theta) \cos(\varphi) + A_y \cos(\theta) \sin(\varphi) - A_z \sin(\theta) \quad (5.4.47)$$

$$A_{\varphi}(\theta, \varphi) = -A_x \sin(\varphi) + A_y \cos(\varphi) \quad (5.4.48)$$

Knowing these two components, we can then determine the far field radiated by the antenna :

$$E_{\theta} = -j\omega A_{\theta} \quad (5.4.49)$$


$$E_{\varphi} = -j\omega A_{\varphi} \quad (5.4.50)$$

### Results of the simulation

In the page depicting the MoM simulation (FIGURE 5.17), we can introduce the input parameters in two different ways : we can send a file to the server or introduce numerical data. If we introduce as input parameters the values summarized in TABLE 5.1 the results obtained are shown in FIGURE 5.18 and FIGURE 5.19.

Otherwise, in the case of a geometrical file, it must contain the co-ordinates of the segments placed in six columns (Xn Yn Zn Xm Ym Zm). Furthermore, a first line must be added to this file in order to provide additional information. The first element of the first column provides the number of the feeding point of the antenna, while the first element of the second column must be set equal to 1 in the case of a linear wire antenna, or to 2 for a loop antenna. The current file must contain the current value placed in two columns : the first column is the real part of the current and the second column the imaginary part.

# CHAPTER 5. REMOTE COURSE ON ANTENNA TEACHING



ÉCOLE POLYTECHNIQUE  
FÉDÉRALE DE LAUSANNE

LABORATOIRE D'ELECTROMAGNETISME ET D'ACOUSTIQUE (LEMA)

Autre Laboratoire : NAM | TCOM

EPFL > LEMA > R&ANT > COURS > Chapitre2 > MoM

Log in

---

**Paramètres**

Type d'antenne  
Antenne Rectiligne

Paramètres d'entrée

Nombre de Segments: 61

Rayon/Largeur du Fil: 0.001

Longueur/Rayon de l'Antenne: 1

Nombre de Branches: 6

Angle: 14

Ecart entre Branches: 0.1

Données dans un fichier

Géométrie:  Browse...

Courant:  Browse...

Paramètres de Sortie



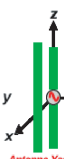
Courant  
 Champ

Executer Matlab    Reset

Afficher les graphes

LA METHODE DES MOMENTS

La méthode des moments est une technique qui permet de modéliser les antennes en donnant la distribution du courant sur l'élément considéré et en mettant en évidence l'influence de la géométrie et de la disposition des éléments rayonnants sur les caractéristiques d'une antenne. Dans cet exercice il sera question de sectionner une antenne filiforme quelconque en éléments infinitésimaux puis de sauvegarder cette géométrie dont chaque coordonnée sera exprimée en longueur d'onde dans un fichier. Ensuite d'utiliser cet utilitaire pour déterminer la distribution de courant le long de l'antenne. Le fichier devra contenir les coordonnées des segments en six colonnes (Xn Yn Zn Xn Yn Zn). On ajoutera une première ligne supplémentaire à chaque colonne qui contiendra des informations complémentaires. Le premier élément de la première colonne doit contenir le numéro du segment qui contient le point d'alimentation de l'antenne et le premier élément de la deuxième colonne doit contenir le numéro 1 dans le cas d'une antenne rectiligne normale, ou bien le numéro 2 dans le cas d'une antenne rectiligne en boucle fermée.








Figure 1 : Liste des antennes

**Exemple :** Soit une antenne rectiligne divisée en trois segments et alimentée en son centre (segment 2). Le fichier de la géométrie de cette antenne sera la suivante :

2	1	0	0	0	0
0	0	-1.5	0	0.025	-1.5
0	0	-0.5	0	0.025	-0.5
0	0	0.5	0	0.025	0.5
0	0	1.5	0	0.025	1.5

N.B. : Les dimensions des données se trouvant dans la fenêtre "Paramètres" sont exprimées en longueur d'onde. L'angle est exprimé en degré.

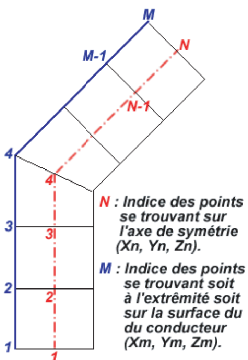


Figure 2 : Segmentation de l'antenne

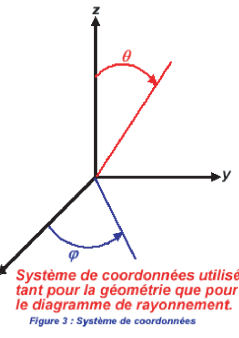


Figure 3 : Système de coordonnées

©2006 Olivier Vidémé Bossou [olivier.videmebossou@epfl.ch](mailto:olivier.videmebossou@epfl.ch)  
Mise à jour : December 20 2006 15:27:26.

FIGURE 5.17: Web page of the MoM simulation

## 5.4. SOME EXAMPLES OF AVAILABLE SIMULATIONS

---

TABLE 5.1: Input parameter values

Linear wire antenna	Circular loop antenna	Square loop antenna	Archimedean spiral antenna	Helical antenna	Yagi antenna
Segment number 61	Segment number 36	Segment number 31	Segment number 15	Segment number per spire 36	Segment number per element 21
Radius of the wire 0.001 (wavelength)	Radius of the wire 0.001 (wavelength)	Radius of the wire 0.001 (wavelength)	Width of the wire 0.001 (wavelength)	Radius of the wire 0.0001 (wavelength)	Radius of the wire 0.003 (wavelength)
Length of the antenna 1 (wavelength)	Radius of the antenna 0.05 (wavelength)	Width of the antenna 4.44 (wavelength)	Length of the central branch 0.005 (wavelength)	Spire circumference 0.73 (wavelength)	Elements length [0.406; 0.406; 0.5; 0.47] (wavelength)
			Branch number 5	Number of spire 6	Spacing between elements [0.334 0.334 0.244] (wavelength)
			Spacing between branches 0.0001 (wavelength)	Angle 14 (degree)	

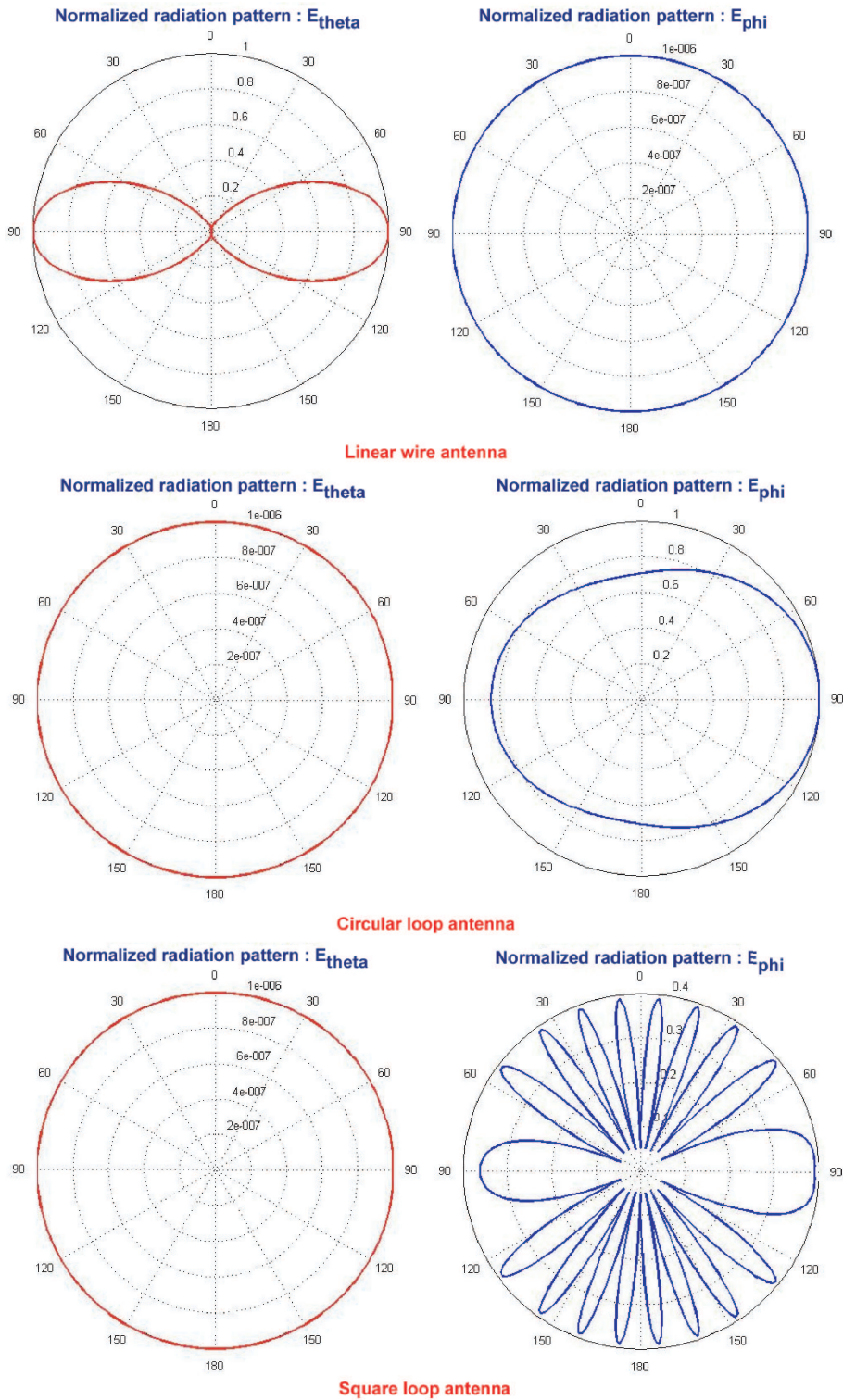


FIGURE 5.18: MoM simulation results (a)

## 5.4. SOME EXAMPLES OF AVAILABLE SIMULATIONS

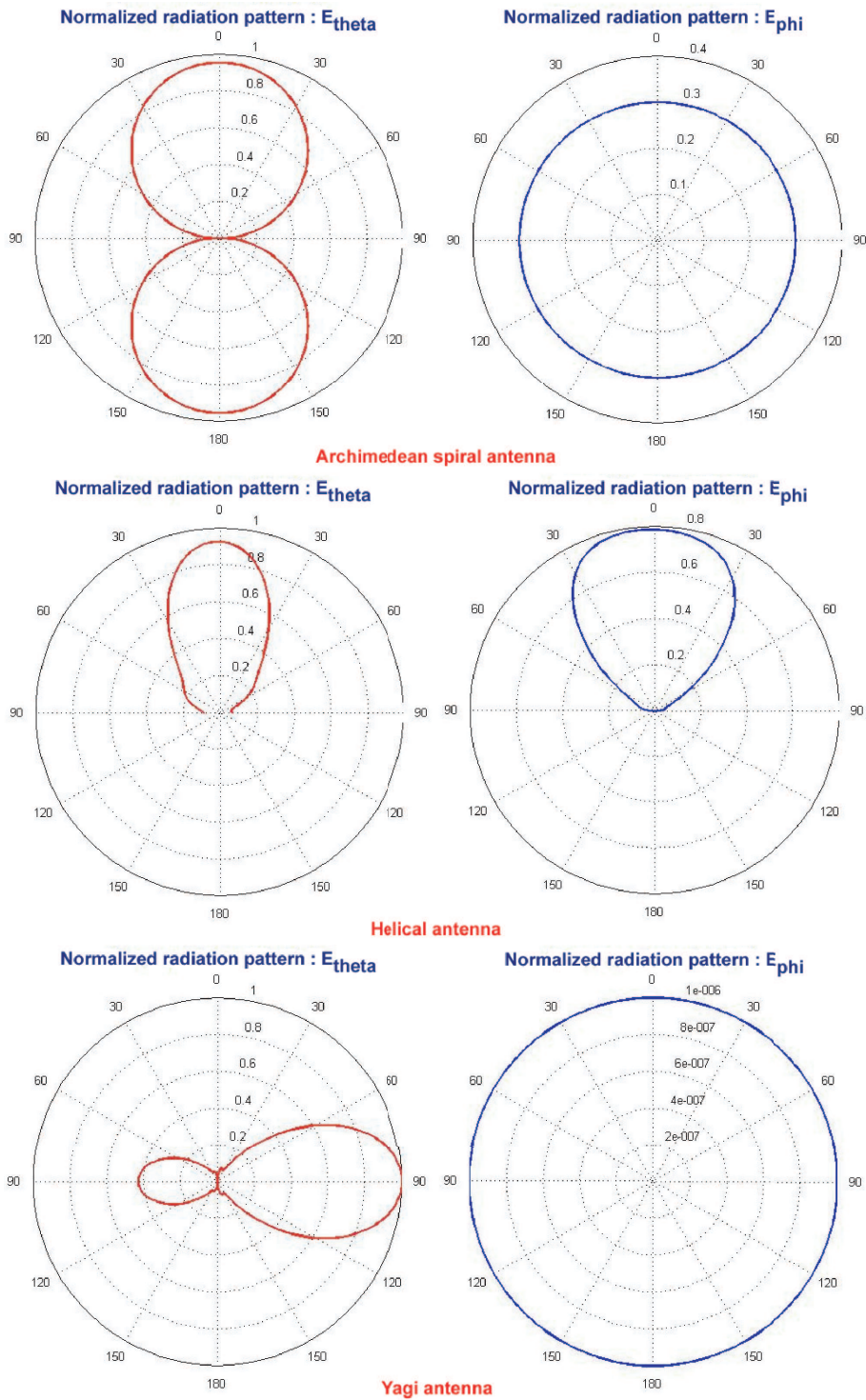


FIGURE 5.19: MoM simulation results (b)

## CHAPTER 5. REMOTE COURSE ON ANTENNA TEACHING

The screenshot shows a web application interface for antenna simulation. At the top, there is a header for the EPFL (École Polytechnique Fédérale de Lausanne) and the Laboratory of Electromagnetism and Acoustics (LEMA). The navigation bar includes links for 'Autre Laboratoire : NANT | TCOM', 'EPFL > LEMA > R&ANT > COURS > Chapitre3 > Diagramme', and a 'Log in' button.

The main content area is titled 'PARAMETRES CARACTERISTIQUES D'UNE ANTENNE'. It is divided into two columns. The left column contains a 'Paramètres' sidebar with several sections:

- Champ Electrique**: 'Données Analytiques' section with a 'Nom de l'antenne' input field containing '1' and a 'Données Numériques' section with a 'Browse...' button.
- Type de Représentation**: Radio buttons for 'Dimension 2' (selected), 'Dimension 3', and 'Projection'.
- Paramètres de Sortie**: 'Résultat Numérique' section with a 'Puissance Rayonnée' input field containing '1' and a unit 'W'. Below it, 'Caractéristique à Représenter' section has radio buttons for 'Puissance' (selected), 'Champ', 'Directivité', and 'Polarisation'.
- Buttons for 'Executer Matlab', 'Reset', and 'Afficher les graphes'.

The right column contains the following text:

Cette simulation permet de faire une représentation graphique en 2D, en 3D et en projection de certains paramètres caractéristiques d'une antenne. Elle utilise soit des données numériques enregistrées dans un fichier, soit des expressions analytiques des deux composantes transverse du champ électrique :

$$(E_{\theta}, E_{\phi})$$

Les expressions analytiques sont enregistrées dans une base de données. Vous pouvez les consulter en [cliquant ici](#).

Pour rentrer les données analytiques il suffira juste de mettre dans la case ci-contre le numéro d'enregistrement de l'antenne figurant dans la base de données.

Pour rentrer les données numériques vous devez envoyer un fichier texte contenant les données numériques des champs  $E_{\theta}$  et  $E_{\phi}$ . Ce fichier devra avoir soit **361 lignes et 364 colonnes**, soit **361 lignes et 724 colonnes**. Les colonnes correspondent aux valeurs de l'angle  $\theta$  alors que les lignes correspondentent aux valeurs de l'angle  $\phi$ . La structure du fichier devra être la suivante :

**Valeur réelle( $E_{\theta}$ ) Valeur Imaginaire( $E_{\theta}$ ) Valeur réelle( $E_{\phi}$ ) Valeur Imaginaire( $E_{\phi}$ ).**

©2006 Olivier Videmé Bossou [olivier.videmebossou@epfl.ch](mailto:olivier.videmebossou@epfl.ch)  
Mise à jour : March 29 2007 15:50:35.

FIGURE 5.20: Web page of antenna characteristics



### 5.4.3 Antenna characteristics graphical representation

In this simulation (FIGURE 5.20) we graphically represent some characteristics of the antennas. The graphs will be drawn in the plane or in space. We have two ways of communicating parameters to the software :

- The first one is mainly the analytical expressions of the fields stored in a database. The user can consult what is in the database and then put the number related to the selected antenna.
- Or, for the second one, the input parameters can be of numerical type stored in a file.

The file must have 361 lines and 364 columns, or 361 lines and 724 columns. The columns correspond to the values of the elevation angles theta whereas the lines correspond to the values of the azimuth angles phi. The structure of the file will be the following one :

Real value(Etheta[361, 91]) Imaginary value(Etheta[361, 91]) Real value(Ephi[361, 91]) Imaginary value(Ephi[361, 91])

or

Real value(Etheta[361, 181]) Imaginary value(Etheta[361, 181]) Real value(Ephi[361, 181]) Imaginary value(Ephi[361, 181])

If we choose the third registration in the database, with the following expression for the fields :

$$E_{\theta} = \frac{\sin(3\theta)}{\sin(\theta)} + \sin(\theta) \cos(\varphi)$$

$$E_{\varphi} = \sin(\theta) (j + \sin(\varphi))$$

the results will be those of FIGURE 5.21 and FIGURE 5.22.

## CHAPTER 5. REMOTE COURSE ON ANTENNA TEACHING

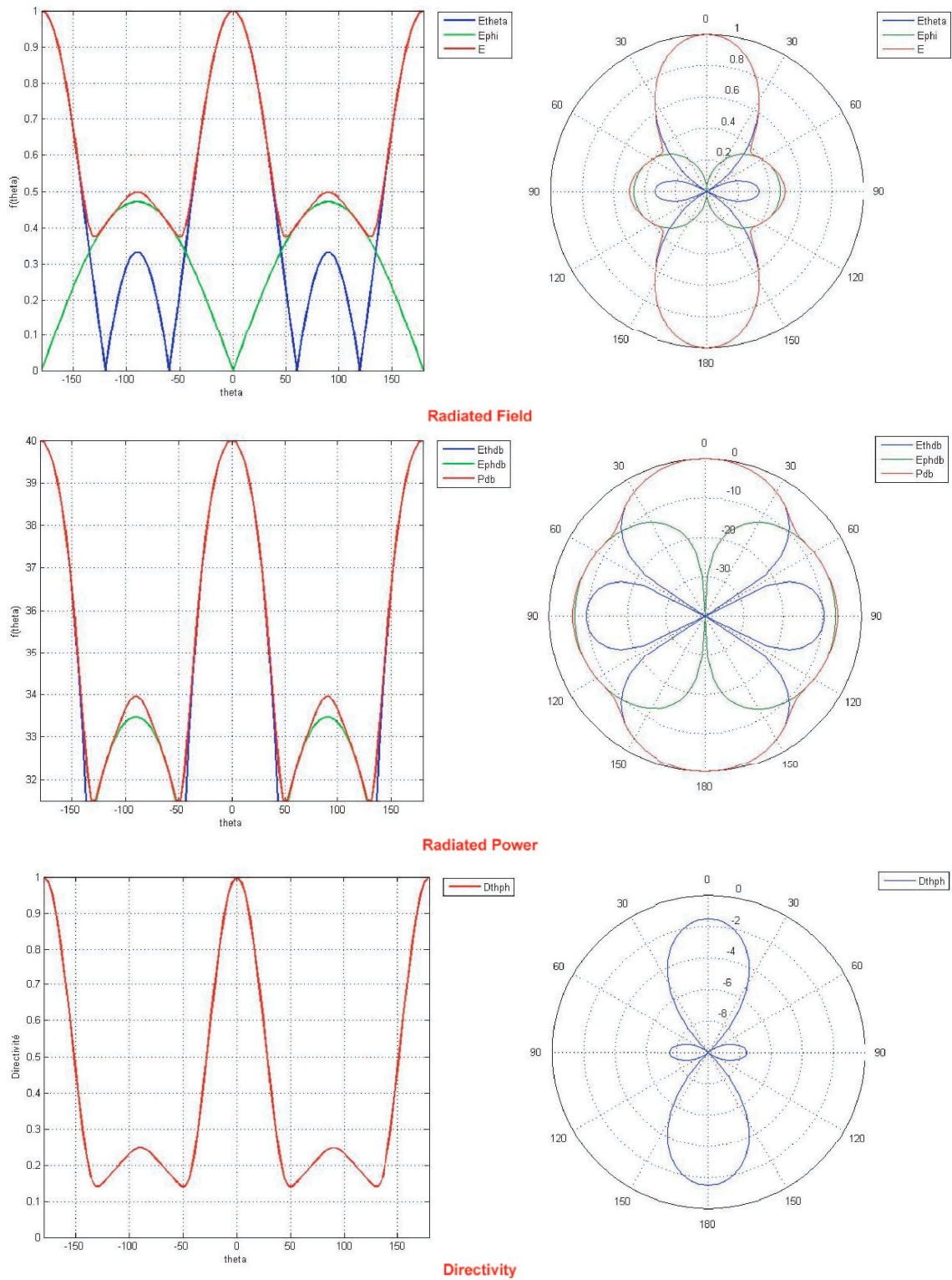


FIGURE 5.21: Simulation results (a) for the antenna characteristics

## 5.4. SOME EXAMPLES OF AVAILABLE SIMULATIONS

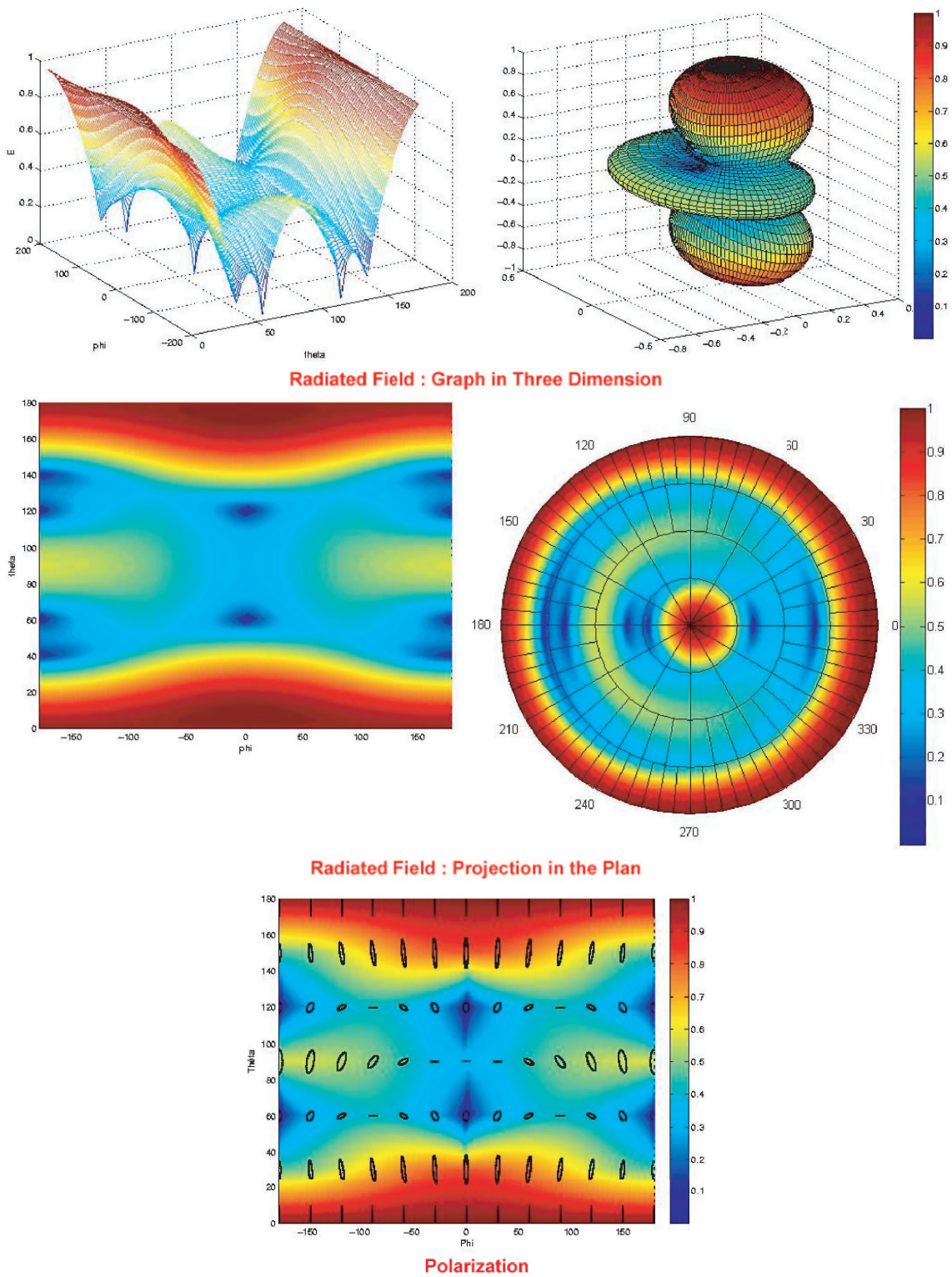


FIGURE 5.22: Simulation results (b) for the antenna characteristics

### 5.5 Conclusion

Teaching the electromagnetic theory of antennas at an undergraduate level usually requires vector mathematics in a 3D continuous space. This makes the average course hard to understand by today's students, more used to deal with digital/discrete quantities in 1D or 2D spaces. With the purpose of rendering these courses more attractive, we have developed a series of teaching tools in MatLab environment. To make this process more interactive, and also to access a much wider number of students, we used the nowadays well developed web-based tools for e-learning. The MatLab environment with his Matlab Web Server enables us to create Matlab applications that use the capabilities of the World Wide Web for inputting data and graphically displaying the output results with just a Web browser. Once the application was download via the designed receiver, the functioning of the website becomes easy. Only the server needs to have Matlab installed on it. The customer just needs a browser to launch the website, which requires only a narrow bandwidth. Since this courseware was an "open" strategy, the user could himself derived calculations and introduced his results values saved in a file and compared them with those of the website. This way of proceeding would help the user to understand the principle of the method described.

This courseware was found to be a useful tool for teachers to enhance the understanding of the antenna courses by the students. All these simulations helped the students to gain a practical sense for the analysis of antennas. Once the website was set up, any number of simulations could be carried out if the specified rules were respected when writing the program files. This web course increases the number of potential users, but reduces the interactivity of the Matlab program. The use of the matlabserver was time consuming for the user who must wait for the response from the server. But despite this drawback, the development of this web site contributed to make the antenna course more understandable and accessible for the average student.

## Chapter 6

# CONCLUSION AND PERSPECTIVES

The purpose of our thesis project was to make available to African universities a low cost system of telecommunications, developed with local material and a simple process to manufacture antennas.

At the beginning of this project, our aim was to use free satellite communication for amateurs. This was the initial suggestion that was included in our proposal for the research project "Antenna for inter-university system of communication" accepted among four other projects submitted for financing by the Swiss Agency for Development and Cooperation (SDC) (2004-2007). Afterwards, reading carefully the regulations for radioamateurs [83], we realized that this system of telecommunications could not be used for our application. Because an amateur service is a radiocommunication service for the purpose of self-training, intercommunication and technical investigations carried out by amateurs, that is, by duly authorized persons interested in radio technique solely with a personal aim and without pecuniary interest. Then we shifted our selection to commercial low cost satellites of telecommunications. This change in telecommunications system had also a relevant impact on the receiving equipments. Instead of using an array of adaptive antennas, we designed only one patch antenna, for which there is no need to use an optimization technique. On the one hand, the design of equipment is less free and flexible when dealing with commercial

## CHAPTER 6. CONCLUSION AND PERSPECTIVES

---

system than with amateur system. This added some extra constraints to our design effort. On the other hand, some rules must be observed while using a commercial system of telecommunications. We chose the more affordable one and we designed an Earth station for the reception of signals in a satellite system of telecommunications.

First of all, we evaluated some systems of telecommunications which are already available and focused our choice on the least expensive system, both in terms of receiver cost and telecommunication fees : the Worldspace system of telecommunications. Among all the Worldspace receiver manufacturers, there is one, Tongshi, which proposes the lowest price for a receiver that can be connected to a computer. With the help of a standard computer, it will become possible for African universities to transfer scientific information from the North to the South. Once we had decided to use the Tongshi receiver equipment, we obtained characteristics of the the Tongshi Worldspace receiver, in order to design aluminium-wood antennas providing compatible performances. Before using wood as dielectric we must know its characteristics.

Then, for the first time, we characterized a series of samples of tropical wood, in order to select the type of wood that exhibits the lowest loss tangent. The measurement of wood dielectric properties is the first original contribution of this thesis. It has resulted in exchanges between our laboratory at EPFL and a German small and medium enterprize (IMST) interested by the possible experimental applications. We used two available methods in the laboratory : the waveguide method, which gave us the reference values and the open resonator method, which will be used to confirm the values measured by the first method. We noticed that all the wood samples that we characterized are linear anisotropic dielectric media. When we measured the dielectric values of all our samples we realized that wood is an anisotropic linear dielectric medium, which has an uniaxial character for all the species of wood considered. Among the indexed wood available in the Cameroon forests, the one having the lowest density is Ayous. Our measurements show that the dielectric loss tangent increases with the density of the wood. Since we had determined which sample of wood has the lowest density, we concluded that it is no longer necessary to characterize all the Cameroonian species of wood. Among all the wood samples that we characterized, we

---

arrived at a conclusion that the best approach would be to use Balsa wood for the patch substrate and Ayous for the line substrate.

We used these two species of wood to simulate and design the first aluminium-wood antennas, with both linear and circular polarizations, by using a simple assembling process : gluing. First we try to measure the loss of quality between SSFIP antenna and the aluminium-wood antenna. The measurement of gain gives us 8.54 dB for the aluminium-wood antenna. This value is larger than the one exhibited by a standard patch microstrip antenna, and sufficient enough for our purposes. Moreover, if we compare this gain with the SSFIP reference antenna's gain we have a loss of only 1.5 dB. From this small reduction in gain, we can conclude that the loss of quality is small between the two types of antennas : we can therefore use the aluminium-wood antenna at the place of the SSFIP antenna. The measured characteristics of the antennas we designed showed us that we can use only two types of aluminium-wood antennas to receive Worldspace satellite signals : the antenna with only Balsa as patch substrate or the antenna with Balsa as patch substrate and Ayous as line substrate. With these two antennas we measured gains which fit the Tongshi Worldspace receiver system characteristics. We want to thank the German company IMST which allowed me to spend one week for a short term scientific mission supported by COST-284 funds. During this mission we have characterized Balsa wood, manufactured the first wood antenna and measured its parameters. We also discussed some technical aspects of antenna manufacturing using local material. All these experiences gained were used within the framework of this thesis.

Then we proceeded to design a simplified low noise amplifier with characteristics similar to those of the Tongshi receiver. Standard microwave and circuit design theory was used to provide an initial topology and to check the viability of our proposed design. However, since the simplifications of the theoretical model led to inconclusive results, the final characterization of the LNA performance had to be obtained by direct measurement. The measured characteristics of the designed LNA were adequate for our application. After the design of our simplified LNA we connected it to the antennas that we had also designed. The reception tests of satellite signals confirmed that this combination of the simplified LNA

and the aluminium-wood antenna works perfectly. During the test, we received the signals from all the radio stations which are located in the west beam of Afristar Worldspace satellite. These positive receptions confirmed that we can use wood, aluminium and a simple manufacturing process to design antennas for the reception of satellite signals. The RF front-end we designed here can be manufactured locally with a minimum of specific training. Already at the prototype/university level, costs are certainly much lower than for buying a commercial equipment.

Finally we designed a course for the remote study of antennas by associating our Matlab codes to PHP codes through the Matlab Webserver software. It enabled us to make our Matlab codes available to a large number of students, so that students can better understand antenna theory. We designed an "open" strategy course to help the user to understand the antenna course by practising himself. The development of this web site contributes to making antenna courses more understandable and accessible to the average student. These codes were successfully tested in EPFL in the course "Antennas and Radiation".

Within our project, we built the first aluminium-wood antenna and convincingly demonstrated its application to a satellite receiver. There is still room enough to improve the characteristics, in particular for the circularly polarized antenna, as we did not yet get the best possible ellipticity in our radiation pattern. The next first step will be to pursue simulation, in order to realize a circularly polarized wood antenna with a more optimal ellipticity. The second step will be to realize a wood antenna with dual circular polarization since this could double the possibilities for receiving different channels from the targeted satellites.

### **Some Future Perspectives**

Back to other more general perspectives for further development and improvement, the following can be said :

- The obvious power source for our antennas is power provided by solar cells. Indeed, in our prototype we have used solar cells to power and bias the LNAs. LEMA-EPFL has conclusively demonstrated that low cost amorphous silicon solar cells can be used as "solar antennas" [84]. Therefore we could replace the aluminium patch by a solar



---

cell, solving in this way simultaneously the problem of RF signal reception and of power generation. This insight is fully confirmed by the fact that several companies in Switzerland (VHF Technologies [87]) are developing cheap mass production of flexible film solar cells that could fit our design and provide in addition another chance for a successful North-South technological transfer.

- Recently, the idea of replacing satellites by high altitude platforms (HAPS) has received a lot of attention [85]. In Europe, several projects funded by the European Commission (CAPANINA, ...) aim at this goal. HAPS could provide a good solution for communications in Africa, and this has recently been acknowledged in a document of the "Fonds Mondial de Solidarité Numérique" [88]. Again, LEMA-EPFL is fully aware of these developments and collaborates in some Swiss initiatives like ASOLANT [84] and STRATXX [86]. Therefore, this will be an excellent new challenge for our RF front ends and receiving wood antennas.
- Finally a market study is being conducted in parallel with this thesis. At the end of this study, mass production of the aluminium antennas should begin in Cameroon. Then a didactic video and a simulation of the manufacturing process of Cameroonian local antennas would be added to the courseware and make of this e-course a very valuable tool for teaching and manufacturing of antennas.



# Bibliography

- [1] A. H. G. Nkama, *Sources of growth and realizing Cameroon's potentials for future development*, Global development network, Faculty of Economics and Management, University of Yaounde II, Cameroon, September, 2006, [http://ctool.gdnet.org/conf\\_docs/Nkama\\_paper\\_parallel\\_2.5.doc](http://ctool.gdnet.org/conf_docs/Nkama_paper_parallel_2.5.doc).
- [2] <http://www.world66.com/africa/cameroon/economy>.
- [3] <http://www.inmarsat.com>.
- [4] <http://www.satellite-provider.pl/inmarsat.html>.
- [5] <http://www.globalstar.com>.
- [6] <http://www.iridium.com>.
- [7] <http://www.satellitephonestore.com/iridium/iridium-satellite-phones.php>.
- [8] <http://www.thuraya.com>.
- [9] <http://www.worldspace.com>.
- [10] <http://www.europesatellite.com/wordspa/techno#techno>.
- [11] <http://194.117.210.39/Fichiers/ecouter/Frequences/satellites/afristar.pdf>.
- [12] [http://www.tongshi.com/cp\\_dab\\_e.htm](http://www.tongshi.com/cp_dab_e.htm).
- [13] <http://contracts.onecle.com/worldspace/worldspace.mfg.2001.08.18.shtml>.
- [14] S. R. Saunders, *Antennas and propagation for wireless communication systems*, John Wiley & Sons, England, 1999.
- [15] J. R. James & P. S. Hall, *Handbook of microstrip antennas*, Peter Peregrinus Ltd, London, UK, 1989.

## BIBLIOGRAPHY

---

- [16] D. M. Pozar and D. H. Schaubert, *Microstrip antennas : the analysis and design of microstrip antennas and arrays*, IEEE Press, New York, USA, 1995.
- [17] J.F. Zürcher, F. E. Gardiol, *Broadband patch antennas*, Artech House, London, UK, 1995.
- [18] F. Gardiol, *Traité d'électricité volume III : électromagnétisme*, Presses Polytechniques Romandes, Lausanne, Suisse, 1989.
- [19] J. Chamberlain and G. W. Chantry, *High frequency dielectric measurement*, IPC Science and Technology Press Ltd, London, UK, 1973.
- [20] P. Kabos, R. G. Geyer and J. Baker-Jarvis, *Dielectric sleeve resonator techniques for microwave complex permittivity evaluation*, IEEE Transactions on Instrumentation and Measurement, **Vol. 51**, No. 2, April, 2002, pp 383–392.
- [21] D. Li, C.E. Free, K.E.G. Pitt and P.G. Barnwell, *Perturbation method for dielectric constant measurement of thick-film dielectric materials at microwave frequencies*, IEE Electronics Letters, **Vol. 34**, No. 21, 15 October, 1998, pp 2042-2044.
- [22] P. A. Rolla M. Martinelli and E. Tombari, *A method for dielectric loss measurements by a microwave cavity in fixed resonance condition*, IEEE Transactions on Microwaves Theory and Techniques, **Vol. MTT-33**, No. 9, September, 1985, pp 779–783.
- [23] K. Sarabandi and E. S. Li, *Microstrip ring resonator for soil moisture measurements*, IEEE Transactions on Geoscience and Remote Sensing, **Vol. 35**, No. 5, September, 1997, pp 1223—1231.
- [24] R. G. Sumesh Sofin and R. C. Aiyer, *Measurement of dielectric constant using a microwave microstrip ring resonator (MMRR) at 10 GHz irrespective of the type of overlay*, Microwave and Optical Technology Letters, **Vol. 47**, No. 1, 5 October, 2005, pp 11–14.
- [25] T. M. Hirvonen, P. Vainikainen, A. Lozowski and A. V. Räsänen, *Measurement of dielectrics at 100 GHz with an open resonator connected to a network analyzer*, IEEE Transactions on Instrumentation and Measurement, **Vol. 45**, No. 4, August, 1996, pp 780—786.
- [26] B. Komiyama, M. Kiyokawa and T. Matsui, *Open resonator for precision dielectric measurements in the 100 GHz band*, IEEE Transactions on Microwave Theory and Techniques, **Vol. 39**, No. 10, October, 1991, pp 1792—1796.
- [27] B K Chung, *A convenient method for complex permittivity measurement of thin materials at microwave frequencies*, Journal of Physics D: Applied Physics, **Vol. 39**, 2006, pp 1926—1931.

- [28] R. Zoughi, *Microwave non-destructive testing and evaluation*, Kluwer Academic Publishers, Dordrecht, Netherlands, 2000.
- [29] F. Gardiol, *Traité d'électricité volume XIII : hyperfréquences*, Troisième édition, Presses Polytechniques Romandes, Lausanne, Suisse, 1991.
- [30] S. Ramo, J. R. Whinnery, T. Van Duzer, *Fields and waves in communication electronics*, Second edition, John Wiley & Sons, USA, 1965.
- [31] Hewlett Packard, *Measuring the dielectric constant of solids with the HP 8510 network analyser*, Materials measurement, Product note 8510-3.
- [32] L. Solymar and D. Walsh, *Lectures on the electrical properties of materials*, Second edition, Oxford University Press, London, UK, 1979, p. 257.
- [33] Damaskos, Inc, *Model 600T Open Resonator*.
- [34] O. Vidémé Bossou, J.R. Mosig, J-F. Zürcher, *Le bois comme diélectrique pour une antenne microruban*, 9ième Journée de Caractérisation Microondes et Matériaux (JCMM 2006), St. Etienne, France, 28-30 mars, 2006, Session Posters, P13.
- [35] Y. Amino, *Mechanical performance evaluation of bamboo-timber composite beams*, Ph.D. thesis, École Polytechnique Fédérale de Lausanne, Faculté Environnement Naturel Architectural et Construit, 2002, <http://library.epfl.ch/theses/?nr=2582>.
- [36] Kurt Galik, M. Tabassum Afzal, B. Colpitts, *Dielectric properties of softwood species measured with an open-ended coaxial probe*, Proceedings 8th International IUFRO Wood Drying Conference 2003, Brasov, Romania, 24-29 August, 2003, pp 110–115.
- [37] H. Sahin, N. Ay, *Dielectric properties of hardwood species at microwave frequencies*, Journal of Wood Science, **Vol. 50**, No 4, August, 2004, pp 375–380.
- [38] R. H. Lang, A. Franchois, Y. Piñeiro, *Microwave permittivity measurements of two conifers*, IEEE Transactions on Geoscience and Remote Sensing, **Vol. 36**, No. 5, September, 1998, pp 1383–1395.
- [39] [http://www.kayelaby.npl.co.uk/general\\_physics/2\\_6/2\\_6\\_5.html](http://www.kayelaby.npl.co.uk/general_physics/2_6/2_6_5.html).
- [40] Association Internationale Technique des Bois Tropicaux (ATIBT) (ed.), *Atlas des bois tropicaux*, Tome I - Afrique.
- [41] C. P. Aron, *Effect of degenerate  $E_{11}$  mode in  $H_{01}$  mode cavity on the measurement of complex permittivity*, Proc. IEE, **Vol. 114**, No. 8, 1967, pp 1030–4.

## BIBLIOGRAPHY

---

- [42] J. Pellet, L. Rechsteiner, A. Skrivervik, J-F. Zürcher, N. Perrin, *Use of the harmonic direction finder to study the terrestrial habitats of the European tree frog (Hyla arborea)*, Amphibia-Reptilia, No. 27, March 3, 2006, pp 138–142.
- [43] S. Vaccaro, J.R. Mosig, P. de Maagt, *Patch and slot antennas integrating high efficiency GaAs solar cells for space applications*, Journées Internationales de Nice sur les antennes (JINA'02), Nice, France, **Vol. II**, 12-14 Novembre, 2002, pp 117–120.
- [44] S. Vaccaro, *SOLANT : study and development of planar antennas integrating solar cells*, Ph.D. thesis, École Polytechnique Fédérale de Lausanne, Faculté Sciences et Techniques de l'Ingénieur, 2003, <http://library.epfl.ch/theses/?nr=2689>.
- [45] S. Vaccaro, P. Torres, J.R. Mosig, A. Shah, J.-F. Zürcher, A.K. Skrivervik, P. de Maagt and L. Gerlach, *Stainless steel slot antenna with integrated solar cells*, IEE Electronics Letters, **Vol. 36**, No 25, 7th December, 2000.
- [46] <http://www.f8byc.net/menu4/page8.html>.
- [47] <http://www.nodomainname.co.uk/Omnicolinear/2-4collinear.htm>.
- [48] <http://www.myotis.ch/exoops/modules/mydownloads/cache/files/pringles.pdf>.
- [49] Wayne S. T. Rowe and Rod B. Waterhouse, *Theoretical investigation on the use of high permittivity materials in microstrip aperture stacked patch antennas*, IEEE Transactions on Antennas and Propagation, **Vol. 51**, No. 9, September, 2003, pp 2484–2486.
- [50] Ch. Gentili, *Amplificateurs et oscillateurs micro-ondes*, Masson, Paris, France, 1984.
- [51] Pieter L. D. Abrie, *Design of RF and microwave amplifier and oscillators*, Artech House, London, UK, 1999.
- [52] <http://www.avagotech.com/products/product-detail.jsp?navId=H0,C1,C4936,C5230,C5010,C5088,P93933>.
- [53] <http://www.iit-online.iit.edu/businesses/>.
- [54] <http://cpd.asu.edu/ant/>.
- [55] [http://cpd.asu.edu/online/?page=course\\_eee443\\_spr2005](http://cpd.asu.edu/online/?page=course_eee443_spr2005).
- [56] <http://blackboard.uic.edu/webapps/blackboard/execute/viewCatalog?type=Course>.
- [57] [http://blackboard.uic.edu/webapps/portal/frameset.jsp?tab=courses&url=%2Fbin%2Fcommon%2Fcourse.pl%3Fcourse\\_id%3D\\_83\\_1](http://blackboard.uic.edu/webapps/portal/frameset.jsp?tab=courses&url=%2Fbin%2Fcommon%2Fcourse.pl%3Fcourse_id%3D_83_1).
- [58] <http://www.den.usc.edu/programs/ee/index.htm>.

- [59] <http://www.engineeringlab.com/rfwireless5.html>.
- [60] K. E. Lonngren, S. V. Savov, R. J. Jost, *Fundamentals of electromagnetics with Matlab*, Second edition, Scitech publishing inc., Canada, 2007.
- [61] [http://www.technolab.org/index\\_F\\_CH.htm](http://www.technolab.org/index_F_CH.htm).
- [62] <http://www.fbk.com/pdfs/telecom/telecommunications-range.pdf>.
- [63] [http://www.lucas-nuelle.de/299/Products/Training\\_Systems/Information\\_and\\_Communication\\_Technology/tan.htm](http://www.lucas-nuelle.de/299/Products/Training_Systems/Information_and_Communication_Technology/tan.htm).
- [64] E. Tonyé and O. Vidémé Bossou, *CAL-Antennas : Computer-Aided Learning of Antennas*, Applied Computational Electromagnetics Society Journal (ACES), **Vol. 8**, No 1, 1993, pp 138–156.
- [65] J. M. Bélinga Bélinga, *Définition et élaboration d'un cours hypermédia sur le télé-enseignement distant*, DEA thesis, École Nationale Supérieure Polytechnique, Département du Génie Electrique, 1997.
- [66] <http://www.prepaly.com>.
- [67] O. Vidémé Bossou, J. R. Mosig, E. Tonyé, *Kit Didactique Matlab pour le Traitement d'Antenne de Type Filiforme*, 1st International Symposium on Electromagnetism, Satellites and Cryptography (ISESC'05), Jijel, Algeria, June 19-21, 2005.
- [68] O. Vidémé Bossou, J. R. Mosig, *Teaching Matlab Based Toolbox for Antenna Course*, International Conference on Engineering Education (ICEE 2005), **Volume 2**, Gliwice, Poland, July 25–29, 2005, pp 633–641.
- [69] O. Vidémé Bossou, J. R. Mosig, E. Tonyé, *Integrated system for the support of teaching, design and manufacturing of antennas*, International Conference on Engineering Education (ICEE 2003), Valencia, Spain, July 21-25, 2003.
- [70] O. Vidémé Bossou, J. R. Mosig, E. Tonyé, *e-Antenna : antenna web based course using matlabserver*, IV International Conference on Multimedia and Information and Communication Technologies in Education (m-ICTE 2006), **Vol. II**, Sevilla, Spain, November 22-25, 2006, pp 1239–1243.
- [71] <http://ephotonics.epfl.ch>.
- [72] MathWorks Inc., *MATLAB Web Server*, 2005.
- [73] P. Hudson, *PHP in a nutshell*, O'Reilly, London, UK, 2006.

## BIBLIOGRAPHY

---

- [74] G. Schlossnagle, *Advanced PHP programming*, Developer's library, London, UK, 2004.
- [75] R. F. Harrington, *Field computation by moment methods*, IEEE Press, New York, USA, 1993.
- [76] E. K. Miller, L. Medgyesi-Mitschang, E. H. Newman, *Computational electromagnetics : frequency-domain method of moments*, IEEE Press, New York, USA, 1992.
- [77] J. D. Kraus, *Antennas*, Second edition, McGraw-Hill Book Company, New York, USA, 1988.
- [78] C. A. Balanis, *Antenna theory : analysis and design*, Third edition, John Wiley and Sons Inc., New Jersey, USA, 2005.
- [79] S. D. Rogers and C. M. Butler, *An efficient curved-wire integral equation solution technique*, IEEE Transactions on Antennas and Propagation, **Vol. 49**, No 1, January, 2001, pp 70–79.
- [80] N. J. Champagne II, J. T. Williams, D. R. Wilton, *The use of curved segments for numerically modeling thin wire antennas and scatterers*, IEEE Transactions on Antennas and Propagation, **Vol. 40**, No 6, June, 1992, pp 682–689.
- [81] G. A. Thiele, *Analysis of Yagi-Uda-Type antennas*, IEEE Transactions on Antennas and Propagation, **Vol. AP-17**, No 1, January, 1969, pp 24–31.
- [82] L. Sevgi and G. Çakir, *A broadband array of archimedean spiral antennas for wireless applications*, Microwave and Optical Technology Letters, **Vol. 48**, No 1, January, 2006, pp 195–200.
- [83] <http://www.iaru.org/iarucnst.html>.
- [84] <http://itopwww.epfl.ch/LEMA/Asolant/>.
- [85] Fonds mondial de Solidarité Numérique (FSN), FSN-infos, No 10, Mars, 2007.
- [86] <http://www.stratxx.com/>.
- [87] <http://www.flexcell.com>.
- [88] <http://www.dsf-fsn.org>.



# Curriculum Vitae

**Name and first name :** VIDÉMÉ BOSSOU Olivier

**Date and place of birth :** 26th July 1963, Maroua - Cameroon

## EDUCATION

**1999-2000:** National Advanced School of Engineering (ENSP), University of Yaounde I, Cameroon, (DEA diploma in Engineering Science, Telecommunication option)

**1989-1991:** Ecole Normale Supérieure de l'Enseignement Technique - Annexe de Nkolbisson (Yaoundé), University of Douala, Cameroon, (Professorship Diploma for technical high school, Electrical Engineering)

**1986-1989:** National Advanced School of Engineering, University of Yaounde I, Cameroon, (Electronic Engineer diploma)

**1982-1985:** Secondary High School of Maroua, Cameroon (High school diploma)

## RESEARCH EXPERIENCE

**2004-2007:** Research Assistant at the Swiss Federal Institute of Technology in Lausanne (EPFL), Sciences Institute, Electromagnetic and Acoustic Laboratory, Lausanne, Switzerland, sponsored by EPFL-SDC, Switzerland

**2005:** Invited stay in IMST-Germany in the frame of an European COST project on wood antenna measurement, sponsored by European action COST 284

**2002-2003:** Post-graduate research training at the Swiss Federal Institute of Technology in Lausanne (EPFL), Sciences Institute, Electromagnetic and Acoustic Laboratory, Lausanne, Switzerland, sponsored by AUF, France

## TEACHING EXPERIENCE

**2005:** Improved the codes of the teaching web site <http://ephotonics.epfl.ch/>

**2003-2005:** Design two teaching module in PREPALY ([www.prepaly.com](http://www.prepaly.com)) project sponsored by Fonds Francophones des Inforoutes (F.F.I.)

**1999-2002:** Part time teacher at National Advanced School of Engineering (ENSP-Cameroon) - Department of Electrical Engineering and Telecommunication

**2000:** Trainer in "5th edition CITI program: Training on Internet Applications Experts

## BIBLIOGRAPHY

---

(ENSP-Cameroon)"

**1994-1996:** Taught informatics and electronic maintenance at Jobbers Computer Company (Yaoundé-Cameroon)

**1992-1997:** Teacher at technical high school (Sangmelima, Ebolowa-Cameroon)

# Publications

## Conference Proceedings

Olivier Vidémé Bossou, J. R. Mosig, E. Tonyé, *Integrated system for the support of teaching, design and manufacturing of antennas*, International Conference on Engineering Education (ICEE 2003), Valencia, Spain, July 21-25, 2003.

Olivier Vidémé Bossou, J. R. Mosig, *Teaching Matlab Based Toolbox for Antenna Course*, International Conference on Engineering Education (ICEE 2005), **Volume 2**, Gliwice, Poland, July 25–29, 2005, pp 633–641.

O. Vidémé Bossou, J.R. Mosig, J-F. Zürcher, *Le bois comme diélectrique pour une antenne microruban*, 9ième Journée de Caractérisation Microondes et Matériaux (JCMM 2006), St. Etienne, France, 28-30 mars, 2006, Session Posters, P13.

Olivier Vidémé Bossou, J. R. Mosig, E. Tonyé, *e-Antenna : antenna web based course using matlabsolver*, IV International Conference on Multimedia and Information and Communication Technologies in Education (m-ICTE 2006), **Vol. II**, Sevilla, Spain, November 22-25, 2006, pp 1239–1243.